ARO 36100.1-PH-CF

PROCEEDINGS PIERS 1997

Volume 1

DISTRIBUTION STATEMENT A
Approved for public release;
Distribution Unlimited



19970514 059

香港城市大學
City University
of Hong Kong

6 - 9 January 1997

Telecommunications Research Centre

REPORT DOCUMENTATION PAGE

Form Approved
OMB NO. 0704-0188

Public reporting burden for this collection of information is estimated to average 1 hour per response, including the time for reviewing instructions, searching existing data sources, gathering and maintaining the data needed, and completing and reviewing the collection of information. Send comment regarding this burden estimates or any other aspect of this collection of information, including suggestions for reducing this burden, to Washington Headquarters Services, Directorate for information Operations and Reports, 1215 Jefferson Davis Highway, Suite 1204, Arlington, VA 22202-4302, and to the Office of Management and Budget, Paperwork Reduction Project (0704-0188), Washington, DC 20503.

1. AGENCY USE ONLY *(Leave blank)*	2. REPORT DATE	3. REPORT TYPE AND DATES COVERED
	March 1997	Final 1 Sep 96 - 31 Aug 97

4. TITLE AND SUBTITLE

Proceedings of Conference on Progress In Electromagnetics Research Symposium, PIERS 1997, Volumes 1 and

5. FUNDING NUMBERS

DAAH04-96-1-0411

6. AUTHOR(S)

Zu-Han Gu (principal investigator)

7. PERFORMING ORGANIZATION NAMES(S) AND ADDRESS(ES)

Surface Optics Corp.
San Diego, CA 92126

8. PERFORMING ORGANIZATION REPORT NUMBER

9. SPONSORING / MONITORING AGENCY NAME(S) AND ADDRESS(ES)

U.S. Army Research Office
P.O. Box 12211
Research Triangle Park,, NC 27709-2211

10. SPONSORING / MONITORING AGENCY REPORT NUMBER

ARO 36100.1-PH-CF

11. SUPPLEMENTARY NOTES

The views, opinions and/or findings contained in this report are those of the author(s) and should not be construed as an official Department of the Army position, policy or decision, unless so designated by other documentation.

12a. DISTRIBUTION / AVAILABILITY STATEMENT

Approved for public release; distribution unlimited.

12 b. DISTRIBUTION CODE

13. ABSTRACT *(Maximum 200 words)*

NO ABSTRACT FURNISHED

14. SUBJECT TERMS	15. NUMBER IF PAGES
	16. PRICE CODE

17. SECURITY CLASSIFICATION OR REPORT	18. SECURITY CLASSIFICATION OF THIS PAGE	19. SECURITY CLASSIFICATION OF ABSTRACT	20. LIMITATION OF ABSTRACT
UNCLASSIFIED	UNCLASSIFIED	UNCLASSIFIED	UL

PIERS 1997

Progress In Electromagnetics Research Symposium

Volume 1
Monday and Tuesday Sessions

Proceedings

January 6-9, 1997

Telecommunications Research Centre
City University of Hong Kong
Tat Chee Avenue, Kowloon , Hong Kong

DTIC QUALITY INSPECTED 4

This Publication was prepared by the Telecommunications Research Centre, City University of Hong Kong.

PIERS 1997 TECHNICAL COMMITTEE

PIERS Chair:	Prof J.A.Kong, Massachusetts Institute of Technology
General Chair:	Prof Edward K.N.Yung, City University of Hong Kong
Technical Program:	Prof K.M.Luk (Chair), City University of Hong Kong
	Prof K.F.Lee (Co-Chair), University of Missouri-Columbia
	Prof A.L.Cullen, University College London
	Prof Shenggang Liu, Univ. of Electronic Science and Tech. of China
	Prof W.A.Gambling, City University of Hong Kong
	Prof K.K.Mei, City University of Hong Kong
	Prof Y.L.Chow, City University of Hong Kong
	Prof C.H.Chan, City University of Hong Kong
Local Arrangement:	Dr K.F.Tsang (Chair), City University of Hong Kong
	Dr Ross D.Murch, Hong Kong Univ. of Science and Technology
	Mr K.T.Ng, City University of Hong Kong
Publication:	Mr L.L.Cheng (Chair), City University of Hong Kong
	Dr Beatrice Chu (Co-Chair), City University of Hong Kong
	Dr Y.T.Chow, City University of Hong Kong
Registration:	Dr Y.Hwang (Chair), City University of Hong Kong
Finance:	Dr K.W.Leung (Chair), City University of Hong Kong
Social Program:	Dr Albert K.Y.Lai (Chair), Chinese University of Hong Kong
Souvenir:	Dr W.Y.Tam (Chair), Hong Kong Polytechnic University
	Dr Y.Chen, Hong Kong Polytechnic University
	Dr W.H. Lau, City University of Hong Kong
Web Page:	Dr Terry C. K. Ng, City University of Hong Kong
Secretary:	Dr W.S.Chan, City University of Hong Kong

SPONSORS

Likely Industries Ltd.
Hewlett-Packard Hong Kong Ltd.
Hong Kong Telecom Foundation
K.C. Wong Education Foundation
Treasure Floating Restaurant
Computer Products Asia-Pacific Ltd.
Hong Kong Industrial Technology Corporation
Gold Peak Industries (Holdings) Ltd
New Asia Grocery Co., Ltd.
US Army Research Office

ABSTRACT

The Progress in Electromagnetics Research Symposium (PIERS 1997) was held in Hong Kong, on the campus of the City University of Hong Kong, January 6-9, 1997. More than 650 presentations were made, and those abstracts are included in this publication.

Progress in Electromagnetics Research Symposium, PIERS 1997 ISBN 962-442-097-1

CONTENTS

Session 6P18	Microstrip and Printed Antennas 1	7
Session 6P17	Electromagnetic Compatibility	18
Session 6P16	Computational Techniques 1	30
Session 6P15	Scattering and Diffraction 1	40
Session 6P14	Millimeter, Submillimeter and Lightwaves 1	50
Session 6P13	RF and Microwave Circuits 1	57
Session 6P12	Radar	68
Session 6P11	Inverse Scattering & Polarimetry	78
Session 6P10	Wave Propagation in Planar Structures	89
Session 6P9	Optical Waveguide Structures	99
Session 6P8	Semiconductor Lasers & Photonic Devices	108
Session 6P7	Electromagnetics - Efficient in Cancer Treatment	119
Session 7A18	Microstrip & Printed Antennas 2	126
Session 7P18	Microstrip & Printed Antennas 3	136
Session 7A17	Antenna Measurements	144
Session 7P17	Six-Port Technology	155
Session 7A16	Computational Techniques 2	164
Session 7P16	Measured Equation of Invariance	172
Session 7A15	Scattering & Diffraction 2	181
Session 7P15	Scattering & Diffraction 3	191
Session 7A14	Non-Radiative Dielectric Waveguide and Its Millimeter-Wave Applications	201
Session 7P14	Millimeter, Submillimeter & Lightwaves 2	212
Session 7A13	RF & Microwave Circuits 2	222
Session 7P13	RF & Microwave Circuits 3	234
Session 7A12	Microwave-to-Optical Polarimetry : Basic Concepts	245
Session 7P12	Microwave-to-Optical Polarimetry : Applied Concepts	256
Session 7A11	Remote Sensing of Precipitation	265
Session 7P11	Advanced Image and Signal Processing for Remote Sensing	273
Session 7A10	International Workshop "Related Correlation Effects in Optics and Condensed Matter Physics 1"	281
Session 7P10	International Workshop "Related Correlation Effects in Optics and Condensed Matter Physics 2"	286
Session 7A9	Analytical and Numerical Techniques in Photonics 1	291
Session 7P9	Analytical and Numerical Techniques in Photonics 2	301
Session 7A8	Photonics, Nonlinear Optics & Devices 1	309
Session 7P8	Nonlinear Optics & Applications	320
Session 7A7	Bioelectromagnetic Image and Visualization	329
Session 7P7	Medical Applications & Biological Effects 1	341
Session 8A18	Propagation and Antennas in Mobile Communications	353
Session 8P18	DR Antennas & Mobile Antennas	363
Session 8A17	Antenna Theory & Measurement 1	374
Session 8P17	Antenna Theory & Measurement 2	382
Session 8A16	Computational Techniques 3	388
Session 8P16	Wavelets in Electromagnetics & Neural Network Techniques in Electromagnetics	395
Session 8A15	Scattering & Diffraction 4	404
Session 8P15	Time-Domain Electromagnetics	412
Session 8A14	Millimeter, Submillimeter & Lightwaves 3	420
Session 8P14	Millimeter, Submillimeter & Lightwaves 4	429
Session 8A13	RF & Microwave Circuits 4	436
Session 8P13	RF & Microwave Circuits 5	446

Session 8A12	Scattering by Rough Surface and Random Media 1	457
Session 8P12	Scattering by Rough Surface and Random Media 2	467
Session 8A11	Remote Sensing 1	479
Session 8P11	Remote Sensing 2	487
Session 8A10	International Workshop "Related Correlation Effects in Optics and Condensed Matter Physics 3"	495
Session 8P10	International Workshop "Related Correlation Effects in Optics and Condensed Matter Physics 4"	500
Session 8A9	Computational Methods in Lightwave Technology	503
Session 8P9	Integrated Optics & Fiber Optics	511
Session 8A8	Photonics, Nonlinear Optics & Devices 2	518
Session 8P8	Photonics, Nonlinear Optics & Devices 3	530
Session 8A7	Medical Applications & Biological Effects 2	542
Session 8P7	Low Frequency Applications	552
Session 9A18	Microstrip & Printed Antennas 4	559
Session 9P18	Microstrip & Printed Antennas 5	570
Session 9A17	Wireless Communications	580
Session 9A16	Computational Techniques 4	588
Session 9P16	Computational Techniques 5	597
Session 9A15	FDTD & Applications	604
Session 9P15	Development & Applications in Finite Difference Time Domain Method	615
Session 9A14	Millimeter, Submillimeter and Lightwaves 5	624
Session 9P14	Millimeter, Submillimeter and Lightwaves 6	633
Session 9A13	Superconducting Electronics	639
Session 9P13	RF Circuits for Mobile Applications	650
Session 9A12	Rough Surface Scattering	657
Session 9A11	Remote Sensing of the Atmosphere	664
Session 9A10	Waves in Composite and Complex Media	677
Session 9P10	Random Media, Nonlinear Media and Turbulent Media	687
Session 9A9	Blue-Green Light Emitters, Photonics and Nonlinear Optics	699
Session 9A8	Photonics, Nonlinear Optics and Devices 4	706
Session 9P8	Optoelectronics	715
Session 9A7	Electromagnetics & Microwaves	727
Session 9P7	Ferrite Devices & Measurements	737

Author Index .....

SESSION 6P18

Monday, January 6, PM 1330-1710, Lecture Theatre 18, City University of Hong Kong

Microstrip and Printed Antennas 1

Organizer: Kin-Lu Wong

Chairperson: Kin-Lu Wong, National Sun Yat-Sen University
Co-Chairperson: Ching-Her Lee, National Changhua University of Education

13:30 ***Studies of Cylindrical Microstrip Antennas*** 8
Kin-Lu Wong, Nan-Cheng Chen
National Sun Yat-Sen University

13:50 ***Theory and Experiment of Spherical Microstrip Antennas*** 9
*Hong-Twu Chen, **Horng-Dean Chen, *Yuan-Tung Cheng
*Chinese Military Academy
**Nan-Tai College

14:10 ***Dual-Frequency Operation of Rectangular Microstrip Antennas*** 10
*Horng-Dean Chen, **Shang-Jen Chuang
*Nan-Tai College
**National Kaosiung Institute of Marine Technology

14:30 ***Modified Annular-Ring Microstrip Antennas with a Sectorial Cut*** 11
*Wen-Shyang Chen, **Jinn-Chyuan Yang
*Cheng-Shiu College of Technology & Commerce
**Chung Cheng Institute of Technology

14:50 ***Scattering from Conformal Microstrip Antennas*** 12
Yuan-Tung Cheng, Hong-Twu Chen, Tsurng-Jeng Chang
Chinese Military Academy

15:10 **Break**

15:30 ***Analysis of Cylindrical Microstrip Discontinuities*** 13
Ching-Her Lee, Wei-Chen Hsu
National Changhua University of Education

15:50 ***Coplanar Waveguides on a Cylindrical Surface*** 14
Hsin-Cheng Su, Kin-Lu Wong
National Sun Yat-Sen University

16:10 ***Some Results on Slot-Coupled Double-Sided Microstrip Lines*** 15
Jui-Han Lu, Kin-Lu Wong
National Sun Yat-Sen University

16:30 ***Printed Antennas for A Portable Handset*** 16
Shyh-Yeong Ke, Chewn-Pu Jou
Industrial Technol. Research Institute

16:50 ***Characteristics of a Rectangular Patch Antenna Using Foam as Substrate*** 17
Jeen-Sheen Row
RF-Link Inc.

STUDIES OF CYLINDRICAL MICROSTRIP ANTENNAS

*Kin-Lu Wong and Nan-Cheng Chen
Department of Electrical Engineering
National Sun Yat-Sen University
Kaohsiung, Taiwan 804, R.O.C.

This paper presents a review of several recent publications for the analysis of probe-fed and slot-coupled cylindrical microstrip antennas using various theoretical techniques, including the full-wave approach, the cavity-model analysis, and the generalized transmission line model (GTLM) theory. The formulation of the input impedance of a single antenna and the mutual coupling coefficient between two antennas is described. Numerical results showing the curvature effects on the input impedance and mutual coupling of cylindrical microstrip antennas are discussed. Experimental measurements conducted to verify the theoretical results are also shown.

For the full-wave approach [S. Y. Ke and K. L. Wong, *Microwave Opt. Technol. Lett.*, vol. 7, pp. 232-236, 1994], a set of electric-field integral equations is first derived, which in turn is reduced to a matrix equation using the Galerkin's moment-method procedure. The unknown electric currents on the microstrip patch can then be calculated from solving the matrix equation. Once the unknown patch currents are obtained, the input impedance of the antenna or the mutual coupling between two antennas can readily be calculated. Among various theoretical results obtained, the full-wave solutions are usually the most accurate. However, the numerical computation for the full-wave approach is usually inefficient and requires more careful programming.

As for the cavity-model analysis [K. L. Wong and J. S. Chen, *Microwave Opt. Technol. Lett.*, vol. 9, pp. 124-127, 1995] and the GTLM theory [K. L. Wong, C. Y. Huang and Y. H. Liu, *Microwave Opt. Technol. Lett.*, vol. 8, pp. 63-68, 1995], the formulation is relatively simpler and the numerical computation is also more efficient. The cavity model considers the microstrip antenna as a cavity bounded by a perfect magnetic wall around the cavity and two electric walls on top and bottom of the cavity. From solving this cavity problem with a probe feed or a coupling slot, the equivalent magnetic current around the cavity at the magnetic wall is evaluated, and in turn the radiation power of the antenna can be obtained, which in turn gives the antenna's input impedance. On the other hand, the GTLM theory models the microstrip antenna as a section of transmission line loaded with a wall admittance at the radiation aperture around the patch edge. The section of the transmission line is further replaced by an equivalent π network, and an equivalent circuit for the microstrip antenna can be derived. From solving the circuit elements in the equivalent circuit, the input impedance or the mutual coupling of the antenna can be determined. And it should be noted that, due to the thin-substrate condition assumed in the cavity-model and GTLM analyses, the calculated results may be less accurate. The comparison of the theoretical solutions obtained from the full-wave approach, the cavity-model analysis, and the GTLM theory with the experimental results will be given in the presentation.

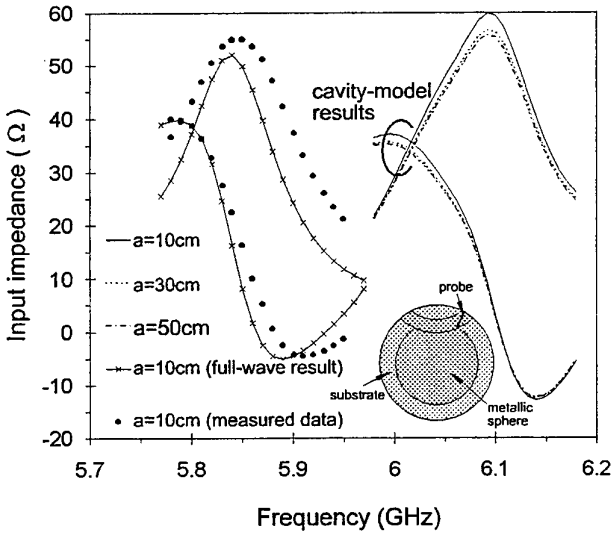
THEORY AND EXPERIMENT OF SPHERICAL MICROSTRIP ANTENNAS

***Hong-Twu Chen[1], Horng-Dean Chen[2], and Yuan-Tung Cheng[1]**

[1]Department of Electrical Engineering, Chinese Military Academy
Fong-Shan, Taiwan 830, R.O.C.

[2]Department of Electronic Engineering, Nan-Tai College
Tainan, Taiwan 710, R.O.C.

The characteristics of probe-fed circular and annular-ring microstrip antennas on a spherical body are studied in this paper. Both the cavity-model method and full-wave analysis are used for theoretical treatments. The cavity model is first proposed by Y.T. Lo et al. in 1979, in which the region bounded by the patch and ground plane is treated as a cavity and it is valid only for thin-substrate conditions. On the other hand, the full-wave analysis, a Green's-function formulation in the spectral domain incorporating with a Galerkin's moment-method calculation, is applicable for thicker substrates and more rigorous for analyzing microstrip antennas. However, the computation of full-wave analysis is relatively more complicated and requires careful programming to be computationally efficient. Various characteristics obtained using these two methods are compared with those obtained from the generalized transmission line model (GTLM) or measured data. It is seen that, as shown in the figure, the resonant frequency, obtained from the zero crossing of the reactance curve, is not affected by the curvature radius. This behavior is due to the approximation adopted in the cavity-model analysis. However, the resonant peak value of input resistance is decreased as increasing the curvature radius, this phenomena is similar to the observation of the full-wave analysis. More numerical and experimental results for the resonance, input impedance, and radiation characteristics of the spherical microstrip antennas will be presented at the meeting.



Besides the analysis of the single patch case, the coupling problems between two patches will also be investigated. A driven patch loaded by a parasitic element case is first studied. It is found that, by adjusting a suitable parasitic patch size, the impedance bandwidth of the spherical microstrip antenna could be increased considerably. For the mutual coupling between two probe-fed patches, this problem is treated as a two-port network with a 2×2 port impedance matrix $[Z^P]$, and the scattering matrix [S] can be evaluated. Then the coupling coefficient S_{12} can be calculated. The theoretical results for the coupling problems between two patches on a spherical surface will be discussed in the presentation.

DUAL-FREQUENCY OPERATION OF RECTANGULAR MICROSTRIP ANTENNAS

*Horng-Dean Chen[1] and Shang-Jen Chuang[2]

[1]Department of Electronic Engineering
Nan-Tai College, Tainan, Taiwan 710, R.O.C.

[2]Department of Telecommunication Engineering
National Kaohsiung Institute of Marine Technology, Kaohsiung, Taiwan 811, R.O.C.

Several methods of obtaining dual-frequency operations have been developed. In this artical a simple design method using a single-layer rectangular patch fed by a single coaxial probe is introduced (see Figure 1). For the antenna which is to operate at two desired operation frequencies, the rectangular patch dimensions are initially chosen in a mannar that the wide and narrow dimensions are determined, respectively, by the lower and upper operation frequencies. The feed location is selected for a good matching to the 50Ω feeding coax for the two frequencies. A typical example of a C-band rectangular patch antenna is construced and tested. For operation at 4 and 6 GHz, the patch dimensions are chosen to be 21.6× 13.9 mm. By moving the feed position along the x axis, we can find a 50Ω input impedance at (2.2 mm, 0) for the excitation of the TM_{10} mode at f = 4 GHz; by selecting a feed position at (0, 2.7 mm), a 50Ω input impedance is obtained for the TM_{01} mode at f = 6 GHz. By changing the feed position to be at (2.2 mm, 2.7 mm), two resonant modes are excited at frequencies about 4 GHz and 6 GHz with a good matching condition. The measured results for S_{11} are shown in Figure 2. Theoretical results calculated using a full-wave approach are in good agreement with measurement. However, due to the feed position moved away from the center lines (x and y axes), the cross-polarization performance may be affected at the two operation frequencies, and details of the results will be presented in the symposium. The dual-frequency operation results for the L- and X-band rectangular patch antennas will also be given in the symposium.

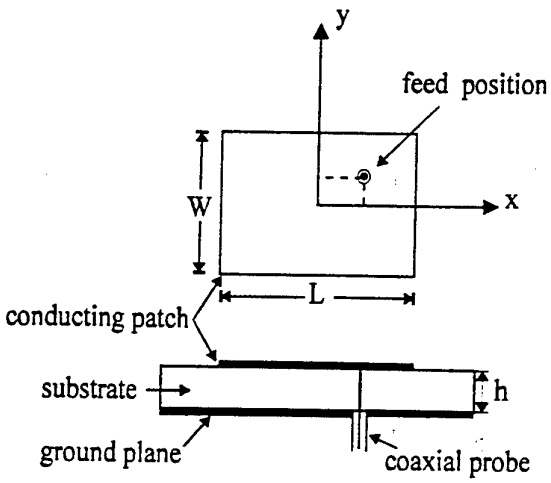


Figure 1 Geometry of a dual-frequency rectangular microstrip antenna with a coaxial probe

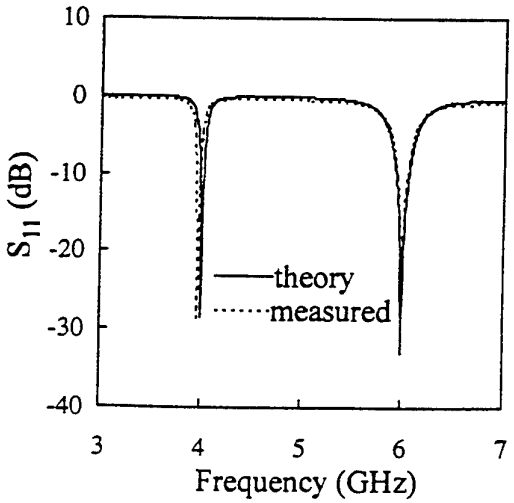


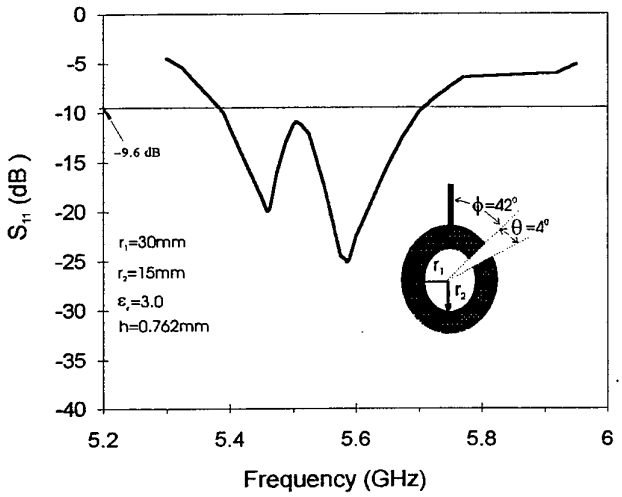
Figure 2 S_{11} for the feed position at (2.2mm, 2.7mm); L = 21.6mm, W = 13.9mm, h = 0.762mm, $\varepsilon_r = 3.0$, $\tan\delta = 0.0045$.

MODIFIED ANNULAR-RING MICROSTRIP ANTENNAS WITH A SECTORIAL CUT

*Wen-Shyang Chen[1] and Jinn-Chyuan Yang[2]

[1]Department of Electrical Engineering
Cheng-Shiu College of Technology & Commerce, Kaohsiung, Taiwan 833, R.O.C.

[2]Department of Electronic Engineering
Chung Cheng Institute of Technology, Taoyuan, Taiwan, R.O.C.



A microstripline-fed annular-ring microstrip antenna with a 50Ω matching condition in the TM_{12} mode can be easily achieved by cutting a small sectorial slit in the annular-ring patch (see inset in the figure). For an ordinary annular-ring microstrip patch antenna, due to its symmetric geometry, using a microstrip line to excite the patch with a 50Ω matching condition is usually impractical. However, with a small sectorial cut in the annular-ring patch, the surface current density on the patch is perturbed, and this makes it possible to obtain various input impedances by changing the angle between the feeding microstrip line and the sectorial cut. This matching technique has been experimentally verified. The figure shown here presents a typical example of a constructed annular-ring microstrip patch antenna with a sectorial cut of 4° matched to a 50Ω microstrip line. In this case the angle between the microstrip line and the sectorial cut is 42°, and the obtained antenna bandwidth (VSWR $\leq$ 2) is about 5.5%. It is also found that this antenna bandwidth is about twice as large as that of a probe-fed annular-ring microstrip patch antenna without a sectorial cut. And, since the excited patch surface current is perturbed in the modified annular-ring microstrip patch antenna, the radiation pattern may be varied as compared to the case without a sectorial cut. Results of the radiation properties from this modified structure will be discussed in the symposium.

In addition to the broadband impedance matching obtained for the modified annular-ring microstrip patch antenna fed by a microstrip line, a circular polarization design using such a modified antenna has been found to be possible. A circularly polarized microstripline-fed annular-ring microstrip antenna with a sectorial cut has been successfully implemented. Details of the experimental results will be illustrated in the symposium.

Scattering from Conformal Microstrip Antennas

Yuan-Tung Cheng*, Hong-Twu Chen, and Tsurng-Jeng Chang

Department of Electrical Engineering,
Chinese Military Academy
Fong-Shan, Taiwan 830, R.O.C.

Due to the major advantage of the microstrip patch antenna to be flushed-mounted on curved surfaces, the scattering characteristics of the conformal microstrip antenna are worthy of investigations. In this paper, the radar cross section (RCS) of conformal microstrip antennas, such as a rectangular microstrip patch antenna mounted on a grounded circular-cylindrical substrate and a circular microstrip patch antenna mounted on a grounded spherical substrate, is studied. The feeding of the patch antenna is neglected in the theoretical formulation for simplicity.

The theoretical treatment is based on the full-wave formulation, and the numerical calculations are performed using Galerkin's moment method. It is seen that, as shown in figures, the conformal microstrip antennas have a higher RCS resonant response than the planar microstrip patch antenna, and the curvature of the conformal microstrip antennas also causes a shift of the RCS resonant peak to higher frequencies.

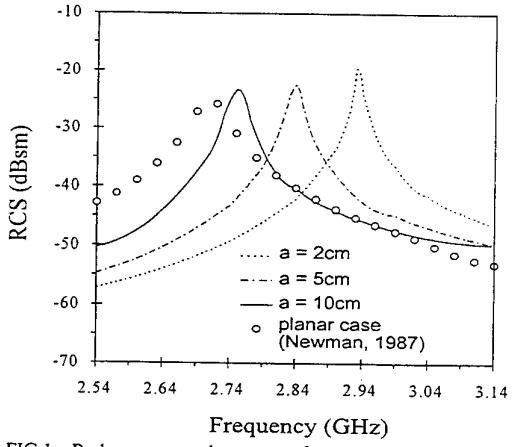


FIG.1. Radar cross section versus frequency for a cylindrical-rectangular with different curvature

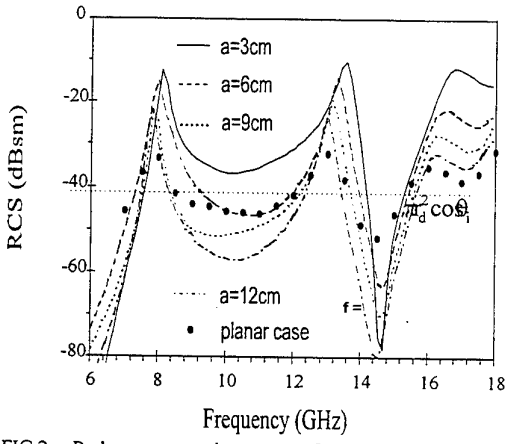


FIG.2. Radar cross section versus frequency for a spherical-circular microstrip antenna.

Since many substrate materials commonly used for microstrip antennas exhibit uniaxial anisotropy, we have investigated the effects of uniaxial substrate's anisotropy and thickness on the scattering behavior. For the substrate's uniaxial anisotropy, it is found that the uniaxial anisotropy causes a shift of the resonant peak of the RCS values. The negative uniaxial anisotropy shifts the resonant RCS peak to lower frequencies and the positive uniaxial anisotropy moves the resonant peak to higher frequencies. For the substrate's thickness, it is also found that the frequency locations of RCS resonant peaks move to lower frequencies with the increasing of the substrate's thickness. The RCS resonant peak value is, however, found to be insensitive to the substrate thickness and the uniaxial anisotropy in the substrate. The extensive numerical results will be presented in the symposium.

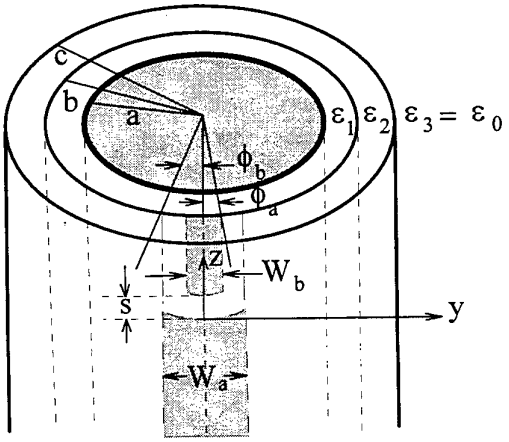
ANALYSIS OF CYLINDRICAL MICROSTRIP DISCONTINUITIES

Ching-Her Lee and Wei-Chen Hsu
Department of Industrial Education
National Changhua University of Education
Changhua, 500, Taiwan, R. O. C.

Microstrip gap and step discontinuities are useful in the design of coupled filters and impedance transformers. In the past, planner microstrip discontinuities have been well worked out by D. M. Pozar [IEEE/MTT, vol. 33, pp. 1036-1042, 1985], N. G. Alexopoulos [IEEE/MTT, vol. 33, pp. 1029-1035, 1985], and other researchers. The corresponding problems of cylindrical microstrip lines have just been gaining attentions recently. The geometries of microstrip open-end and gap discontinuities with uniform line width have been analyzed by H. M. Chen and K. L. Wong [Microwave Opt. Technol. Lett., vol. 9, pp. 260-263, 1995]

In this paper, we present the analysis and modeling of cylindrical microstrip discontinuity in a substrate-superstrate structure (as depicted in the figure) using the numerical solution of an integral equation. For numerical solution, a combination of entire-domain sinusoidal basis functions, which represents the fundamental traveling mode incident, reflected and transmitted near the discontinuity, and piecewise sinusoidal basis functions, which represents the higher order modes excited due to the discontinuity, is used to represent the currents on the microstrip lines. Moment-method is used to solve the unknown frequency-dependent reflection and transmission coefficients and the expansion coefficients of the PWS functions. The effects due to the superstrate depth, line width, and the gap spacing on the characteristics of cylindrical microstrip gap discontinuities are analyzed.

Some example structures are computed in this work. The dimension parameters used are as follows: the substrate thickness h, the thickness of superstrate t, and the microstrip lines width W_a, W_b, are all about 0.5 to 1.5 mm; the ratio of the radius of the conducting cylinder to that of the substrate, a/b, varies from 0.8 to 0.95. The dielectric constants used for substrate is 9.6, and that for superstrate is 2.32 or 5.0. Details of the calculated results will be presented in the symposium.

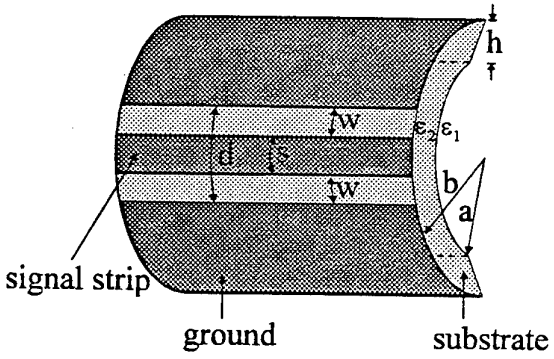


COPLANAR WAVEGUIDES ON A CYLINDRICAL SURFACE

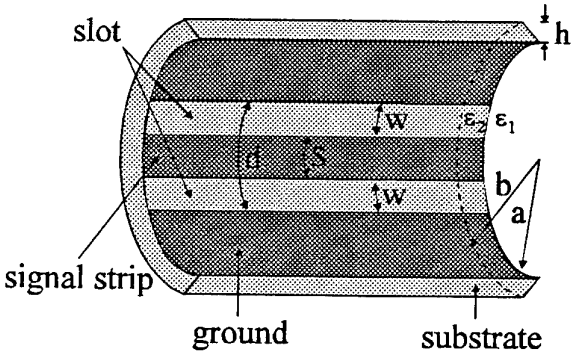
*Hsin-Cheng Su and Kin-Lu Wong
Department of Electrical Engineering
National Sun Yat-Sen University
Kaohsiung, Taiwan 804, R.O.C.

Although coplanar waveguides (CPW's) on a planar structure have been widely studied, the CPW's mounted on nonplanar surfaces have received relatively less attention. In this article we report the characteristics of the CPW mounted on a cylindrical surface (see figures below). Both cases of the outside and inside cylindrical CPW's are studied, which can find applications in the design of conformal microstrip circuits or in feeding cylindrical printed antennas. In the study a full-wave approach is applied, and exact Green's functions for the cylindrical structure are derived and used in a Galerkin's moment-method calculation [H. C. Su and K. L. Wong, *Microwave Opt. Technol. Lett.*, vol. 12, June 5, 1996]. And the dynamic effective relative permittivity and characteristic impedance are formulated and calculated. Theoretical results are found to agree with the experimental measurements.

In this study only the odd-mode propagation of the CPW is considered. In the experiment the ground planes on both sides of the signal strip are made in contact and the excitation of the parasitic mode (even mode) is suppressed. From the calculated results and measured data, it is found that the curvature effect on the effective relative permittivity is much greater for the inside cylindrical CPW case. And the effective relative permittivity of the outside cylindrical CPW is relatively insensitive to the curvature variation. This behavior is similar to the observations of outside and inside cylindrical microstrip lines [R. B. Tsai and K. L. Wong, IEEE/MTT, vol. 43, pp. 1607-1610, 1995]. Characteristic impedances for the cylindrical CPW with various curvatures are also studied, and significant curvature effects are observed. Details of the theoretical formulation and the calculated and measured results will be presented in the symposium.



Outside Cylindrical CPW



Inside Cylindrical CPW

SOME RESULTS ON SLOT-COUPLED DOUBLE-SIDED MICROSTRIP LINES

*Jui-Han Lu and Kin-Lu Wong
Department of Electrical Engineering
National Sun Yat-Sen University
Kaohsiung, Taiwan 804, R.O.C.

Slot-coupled double-sided (SCDS) microstrip lines have recently found applications in the design of interconnects in multilayer microwave and millimeter-wave integrated circuits. The structure of SCDS parallel microstrip lines with a narrow rectangular coupling slot in the common ground plane has also been studied by many authors. To provide more flexibility for the applications of SCDS microstrip lines, we present in this article several related novel structures, including the SCDS microstrip lines using end-loaded coupling slots (H-shape or dumbbell slots; see inset in Fig. 1), the SCDS perpendicular microstrip lines with an arbitrarily inclined narrow rectangular coupling slot (see inset in Fig. 2), and the SCDS cylindrical microstrip lines, etc.

For various structures we apply the reciprocity theorem and use the exact Green's functions in a moment-method calculation for the unknown electric field in the coupling slot. The S parameters are formulated and calculated, and experiments are also conducted to compared with the theoretical results. Fig. 1 shows the effects of the end-loaded coupling slots on the coupling coefficient (S_{31}). Results indicate that the end-loaded slots increase the coupling between the SCDS microstrip lines. For the SCDS perpendicular microstrip lines good agreement between the theoretical results and measured data has been obtained (Fig. 2). It is also found that, when the coupling slot is at resonance, there exists a maximum coupling between the feed and coupled lines. In this case the coupling slot also acts as a radiator, and the radiated power loss is estimated to be about 10%. More theoretical and measured results such as the curvature effects on the characteristics of SCDS microstrip lines will be discussed in the presentation.

Fig. 1

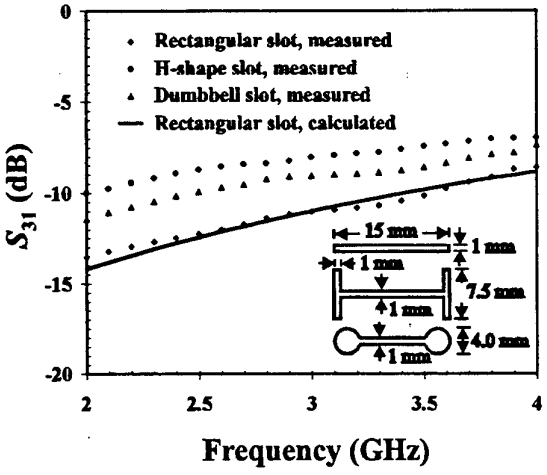
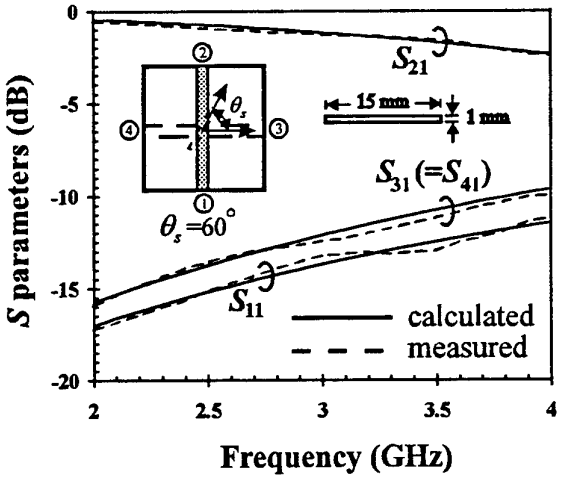


Fig. 2



PRINTED ANTENNAS FOR A PORTABLE HANDSET

*Shyh-Yeong Ke and Chewn-Pu Jou
Computer and Communication Research Lab., Industrial Technol. Research Institute
Hsinchu, Taiwan 310, R. O. C.

This paper describes novel designs of printed antennas applicable for portable communication transceivers. The antenna elements are etched on the printed circuit board and excited by a microstrip-line feed. Two printed antennas, respectively, referred to "non-coplanar resonant element printed circuit board antenna" and "top-loaded triangular printed antenna", have been exploited by using an empirical designing procedure. We will present the input impedance and the radiation pattern characteristics of such two antennas. The effects of the shielding metal case on the antenna performance are also discussed.

The current trend in miniaturizing portable communication equipments, such as cellular phones, has prompted engineers to study the design of small antennas and built-in antennas. On the other hand, a wideband antenna is also necessary for a multi-channel telephone system and can help cope with the effect of operator proximity. Moreover, the antenna gain (efficiency) should be as high as possible for the receiver sensitivity. Several antennas such as whip antennas, sleeve antennas, helical antennas, and inverted-L antennas are commonly used for protable telephones. However, the reliabilities of wire antennas are dependent on the manual assembly. And wire antennas mounted outside the portable equipments will abate the user's portability.

In order to meet the above noted requirements and reduce the manufacturing cost, we attempt to investigate printed antennas for a portable handset. The first one is a non-coplanar resonant element printed circuit board antenna that comprises an F-shaped strip and an L-shaped strip printed on the two sides of the printed circuit board. It has a -1 dBi antenna gain and its impedance bandwidth is 23 % (VSWR ≤ 2, $Z_o = 50\ \Omega$). The other designed antenna is top-loaded triangular printed antenna, which has a 0.5 dBi antenna gain and 6 % bandwidth. Both the printed antennas show a fairly uniform radiation pattern in the horizontal plane. Besides, the antennas provides both horizontally and vertically polarized radiations. Without additional diversity elements, such a configuration could improve the reception problem in urban enviroment. The printed antennas integrated with RF circuit module are also considered in our study. Two metal covers mounted on the two sides of the printed circuit board are used to be an electromagnetic shielding between the antenna and the inside RF circuit. The measured results show that shielding metal cases have a significant effect on the antenna impedance and the radiation pattern.

Characteristics of a Rectangular Patch Antenna Using Foam as Substrate

Jeen-Sheen Row
Antenna Section, RF-Link Inc.
Hsinchu, Taiwan, R.O.C.

Narrow bandwidth has been one of the most serious limitations of a microstrip patch antenna. Many elements with enhanced bandwidth have already been investigated; e.g., electrically thick elements, stacked multipatch, mutilayer elements, multiple-resonator elements. All these wide band elements' increased impedance bandwidth is also paid for their high cost and complex structure. In this paper, a rectangular microstrip patch antenna using foam as substrate is experimentally investigated in order to increase the bandwidth. The conventional three types of antennas fabricated on different material (Teflon, Duroid, FR4) are manufactured to compare with the performance of the antenna using foam as substrate, emphasis on bandwidth and gain especially. Experimental results show that the bandwidth of the antenna with foam as substrate is 1.5 times than the conventional antennas, while the gain is also increased 2-5 dB. The cost of this antenna is also much less than the conventional antennas.

The bandwidth of the antenna with foam as substrate depends on the thickness of the foam and the aspect ratio of the patch. The effects of the thickness and aspect ratio on the bandwidth and gain of the antenna are discussed. The CP characteristics of the square patch with trimmed corner fabricated on foam substrate are also presented. It is found that the bandwidth of the 3-dB axial ratio is enhanced when the foam is used to replace the conventional material.

Finally, the bandwidth and gain of microstrip patch arrays of 4, 8, 16, 32 elements with foam as substrate are measured. The experimental data indicate that the bandwidth is considerably increased. However, the antenna loss due to the coplanar corporate feed network is not negligible when the antenna arrays use foam as substrate.

Progress in Electromagnetics Research Symposium, PIERS 1997 ISBN 962-442-097-1

SESSION 6P17

Monday, January 6, PM 1330-1730, Lecture Theatre 17, City University of Hong Kong

Electromagnetic Compatibility

Organizer: S W Leung

Chairperson: S W Leung, City University of Hong Kong
Co-Chairperson: A C Marvin, University of York

13:30	***An Overview of EMC Development in Hong Kong*** S W Leung, Y M Siu, James W Minett, H S Liu City University of Hong Kong	19
13:50	***Theoretical Investigation on Changing Matching Frequency Characteristics with a Punched Ferrite EM-Absorber*** Youji Kotsuka, Atsushi Maeda Tokai University	20
14:10	***Multipoint Connections of Wires to Surfaces in the Combination of GTD and MOM*** *Holger Wagner, **Karl-Heinz Gonschorek *TU Hamburg-Harburg, **TU Dresden	21
14:30	***Time Domain Magnetic Field Measurement near Printed Circuit Boards*** Hideki Sasaki, Takashi Harada NEC Corporation	22
14:50	***Screening of Electromagnetic Fields by an Ellipsoid Shaped Shield with Constant Wall Thickness*** *E Baum, **G Mrozynski *School of Engineering, Fulda, **University of Paderborn	23
15:10	**Break**	
15:30	***The Effects of Cross-Polarisation Terms in the Measurement of Radiated Emissions on Open-Area Test Sites and in GTEM Cells*** A C Marvin, L Turnbull, A Nothofer University of York	24
15:50	***Solution for the EMC-Immunity Measuring Problem for Interactive and Non-Interactive Satellite Earth Stations*** Uwe Kartmann Bundesamt für Zulassungen in der Telekommunikation	25
16:10	***EMC Re-Design Technique*** C N Wong, H W Ma City University of Hong Kong	26
16:30	***Progress Research in Microwave EMC*** Sheng-chuan Zhu Peking University	27
16:50	***The Use of the Sequent Diffraction in EMC Problems*** A S Batoroev, D B Dugarzhapova, V E Munkoev Buryat Institute of Natural Sciences	28
17:10	***Development of 0° and 180° Hybrid Junction in the Test System of EMC*** Zhong Wang, Jihong Zhang, Jiasheng Zhao, Shunji Huang University of Electronics Science and Technology of China	29

An Overview of EMC Development in Hong Kong

S.W. Leung, Y.M. Siu, James W. Minett & H. S. Liu
Department of Electronic Engineering
City University of Hong Kong
Kowloon, Hong Kong

Abstract

Hong Kong is a focal point for economic activity throughout the Asia Pacific Rim region, with a per-capita gross domestic product of HK$143,236. Electronics is the second largest industry in Hong Kong with more than 2,000 electronics products designed here each year. To remain competitive in world markets, the electronics industry has started to focus on designing high-quality, reliable products. In particular, Hong Kong's relationship with China has changed dramatically. The Hong Kong electronics industry now concentrates on product design and engineering services, while higher value-added products are manufactured in both Hong Kong and China. Cheaper OEM products which were formerly made in Hong Kong are now typically manufactured in China.

One of the most significant challenges for the Hong Kong electronics industry is to align with the world-wide effort to purify the electromagnetic environment. Many countries stipulate stringent EMC regulations with which each electronics product must comply. In view of these regulations, local manufacturers have become concerned about the possible impact on their products' viability. Many manufacturers consider EMC compliance just prior to production rather than during the initial design stage. This reflects a general lack of awareness of efficient methods to achieve EMC compliance. In addition, most manufacturers rely on guidance from the small number (6–7) of EMC test houses currently set up in Hong Kong. Demand far exceeds the services these test houses provide. Again, the supply of these training courses does not meet the industry's demand. There is now much research on EMC being carried out in Hong Kong, both in the academic sector and the commercial sector.

The design of EMC compliant products is a skill learned only through hands-on experience. The City University of Hong Kong currently offers undergraduate students modules in product design, emphasising good EMC techniques. Practical workshops and laboratory sessions are also offered to professional engineers. With more courses such as these, the awareness of EMC issues in Hong Kong will continue to improve.

Theoretical Investigation on Changing Matching Frequency Characteristics with a Punched Ferrite EM-Absorber

Youji Kotsuka, Atsushi Maeda
Faculty of Engineering
Tokai University

1117, Kitakaname, Hiratsuka City 259-12, Japan

A simple method is proposed for widely changing the matching frequency characteristics of an EM-wave absorber using a punched ferrite material. A conventional EM-wave ferrite absorber has its own matching frequency, which depends upon ferrite thickness and material constant. That is, the ferrite EM-wave absorber has only one matching frequency, which is determined by its proper thickness. However, the matching frequency characteristics we want can be easily adjusted by punching holes in the ferrite material.

In this paper, to find an optimum method of widely changing the matching frequency by means of a punched ferrite absorber, a theoretical investigation based upon the Spatial Network Method was performed. It was found that the theoretical results can closely represent the experimental matching characteristics of a punched ferrite absorber. Accordingly, on the basis of the Spatial Network Method, the matching characteristics of various shapes of punched holes were also simulated and the optimum shape was investigated.

In the present study, rubber ferrite material is used as the punched ferrite absorber. A material with the matching frequency of 2.2 GHz is used as an example. In this ferrite, if a small rectangle with dimensions of 8 (width) x 7 (height) mm is used, the matching frequency can be changed to 2.5 GHz from its original matching frequency of 2.2 GHz in its center frequency. Further, in the case of a small cross-shaped hole with maximum lengths of vertical and horizontal axes of 2 mm, 1 mm in width, the matching frequency band is improved widely from 2.3 GHz to 3.8 GHz.

Consequently, from the Spatial Network Method's analysis, it is clarified that it becomes possible to change the matching frequency of a ferrite EM-wave absorber using a simple method of punching holes without changing the material constant.

MULTIPOINT CONNECTIONS OF WIRES TO SURFACES IN THE COMBINATION OF GTD AND MOM

Holger Wagner
TU Hamburg-Harburg, Germany
h.wagner@tu-harburg.d400.de

Karl-Heinz Gonschorek
TU Dresden, Germany
gonscho@eeiwzb.et.tu-dresden.de

Building models and measuring fields was the only way to estimate the influence of electromagnetic fields on electrical equipment in the past. Because of numerical field calculation methods this is no longer necessary in most cases.

The Method of Moments (MoM) is a very powerful tool for the calculation of electromagnetic fields in the high frequency region (MHz). Its use is limited by the size of the coupling equations forming the coupling impedance matrix and the time to solve these equations. Both restrictions depend on the relationship of the size of the investigated bodies to the wave length (λ). As a function of the frequency (f) the needed memory of this coupling matrix is proportional to $(2\,f^2)^2 = 4\,f^4$. The calculation time to solve these equations increases by $8\,f^6$ using the Gaussian algorithm.

Another method to calculate electromagnetic fields is the Geometrical Theory of Diffraction (GTD) and its extended version, the Uniform Geometrical Theory of Diffraction (UTD). These methods are asymptotic procedures to calculate electromagnetic fields in very high frequency regions (GHz). Here, the dimensions of the bodies have to be large in terms of the wavelength. Configurations of smaller bodies cannot be examined. The distance between the field source and the bodies has to be greater than approximately $\lambda/2$. The influence of the bodies on the field sources is neglected.

By combining these two methods and using their advantages it is possible to avoid their restrictions. This combination is called Hybrid Method (HM). With the HM it is possible to calculate arrangements containing both electrically small (for instance linear antennas) and electrically large bodies (for instance platforms like ships or airplanes).

But up to now antennas cannot be connected to conducting surfaces in this HM.

The main idea to make this connection possible is to fill the coupling impedance matrix, which describes the dependency of each segment to another, in a way that the single elements are calculated by the best method: MoM or HM:

- Using HM if the segments are neither neighbours nor too close to the body. With the use of a special description of the sources (Ekelman point sources) the GTD distance of $\lambda/2$ can be limited down to $\lambda/10$ in the HM calculation.
- Using MoM if the segments are close to the body. In this case the body can be approximated as an infinitely large conducting plane.
- Using MoM for the direct coupling factor of two neighboured segments because the distance between them is too small for calculation by GTD. The indirect coupling factor (i.e. influence of the body) can be calculated by GTD. So the curvature of the body is considered without its subdivision in patches (normally necessary for MoM).

Vivid, this technique can be described as to cut the antenna into two parts (part 1 and part 2) in a way that only antenna part 2 has a connection to the electrically large body. A coupling matrix only for the linear antenna is set up by HM and MoM:

First step: The matrix part of antenna part 1 and the body is calculated by HM. The distance of antenna part 1 to the large body must fulfil the requirements of HM.

Second step: As long as antenna part 2 is very short the curvature of the body can be neglected. An infinitely large conducting plane can be used instead. This arrangement is calculated by MoM very easily. The shorter antenna part 2 the smaller the error of the approximation.

Third step: The coupling between the two antenna parts has to be considered. This can also be done by MoM or in a further improvement by MoM and HM.

After these three steps the calculated matrix parts are assembled to a complete matrix. This system of equations can be solved by the Gaussian algorithm. After that all currents on the antenna are known. The field strength in any observation point P can be calculated as a sum of

- the direct electromagnetic rays of the current on the linear antenna and
- the additional electromagnetic rays of the GTD processes (if they exist):

$$\underline{\vec{E}}(P) = \underline{\vec{E}}^{\mathrm{MoM}}_{\mathrm{dir}}(P) + \sum \underline{\vec{E}}^{\mathrm{GTD}}_{\mathrm{refl}}(P) + \sum \underline{\vec{E}}^{\mathrm{GTD}}_{\mathrm{edge}}(P) + \sum \underline{\vec{E}}^{\mathrm{GTD}}_{\mathrm{creep}}(P) \quad .$$

With this procedure all influences of the arrangement are considered. By extending this procedure it is not only possible to treat linear antenna structures but also multipoint connections.

Time Domain Magnetic Field Measurement near Printed Circuit Boards

Hideki Sasaki and Takashi Harada

NEC Corporation
Kanagawa, Japan

Time domain magnetic field measurement near printed circuit boards (PCBs) is described. Such magnetic field measurement near PCBs is effective in analyzing the sources responsible for radiated EMI. Since the waveforms of magnetic fields depend on the circuit active condition, they provide very detailed information on EMI sources.

We measured the waveforms of magnetic fields with a small loop probe, a high-bandwidth digitizing oscilloscope, and a personal computer to capture and to process waveforms of emergent voltage from the oscilloscope input port. The waveform of magnetic field h(t) is obtained from the oscilloscope input voltage waveform v(t) as

$$h(t) = f^{-1}\,[\,F(\omega) \cdot f\{v(t)\}\,]$$

where $F(\omega)$ is a loop probe calibrating coefficient, and $f\{\ \}$ and $f^{-1}\,[\ ]$ denote the Fourier and inverse Fourier transform, respectively. The loop probe calibrating coefficients are determined by applying a microstrip line as the standard magnetic field source.

The waveforms of a magnetic field near a PCB designed with a four layer signal-ground-power-signal construction were measured. The PCB's upper signal layer containes a quartz crystal oscillator IC, a 74AS04 type driver IC, decoupling capacitors, around 10 cm signal traces, and load resisters. The waveform of the component orthogonal to the signal traces and parallel to the surface of the PCB at the point directly above the signal traces closely reflects the characteristics of the EMI radiated from this PCB. The waveform indicates that, apart from the magnetic field which is radiated from the signal traces, a magnetic field causing EMI to radiate from the PCB is generated when the output level of the drive IC is high, i.e. when the driver IC draws a current from a capacitor consisting of the ground layer and the power layer. We conclude from this result that the source of the EMI radiated from this PCB is in the power system.

Progress in Electromagnetics Research Symposium, PIERS 1997 ISBN 962-442-097-1

Screening of Electromagnetic Fields by an Ellipsoid Shaped Shield with Constant Wall Thickness

*E. Baum,*Department of Electrical Engineering, School of Engineering, Fulda, Germany
Tel./Fax: +49-661-9640-558/559, E-mail: baum@et.fh-fulda.de
*G. Mrozynski,*Institute of Electromagnetic Theory, University of Paderborn, Germany
Tel./Fax: +49-5251-60-3015/3524, E-mail: mrozynski@tethp1.uni-paderborn.de

The inner and outer surfaces of an prolate ellipsoidal shield of finite wall thickness can only be described in spheroidal coordinates if the ratio of the major axis of the ellipsoid is nearly equal to one, i.e. the ellipsoid is almost degenerated to a sphere.

For other ratios of the major axis and constant wall thickness an approximation is introduced:

The electric and the magnetic field strengths along a coordinate directed normal to the (inner or outer) surface of the shield can be approximated by a step function if the shield is thin. Thus the shield can be replaced by electric and magnetic current sheets flowing on an ellipsoidal surface positioned between the inner and outer surfaces of the shield. The intensity of the electric and magnetic current sheets depends on the material parameters of the shield, of the local wall thickness and of the operating frequency.

As an example the exciting field of a magnetic dipole with arbitrary position and orientation inside the shield is considered.

The total fields inside and outside the shield are represented with the help of associated Legendre functions.

To check the validity of the calculations the limiting case of a sphere was considered; for this case shielding factors are reported in literature. A good agreement of the computed shielding factors and the ones taken from literature could be observed for this special geometry.

If the field is excited by current flowing in a loop of arbitrary shape the total field can be computed by integrating the elementary contributions of dipoles in a surface bounded by the contour of the current loop.

'The effects of cross-polarisation terms in the measurement of radiated emissions on Open-Area Test Sites and in GTEM Cells'

Prof A.C. Marvin, Mr L. Turnbull & Miss A Nothofer.

University of York
Department of Electronics
UK

tel +44 1904 432342
fax +44 1904 433224

Abstract

The measurement of radiated emissions from equipment-under-test (EUT) is well established for open-area test sites (OATS) and more recently for GTEM Cells. Recent studies have indicated that there still remain problems with these measurements, particularly in terms of repeatability between different test sites in the case of OATS and in correlating the measurements made in GTEM Cells with those made on OATS.

We propose that one of the reasons for the discrepancies is that the test environment are calibrated with techniques that utilise emitters with well defined polarisation properties, for example, half-wave dipoles are used to measure site attenuation on OATS. The EUT's measured are not so well defined and, in general, can be considered to be ensembles of radiating dipoles (electric and magnetic) oriented in three orthogonal directions. Thus a typical EUT will radiate a vertically polarised wave, a horizontally polarised wave (as measured on the OATS) and also a wave we define as longitudinally polarised because its source dipole is aligned along the axis of the OATS. This latter wave couples to the vertically polarised receiving antenna when the EUT and the antenna are at different heights and also through the image of the EUT in the groundplane when they are at the same height. In general, the receiving antenna will receive energy from the cross-polarised waves as well as its co-polarised wave.
This phenomenon is not accounted for in site assessment procedures. Our paper presents an analysis of this effect and describe a technique for assessing the cross-polarisation properties of an OATS which enables a judgement of the suitability of the site to be made. We also demonstrate how estimates of the measurement uncertainties associated with the polarisation problems can be obtained.

Our work has also been extended to include similar effects observed in GTEM Cell measurements where the EUT has to be rotated to a number of orientations in the cell to complete the measurement. We show how a similar analysis can be utilised to estimate the uncertainties in the GTEM to OATS correlation.

Solution for the EMC-Immunity Measuring Problem for Interactive and Non-Interactive Satellite Earth Stations

Dipl.-Ing. Uwe Kartmann
Bundesamt für Zulassungen in der Telekommunikation
Postfach 10 04 43
66004 Saarbrücken
Germany
Tel.: +49 681 598-1300
Fax: +49 681 598-1613

In Germany satellite earth stations must comply to the horizontal EMC-Directive 89/336/EEC and the vertical Telecommunication Terminals Equipment Directive 91/263/EEC together with the Satellite Earth Station Directive 93/97/EEC. According to these directives, a type examination for receive/transmit satellite earth stations by a Notified Body according to the EMC-Directive Article 10.2 is not necessary. Nevertheless the manufacturer, his authorised representative within the European Union or the person who places this kind of equipment on the market has to draw up a written Declaration of Conformity. This procedure corresponds to that for receive-only satellite earth stations. An EMC-Declaration of Conformity normally grounds in European harmonised standards published in the Official Journal of the European Union. A number of telecom standards are being developed by the European Telecommunications Institute ETSI but non has yet been harmonised to the EMC-Directive. Therefore for satellite earth stations equipment the consultation of a Competent Body according to the EMC-Directive will be necessary. This body can determine the way to the required declaration. In general tests according to related harmonised standards, standards or draft standards will be proposed. Satellite earth stations for example, could be tested against the ETSI STC RES 09 draft prETS 300 673 „Electromagnetic Compatibility (EMC) standard for 4/6 GHz and 11/12/14 GHz Very Small Aperture Terminal (VSAT) equipment and 11/12/13/14 GHz Satellite News Gathering (SNG) Transportable Earth Station (TES) equipment", a draft Standard. The latter will soon be published in the Official Journal of the European Union.

The main question for an accredited testhouse like the Bundesamt für Zulassungen in der Telekommunikation is how to realise this standard technically. The required emission tests have been unproblematic because they are done according to EN 55022, the European Standard which in the past had been part of type approval. The realisation of the test configuration for each immunity phenomenon (RF electromagnetic field, fast transients, voltage dips and interruptions etc.) is technically practicable. The main problem is how to activate and to operate the equipment during the test and the monitoring during the immunity influence. In this matter the standard requires that the manufacturer arrange the conditions to put the EUT in its operating modes. The standard does not tell how this can be done respectively whether it can be done at all. This problem shall be analysed in my presentation. In a first step, a solution for non-interactive satellite earth stations, i.g. a SNG satellite earth station, will be presented. Test performance, putting into operation, radiation and monitoring will be discussed. In a second step interactive systems will be examined. In this case an external transmitting signal, i.g. from a hub-station, is required by the EUT. The way this can be realised will be presented for meshed, point to point and star networks. In the latter case the EUT must have contact to a hub-station via satellite (or a hub simulator), a real problem for the equipment under test which is placed in an anechoic chamber. For this case different approaches to solutions will be presented and discussed.

EMC Re-Design

Wong Chak Nam
Department of Electronic Engineering,
City University of Hong Kong,
Tat Chi Avenue, Kowloon Tong,
Kowloon, Hong Kong.
Tel : (852)2784-4153

Ma Hon Wah
Department of Electronic Engineering,
City University of Hong Kong,
Tat Chi Avenue, Kowloon Tong,
Kowloon, Hong Kong.
Tel : (852)2784-4153

ABSTRACT

All electrical and electronic products to be sold in the European market must be so constructed to comply with EMC regulations and carry a CE mark since 1st January 1996. It is obviously better to anticipate EMC problems at the start of development. Unfortunately, there were many products has already designed in traditional way, only later doing any redesign necessary to meet EMC requirement.

This paper is going to provide the direction for EMC re-design and modification. Two main aspects to perform satisfactorily EMC and EM emission (EME) and EM susceptibility (EMS). The basic ideal for EMC re-design is to identify the noise source group and victim group. The noise propagation path through conductor and radio wave could be suppressed by different method such as inserting EMI suppresser, shielding and screening etc.

In high speed digital circuit, almost all noise generated form ICs in digital equipment was caused by high harmonic waves contained in digital signals. The higher speed operation would be increase the noise and expansion in upper limit of noise frequency range. Two type of EMI filters could be used in signal and power line for high harmonic noise suppression which were noise limiter type filter and noise by-pass type filter. The common mode noise suppression products were used to suppress noise current and by-pass noise current to ground.

The education training product "POWER PAD" had been EMC re-designed successfully by using about method and would be shown in the paper.

PROGRESS RESEARCH IN MICROWAVE EMC

Sheng-chuan Zhu
Department of Physics, Peking University, Beijing 100871, China

In the standard documents of Electromagnetic Compatibility(EMC), the relative frequency region is very broad, it may from ELF to mm-wave (f =10Hz - 100GHz). As we know, the frequency region of microwave is 30MHz - 30THZ. There is a overlapping range with 30MHz - 100GHz. Owing to the characteristics and impordance of microwave, the EMC problems in microwave band attract the attention of many scholars in the world. The microwave is applied broadly in the systems of radar, navigation, communication, control and command, so that the microwave EMC(MEMC) problems are appeared naturally[1][2].

Some directions of interest to research[3,4,5,6]:

EMC in radar and communication systems -- The MEMC problems come from radar system, nevigation system, airborne system, space flight measuring ship and ground settite station. Whether military affairs or production fields, it is an impordant project to research the EMC of all sorts of EM system and equipment in the EM enviroment.

Elecromagnetic pulse (EMP) and nuclear electromagnetic pulse (NEMP)- - The transient electromagnetic field must be pay close attention to the MEMC research. EMP come from the natural phenomena (thunder & lighting). The manufactures, productions and experiments of nuclear equipments are in object existance.

The hardware construction of EMC/EMI measurement -- The experimental research and theoretical analysis of TEMcell series(parallel plate TEM cell, TEM transmission cell and GHz TEM cell) are developed. By the point of MEMC, GHZ TEM cell has the larger meaning.

Basical materials and theoretical research -- People pay attention to the research on basical materials concerned with EMC/EMI technique . The proformances of the shield materals, the microwave absorption materials and high T_c superconductor have been studied by experiment and theory. In the stealthy technique, the exploration of basical theory must be strengthened, for example, to realize stealthy in a more broaden frequency region.

To sum up, we can understand the region, content, significiance method and scope of MEMC. It is very complicated with the related science technique, and is interweaved with other banches of learning. MEMC will develop as a brimmig with vigour banch of subject.

[1] W. G. Lin, "Encyclopedic Knowledge", No. 3, p.p. 35-37, 1991.
[2] Z. X. Huang, "Wuli", No. 4, p.p. 244-247, 1991.
[3] " Proceedings of 1st Natioal Symposium of Microwave EMC", Qingdao, China,1992.
[4] " Proceedings of 2rd Natioal Symposium of Microwave EMC", Xiamen, China,1994.
[5] IEEE Trans. MTT, Vol. 43, No. 1-12, 1995.
[6] IEEE Trans. EMC, Vol. 37, No. 1-4, 1995.

The use of the sequent diffraction in EMC problems

A.S. Batoroev, D.B. Dugarzhapova, V.E. Munkoev

Buryat Institute of Natural Sciences
Siberian Department of Russian Academy of Sciences
6 Sakhyanova st., Ulan-Ude, 670042, Russia.
Phone: +7(30122) 31254, Fax: +7(30122) 2841, E-mail:root@bien.buriatia.su

The paper presents the possibilities of using the sequent diffraction peculiarities at two obstacles with the view of two important practically applied problems.

The first problem considers the possibilities of additional field attenuation in case of diffraction at two sequent semiplanes using the system of longitudinal opaque strips in one of the semiplanes. This problem is of great interest for radiosystem isolation operating in the complicated relief areas, when the model of two prevailing peaks serves as an approximating model. We managed to adapt the earlier elaborated hodograph method [1] to define the optimum system parameters of opaque strips providing the maximum field attenuation. In case of the sequent diffraction at two semiplanes the use of the above-mentioned method is reduced to the solution of the equation such as :

$$\Phi = \sum_{j=1}^{2k+1} (-1)^{j-1} F(v_1, v_{2j}, \alpha) = 0 , \qquad (1)$$

where Φ is a diffraction attenuation factor, which serve as a purpose function; v_{2j} – optimum parameters of the strip system, necessary to be defined, $F(v_1, v_{2j}, \alpha)$ is some generalised function, depending on the geometrical parameters of the path and the parameters of horizontal strip system. As a result of the solution of the equation using the above-mentioned method optimum parameters of the system have been found in general, and space and frequency dependances characterizing the picture of the field distribution near the minimum field have been calculated.

In the second problem the areas of low field levels in case of diffraction at two sequent strips are found by means of investigation of space and frequency characteristics. This problem can be used for isolation of radiosystems operating in direct visibility, as well as for attenuation of interfering signals reflecting from the earth surfase. Using analitical methods in the given problem the expression for diffraction field is reduced to the known solution of the sequent diffraction at two semiplanes [2] such as :

$$\Phi = 1 - [F(v_{11}) - F(v_{12}) + F(v_{21}) - F(v_{22})] + [F(v_{11},v_{21}) - F(v_{11},v_{22}) - F(v_{12},v_{21}) + F(v_{12},v_{22})], \qquad (2)$$

where Φ is the diffraction attenuation factor at two strips, $F(v_{jk})$ and $F(v_{jk},v_{kj})$ are attenuation factors in case of the diffraction in one semiplane and in two sequent semiplanes correspondingly.

Using the given solution (2) space and frequency field characteristics have been obtained, analizing which areas of rather low field levels have been revealed, that can be used in above-mentioned problems for providing EMC conditions of radiosystems.

References

1. Batoroev A.S., Maltuguev A.A., Dugarzhapova D.B. Slot-type diffraction screens for interfering field suppression. Summuries of the Eighth International Wroclaw Symposium on Electromagnetic compatibility, part II, 1986, pp114-115.

2.Millington G., Hewitt R., Immirsi F.S. Double khife edge diffraction in field-strength predictions . – Proc. IEE, Monograph № 507 E, March, 1962.-11 p.

DEVELOPMENT OF 0°AND 180° HYBRID JUNCTION IN THE TEST SYSTEM OF EMC

(Wang Zhong Zhang Jihong Zhao Jiasheng Huang Shunji)

Dr. Wang Zhong
95B1
Department of Electronic Engneering
University of Electronics science &.
Technology of China
Chengdu.Sichuan 610054
P. R. China
Tel:(028)3201140

Abstract——This paper provides a development of key device (0^0 and 180^0 Hybrid Junction) in the test system of TEM cell radiated emission. Outputs of sum and difference of two signals could be obtained with high quality magic Tee hybrid network. At last, it gives the result of hybrid junction.

SESSION 6P16

Monday, January 6, PM 1330-1650, Lecture Theatre 16, City University of Hong Kong

Computational Techniques 1

Organizer: The-Nan Chang

Chairperson: The-Nan Chang, Tatung Institute of Tech.
Co-Chairperson: Wei-Ching Chuang, National Yunlin Polytechnic Institution

13:30 ***Simulation and Measurement of the Deflected Electron Beams in a Color Cathode-Ray Tube*** 31
*D M MacGregor, **C-W Su, **P-H Kuo, **J-J Wang, **C-H Yeh, **C-F Huang
*Electrocon International, Inc.
**Chunghwa Picture Tubes, Ltd.

13:50 ***Analysis of Multislot Line by Charge-Field Integral Equation Method*** 32
The-Nan Chang
Tatung Institute of Technology

14:10 ***Novel Differential Approach for Scattering from a Laminated and Anisotropic Cylindrical Shell of Arbitrary Cross-section*** 33
Cheng-Nan Chiu, Chun Hsiung Chen
National Taiwan University

14:30 ***Analysis of the Four-Layer Optical Waveguides by Galerkin's Method*** 34
*Kun-Hua Tsai, *Wei-Yu Lee, *Kun-Yi Lee, **Wei-Ching Chuang
*Tatung Institute of Technology
**National Yunlin Polytech Institution

14:50 ***A Simple Mathematica Algorithm for Computation of Spheroidal Wave Functions and their Derivatives*** 35
L W Li, P S Kooi, T S Yeo, M S Leong, C L Quek
National University of Singapore

15:10 **Break**

15:30 ***Addition to Spectral Domain Technique to Analysis of Planar Transmission Lines*** 36
Yung-Hong Chen, The-Nan Chang
Tatung Institute of Technology

15:50 ***Analysis of EM Scattering from Microstrip Circular Patch Using Hybrid Method: A Closed Form Solution*** 37
L W Li, P S Kooi, T S Yeo, M S Leong, Y L Qiu
National University of Singapore

16:10 ***Capacitance Computation for CPW Discontinuities with Finite Metallization Thickness by Hybrid Finite Element Method*** 38
Chien-Wen Chiu, Ruey-Beei Wu
National Taiwan University

16:30 ***Design Considerations for Microstrip Antennas Excited by Coplanar Waveguides*** 39
Powen Hsu, Shih-Wen Lu
National Taiwan University

Simulation and Measurement of the Deflected Electron Beams in a Color Cathode-Ray Tube

D. M. MacGregor[§],
*C.-W. Su, P.-H. Kuo, J.-J. Wang, C.-H. Yeh, and C.-F. Huang[#]

[§] Electrocon International, Inc.
715 West Ellsworth Rd., Ann Arbor
Michigan, USA

*CRT R&D Div.
Chunghwa Picture Tubes, Ltd
80 Hsing-Shan Rd., Yangmei
Taoyuan County, TAIWAN

Abstract:

Based on a certain literature, which had developed a theory for calculating the beam's spot size on a CRT (Cathode-Ray-Tube) screen by using the measured magnetic field along the boundary of the deflection yoke (DY), this presented work is to extend a commercial package - DMEGA/GUN3D to calculate the spot size everywhere on a CRT screen when considering the excited deflecting magnetic field of a deflection yoke. DMEGA/GUN3D was originally only capable of predicting the static spot size on the center of CRT screen, but has been well employed as a practical design tool for electron gun in the CRT industry. As known, deflection yoke functions as a mean of deflecting the electron beams inside a CRT for information display on the screen, when it is mounted on the neck of a CRT.

The azimuthal component of the magnetic field of a deflection yoke is measured first along the CRT funnel boundary by a Hall-probe based 3-dimensional index moving system. And the data acquisition then is followed to compute the corresponding mode function of that magnetic field by employing a FFT procedure. Moreover, a formula is further used to compute the mode function value of the magnetic scalar potential function along boundary. Finally, by solving a finite-difference problem using numerical method, we may have the clear potential distribution inside the tube which is for the trajectory computation of the electron beams originating from the electron gun. By only feeding the boundary values of mode functions, computation steps above have been built into the commercial package DMEGA/GUN3D as an extended utility when the deflected beam spot consideration is asked for.

The simulated spot size of deflected beams of a CRT are to be represented and compared with the measured ones also.

Key words: Cathode-Ray-Tube (CRT), deflection yoke, FFT, scalar potential Finite-Difference Technique

[#] To whom for corresponding
Dr. Chi-Fang Huang
Home Address: 12F-2, #8, Hsin-Hai Rd., Sec. 1, Taipei, TAIWAN
Tel: +886-3-4786121 Ext.8465, Fax: +886-3-4858092
E-mail address: ras@wave.ee.ttit.edu.tw

Analysis of Multislot Line by Charge-Field Integral Equation Method

The Nan Chang
E.E. Department, Tatung Institute of Technology
No.40, Sec.3, Chung Shan North Road

Quasi-static analysis of various printed circuit transmission lines is widely used in the literature to model their electromagnetic behaviors at low frequency. To achieve this goal, a potential-charge density (PC) integral equation is usually derived considering unknowns to be free charges on metallizations. However, for slot-dominated structure (such as CPW), it is more efficiently characterized with the aperture electric fields than in terms of the charge density distribution. It then requires the derivation of a charge-field (QE) integral equation. Though many formulations for quasi-static analyses are based on PC method, QE method has hardly been seen in the literature.

For a layered structure, an operator L can always be found out such that $L(E)=\rho$ on the source plane. The QE integral equation appears as $M(E)=Q(x)-Qo$, where $M(E)=\int L(E)dx'$, $Q(x)$ is the accumulation charge on the source plane ; and Qo is the initial charge at some reference point. The main difficulty met with to solve this QE integral equation is that the initial charge is not known. A method that requires reformulating the equation by cancelling out the initial charge was proposed before. In this paper, a different approach that allows the initial charge be arbitrarily assigned is investigated. If the initial charge is arbitrarily assigned as Qa, one can get the "pseudo" fields Ea. It is first investigated in this paper that the true fields E can still be obtained through "pseudo" fields by extracting out error terms.

On contrast to assign known constant potential on conducting part as in conventional potential-charge density (PC) integral equation, we now assign "assumed" known accumulation charge, say Qa, on the non-conducting part. Introducing the inverse operator M^{-1} for the QE integral equation, we have $E=Ea-M^{-1}(Qa-Qo)$. Since E represent true fields, integration of E along source plane from $-\infty$ to ∞ is zero. Therefore, Qo can be extracted out after taking integrations from $-\infty$ to ∞ on both sides of the above equation.

Based on this new method, we have calculated capacitive matrix of a 4-slot CPW structure, the characteristic impedances of microstrip and suspended lines. All data are found agreeable with those in the literature. For slot-dominated structure, QE method is more suitable than PC method as less memory is required for numerical simulation. By the present method, QE method can directly be handled by assuming Qa first, then extract out Qo.

Novel Differential Approach for Scattering from a Laminated and Anisotropic Cylindrical Shell of Arbitrary Cross-section

Cheng-Nan Chiu and Chun Hsiung Chen
Department of Electrical Engineering, National Taiwan University,
Taipei, Taiwan 10617, R.O.C.
Tel: 886- 2- 3625252- 221, Fax: 886- 2- 3638247, E-mail: albert@ew.ee.ntu.edu.tw

Introduction Advanced composite materials [1] have been widely used in modern aircraft systems due to their superior mechanical properties. These materials are generally laminated, anisotropic, and lossy. The purpose of this study is to develop a rigorous theory based on differential equation approach for characterizing the electromagnetic fields in a laminated, anisotropic, and lossy cylindrical shell of arbitrary cross-section which is illuminated obliquely by a plane wave. Based on this new theory, numerical results of monostatic and bistatic echo widths are presented and discussed for boron/epoxy (B/E) fiber-reinforced laminated composite cylindrical shells of elliptical cross-section.

Formulation Consider a two-dimensional scattering problem (Fig. 1) in which a plane wave is obliquely incident upon a laminated and anisotropic cylindrical shell of arbitrary cross-section. This shell structure may be discussed by a 9-element complex permeability and permittivity tensors in which the elements may depend on ρ and ϕ. A novel theory may then be established using a differential equation approach together with a finite difference approximation. This theory can also deal with the scattering problem associated with a two-dimensional bound structure of arbitrary inhomogeneity and anisotropy.

Results and Conclusion An anisotropic bulk model for B/E elliptic cylindrical shells is proposed. By the new theory and anisotropic bulk model, the echo widths for scattering from a B/E elliptic cylindrical shell are obtained and discussed. In particular, the scattering characteristics of the shells with different size and thickness as well as the plane wave with different incident angle and polarization are investigated in detail.

References [1] C.-N. Chiu and C. H. Chen, IEEE Trans. EMC, 1, pp. 109-113, 1995.

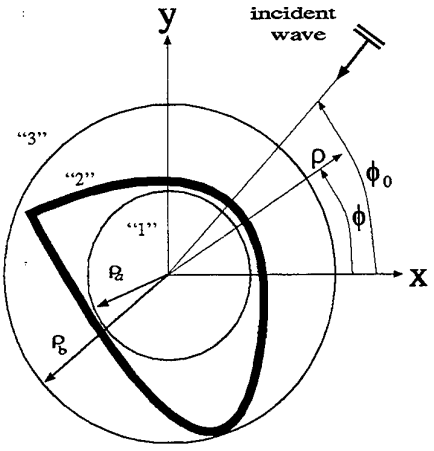


Fig. 1: Geometry of laminated and anisotropic cylindrical shell of arbitrary cross-section.

Analysis of the four-layer optical waveguides by Galerkin's method

Kun-Hua Tsai[+], Wei-Yu Lee[+], Kun-Yi Lee[+], Wei-Ching Chuang[*]
[+]Department of Electrical Engineering, Tatung Institute of Technology
[*]Department of Electro-Optic, National Yunlin Polytech Institution
[+]40 Chung-Shan North Road, Sec. 3, Taipei, Taiwan, 10451, ROC
TEL: 886-02-5957005
FAX: 886-02-6481583

Four-layer planar optical waveguides with semiconductor-cladding, owing to the coupling between the lossless and lossy modes, are useful in some optical devices such as optical polarizers, couplers, IR photo-detectors, and distributed feedback lasers etc. Therefore, in order to design a four-layer waveguide structure which can support these two different modes, it is important to have a simple and fast method to get propagation characteristics, namely, mode spectra and optical field distribution of such waveguides.

In this work, we propose a simple and easy method to analyze the four-layer waveguide structures based on the Galerkin's method which expands the unknown field in a complete set of orthogonal functions and converts a linear differential equation into a set of linear equations. The linear equations, i.e. the matrix equation, will yield all the possible modes of the waveguide without any recurrence. We choose two different basis functions, the trigonometric and Hermite-Gaussian functions, to deal with the four-layer waveguide structures with three different refractive index profiles, namely, the Step index Slab Waveguide(SSW), Semi-Parabolic index Slab Waveguide(SPSW), and Exponential index Slab Waveguide(ESW). Then, we get similar field distributions between the two different basis functions. In the case of the ESW structure, it is found that the field in the guiding region is maximum. On the other hand, in the SPSW is minimum. The results are shown in Fig. 1. It means that when we want to fabricate a waveguide which has a more better guiding effect, we can choose the ESW structure; when we fabricate a coupler, we can choose the SPSW structure. Furthermore, when we increase the thickness of the guiding region or the buffer region, the waveguide will support another guiding mode. This can give us a consideration to design four-layer planar optical waveguides. To the authors' best knowledge, this is the first time that we use the Galerkin's method to analyze the four-layer waveguide problems and we believe that the method can also be applied to other integrated optics devices.

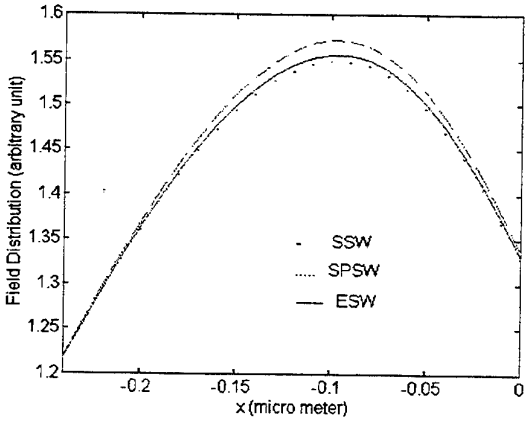


Fig. 1 The field distributions in the guiding region

A Simple Mathematica Algorithm for Computation of Spheroidal Wave Functions and Their Derivatives

L.W. Li, P.S. Kooi, T.S. Yeo, M.S. Leong, and C.L. Quek
Communications & Microwave Division, Department of Electrical Engineering
National University of Singapore, 10 Kent Ridge Crescent, Singapore 119260
Phone: (+65) 772 6658; Fax: (+65) 779 1103; Email: eleLiLW@nus.sg

Spheroidal Wave Functions

The spheroidal wave functions, as a kind of special functions in Mathematical Physics, have found many important and practical applications in science and engineering. In the evaluation of electromagnetic fields in the spheroidal structures, the spheroidal wave functions are frequently employed especially when the boundary-value problems are solved using full-wave analysis. By applying the separation of variables to the Maxwell's equations of either electric or magnetic field, two types of the spheroidal wave functions, i.e. the prolate and oblate functions corresponding to their respective coordinates system, can be obtained. Symbolically, one type of functions can be obtained from another simply by making the changes $c \rightarrow -ic$ and $\xi \rightarrow i\xi$. Computationally, values of the prolate and oblate spheroidal wave functions are calculated in quite different ways.

Previous Progress and Current Status

In either the prolate or the oblate spheroidal coordinates, the separation of the variables results in three independent functions: (1) the spheroidal radial function $R_{mn}^{(i)}(c,\xi)$ $(i = 1,2,3,4)$, (2) the spheroidal angular function $S_{mn}(c,\xi)$ (also referred to as the generalized Legendre function $\mathcal{P}_n^m(c,\xi)$), and (3) the sine and cosine functions. The latter is well-known, but the first two are not so easily computed. The computation of the spheroidal prolate/oblate, radial/angular, functions is involved in the eigenvalue computation and the forward and backward recursion formulation. Theoretically, the formulation of these functions was well-documented by C. Flammer earlier in 1957 [1]. Later on, the eigenvalues, the spheroidal wave functions, and their first-order derivatives were computed and the C-[2] and Fortran-programs [3-4] were developed.

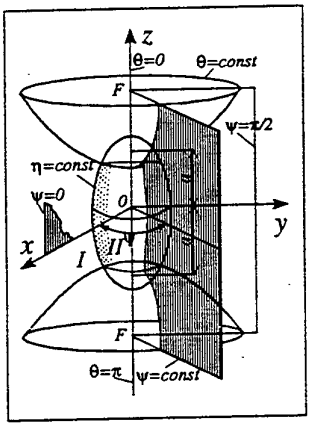


Figure 1: Prolate spheroidal coordinates (ζ,θ,ψ).

Motivation of the Work

The programs available in the literature are applicable only to the **lossless** problems where the permittivity of each spheroidal region is a real quantity. In this paper, a *Mathematica*^{TM} routine consisting of functional commands of eigenvalues λ, radial $R_{mn}^{(i)}(c,\xi)$ and angular $S_{mn}(c,\xi)$ spheroidal functions, and their first and second order derivatives has been developed so that users can call the functional commands directly. Both the prolate and oblate coordinates systems are considered and there is no restriction on the dielectric properties (i.e. the medium can be either *lossless* or *lossy*). The software routine package is soon available from the *MathSource* on the WWW Page of Wolfram's Mathematica^{TM}.

References

[1] C. Flammer, *Spheroidal Wave Functions*, California: Stanford Univ. Press, 1957.
[2] Louis Baker, *C Mathematical Function Handbook*, New York: McGraw Hill, Ins., 1992.
[3] A. L. van Buren, R. V. Baier, S. Hanish, and B. J. King, *J. Acoust. Soc. Amer.*, vol. 51, pp. 414-416, 1972.
[4] B. P. Sinha and R. H. MacPhie, *J. Math. Phys.*, vol. 16, pp. 2378-2381, 1975.

Addition to Spectral Domain Technique to Analysis of Planar Transmission Lines

Yung-hong Chen and *The-nan Chang
Department of Electrical Engineering, 40, Chung-Shan N. Road 3rd Sec.
Taipei, Taiwan.
E-mail : cyh@wave.ee.ttit.edu.tw, tnc@wave.ee.ttit.edu.tw

In this paper, we present an addition to spectral domain technique to analysis of planar transmission lines. In traditional spectral domain approach (SDA), two field equations on each dielectric boundary are derived, but there are four field quantities, two tangential electric fields ($[E_t]$) and two current densities ($[J_t]$)which are unknowns. Two of them can be eliminated by Galerkin's method in transform domain. In this way, the dimension of singular matrix depends on the number of basis function. Generally, it generats a small matrix in the literature. However, the elements of this matrix that are an integration of product of Green's function and basis functions in the transform domain are usually hard to compute. To present a different numerical solving process, the electric fields over the boundary are taken as the unknowns. Furthermore, two more equations derived from the inverse Discrete Fourier Transform (DFT) of $[E_t]$ are added in this paper. Since $[E_t]=0$ holds true on the strip, that is,

$$E_t[x] = \sum_{n=-\frac{N}{2}}^{\frac{N}{2}+1} \tilde{E}_t[n]\exp(-\frac{2\pi}{N}nx) = 0 \qquad (1)$$

We can set up this as the first equation, namely, $\left[\tilde{Y}_1\right]\left[\tilde{E}_t\right]^t = 0$, where $\left[\tilde{E}_t\right]^t$ is the spectral quantity of $[E_t]$. The element of $\left[\tilde{Y}_1\right]$ is simply the kernel in definition of DFT. The second equation is obtained viewing that $[J_t]$ is zero on the metal-less region.

$$[J_t(x)]^t = \mathrm{DFT}\left\{\left[\tilde{G}\right]\left[\tilde{E}_t\right]^t\right\} = \left[\tilde{Y}_2\right]\left[\tilde{E}_t\right]^t = 0 \qquad (2)$$

The elements of $\left[\tilde{Y}_2\right]$ is the product of Green's function and the kernel of DFT.

The combination of $\left[\tilde{Y}_1\right]$ and $\left[\tilde{Y}_2\right]$ will make a square matrix. In order that $\left[\tilde{E}_t\right]^t$ has nontrivial solution, the determinant of this matrix must be zero. Hence, the propagation constant can be determined at each frequency. Although the final matrix is similar to that by point matching in SDA, the process is somewhat different.

The main reason to use this technique is for easy calculation of the distributions of field on the boundary. $\left[\tilde{E}_t\right]^t$ is directly solved without any simplification. Once it is obtainable, all the field distributions along with the line parameters can readily be calculated.

* : Corresponding author.

Analysis of EM Scattering from Microstrip Circular Patch Using Hybrid Method: A Closed Form Solution

L.W. Li, P.S. Kooi, T.S. Yeo, M.S. Leong, and Y.L. Qiu
Communications & Microwave Division, Department of Electrical Engineering
National University of Singapore, 10 Kent Ridge Crescent, Singapore 119260
Phone: (+65) 772 6658; Fax: (+65) 779 1103; Email: eleLiLW@nus.sg

Background of Scattering from Circular Disk

Over several decades, electromagnetic scattering from a circular disk has attracted researchers working on the (monostatic or backscattering) *r*adar *c*ross *s*ection (RCS) of large dynamic range. Usually, there are four groups of techniques applied to the analysis of the electromagnetic scattering from circular disks. The first is the *p*hysical *o*ptics (PO) [1] which is an approximate technique and is accurate to predict the far-field pattern near the main beam. The second is the *p*hysical *t*heory of *d*iffraction (PTD) [2] which is more accurate than the PO technique and consists of the following three methods: (a) Mitzner's incremental length diffraction coefficients, (b) Michaeli's equivalent edge currents, and (c) Ando's modified physical theory of diffraction. The third is the *g*eometrical *t*heory of *d*iffraction (GTD) [2] that is of similar accuracy to the PTD and also consists of (a) geometrical theory of diffraction, (b) uniform geometrical theory of diffraction, and (c) uniform asymptotic technique. The last one is the *m*ethod *o*f *m*oments (MoM) or *m*oment *m*ethod (MM) [2] that is considered to be numerically exact.

Formulation of the Problem

This paper presents a novel analysis of the classical electromagnetic scattering from a microstrip circular patch. A hybrid method which combines the vector wave eigenfunction expansion technique, the mode-matching method, and the dyadic Green's function is applied to the derivation of the unknown scattering coefficients of the expanded eigenfunctions of scattered fields. This method is similar to the MoM and therefore has the same order of accuracy as the MoM. Orthogonality of the vector wave functions is also utilized. The scattering coefficients are obtained in closed form and expressed in terms of compact matrices. Numerical computation of the radar cross sections (RCSs) of the perfectly conducting disk is carried out. Experimental data and theoretical results published elsewhere are compared with the results obtained here. A good agreement has been found confirms the applicability of the hybrid method developed in this paper.

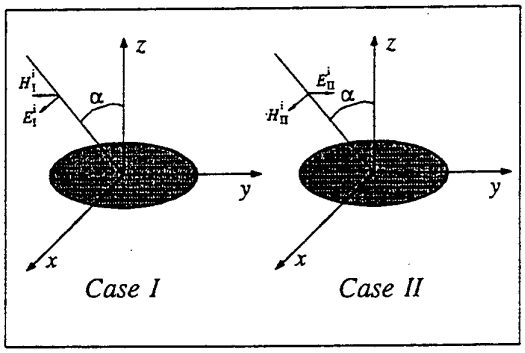


Figure 1: Geometry of plane waves scattered by a conducting circular disk. Case I: parallel polarization and Case II: perpendicular polarization.

References

[1] C. A. Balanis, *Advanced Engineering Electromagnetics*, New York: John Wiley & Sons Ins., 1989.

[2] D-W Duan, Y. Rahmat-Samii, and J.P. Mahon, *Proc. IEEE*, vol. 79, No. 10, pp. 1472-1480, Oct. 1991.

Capacitance Computation for CPW Discontinuities with Finite Metallization Thickness by Hybrid Finite Element Method

Chien-Wen Chiu, and Ruey-Beei Wu

Department of Electrical Engineering, Rm. 523
National Taiwan University
Taipei, Taiwan, R.O.C.

Abstract

The uni-planar transmission line structure based on the coplanar waveguide (CPW) has been proposed as a circuit element for monolithic microwave integrated circuits (MMIC) and accurate analysis of the characteristics of CPW discontinuity is important in designing the MMIC. As we know, the influence of the metallization thickness becomes not negligible and should be taken into account due to the miniaturized lines geometries used in MMIC's.

In this paper, a variational equation is derived for the capacitances of CPW structures with finite metallization thickness. Introducing a vector electric potential and a scalar potential ϕ, the stored energy can be related to the scalar potential in the slot regions. Hence, the total electric energy can be expressed in terms of the scalar potential by

$$\begin{aligned} W_e &= \frac{1}{2}\int_{\Gamma^u}\int_{\Gamma^u} G^u(\vec{\rho};\vec{\rho}')\,\nabla_\rho\,\phi(\vec{\rho},z=t)\cdot\nabla'_\rho\phi(\vec{\rho}',z'=t)\,d\Gamma\,d\Gamma' \\ &+ \frac{1}{2}\int_{\Gamma^l}\int_{\Gamma^l} G^l(\vec{\rho};\vec{\rho}')\,\nabla_\rho\,\phi(\vec{\rho},z=0)\cdot\nabla'_\rho\phi(\vec{\rho}',z'=0)\,d\Gamma\,d\Gamma' \\ &+ \frac{1}{2}\int_{\Omega}\epsilon\,\nabla\,\phi(\vec{\rho},z)\cdot\nabla\phi(\vec{\rho},z)\;\;d\Omega \end{aligned} \tag{1}$$

where G^u and G^l are the space-domain Green's function for the upper and lower spaces. Here, the superscript u and l denote the contributions from the upper and lower regions, respectively. It is well-known that the variational equation for capacitance (1) can be solved by applying the Ritz procedure. Here, the potential distribution $\phi(x,y,z)$ over each element is modeled as a linear combination of first-order shape functions.

By using this formula, some numerical results for the equivalent capacitances of CPW discontinuities with finite metallization thickness will be presented and compared with measured data. The reasonable agreement between the measured data and the theoretical results validates the present approach. Being simple and computationally efficient, the method is suitable to deal with extensive CPW discontinuity problems where the metallization thickness is not negligible.

Design Considerations for Microstrip Antennas Excited by Coplanar Waveguides

Powen Hsu and Shih-Wen Lu
Department of Electrical Engineering
National Taiwan University
Taipei, Taiwan 10617
R. O. C.

Coplanar waveguide fed microstrip antennas have been studied by many investigators [1]-[4]. They either concentrated on the numerical analysis technique [1], [2], or on the effect of the coupling slots between the coplanar line and the microstrip patch [3], [4]. Besides the coupling slot dimensions, in order to have a good design, it is also important to study the effect of the substrate, including the dielectric permittivity and the substrate thickness. This is the purpose of this study.

All of the data to be presented were calculated by a moment method solution. A detailed description of this method, with comparisons of calculated and measured results for input impedances, has already appeared in the literature [2], only a brief description will be given.

The effect of the substrate on the performance of the coplanar waveguide fed microstrip antenna is presented through calculations of the resonant length, resonant resistance, bandwidth, and loss due to surface waves. All of these data should be helpful to the antenna designers, especially those designing the millimeter wave antennas.

[1] M. I. Aksun, S. L. Chuang, and Y. T. Lo, "Coplanar waveguide-fed microstrip antennas," *Microwave and Opt. Tech. Lett.*, vol. 4, no. 8, pp. 292-295, July 1991.
[2] S. M. Deng, M. D. Wu, and P. Hsu, "Analysis of coplanar waveguide-fed microstrip antennas," *IEEE Trans. Antennas Propagat.*, vol. 43, no. 7, pp. 734-737, July 1995.
[3] W. Menzel and W. Grabherr, "A microstrip patch antenna with coplanar feed line," *IEEE Microwave and Guided Wave Lett.*, vol. 1, no. 11, pp. 340-342, Nov. 1991.
[4] S. M. Deng, M. D. Wu, and P. Hsu, "Impedance characteristics of microstrip antennas excited by coplanar waveguides with inductive or capacitive coupling slots," *IEEE Microwave and Guided Wave Lett.*, vol. 5, no. 11, pp. 391-393, Nov. 1995.

SESSION 6P15

Monday, January 6, PM 1330-1650, Lecture Theatre 15, City University of Hong Kong

Scattering and Diffraction 1

Organizer: Weng Cho Chew, Uni. of Illinois at Urbana-Champaign

Chairperson: Jian-Ming Jin, Univ. of Illinois at Urbana-Champaign
Co-Chairperson: Cai-Cheng Lu, Univ. of Illinois at Urbana-Champaign

13:30 ***Application of the Element Residual Method for Adaptive Refinement in Finite Element Design*** 41
*Tom Cwik, *Vahraz Jamnejad, *Cinzia Zuffada, **C H Chan
*California Institute of Technology
**City University of Hong Kong

13:50 ***Microwave Specific Attenuation by Lossy Raindrops of Spheroidal Shapes: An Exact Formulation*** 42
L W Li, T S Yeo, P S Kooi, M S Leong, C L Quek
National University of Singapore

14:10 ***A Novel Hybrid EFIE-MFIE Iterative (HEMI) Method: Application to Radiation and Scattering Problems*** 43
Richard E Hodges, Yahya Rahmat-Samii
University of California, Los Angeles

14:30 ***Complementary Perfectly Matched Layers for Use as an Absorbing Boundary Condition*** 44
Jian-Ming Jin, Shawn Carolan, Weng Cho Chew
University of Illinois at Urbana-Champaign

14:50 ***Acceleration of the Convergence Rate for the Iterative Solution of EM Scattering from Objects with Open-End Cavities*** 45
Cai-Cheng Lu, Weng Cho Chew
University of Illinois at Urbana-Champaign

15:10 **Break**

15:30 ***MLFMA for Electromagnetic Scattering with the Impedance Boundary Condition*** 46
J M Song, Cai-Cheng Lu, Weng Cho Chew
University of Illinois at Urbana-Champaign

15:50 ***Detection of a Buried Target Based on Angular Correlation Function Measurement*** 47
T K Chan, Y Kuga, A Ishimaru
University of Washington

16:10 ***Comparison Study of Numerical Simulations of Random Rough Surfaces at Near Grazing Incidence*** 48
*C H Chan, **L Tsang
*City University of Hong Kong
**University of Washington

16:30 ***Research on Solution Stability of Born Iterative Method and Distorted Born Iterative Method in Low-Frequency Inverse Problem*** 49
Zaiping Nie, Yerong Zhang
University of Electronic Science and Technology of China

Application of the Element Residual Method for Adaptive Refinement in Finite Element Design

*Tom Cwik, Vahraz Jamnejad, Cinzia Zuffada and Chi Chan**

Jet Propulsion Laboratory
California Institute of Technology
Pasadena, CA 91109

Department of Electrical Engineering
University of Washington
Seattle, WA 98195

Finite element modeling has proven useful for accurately simulating scattered or radiated electromagnetic fields from complex three-dimensional objects whose geometry varies on the scale of a fraction of a wavelength. Convergence of the simulation can be assessed by uniformly increasing the mesh density until an observable quantity stabilizes. Depending on the electrical size of the problem, uniform refinement of the mesh may be computationally infeasible due to memory limitations. Similarly, depending on the geometric complexity of the object being modeled, uniform refinement can be inefficient since regions that do not need refinement add to the computational expense. In either case, convergence to the correct (measured) solution is not guaranteed.

Adaptive methods attempt to selectively refine the region of the mesh that is estimated to contain proportionally higher solution errors. The refinement may be obtained by decreasing the element size (h-refinement), by increasing the order of the element (p-refinement) or by a combination of the two (h-p refinement). A successful adaptive strategy refines the mesh to produce an accurate solution measured against the correct fields without undue computational expense. This is accomplished by the use of a) reliable *a posteriori* error estimates, b) hierarchical elements, and c) automatic adaptive mesh generation. Various *a posteriori* error estimates have been used in internal region problems in the past. In this paper, mathematical developments of *a posteriori* error estimates based on the element residual method developed in structural mechanics and fluid dynamics (M. Ainsworth and T. Oden, *Comput. Methods Appl. Mech. Engrg.*, 101, 73-96, 1992), and tried in electromagnetic problems (F. Meyer and D. Davidson, *Electr. Lett.*, 30, 936-938, 1994) will be examined for internal and external scattering problems. The element residual method estimates error in the field solution over the mesh by solving very small problems at each element. Based on this error estimate a new refined mesh is developed and the method is repeated until the error is below a given tolerance.

Microwave Specific Attenuation by Lossy Raindrops of Spheroidal Shapes: An Exact Formulation

L.W. Li, T.S. Yeo, P.S. Kooi, M.S. Leong, and C.L. Quek
Communications & Microwave Division, Department of Electrical Engineering
National University of Singapore, 10 Kent Ridge Crescent, Singapore 119260
Phone: (+65) 772 6658; Fax: (+65) 779 1103; Email: eleLiLW@nus.sg

ABSTRACT

Scattering and attenuation of radio waves by raindrop scatterers have attracted many researchers worldwide over the past several decades. The most popular raindrop model, used for the analysis of rainfall attenuation in the published literature, considers the raindrops as spheroidal raindrop scatterers. The methods and techniques employed for the analysis of specific rainfall attenuation are the boundary-perturbation and point-matching techniques by Oguchi (J. Radio Res. Labs., vol. 7, pp. 467-485, 1960 and vol. 11, pp. 19-44, 1964), the least-squares fitting process of boundary conditions by Morrison and Cross (Bell Syst. Tech. J., vol. 53, pp. 955-1019, 1974), the T-matrix method by Waterman (Proc. IEEE, vol. 53, pp. 805-812, 1965; Alta Freq., vol. 38, pp. 348-352, 1969) or the method of extended boundary conditions by Warner (Electron. Lett., vol. 11, pp. 328-330, 1975; Radio Sci., vol. 11, pp. 921-930, 1976) and so forth.

However, the above-mentioned methods cannot produce exact FORMULATION of the scattered fields and therefore the total cross sections. So the specific microwave attenuation due to rainfall cannot be exactly formulated. To accurately calculate the scattered fields by the dielectric spheroid and its total cross sections, the expansion method of spheroidal vector wave eigenfunctions is developed by Asano and Yamamoto (Applied Optics, vol. 14(1), pp. 29-49, 1975; errata, vol. 15, p. 2028, 1976) where the expansion coefficients are determined using the boundary conditions. However, since only the tabulated values given in the published work were used, Asano and Yamamoto presented the extinction cross sections which are valid only for the scattering from the lossless dielectric spheroid. Even with the modification made later by Asano & Yamamoto and Cooray & Ciric, there is still no available extinction cross section data that are necessary for the calculation of rainfall attenuation.

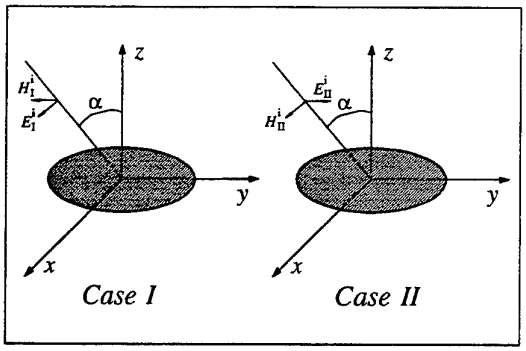


Figure 1: Geometry of electromagnetic scattering and attenuation by oblate spheroidal raindrops.

In a similar fashion, RIGOROUS formulation of the electromagnetic scattering from a LOSSY dielectric spheroid is given in this paper. The experimental data show that the specific microwave attenuation due to rainfall in Singapore's tropic environment are much LARGER than those recommended by the CCIR. With the EXACT expressions of the scattered fields and the extinction cross sections in terms of spheroidal vector wave eigenfunctions, the specific attenuation is integrated numerically by making use of the distribution of raindrop sizes in Singapore. The computed results are also COMPARED with the experimental data collected in Singapore in the last THREE years and with the results previously published by the authors (IEEE Trans. on Antennas Propagat., vol. 43(8), pp. 811-28, 1995). Numerical techniques are also used in the data interpolation and an interpolated three-dimensional MODEL of the extinction cross sections is established. With this model, the computational speed of the specific attenuation is increased significantly.

A NOVEL HYBRID EFIE-MFIE ITERATIVE (HEMI) METHOD: APPLICATION TO RADIATION AND SCATTERING PROBLEMS

Richard E. Hodges and Yahya Rahmat-Samii
Department of Electrical Engineering
University of California, Los Angeles
Los Angeles, CA 90095-1594
e-mail: rahmat@ee.ucla.edu

Both current-based and ray-based hybrid methods are increasingly used to solve the problem of small, intricate antennas mounted on large structures such as aircraft. This approach offers a significant advantage since one may utilize the known asymptotic behavior to reduce computation time for large structures. For example, the physical optics (PO) solution may be utilized in current-based methods and geometrical optics (GO) is used in ray-based methods. In order to obtain accurate results, the hybrid construction must properly account for errors introduced by the asymptotic approximations. This paper presents a general current-based hybrid method which applies the Electric Field Integral Equation (EFIE) and Magnetic Field Integral Equation (MFIE) to geometrically distinct regions of an object. The EFIE region is used to model small, geometrically complex antennas while the MFIE region is used to model closed surfaces (e.g. an airplane fuselage). The formulation is rigorous and is intended for intermediate frequency regimes which are too computationally demanding for numerically exact methods such as the Moment Method (MM) and are not amenable to pure asymptotic approximations.

The theoretical formulation is hybrid in that Fredholm integral equations of the first and second kind are applied to separate regions of an object to generate a pair of coupled integral equations. In addition, the solution method is also hybrid in that two distinct methods are used to solve the two integral equations. The solution technique is a dual iterative method called HEM iterative (HEMI). HEMI uses the Moment Method (MM) in the EFIE region and an iterative Neumann series technique in the MFIE region. Coupling between the regions is handled by a successive approximations approach. The advantage of MFIE is that it permits one to utilize the physical optics (PO) approximation to start the iterative process. In this way, the number of iterations required for solution are substantially reduced and the solution time is considerably less than $O(N^3)$ required by a standard linear equation solver. In effect, it provides a general and systematic mechanism to correct the inherent error in PO. The HEMI solution method is also naturally suited to parallel processing computer architectures such as Multiple Instruction Multiple Data (MIMD) machines. Accurate solution of relatively large problems is achieved by efficient use of the large distributed memory available on a parallel machine.

A computer code has been designed to implement the HEMI algorithm for the general class of problems that can be represented by an arbitrary three-dimensional system of metallic wires and bodies. For example, the program can model complex wire antennas (e.g. bent wire Yagi) mounted on curved structures (airplane fuselage). Numerical results comparing MM and HEMI are given for representative examples to demonstrate the accuracy of computed input impedance, mutual impedance, surface currents, gain and radiation patterns. The results show that HEMI calculations are in good agreement with MM calculations and experimental data, and also indicate that the HEMI solution method is significantly faster than MM.

COMPLEMENTARY PERFECTLY MATCHED LAYERS FOR USE AS AN ABSORBING BOUNDARY CONDITION

Jian-Ming Jin, Shawn Carolan, and Weng Cho Chew
Center for Computational Electromagnetics
Department of Electrical and Computer Engineering
University of Illinois at Urbana-Champaign
Urbana, Illinois 61801-2991

The perfectly matched layer (PML) has recently been introduced by Berenger (*J. Comp. Phys.*, 114:185-200, 1994) as a material absorbing boundary condition (ABC) for electromagnetic waves. An infinitely thick PML has no reflection for all incident angles and all frequencies at its interface with another medium. However, when the PML is used to truncate the finite difference or finite element solution domain, it must be terminated or backed by a perfectly conducting or impedance surface. As a result, the PML does not possess zero reflection for all incident angles. Instead, the reflection coefficient increases as the incident angle and reaches the value of one at grazing. To reduce the error associated with this artificial reflection, one must either place the PML at some distance away from the object or increase the PML thickness. Both would result in a large solution domain and reduce the efficiency of the numerical solution. Recently, we have proposed a combination of the PML with ABC to reduce the artificial reflection (Jin and Chew, *1996 ACES Proceedings*, 2:962-971).

In this paper, we propose a new approach to reduce the numerical error associated with the artificial reflection of the PML. This approach employs a pair of PMLs that have exactly the same material composition or parameters, but one is backed by a perfectly electric conducting (PEC) surface and the other is backed by a perfectly magnetic conducting (PMC) surface. As a result, the PEC-backed PML has a reflection coefficient that is the negative of the reflection coefficient of the PMC-backed PML, or in other words, the PEC- and PMC-backed PMLs are complementary to each other. Assuming that the PEC-backed PML has a reflection coefficient R, the numerical solution obtained with this PML has an error proportional to R. When the same problem is solved using the PMC-backed PML, the error is proportional to $-R$. Averaging the two solutions eliminates the error proportional to R and the remaining error is proportional to R^2, which can be significantly smaller than $O(R)$. The smaller error $O(R^2)$ is due to the double reflections of waves, which cannot be eliminated by averaging. The use of the complementary PMLs is demonstrated by several numerical examples of wave scattering in waveguides and free space. Although the proposed approach requires to solve the problem twice, the saving resulting from the reduction of the solution domain overcompensates this disadvantage. This work can be considered as an extension to the material ABC of the work by Ramahi (*IEEE Trans. Antennas Propagat.*, 43:697-704, 1995), in which the complementary ABCs were developed for the finite difference time domain (FDTD) solution of partial differential equations.

ACCELERATION OF THE CONVERGENCE RATE FOR THE ITERATIVE SOLUTION OF EM SCATTERING FROM OBJECTS WITH OPEN-END CAVITIES

CAI-CHENG LU AND WENG CHO CHEW

CENTER FOR COMPUTATIONAL ELECTROMAGNETIC
DEPARTMENT OF ELECTRICAL AND COMPUTER ENGINEERING
UNIVERSITY OF ILLINOIS
URBANA, IL 61801, USA

Abstract

In the solution of electromagnetic scattering from arbitrary objects, the integral equation method with an iterative solution for the matrix equation has become an important method. The computational cost for solving a matrix equation iteratively consists of two factors: one being the operation count in each iteration which, in most cases, is proportional to that of a matrix-vector multiplications. Another being the number of iterations, which is related to the convergence rate of a system. The matrix-vector multiplication can be realized in $O(N \log N)$ operations via the multilevel fast multipole approach (FMM). Moreover, the fast multipole method reduces the memory requirement to $O(N \log N)$ for an $N-$unknown problem. Usually, the convergence rate is closely related to the condition number of the system. The iterative method is unstable for systems with large condition numbers. In the electromagnetic scattering problems, there are many causes for the ill conditioning of the system, such as internal resonances and multiple bounces of the waves. The combined field integral equation can successfully eliminate the ill conditioning resulting from the internal resonances. However, it has no effect on those caused by multiple bounces in open-ended cavities. In the high frequency method, the multiple wave bounces are usually accounted for by ray expansion method and ray tracing method.

In this paper, the equivalence principle is applied to separate the cavity region from the rest of the object, hence, the cavity problem can be solved independently. In this method, the first step is to cover the aperture of the cavity by a conducting sheet of zero thickness. Then an equivalent magnetic current $\mathbf{M}$ is impressed on both sides of the conducting cover sheet. In this way, we can solve the internal problem independently. By solving the integral equation that is formulated on the closed cavity interior surface, we obtain an admittance matrix $\overline{\mathbf{Y}}$ such that $\mathbf{J} = \overline{\mathbf{Y}}\mathbf{M}$. By solving the external boundary integral equation, we determine the induced current on the external surface (including the aperture region) in terms of incident field. If the cavity is a long one, i.e., the aperture dimension is much smaller than its depth, the interior region can be divided into several sections and the $\overline{\mathbf{Y}}$-matrix is solved recursively. The major advantage of this method is to isolate the cavity from the rest of the object and the multiple wave bounces inside the cavity are taken care of by a Y-matrix, reducing the iteration number. In numerical simulations, we observed significant reduction in the number of iterations.

Progress in Electromagnetics Research Symposium, PIERS 1997 ISBN 962-442-097-1

MLFMA FOR ELECTROMAGNETIC SCATTERING WITH THE IMPEDANCE BOUNDARY CONDITION

J. M. Song, C. -C. Lu and W. C. Chew
Center for Computational Electromagnetics
Department of Electrical and Computer Engineering
University of Illinois, Urbana, IL 61801, USA
Phone: (217)333-4468, Fax: (217)244-7345, email: j-song4@uiuc.edu

Scattering of an electromagnetic wave by a conducting body can be controlled or modified by coating the body with a lossy material sheet. If the coating materials are homogeneous media, surface integral equations can be solved for electromagnetic scattering. If they are inhomogeneous, volume integral equations, finite element method (FEM) with absorbing boundary condition (ABC), or with surface integral equations can be used. But all these methods are computationally expensive. When the coating sheet is very thin, it can be modeled as infinitesimally thin structures, and described in terms of impedance boundary condition (IBC). Thus, the scattering problems can be expressed as solving surface integral equations with IBC. IBC also can be used for lossy, electrically large scatterers, such as the earth, and ocean surface.

Fast multipole method (FMM) [1-2] and multilevel fast multipole algorithm (MLFMA) [3-4] have been applied for solving integral equations of electromagnetic scattering from perfect electric conductors. FMM reduces the complexity of a matrix-vector multiply from $O(N^2)$ to $O(N^{1.5})$, where N is the number of unknowns. MLFMA further reduces the complexity to $O(N\log N)$. It requires $O(N\log N)$ memory, and hence, can solve a large problem on a small computer.

MLFMA has been implemented to solve electric field integral equation (EFIE) with IBC. The fast multipole expressions for basis functions with IBC are derived. The code is verified by comparing the results with known ones in published articles for conducting objects with different shapes like sphere, plate, etc. Our numerical results agree very well with analytical solution, measurements, and LUD solutions.

In conclusion, electromagnetic scattering from thin coated conductors, lossy, electrically large scatterers can be found by solving surface integral equations with impedance boundary condition (IBC). MLFMA has been implemented to speed up the matrix-vector multiplies. Both memory requirements and CPU time per iteration are of $O(N\log N)$. The code is verified by comparing the results calculated using MLFMA with the results calculated using Mie series with IBC.

[1] R. Coifman, V. Rokhlin, and S. Wandzura, "The fast Multipole Method for the Wave Equation: A Pedestrian Prescription," *IEEE Antennas Propagat. Mag.*, vol. 35, no. 3, pp. 7-12, June 1993.
[2] J.M. Song and W.C. Chew, "Fast Multipole Method Solution Using Parametric Geometry," *Micro. Opt. Tech. Lett.*, vol.7, no. 16, pp.760-765, November 1994.
[3] C.C. Lu and W.C. Chew, "A Multilevel Algorithm for Solving Boundary Integral Equations of Wave Scattering," *Micro. Opt. Tech. Lett.*, vol. 7, no. 10, pp. 466-470, July 1994.
[4] J.M. Song and W.C. Chew, "Multilevel Fast Multipole Algorithm for Solving Combined Field Integral Equations of Electromagnetic Scattering," *Micro. Opt. Tech. Lett.*, vol.10, no. 1, pp.14-19, September 1995.

Detection of a Buried Target Based on Angular Correlation Function Measurement

T. K. Chan, Y. Kuga, and A. Ishimaru

Department of Electrical Engineering,
University of Washington,
Box 352500,
Seattle, WA 98195–2500

A new target detection technique based on amplitude angular correlation function (ACF) measurement is proposed in this study. Given a target buried in a random scattering medium it was shown that this technique proves to be a useful means to discriminate the ACF response of the target from that of the medium.

Recent studies suggest that scattering of random media exhibits a correlation property known as the angular memory effect when the generalized Snell's law, which governs the angular relationship between the reference and variable transmitter-receiver positions, is satisfied. This memory effect results in non-zero angular correlation between scattered wave amplitudes in response to a change in incident wave direction.

In this study, a long conducting cylinder of diameter equal to one wavelength was buried in a sand medium with a flat sand-air interface at a depth of one wavelength. The ACF response of the composite scene is therefore the coherent sum of the target and medium ACF responses. A wideband (80–105 GHz) millimeter-wave scatterometer was used to perform ACF measurements. It was shown experimentally that by adopting a special antenna scanning scheme which aims at suppressing the scattering memory of the medium, the ACF response of the buried target can be clearly discriminated from that of the medium, thus resulting in successful detection. Although in general ACF measurement involves field measurement at two different angles, by orienting the two antennas in a backscattering direction it is possible to implement this ACF-based detection system with a monostatic radar. Comparison with intensity measurements shows that ACF measurement yields better target visibility than intensity measurement does.

In conclusion, it was shown experimentally that enhanced target visibility can be obtained through a special antenna scanning scheme in which the angular clutter is suppressed. This technique is compatible with the existing monostatic radar technology, making it an especially competitive method in detection of targets embedded in strong clutter.

Comparison Study of Numerical Simulations of Random Rough Surfaces at Near Grazing Incidence

C. H. Chan* and L. Tsang**

*Department of Electronic Engineering
City University of Hong Kong
83 Tat Chee Avenue
Kowloon
Hong Kong

**Department of Electrical Engineering, Box 352500
University of Washington
Seattle, WA 98195-2500
USA

In the Monte-Carlo simulations of random rough surface scattering, a popular approach is the integral equation method in which an integral equation is formed in the space domain and subsequently converted into a matrix equation $[Z]\{x\} = \{h\}$ via the use of the method of moments. Recently, two efficient iterative methods have been developed to solve this matrix equation. The first method is the BMIA/Canonical Grid (BMIA/CAG) method [Tsang *et al.*, *IEEE Trans. Antennas Propagat.*, August 1995] in which the matrix equation is converted into the form $([Z^b] + [Z^w])\{x\} = \{h\}$. Here $[Z^b]$ is a banded matrix and the majority portion of the matrix-vector multiplication $[Z^w]\{x\}$ can be performed efficiently using FFTs upon the use of Taylor series expansion. Consequently, both computation time and computer memory can be reduced significantly. On the other hand, the method of ordered multiple interactions (MOMI) [Kapp and Brown, *IEEE Trans. Antennas Propagat.*, May 1996] converts the matrix equation into the form of $[I-L-U]\{x\} = \{h\}$ where [I] is an identity matrix and [L] and [U] is the lower and upper triangular matrices that correspond to the forward- and backward-scattered waves, respectively. In contrast to the BMIA/CAG method, the total solution for MOMI is the sum of all the order of solutions $\{x\}_n$. Each order of solution can be evaluated by solving two matrix equations of the forms $[1-L]\{y\} = \{b\}$ and $[1-U]\{x\}_n = \{y\}$. These solutions only require backsubstitutions as no LU decomposition is required. Computer memory storage problem is alleviated as [L] and [U] are recomputed for each order of solution. To have a fair comparison, we establish the same truncation criterion for the two iterative schemes, i.e., error $= \sqrt{\|\{h\} - [Z]\{x\}\| / \|\{h\}\|} \times 100\% < \varepsilon$. It is not difficult to see that Taylor series expansion and FFT operations in computing $[Z^w]\{x\}_n$ can also be employed in handling the corresponding portions of evaluating $[1-U]\{x\}_n$ and $[1-L]\{x\}_n$. Therefore, repetitive evaluations of the nonstored portions of [L] and [U] can be eliminated. However, the matrix equations of $[1-L]\{y\} = \{b\}$ and $[1-U]\{x\}_n = \{y\}$ can no longer be solved by backsubstitutions but can be solved by CG-FFT instead. We denote this improved MOMI by IMOMI. We will compare BMIA/CAG, MOMI and IMOMI when applied to near grazing incidence.

Research on Solution stability of Born Iterative Method and Distorted Born Iterative Method in Low-Frequency Inverse Problem

Nie Zaiping Zhang Yerong
University of Electronic Science and Technology of China
Chengdu 610054, P. R. China

In many low-frequency electromagnetic (EM) inverse problem, the Born iterative method (BIM) and distorted Born iterative method (DBIM) are widely used to image and reconstruct inhomogeneous media. These methods are based on numerical solution of EM integral equation which described the relationship between incident wave in background media, scattering wave due to the volume current of inhomogeneous part of the media and the measurement data of the field. In BIM and DBIM, the constraint condition of Tikhonov regularization has been used to get a proper solution from the overdetermined equation and underdetermined equation. In the procedure of BIM, the background media and the corresponding Green's function remain unchanged throughout the iteration, and the scattering field and signal-to-noise ratio are also unchanged in the process. Therefore, the method is quite robust to noise contamination, providing a stable solution. However, the convergence speed of BIM is very low. On the other hand, DBIM keep updating the background media and the corresponding Green' function in every iterative step, so its convergence speed is quite faster. But the scattering field becomes less and less in the iterative procedure, and interference of noise is more and more severe. After several iteration, the relative mean square error(RMS) of inversion solution is no longer improved, but increased fast.

In this paper, several methods are proposed for improving the performance of tolerance to noise and convergence speed in the inversion methods.

(1) Combine the Born iterative method and the distorted Born iterative method in a same problem: for first several iterative steps the DBIM is used to enhance the convergence speed, and in the following iterative steps the BIM is used to improve the stability of inversion solution. Numerical computation shows that the results of media reconstruction are very satisfied in the case of low signal-to-noise ratio.

(2) Select proper value of Tikhonov regularization parameter, which ensures solution stable in the iterative procedure.

(3) Let the value of Tikhonov regularization parameter be less and less as the relative residual error (RRE) become small in the iterative procedure, making the weighting factor of the inversion equation to restrained condition relative stable in the procedure.

Numerical results show that the three methods mentioned above apparently improve the stability of solution in the process. So, measurement data with errors and noise would not cause severely distortion to the inversion results. These methods have been applied to engineering areas in media inversion and reconstruction based on the measurement data of Array Induction Imager Tool (AIT) and Multi-Electrode Resistivity Tool (MERT).

SESSION 6P14

Monday, January 6, PM 1330-1550, Lecture Theatre 14, City University of Hong Kong

Millimeter, Submillimeter and Lightwaves 1

Organizer: T Itoh

Chairperson: T Itoh, UCLA
Co-Chairperson: M C Wu, UCLA

13:30 ***Progress in High Power, High Frequency Photodetectors*** 51
M C Wu, T Itoh, L Y Lin
University of California, Los Angeles

13:50 ***High Performance Analog Fiber Link Using Semiconductor Waveguide Modulator and Detectors*** 52
P K L Yu
University of California, San Diego

14:10 ***Progress in Semiconductor Optoelectronic Components for Microwave and Millimeter Wave Signal Distribution*** 53
J C Brock
TRW Space and Electronics Group

14:30 ***Recent Progress in Millimeter Wave Antennas*** 54
A Basu, T Itoh
Univeristy of California, Los Angeles

14:50 ***Manufacturing Issues of Millimeter-Wave Filters and Diplexers*** 55
Y C Shih
Hughes Space & Communications Company

15:10 **Break**

15:30 ***Novel Illuminated FET Model and Optically Controlled LU-FET Oscillator*** 56
Shigeo Kawasaki
Tokai University

Progress in High Power, High Frequency Photodetectors

M. C. Wu, T. Itoh, and L. Y. Lin

Department of Electrical Engineering
University of California, Los Angeles
Los Angeles, CA 90095-1594, U.S.A.
E-mail: wu@ee.ucla.edu

High power, high frequency photodetectors play a key role in determining the performance of analog and microwave fiber optic links. The high power photodetectors allows the use of high power laser sources in externally modulated links. This can significantly reduce the RF insertion loss, and increase the spurious free dynamic range and signal-to-noise ratio of the link. High power photodetectors are particularly important for high frequency links because the electro-optic modulators with low V_π (half-wave voltage) become more difficult to achieve. They are also useful for optoelectronic generation of high power microwaves and millimeter-waves. Though significant progress has been made in high speed photodetectors, the conventional photodetectors tend to saturate at very low optical powers because they employ small absorption volume (typically of the order of 1 μm^3) to reduce transit time and parasitic capacitance. Recently, large-core waveguide photodetectors have been proposed to increase the saturation power. Traveling-wave photodetectors can further extend the absorption volume and achieve even higher saturation power.

In this paper, we will review the recent progress in high speed, high power photodetectors. The design trade-offs among the saturation power, 3-dB bandwidth, and quantum efficiency will be described. The fundamental limit of saturation powers for various types of photodetectors, including surface-illuminated p-i-n photodetectors, waveguide photodetectors, traveling-wave photodetectors, and velocity-matched distributed photodetectors, will be derived and compared. In particular, the figure-of-merit (FOM) for high power, high frequency photodetector will be defined. We will also present the recent experimental results of the velocity-matched distributed photodetectors (VMDP) fabricated at UCLA.

The VMDP consists of an array of localized photodiodes serially connected by a passive optical waveguide, and the photocurrents are collected in phase by a separate output microwave transmission line. The microwave transmission line has an impedance of 50 Ω and is velocity-matched to the optical waveguide, which allows the VMDP to extend its absorption length to several hundred micrometers without penalizing its bandwidth. Therefore, the saturation power is greatly enhanced while the bandwidth is essentially the same as that of a single photodiode. Another unique advantage of the VMDP is that the optical waveguide, active photodiodes, and the microwave transmission line can be independently optimized. A VMDP with nanoscale metal-semiconductor-metal photodiodes and coplanar strips transmission line has been designed and fabricated at UCLA. A record-high peak saturation photocurrent of 56 mA is achieved for the 50 GHz VMDP. Saturation photocurrent above 100 mA is projected with further optimization of the fabrication processes.

High Performance Analog Fiber Link Using Semiconductor Waveguide Modulator and Detectors

P. K. L. Yu

Department of Electrical and Computer Engineering

University of California, San Diego

La Jolla, CA 92093-0407

E-mail: yu@ece.ucsd.edu

Abstract

Optical transmission of analog signals has potential use in high-speed antenna remoting and RF distribution systems. Depending on bandwidth, dynamic range, noise figure, and cost requirements, either direct modulation of a laser diode or external modulation using a waveguide modulator is used. External modulation is typically used for the most demanding broadband link applications. However, two problems continue to plague the use of waveguide modulators, the limited linear dynamic range and the RF efficiency. Improvement in these two areas would provide attractive alternatives for several applications that could benefit from using high fidelity, optical analog links. The majority of studies on improving the linearity of optoelectronic modulators have been geared toward the lithium niobate modulators. Recent works make use of parallel modulation, mixed polarization, or other feedforward compensation schemes that cause partial cancellation of the nonlinear components.

In this paper, we present the results of InGaAsP electroabsorption waveguide modulator for high two-tone spur free dynamic range (SFDR) and high RF efficiency. The approach we adopt is to low-bias the modulator. The advantages of low bias are two-fold. First, the third-order intermodulation distortion is suppressed as the bias approaches a point on the transfer curve that has a null in a given third derivative. Second, the link gain increases when excess optical power is used to compensate the optical loss through low-biasing. Multi-octave SFDR of 107 dB per hertz and suboctave SFDR of 128 dB per hertz have been obtained for a link using the waveguide modulator, and the link RF gain is -17.8 dB, at an input power of 43 mW.

With increasing optical power in the link, the performance of the detector becomes critical. It is important that the photodetector does not saturate under the large optical intensity. In the second half of this talk we present the results on high speed waveguide photodetector for high saturation optical power.

The basic waveguide detector consists of a rib loaded PIN waveguide on semi-insulating InP. The intrinsic layer of the photodetector is 0.45 μm thick and the waveguide rib is 5 μm wide and is approximately 20 μm long. The photodetector has a responsivity of 0.4 A/W and a leakage current of 25 nA at a bias voltage of - 6 V. The detector bias is -6 V and the 3 dB roll-off frequency is 39 GHz. A peak power of 76 mW at a peak photocurrent of 32 mA is measured with a four-layer asymmetric waveguide photodetector.

Progress in Electromagnetics Research Symposium, PIERS 1997 ISBN 962-442-097-1

Progress in Semiconductor Optoelectronic Components for Microwave and Millimeter Wave Signal Distribution

J.C. Brock
TRW Space and Electronics Group
MS D1-1024, 1 Space Park, Redondo Beach, CA, 90278, USA

Recent advances in the performance of laser sources, optical modulators, and photodetectors have now made practical the distribution and processing of broadband microwave and millimeter wave signals on optical carriers. This capability is extending the addressable frequency range of signal processors and phased array antennas to the millimeter and submillimeter spectrum, and may enable large millimeter wave arrays for imaging systems

This paper discusses progress on two key III-V semiconductor device technologies that can result in high levels of integration and straightforward manufacturability of optical microwave and millimeter wave signal distribution networks. These semiconductor components may also prove to be capable of monolithic integration with pre-and post MMIC electronic components.

The first device technology to be discussed is high frequency analog optical modulation using electroabsorption in multi-quantum well semiconductor waveguides. The emphasis will be on modulators optimized for high linearity and low electrical insertion loss. Experimental results and analytical projections on important parameters such as drive voltage, optical throughput, and optical power handling capability will be presented. Potential modulation bandwidth for lumped element and travelling wave devices will also be discussed.

The second device technology to be discussed will be semiconductor optoelectronic integrated circuits for fanout distribution in optical-RF signal networks. Presented will be results on the Microwave Optical Splitter/Amplifier Integrated Circuit (MOSAIC), a 1x4 optical distribution chip with integrated optical amplifiers to mitigate the impact of optical losses on electrical performance. Current performance status and technical challenges for improving electrical signal fidelity will be reviewed.

Recent Progress in Millimeter Wave Antennas

A. Basu and T. Itoh
Dept. of Electrical Engineering
UCLA
Los Angeles, CA 90095-1594
U. S. A.
e-mail: itoh@ee.ucla.edu

Recent interest in millimeter wave technology to applications beyond the traditional military components and systems has enlarged the scope of millimeter-wave antennas as key components to reduce the cost while increasing the functionality and performance. The antenna is particularly important for millimeter wave systems, where the electronic functions of typical semiconductor devices deteriorate as the frequency is increased. The antennas are required to be of low loss, high gain and easily integrated with the RF front end. In this paper, some of the recent work for the millimeter wave antenna will be reviewed.

This talk consists of two parts. The first part is concerned with integrated antennas and in particular active integrated antennas. These antennas conform to a growing demand for the entire RF front end made of integrated circuits. These antennas are typically planar and easily interfacing with the integrated circuits, either monolithically or in a hybrid form. Active integrated antennas provide substantial electronic functionality to otherwise passive antennas. For instance, the active integrated antenna can be an oscillator or an amplifier with its output terminated by free space instead of 50 Ω. Since the typical interconnect between the antenna and the RF front end is eliminated, the insertion loss is reduced in the entire system.

The second part of the talk deals with a specific antenna development. Specifically, a leaky wave antenna for millimeter wave imaging is described. This antenna is made of dielectric waveguide technology and is intended for use at 94 GHz and another version at 212 GHz. The basic operating principle, choice of materials, fabrication techniques and design data are described. The results of experimental demonstration including the near field measurement are presented. Finally, the rigorous full-wave three-dimensional analysis is discussed. It is pointed out that the conventional design method based on the unperturbed dielectric waveguide could have significant design error.

Manufacturing Issues of Millimeter-Wave Filters and Diplexers

Y.C. Shih
Hughes Space & Communications Company
P.O. Box 92919, M/S: SC/S12/W327
Los Angeles, Ca 90009

Abstract

The microwave industry has been predicting massive mm-wave system applications in the past twenty years. The recent market demands in high data-rate wireless communications and short range automotive sensors have finally "discovered" the available frequency band at millimeter wavelength. The question at hand is: can we manufacture the mm-wave systems at large volumes with an affordable cost?

In this presentation we will examine the manufacturing issues related to the filters or diplexers which are almost always appear at the front-end of the system, right next to the antenna feed. To achieve the high-Q, low-loss requirement at mm-wave frequencies, waveguide E-plane filters or direct-coupled-cavity filters are the prime candidates. We will first describe an analysis procedure based on a mode-matching method in conjunction with the generalized scattering matrix technique. The analysis is theoretically exact and numerically very efficiency. It takes into account the thickness of the septa or the iris windows, as well as the higher-order mode couplings between them. We will then use this rigorous analysis to study the sensitivity of the filter's frequency response with respect to the dimensional variations in the septum lengths, window openings, and resonator lengths. From the worst case study, we conclude that the filter response is more sensitive to the random errors than to the systematic errors. Since the manufacturing process of the E-plane filters tend to minimize the random errors, it is a more robust design for high volume batch production. The result of our study should serve as a good guideline in developing a manufacturing method for a high-yield, low-cost production.

Progress in Electromagnetics Research Symposium, PIERS 1997 ISBN 962-442-097-1

Novel Illuminated FET Model and Optically Controlled LU-FET Oscillator

Shigeo Kawasaki

Tokai University
Department of Communications Engineering
1117 Kita-Kaname, Hiratsuka, Kanagawa 259-12 Japan

Recent development of microwave and millimeter-wave technologies plays an important role to realize a multi-media network system consisting of a wireless communication system and an optical fiber communication system. For unification of these two communication systems, microwave-optics interaction is very attractive. This phenomenon inherently happens in the Monolithic Microwave Integrated Circuit (MMIC) incorporated with semiconductor devices.

One of the promising effects from the circuit operation is a photoconductive effect resulting from a photo-current generation mechanism. Due to this effect, gain of an amplifier in the MMIC can be controlled. In addition to this effect, photo-generated carriers make lower the barrier of the Schottky contact involved in the MMIC, corresponding to illumination intensity. As the result, an operating condition is changed by this photovoltaic effect and this change results in variation of characteristics of the MMIC such as tuning of the operating frequency of an MMIC oscillator. By making use of these phenomena, a microwave photonic integrated circuit for the terminal of the wireless LAN constructed by optical fiber can be realized such as an optical-microwave/millimeterwave transducer with light weight, low cost, high efficiency and high speed.

Standing on this view point, S-parameters of the illuminated MESFET were measured in the range of 45 MHz to 30 GHz as fundamental data and compared with those from the non-illuminated MESFET. The MESFET used is a self-aligned GaAs MESFET with a 0.2 μm long and 100 μm wide gate provided by NTT LSI Laboratory.

Using a microwave circuit simulator, first, the illuminated MESFET was characterized with a typical MESFET model. For easily finding variation on the FET model parameters, the Y-parameters from analyzed region consisting of the intrinsic region and the drain-source capacitance due to the substrate were examined. From observation of the Y-parameter, it was found that, by the illumination, strong frequency dependence of the output resistance was enhanced up to 30 GHz. In addition, the pinch-off voltage of the drain current became ambiguous resulting from the photo-current. Based on these data, a new model for the illuminated MESFET with the frequency dependence of Rds by adding a capacitance connected in series was proposed. Using this new model, theoretical curve and the experimental one of Y-parameters were compared. The agreement between them became good.

As a next step, illumination on an oscillator using a line unified FET (LU-FET) with the MESFET above was carried out. The LU-FET oscillator provided by NTT Wireless System Laboratory operated at 9.65 GHz. Since illuminated area was enlarged when the LU-FET was used in the oscillator, a wide tuning range was obtained compared with its electrical tuning range.

From them, fundamental data for a design of a light-weighed, low-cost and high-efficient optical-millimeter wave transducer were obtained.

SESSION 6P13

Monday, January 6, PM 1330-1710, Lecture Theatre 13, City University of Hong Kong

RF and Microwave Circuits 1

Organizers: M S Leong, Le Wei Li

Chairperson: M S Leong, National Univ. of Singapore
Co-Chairperson: Le Wei Li, National Univ. of Singapore

13:30 ***Calculations of Energy Deposition in a Human Head Caused by MRI-RF Coils*** 58
Yoshitsugu Kamimura, Yoshifumi Yamada
Utsunomiya University

13:50 ***Antennas Integrated with Microwaves Solid-State Devices*** 59
*Shyh-Jong Chung, **Kai Chang
*Chiao Tung University, Hsinchu
**Texas A&M University

14:10 ***Design of Microstrip Rectangular Disk Quadrature 3dB Hybrids*** 60
Tadashi Kawai, Yoshihiro Kasuya, Yoshihiro Kokubo, Isao Ohta
Himeji Institute of Technology

14:30 ***A New Empirical Nonlinear Model for MESFET*** 61
B L Ooi, M S Leong, P S Kooi
National University of Singapore

14:50 ***Calculation of Longitudinal Current Distribution Over Microstrip Circuits Using Reaction Iterative Method*** 62
L W Li, M S Leong, P S Kooi, T S Yeo, Y L Qiu
National University of Singapore

15:10 **Break**

15:30 ***Thevenin Equivalent Circuit and Scattered Power of a Receiving Wire Antenna*** 63
K Hirasawa, A Sato, Y Ojiro, T Morioka, S Shibasaki
University of Tsukuba

15:50 ***Investigation of RF Solution for Software Radio*** 64
Ke Gong, Pengyu Shi
Tsinghua University, Beijing

16:10 ***FDTD Characterization of Spiral Inductors for Silicon-based RF Circuit*** 65
Jie Xu, Olli Pekonen
Nokia Research Center

16:30 ***Accurate Modeling GaAs MESFETs for Wireless Communication Power Amplifier Design*** 66
*J Cao, **F J Lin, *P S Kooi, *M S Leong
*National University of Singapore
**Institute of Microelectronics

16:50 ***Design and Experiment of a 60GHz Imaging Array on Optimized Multilayer Substrates*** 67
*Yongxi Qian, *Tatsuo Itoh, **Eikichi Yamashita
*UCLA
**University of Electro-Communications

Calculations of Energy Deposition in a Human Head Caused by MRI-RF Coils

Yoshitsugu KAMIMURA and Yoshifumi YAMADA

Department of Information Science, Utsunomiya Univ.
2753 Ishii-cho, Utsunomiya 321, Japan

Abstract

The patient is exposed to radio frequency (RF) magnetic field when diagnosed by magnetic resonance imaging (MRI). With advancing the technique of MRI, the RF energy absorption in the patient's body is increasing. Therefore it is important problem to discuss about safety of MRI-RF exposure.

Grandolfo et al. calculated the specific absorption rate (SAR) in a human torso by the three-dimensional impedance method in 1990. They obtained also the empirical expression for the frequency dependence of the average SAR. However, the frequency dependence of SAR in human head has not been calculated yet, as far as the authors know.

We calculate the frequency dependencies of the average and peak SAR in a human head by analytical method using a homogeneous spherical model, and compare our results to Grandolfo's work.

The solenoid coil with radius of 15 cm and length of 20 cm are adopted as the RF coil. The dielectric parameters of 2/3 muscle model is used. The radius of sphere is 10 cm. The electric (E-) fields inside sphere are expressed using the vector wave functions. SARs are calculated from squared E-field strength inside body.

As a result, we get $f^{2.10}$ and $f^{2.08}$ dependence for average and peak, respectively, in the frequency range 1 MHz - 100 MHz. These results approximately equal to $f^{2.07}$ dependence for the average SAR in human torso calculated by Grandolfo et al.

Progress in Electromagnetics Research Symposium, PIERS 1997 ISBN 962-442-097-1

Antennas Integrated with Microwaves Solid-State Devices

Shyh-Jong Chung
Dept. of Communication Eng., Chiao Tung Univ.
Hsinchu, Taiwan, ROC

Kai Chang
Dept. of Electrical Eng., Texas A&M Univ.
College Station, TX77843-3128, USA
Tel: (409)845-5285 Fax: (409)845-6259
E-mail: chang@eesun1.tamu.edu

Abstract

Integrated and active integrated antennas receive a great deal of attention because they can reduce the size, weight, and cost of many transmit and receive systems. Passive devices and active solid-state devices can be configured to provide several component functions at the terminals of the antenna. Active solid-state devices, for example, can be used to design active integrated antenna oscillators, amplifiers, and multipliers. These active integrated antennas are ideal for current investigations in spatial and quasi-optical power combining. The topic is intriguing since it involves several different areas of microwave engineering (i.e. solid-state devices, circuits, components, and antennas). Knowledge of circuit integration issues, component specifications, and material characteristics is also important.

Combination of guided-wave circuits with radiating structures in integrated antennas often leads to several performance trade-offs. Material properties that enhance circuit performance often degrade antenna radiation while DC biasing circuits and device packages disturb antenna characteristics. Similarly, an antenna's radiation may degrade a component's performance. Furthermore, component functions are connected directly to free space with little opportunity for non-quasi-optical processing or filtering. Overcoming these difficulties will allow integrated antennas to meet system requirements in military and commercial applications.

In the design of integrated antennas, the antennas play not only the role of radiators but can also share part of the component functions. They can be used as resonantors, feedback networks, power dividers, etc. The multiple use of the antennas can certainly reduce the circuit space and fabrication cost, but it may also deteriorate the radiation performance of the antennas. A careful investigation about these multiple-used antennas is thus necessary. In this study, a method-of-moment analysis is used to analyze a structure containing a patch antenna and a proximity microstrip line. The power can be tapped from the antenna to the microstrip line or can be coupled from the microstrip line to the antenna. In addition to space saving of this structure, due to the resonant characteristics of the antenna, a stronger coupling may be achieved than that of a classical power coupler. The effects of the proximity microstrip line on the current distribution and thus the radiation pattern of the antenna need to be studied. The variation of the coupling coefficient with different designs of the microstrip line is also investigated. Finally, some applications of this structure, including the integration with microwave solid-state devices, are conducted.

Design of Microstrip Rectangular Disk Quadrature 3dB Hybrids

Tadashi Kawai, Yoshihiro Kasuya, Yoshihiro Kokubo, and Isao Ohta
Department of Electronics, Faculty of Engineering, Himeji Institute of Technology
2167 Shosha, Himeji-shi, Hyogo, 671-22 Japan
E-mail : kawai@elnics.eng.himeji-tech.ac.jp

1. Introduction Planar-circuit-type quadrature hybrids in a triplate structure have been proposed, and good characteristics have been realized [1]. This paper presents a design method of microstrip circuit using a modified eigenfunction expansion method with consideration for frequency-dependences of the effective strip width and the relative permittivity. Next, the validity of the approximate analysis is examined by the use of FDTD method. Experimental verification is described also.

2. Circuit configuration and design method Fig. 1 shows the circuit configuration to be considered. This circuit possesses a twofold symmetry about the planes AA' and BB', and hence can be analyzed by a twofold even-odd analysis. For a triplate-type circuit, a quasi-static approximation is sufficient to get its accuracy characteristics [2]. But, for the microstrip-type one, it is insufficient, because of the imbalance of a circuit construction. Therefore, we consider a frequency-dependence of the effective width of strip conductor as following equation [3]:

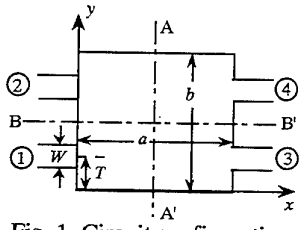


Fig. 1. Circuit configuration.

$$W_{eff}(f) = W + \left(W_{eff\,0} - W\right)/\left(1 + f/f_g\right) \quad (1a)$$

$$f_g = c_0/\left(2W\sqrt{\varepsilon_r}\right) \quad (1b)$$

where W and W_{eff} are a physical and a static effective width of the conductor, f, c_0, ε_r represent frequency in GHz, light velocity, and relative permittivity of the dielectric substrate, respectively. Furthermore, that of the effective relative permittivity is given by [4]

$$\varepsilon_{reff}(f) = \left[\left(\sqrt{\varepsilon_r} - \sqrt{\varepsilon_{reff\,0}}\right)/\left(1 + 4F_1^{-3/2}\right) + \sqrt{\varepsilon_{reff\,0}}\right]^2 \quad (2a)$$

$$F_1 = \left(4df\sqrt{\varepsilon_r - 1}/c_0\right)\left[0.5 + \left\{1 + 2\log\left(1 + W/d\right)\right\}^2\right] \quad (2b)$$

where ε_{eff0} indicates a static effective permittivity, and ε_r a relative permittivity of the dielectric substrate.

We try to analyze and design a 3dB hybrid by expanding a Green's function in terms of eigenfunctions with eqs. (1) and (2). In this design, ε_r and d are chosen as 10.3 and 0.635 mm, respectively, in connection with experiment. Fig. 2 shows the frequency characteristics of S-parameters of the hybrid designed at a center frequency of 8 GHz.

3. Analysis by FDTD method To analyze the circuit property strictly, we apply the method of FDTD [5]. Fig. 3 shows the S-parameters calculated using this method.

4. Experiment In order to confirm the theoretical results, a circuit corresponding to that shown in Fig.2 was made as a trial. Fig. 4 exhibits the magnitude of S-parameters with HP's 8510B network analyzer. This result agree comparably with the computational result shown in Fig.3.

5. Conclusions A method of designing the microstrip-type 3dB quadrature hybrid by the use of a modified eigenfunction expansion has been described. Using this method, we can simply design the microstrip circuit.

Preferences [1] T. Kawai & I. Ohta : *IEEE Trans.*, **MTT-42**, 12, p.2462, Dec. 1994. [2] T. Okoshi : "Planar Circuits," p.32, Springer-Verlag, Berlin, 1985. [3] G. Kompa & R. Mehran : *Electron. Lett.* 11, p.459, 1975. [4] E. Yamashita et. al : *IEEE Trans.*, **MTT-27**, 12, p.1036, Dec. 1979. [5] D. Sheen et. al : *IEEE Trans.*, **MTT-38**, 7, p.849, July 1990.

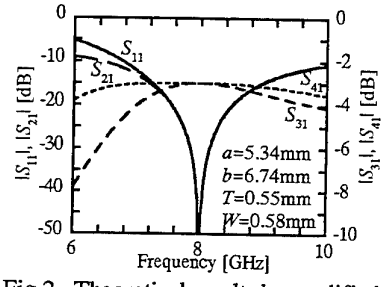


Fig.2. Theoretical results by modified eigenfunction expansion method.

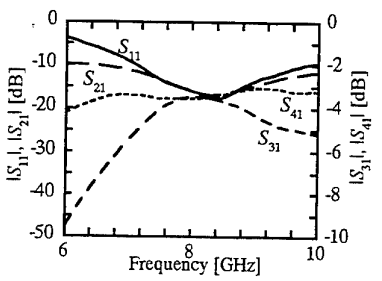


Fig.3. Theoretical results by FDTD method.

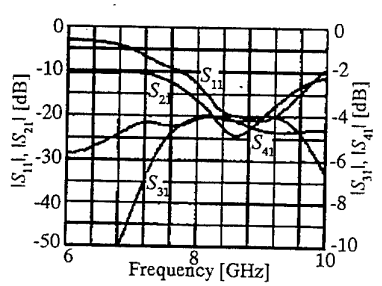


Fig. 4. Experimental results.

A New Empirical Nonlinear Model For MESFET

B. L. Ooi, M. S. Leong and P. S. Kooi
Communication and Microwave Division
Department of Electrical Engineering
National University of Singapore
Singapore 119260, Tel: 7722134, Fax: 7791103
E-mail: blooi@eeserver.ee.nus.sg

Abstracts

Since most active microwave circuits contain nonlinear solid-state devices such as MESFET's or HEMT's, an accurate tool for predicting their nonlinear characteristics such as intermodulation distortion is required. Of all the existing modeling techniques, the empirical modeling technique still plays an important part because of its simplicity and easy implementation in CAD. Numerous empirical models, such as the Curtice model [1], Statz model [2], Materka and Kacprzak model [3] and Angelov model [4] have been developed. In all these models, certain simplified assumptions such as modeling the gate current with the Shockley equation, and ignoring the contribution of $I_{gs}(V_{ds},V_{gs})$ in I_{ds} evaluation have been made. These approximations are often not well-studied and can result in significant errors in the evaluation of the large-signal equivalent circuit elements, namely: I_{ds}, g_m, R_{ds}, C_{gs} and C_{ds}.

It is thus the intention of this paper to study the effect of these assumptions on the extracted large signal equivalent circuit elements. Several empirical models such as the Curtice model [1], Statz model [2], Materka Kacprzak model [3], and Angelov model [4] are adopted for disscusion. A new analytical expression for the modeling of the gate current I_{gs} characteristic is also derived for comparison. Measured and modelled gate current with and without the assumptions are compared. It is found that the application of this new analytical gate current expression in all the above-mentioned models provides the least error. With this new expression and for the first time, some empirical closed form expressions for the components G_{11} and G_{12} of Corbella's work [5] are also presented.

References

1. W. R. Curtice, "A MESFET model for use in the design of GaAs integrated circuits", IEEE Trans. Microwave Theory Tech., vol. MTT-28, pp. 448-456, May 1980.

2. H. Statz et. al., "GaAs FET Device and Circuit Simulation in SPICE", IEEE Trans. Electron Dev., vol. 34, pp. 160-169, Feb 1987.

3. A. Materka and T. Kacprzak, "Computer calculation of large signal GaAs FET amplifier characteristics", IEEE Microwave Theory and Tech., vol. 33, pp. 129-135, Feb 1985.

4. I. Angelov, H. Zirath, and N. Rorsman, "A new empirical nonlinear model for HEMT and MESFET devices", IEEE Trans. Microwave Theory and Tech., vol. 40, pp. 2258-2266, 1992.

5. I. Corbella, J. M. Legido and G. Naval, "Instantaneous model of a MESFET for use in linear and nonlinear circuit simulations", IEEE Trans. on Microwave Theory Tech., vol. 40, pp. 1410-1421, 1992.

Calculation of Longitudinal Current Distribution Over Microstrip Circuits Using Reaction Iterative Method

L.W. Li, M.S. Leong, P.S. Kooi, T.S. Yeo, Y.L. Qiu
Communications & Microwave Division, Department of Electrical Engineering
National University of Singapore, 10 Kent Ridge Crescent, Singapore 119260
Phone: (+65) 772 6658; Fax: (+65) 779 1103; Email: eleLiLW@nus.sg

Technique to be developed

In this paper, a technique referred to as the Reaction Iterative Method (RIM) is further developed based on the work by Gary A. Thiele et al. to calculate the surface current distributions on microstrip lines and circuits. In this technique, the dyadic Green's function (DGF) for various geometries is used as a kernel to represent the electromagnetic field in the area of interest in terms of a series of reactive effects during the field-feedback procedure.

Procedure of Formulation

A constant current distribution is assumed at the beginning. This current distribution will excite waves into the space. Therefore, there will be electromagnetic field surrounding the microstrip circuits. Due to the feed-back of the fields, the uniform current distribution will be distorted causing a new distribution to form. The change of the distribution will vary the field in the space and will further distort the current until the current distribution and electromagnetic fields reach an equilibrium state.

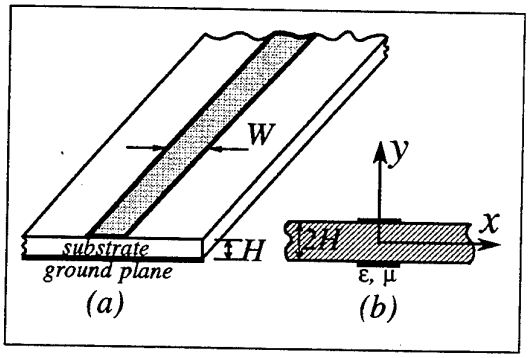


Figure 1: Geometry of a microstrip line flush-mounted on a substrate over the ground plane. (a) An illustration of the geometry, and (b) the equivalent problem by the use of the image theory.

Application to Microstrip Line

As an application of this technique, a microstrip line is considered (see Fig. 1). The current distribution is found by using the DGF and the method where both the electromagnetic fields and current distribution are derived. Comparison of the centre-normalized current distributions is made between the results obtained here and that given by Kobayashi.

In actual computation, the iteration is truncated as soon as the expected accuracy is achieved. The advantages of this method as compared to the Moment Method are that it applies to all the radiation problems regardless of the antenna dimensions and that one can gain an insight into the intermediate physical process and parameters. Besides, it provides an exact solution for the realistic problem by means of a full-wave analysis. As compared with those of Thiele, this method is straightforward.

References

[1] Gary A. Thiele et al., *IEEE Trans. Antennas Propagat.*, vol. 30, pp. 888-897, 1982; vol. 33, pp. 1272-1279, 1985; vol. 34, pp. 1038-1045, 1986; and vol. 34, pp. 1173-1180, 1986.

[2] M. Kobayashi and K. Takaishi, *IEEE Trans. Microwave Theory and Tech.*, vol. 42, pp. 866-869, 1994.

Thevenin Equivalent Circuit and Scattered Power of a Receiving Wire Antenna

K. Hirasawa, A. Sato, Y. Ojiro, T. Morioka and S. Shibasaki
Institute of Information Sciences and Electronics
University of Tsukuba
Tsukuba, Ibaraki 305, Japan

It is well-known that a receiving antenna can be expressed as a Thevenin equivalent circuit with the input impedance Z_{in} of the antenna, a load impedance Z_L and an open-circuit voltage V_0 in a series. The power P_{re} consumed at Z_L is the received power of the receiving antenna and the power P_{sc} consumed at Z_{in} is said to be the scattered (or re-radiated) power from the receiving antenna. Thus when Z_L is equal to the complex conjugate of Z_{in} , P_{re} is equal to P_{sc} and it is expected that the received and scattered power are equal.

In [1] the received and scattered power of a center-loaded straight wire antenna are calculated by the method of moments and the relationship between those powers are investigated. Then it is found that when the antenna length is less than 0.8 wavelength, the received and scattered power are equal for the conjugate-matched antenna. In this case the real part of Z_{in} becomes the re-radiation resistance and the scattered power can be calculated simply from the Thevenin equivalent circuit.

In this paper we consider more general cases such as loops and Yagi-Uda dipole arrays, and investigate the relationship between the received and scattered power for various load points, load impedance values and plane wave incident angles. Then we discuss the validity of the Thevenin equivalent circuit to calculate the scattered power. From the input impedance and current distribution of the receiving antenna we investigate the reason why the received and scattered power are not always equal, even if the antenna is conjugate-matched. Also we show that in general the scattered power cannot be calculated from a Thevenin equivalent circuit.

Reference

[1] K. Hirasawa et al. , "Received and scattered power of receiving antenna," IEEE APS International Symposium, pp.205-208, June 1994.

Investigation of RF Solution for Software Radio

GONG Ke & SHI Pengyu
The State Key Laboratory on Microwave & Digital Communications
Tsinghua University Beijing 100084 China
Fax: (8610)62564176, Email: gongke@sun.ihep.ac.cn

1. INTRODUCTION

To meet the requirement of integration of wireless technologies to provide global Personal Communication Services, Software Radio becomes a hot topic which is based on the ever powerful digital signal processing and frontiers the wireless technology towards the 21st century. However, in the available Software Radio's literature, the RF transceiver is simply represented by "RF converter" without any further description. This paper briefly survey the state of the art RF techniques from the viewpoint of Software Radio, it shows the RF would be a bottle neck of developing Software Radio.

2. ANALYSIS OF TYPICAL RF FRONT-END CONFIGURATION

The challenging of Software Radio to the RF techniques could be summarized by the following keywords: variable working band, multimode T/R duplex, adjustable output level, etc., in short, all hardware realized specifications should be "on-line" adjustable by software. Keeping this in mind, the state of the art RF front-end techniques are analyzed include transmission part, receive part, local oscillator, antenna and duplexes, etc. It is found that the filters , the duplexes, the power amplifiers are the most "hard" specified parts which are hardly met the requirements of the Software Radio..

3. PROPOSED OPTIONS OF MULTIMODE RF TRANCEIVER

Based on the above analysis and a survey of the recent available RF techniques, proposals are made to transmitter, receiver, local oscillator, duplexer and antenna solutions. Discussions are mainly dealing with the comprimization of the contradictory requirements such as fast frequency setting and fine carrier frequency adjustment, FDD and TDD, large dynamic power range and high power efficiency, variable bandwidth and sharp edge of passband, etc. It is point out that to build general software specified RF front-end is economically not suitable, while given multimode ones such as GSM/DCS1800, DECT/DCS1800, AMPS/QCDMA, etc. are not only required by the market but also technical realizable.

4. COMMENTS AND DISCUSSIONS

To conclude the discussion of the Software Radio's RF front-end, some comments are made to the key technology for multimode RF front-end and application issues of multimode terminals.

References:

[1] IEEE Communications Magazine, May 1995

FDTD Characterization of Spiral Inductors for Silicon-based RF Circuit

Jie Xu, Olli Pekonen
Nokia Research Center
P.O. Box 45, 00211 Helsinki, Finland

Abstract—Growing needs to reduce cost in mobile telecommunication industry has boosted widespread research interests in exploring the potential of digital silicon technology for analog circuit designs. The most challenge work in RF MMIC designs, however, is the design of high-Q passive components rather than active devices. One of the most notable devices is the spiral inductor. While accurate models for both active and passive components are vital for a successful MMIC design, there are few accurate models for spiral inductors available to MMIC designers at the moment. In this work the finite-difference time-domain (FDTD) method is employed to characterize spiral inductors manufactured by standard silicon IC technology.

A spiral inductor in compatible with standard digital IC technology commonly uses Metal layer 2 (M2) for inductor spiral and Metal layer 1 (M1) as a connection to another end of the inductor. The minimum dimension of the structure considered in this work is in the range of 0.5 *um* and the maximum 500 *um*. The conventional uniform Yee-cell FDTD method is apparently not suitable for modeling such structures with so large a geometrical ratio, without resorting to huge amount of memory. While it is not possible to utilize sub-cell technique to model complex details of the considered structure, an FDTD code employing the orthogonal non-uniform technique has been written to complete the modeling task. The FDTD code features include full consideration of both conductor losses and substrate losses, variable cell sizes, Mur boundary condition, transparent current excitation scheme and post-processing capability to generate S-parameter data from time-domain results with infinite frequency resolution.

As a case study, a two-turn rectangular spiral inductor has been modeled for the purpose of verification of the FDTD code. The inductor is compatible with standard BiCMOS process and also relatively small thus serves the purpose. The width of layer M2 is 10 *um* and the center feeding line is served by layer M1 with the same width. A perfect PEC contact is assumed between M1 and M2. The outer dimension of the spiral is 80 *um* and spacing between metal traces is 4 *um*. The cell size in the FDTD domain ranges from 0.5 *um* to 2 *um*. The structure is excited at one port by a current source with 50 ohms resistance and another 50 ohms resistor is put at the other port as load. FDTD data has been found to agree very well with measurement results. Full comparisons between simulations results and experimental data will be presented in the symposium.

References

[1] H. Rokainen, et al, "IC compatible planar inductors on Silicon," *submitted to IEE Proceeding, Part. G*, Mar. 1996.

Accurate Modeling GaAs MESFETs for Wireless Communication Power Amplifier Design

J. Cao, F. J. Lin*, P. S. Kooi , M. S. Leong

Department of Electrical Engineering
National University of Singapore
10 Kent Ridge Crescent
Singapore 119260

*Institute of Microelectronics
11 Science Park Road, Science Park II
Singapore 117685

Recently, GaAs MESFET devices are utilizing in RF power amplifiers for wireless communication products. Due to the nature for wireless communication products of low current consumption, high efficiency and high power, large signal MESFET's models are employed to obtain the optimal performance. For industrial users, several harmonic balance simulators (e.g., Libra, Microwave Harmonica, MDS) are commercially available. In these software's, large signal models are already implemented, such as the Curtice models, the Statz model, the HP Roots model. But actually problems are still facing for the users: (1) the selection of the large signal model (2) the model consistency (3) the verification method . Solutions for these problems are examined in this paper.

A large signal model for power amplifier should accurately describe following characteristics: DC I-V characteristics, S-parameters at all working bias points and frequencies, the output power and harmonics as a function of frequency, input power, bias and load impedance. Besides, the model should be simple and the extraction procedure should be practical.

Two popular models are selected to model GaAs MESFET to implement RF power amplifier design. One is the Curtice cubic model which is a typical empirical model and the other is HP Roots model which is a measured data model. The measured data up to 26 GHz , including DC I-V characterization and on-wafer S-parameters required for the modeling, are obtained by ICCAP. The large signal model parameters of the two models are extracted for a 0.5x670 μm MESFET. The s-parameters of measured are compared with the simulated data by the two models for the same transistor. The comparison shows that the slight difference for the S-parameters for the same transistor, especially at high frequency.

A 1-watts RF power amplifier working at 1.9 GHz (such as in the mobile frequency band) is designed implementing the two large signal models separately. To compare the two models, same bias conditions are set within the simulation. The physical sizes of the match circuit are same also. The simulations are performed by MDS. Performance of the power amplifier predicted by the Curtic cubic model and HP Roots model are obtained.

The output power, efficiency, harmonics as a function of bias, frequency, input power of the power amplifier predicted by the two models are carefully compared. The study shows that the improvements are needed for the following problems: (1) Model consistency. (2) Bias dependent self-heating correction for the drain -source current. (3) The frequency dependency of the HP Roots model.

Progress in Electromagnetics Research Symposium, PIERS 1997 ISBN 962-442-097-1

Design and Experiment of a 60GHz Imaging Array on Optimized Multilayer Substrates

Yongxi Qian and Tatsuo Itoh
Electrical Engineering Department IV, UCLA
405 Hilgard Ave., Los Angeles, CA 90024, U.S.A.

Eikichi Yamashita
Department of Electronic Engineering
University of Electro-Communications
1-5-1 Chofugaoka, Chofu, Tokyo 182, Japan

ABSTRACT

Development of millimeter-wave focal plane imaging arrays has been a topic of intensive study by a number of research groups around the world during the past 10-15 years. These imaging array systems possess such unique capabilities like penetration through fog, rain and even clothes, as well as higher spatial resolution than microwave systems. Potential applications include automobile collision avoidance radars, all-weather landing systems, airport security- check systems and many others.

While several recent reports have demonstrated very exciting results which show the capabilities of MMW focal plane imaging arrays, there are still a number of issues to be fully addressed for practical realization of compact, high performance imaging systems. In particular, designing of antenna elements which satisfy all the requirements in a two-dimensional array environment is one of the most important and challenging topics, where much work still needs to be done in the future.

After a brief review of the present status of MMW imaging arrays, we will make a detailed description of a 60GHz focal plane imaging array which uses CPW-fed twin-slot antennas on multilayered dielectric substrates. This is an all-planar structure without having to use an accompanying superhemispherical substrate lens which commonly appears in most of the imaging array systems proposed so far. Our design features a carefully designed CPW-fed twin-slot antenna on top of a dielectric stack with optimized substrate thickness, which results in a symmetrical radiation pattern, low surface wave loss, as well as a controllable beamwidth in order to match the f-number of the objective lens. Optimal design of the quasi-optical receiver is accomplished by using FDTD analysis results for the CPW-fed slot. Other factors such as crosstalk between neighboring antenna elements have also been considered in the design process.

After a rigorous characterization of the electromagnetic properties of the proposed antenna structure, we fabricated a 6-element array and developed a 60GHz experiment system to test its imaging capability. In combination with mechanical scanning, we have been successful in obtaining imaging results for some simple targets such as two parallel acryl bars and a triangular metal plate, both with dimensions in the order of 10cm. This all-planar imaging array is in good compatibility with MMIC technology, and should provide a way of realizing MMW imaging systems at greatly reduced cost.

SESSION 6P12

Monday, January 6, PM 1330-1650, Lecture Theatre 12, City University of Hong Kong

Radar

Organizer: H D Griffiths

Chairperson: H D Griffiths, University College London
Co-Chairperson: Chris Oliver, Defence Research Agency

13:30	***Waveform Design for Satellite Borne Meteorological Radars*** H D Griffiths, L Vinagre University College London	69
13:50	***Review - Information from SAR images*** Chris Oliver Defence Research Agency	70
14:10	***Backscattering Models of Aircraft for Millimetre - Wave Radar Imaging*** Gaspare Galati, Fausto Marti, Maurizio Naldi TorVergata University of Rome	71
14:30	***Large Bandwidth HF Radar Waveforms with Discontinuous Spectra*** S P Kingsley, S D Green The University of Sheffield	72
14:50	***SAR Interferometric Performance Analysis*** Julian Wilson, Stefano Palumbo Estec, Keplerlaan 1	73
15:10	**Break**	
15:30	***Fractal Models of Scattering from Natural Bodies*** *Giorgio Franceschetti, **Maurizio Migliaccio,*Daniele Riccio *Università di Napoli Federico II **Istituto Universitario Navale	74
15:50	***An Overview of Australian HF Radar Research*** S J Anderson Defence Science and Technology Organisation	75
16:10	***Tropospheric Refraction Errors in Radar Target Coordinates*** Ahmed K. Aboul-Seoud, Hanaa M Rashwan, Ahmed E Shaalan Alexandria University	76
16:30	***Non-Gaussian Properties of HF Sea Clutter*** S J Anderson Defence Science and Technology Organisation	77

Waveform Design for Satellite Borne Meteorological Radars

Professor H.D. Griffiths
Mr L. Vinagre
Department of Electrical and Electronic Engineering
University College London
Torrington Place
London WC1E 7JE
UK

Rainfall measurements from spaceborne rain radars present several advantages over current passive techniques, due to the radar capability to discriminate backscattered energy in range. Two spaceborne meteorological missions have already been specified in detail by the U.S.A. and Japan, and by France: TRMM (Tropical Rainfall Measurement Mission) and BEST (Bilan Energétique du Système Tropical). However, the system configuration imposes stringent design requirements in order to guarantee rain detectability, in particular to the radar waveform. Since power is severely restricted on board a satellite, it is necessary to achieve efficient range resolution with low transmit power requirements. Pulse compression theory solves the previous conflicting demand, but the signal needs to be carefully designed in order to allow the significantly large dynamic range (approximately 60 dB) needed to carry out the measurements.

The ouput of a perfectly matched linear FM radar system gives a compressed pulse of a $\mathrm{sinc}(x)$ shape, with a -13 dB sidelobe level. In most applications this sidelobe level does not guarantee a sufficient dynamic range to avoid weak signals (cloud and rain return) being obscured by stronger targets (Earth surface return). Radar FM sidelobe reduction signal processing techniques reported in the literature (amplitude or frequency weighting and nonlinear FM signals) fail to attain a suitable low sidelobe pattern for the spaceborne meteorological radar scenario.

Predistortion functions applied to linear FM signals considerably reduce Fresnel ripples in the signal spectrum. The study of the crosscorrelation properties of predistorted linear FM signals has lead to the development of a novel numerical method for the optimization of the compressed pulse range sidelobe level which improves the original design technique and achieves sidelobe levels of -63 dB, showing significant robustness to Doppler frequency offsets up to hundreds of kHz.

Several options for the provision of a rainfall mode for the RA-2 Radar Altimeter (due to fly on ESA's ENVISAT satellite) are also presented. The fact that meteorological information is only present before the surface return suggests that an asymmetric point target response could be employed since overlapped rainfall can be detected with a significantly lower dynamic range. If most of the energy of the compressed pulse could be displaced to the lower side of the main lobe where there is no rain data, even better performance should be achievable.

Progress in Electromagnetics Research Symposium, PIERS 1997 ISBN 962-442-097-1

Review - Information from SAR images

Prof. Chris Oliver

Defence Research Agency, St Andrews Road, Malvern, Worcs., WR14 3PS, UK.
Tel. 01684 895165; Fax 01684 894481; e-mail chris@sar.dra.hmg.gb

This paper comprises a review of methods for extracting information from SAR images. We begin by providing a strict definition of 'Information' in the context of SAR image exploitation. This combines physical and phenomenological with data and world models, usually expressed in terms of probability distributions characterised by a few parameters. We show the importance of adopting optimum (Maximum Likelihood or Maximum a Posteriori) estimators. Information can then extracted either from an optimised measure for the appropriate parameter or by rigorous likelihood analyis based on the probability distributions.

Throughout the presentation a series of models will be introduced. In each case these will be exploted rigorously to provide a SAR image exploitation capability. Initially we illustrate optimised cross-section estimation based on a speckle model. Additional information about the scene, expressed as models, is progressively incorporated to improve the exploitation capability. In terms of image intensity, this culminates with a structure-sensitive simulated annealing method capable of yielding near photographic image quality from single-look SAR images. In addition to cross-section estimation there are also applications where it would be desirable to segment the scene into regions of uniform cross-section. The optimised approach to intensity segmentation will be discussed and theoretical performance measures derived. In particular we indicate how the desired optimum image interpretation might be achieved in a segmentation process. Information can also be contained within texture. We shall indicate appropriate models to characterise SAR image texture and derive corresponding optimum texture measures which can then be exploited.

Throughout the review, images from both high-resolution airborne and low-resolution space-borne systems will be used as examples. We demonstrate what information can be extracted on the basis of a particular model. In each case we discuss the limitations of the model and indicate where the next level of sophistication might be found. Applications of intensity segmentation and texture classification will be used as illustrations of some of these concepts.

Backscattering Models of Aircraft for Millimetre- Wave Radar Imaging

Gaspare Galati *§, Fausto Marti *, Maurizio Naldi*

* TorVergata University of Rome

Via della Ricerca Scientifica

00131 Rome Italy

§ person to be contacted

telephone:++39 6 72.59.44.64

fax: ++39 6 20.26.266

E- Mail : galati@disp.utovrm.it

Abstract

A backscattering model for commercial aircraft's surfaces, such as B747, MD80 etc, based on multiple scatter-points, Physical Optics theory and random rough surface scattering is described in this paper for millimetre (95 GHz) wave applications.

A commercial aircraft is divided into multiple scattering points (about 90000 for a B747) given a 3D aircraft model by using conical, cylindrical and flat elements. The aircraft parts where there are connections between the wings and the fuselage, the tail wigs / rudder, the engines intake inlets are described by dihedrals or trihedrals. *Model of aircraft's surface and geometry of the scattering are described.*

Scattering from perfectly conducting smooth surface and from perfectly conducting random rough surface are taken into account in order to obtain the complete radiation pattern of each elementary flat plate and finally the complex echo and the radar cross section (RCS) of the considered aircraft.

Algorithm of calculus of RCS as sum of individual contributions are described.

Application of the proposed backscattering model is simulation of radar imaging of aircraft. The need for a millimeter radar signal and image simulator arises from the needs of airport surveillance by means of modern Surface Movement Radar (SMR), particularly from

- the test of target extraction algorithms
- the test of image processing algorithms
- the creation of a database of aircraft image templates from different angles of sight for cross- correlation with the real radar images (correlation is one of the most powerful techniques to extract the target orientation angle, as well as its centre of mass).

Radar simulators suited to the considered application are not available. It does not result that such a model has been implemented for frequancies above the X-band. It has been implemented on an UNIX workstation and it is made up of graphics (X Window) and calculation C language functions. It utilizes the functions to display the results.

Structure and performance of the radar simulator and examples of sequences of simulated images in an airport scenario are described in the full paper.

Large Bandwidth HF Radar Waveforms with Discontinuous Spectra

S.P. Kingsley and S.D. Green
University of Sheffield, Department of Electronic and Electrical Engineering, Mappin Street, Sheffield S1 3JD, UK

High Frequency (HF) Over-The-Horizon (OTH) radar has both civil and military applications. Such radars have been used as early warning defence systems in the past, but recently they have become effective remote sensing devices because of their ability to collect sea surface, wind, wave and tidal information. Most modern HF radar systems use large antenna arrays to gain only modest azimuth resolution and have quite poor resolution in range compared to microwave radar systems.

Range resolution for a given radar is controlled by the amount of bandwidth used. Due to the large number of users in the HF band, quiet regions of the spectrum are often limited to relatively small values (around 10kHz), which lead to narrow waveform bandwidths and thus relatively poor range resolution (typically 15km). In order to improve the radar range resolution, by increasing the bandwidth, the signal spectrum must pass through regions of strong interference from other radio traffic. To avoid a HF radar system causing high levels of interference to other users the transmitted waveform signal must have a discontinuous spectrum. Similarly to stop the return data being corrupted by strong interference from the surrounding signals, discontinuities must be introduced in to the waveform spectrum in the radar receiver system.

In this paper we examine the transmitter and receiver system hardware requirements and analyse the range/doppler performance for a HF radar operating with large bandwidth (>100kHz) discontinuous spectrum waveforms. Results will be presented for long complex doppler sensitive waveforms and short repetitive waveforms. Optimised receiver matched filters, pre-matched filter and post-matched filter data processing algorithms will also be discussed.

SAR INTERFEROMETRIC PERFORMANCE ANALYSIS

Julian Wilson (XRI), Stefano Palumbo (NWP)

Estec, Keplerlaan 1

2200 AG Noordwijk - The Netherlands

e-mail : jwilson@estec.esa.nl - spalumbo@estec.esa.nl

phone: +31-71-565-6565

fax: +31-71-565-6040

ABSTRACT

Interferometric SAR (INSAR) is a method, introduced about twenty years ago by Graham, to provide global digital topography with high spatial resolution and height accuracy.

An interferometric SAR Performance Analysis Model has been developed by the authors to evaluate interferometric engineering performance parameters. This model has been implemented as a software package suitable for a Sun computer X-windows environment. The output parameters (nearly 70), such as the phase resolution, the height resolution, the ambiguity separation height, the maximum resolvable slope, etc., are functions of other input parameters (nearly 50), including the baseline separation and orientation, the incidence angle, the surface slope, the target cross section, the antenna parameters , the system parameters (wavelength, average power, duration of pulse, chirp bandwidth, etc.). The program has been written with the graphical-mathematical toolbox IDL, which is suitable for this type of applications.

The paper describes the central algorithms employed within the program.

FRACTAL MODELS OF SCATTERING FROM NATURAL BODIES

Giorgio Franceschetti [1,2], Maurizio Migliaccio [3], Daniele Riccio [1]

[1] Università di Napoli Federico II, *Dipartimento di Ingegneria Elettronica*, Via Claudio 21, 80125 Napoli, Italy.

[2] Consiglio Nazionale delle Ricerche, *Istituto di Ricerca per l'Elettromagnetismo ed i Componenti Elettronici (I.R.E.C.E.)*, Via Diocleziano 328, 80124 Napoli, Italy. email: francesc@irece1.irece.na.cnr.it

[3] Istituto Universitario Navale, *Istituto Teoria e Tecnica delle Onde Elettromagnetiche*, Via Acton 38, 80133 Napoli, Italy. email: migliaccio@nava1.uninav.it

ABSTRACT

Fractals have been shown to be useful in modelling natural corrugations, e.g. [1] and can be used to evaluate electromagnetic scattering from natural bodies: surfaces and volumes.

We present a surface scattering model based on the Physical Optics (PO) evaluation of the scattered field: the slow components of the surface ondulations are modelled by means of planar facets whereas the fast components are described by a suitable fractal function. To this end we make use of the random Weierstrass-Mandelbrot fractal function [1]:

$$\zeta(x) = \sum_{p=0}^{P-1} C_p a^{-pH} sin[\kappa_o a^p x + \Phi_p] \quad ,$$

to describe the height variations $\zeta(x)$. Note that the formulation is limited to the one dimensional case only for simplicity of presentation. The spatial frequencies of the surface components are determined by κ_0 and by the seed of the geometrical progression a, a non-integer value [1]. The amplitude of the components is governed by the coefficients C_p and by the exponential factor which accounts for the surface roughness by means of the Hurst exponent H. The latter is directly related to the surface fractal dimension [1]. It is possible to select random and non-random amplitude and phase coefficients. Note also that classical statistical parameters have been related to the fractal ones [2]. Followingly, the scattering coefficient ρ [3] can be evaluated [2]:

$$\rho \propto 2L \sum_{m_0,\ldots,m_{P-1}=-\infty}^{+\infty} \exp(j\sum_{p=0}^{P-1} m_p \Phi_p) \prod_{p=0}^{P-1} J_{m_p}(v_z C_p a^{-pH}) \ \mathrm{sinc}[(v_x + \sum_{p=0}^{P-1} m_p a^p)L] \quad ,$$

wherein $\boldsymbol{v} = \boldsymbol{k}_i - \boldsymbol{k}_s$, [3] and $\boldsymbol{k}_i$, $\boldsymbol{k}_s$ are the incident and scattering propagation vectors.

In order to shed light into the model and its dependence on the fractal parameters a number of simulations have been accomplished. The study of the fluctuations of the (random) scattered field has been done by characterizing it through the Normalized Intensity Moments [2]. As expected, the higher the roughness (H decrease) the stronger the fluctuations. When the C_p are changed from deterministic to random values, the proper probability distribution function switches from the negative exponential to the K-distribution [2].

In order to study the volume scattering due to natural bodies a different choice of the fractal function is necessary.

Application to Synthetic Aperture Radar images is made, comparing simulated and real data.

References

[1] K.Falconer, *Fractal Geometry: Mathematical Foundations and Applications*, New York: John Wiley, 1990.

[2] G.Franceschetti, M.Migliaccio, D.Riccio, "An Electromagnetic Fractal-Based Model for the Study of the Fading", submitted.

[3] P.Beckmann, A.Spizzichino, *The Scattering of Electromagnetic Waves from Rough Surfaces*, Norwood, MA: Artech House, 1987.

An Overview of Australian HF Radar Research

S.J.Anderson
HF Radar Division
Defence Science and Technology Organisation
Salisbury SA 5108
AUSTRALIA

Abstract

Australian research into HF skywave radar systems dates from the early 1950's but came of age in 1976 when the first JINDALEE radar commenced operations at sites near Alice Springs in Central Australia. The two decades since then have seen the original radar enhanced almost beyond recognition, with a wide range of surveillance and remote sensing capabilities now being exploited to provide information to a variety of customers. A further revolutionary development presently underway is the construction of two additional radars, over a baseline of some 2500 km, all linked through a common command centre into the JINDALEE Operational Radar Network (JORN).

Besides these skywave radar systems, several HF surface wave radars have been developed and used for remote sensing and surveillance purposes. The early systems, dating from the 1970's, are giving way to a new generation of efficient, low power, low cost designs equipped with very sophisticated signal processing.

To develop and support these systems, a substantial involvement of the Australian applied electromagnetics community has been (and remains) an essential ingredient. At one extreme are the antenna designers, RF engineers, telecommunications specialists and so on, who have solved the practical problems of system implementation. At the other are the ionospheric physicists, signal processing practitioners and electromagnetic scattering theoreticians who are involved with modelling the diverse propagation and scattering phenomena associated with this type of radar and with developing signal analysis and interpretation techniques which extract the required information.

This paper reviews the achievements of the JINDALEE program and its relatives, and identifies some of the crucial problems in applied electromagnetics which confront the scientists and engineers working towards the next generation of HF radars.

Progress in Electromagnetics Research Symposium, PIERS 1997 ISBN 962-442-097-1

TROPOSPHERIC REFRACTION ERRORS IN RADAR TARGET COORDINATES

by
Dr. Ahmed K. Aboul-Seoud Dr. Hanaa M. Rashwan
Ahmed E. Shaalan
Department of Electrical Engineering, Faculty of Engineering
Alexandria University, Alexandria, Egypt

In the troposphere, the radar rays suffer from bending due to variations in the refractive index of air with height. These variations occur due to changes in atmospheric pressure, temperature, and water vapour pressure. The mean refractivity gradient with height in temperate climates is -40 N-units/km. This effect is usually taken into consideration by assuming a hypothetical earth radius equal to 4/3 the actual earth radius. Many radars use this concept in target location processing. Errors in target coordinates occur when the actual air refractivity gradient differs from this standard value. Furthermore, the presence of atmospheric layers with different refractivity gradients is another source of errors. For radars pointing at targets at small elevation angles, significant errors occur in determining target heights. However, differences in target ground range are insignificant.

The above problem is of great importance specially for early warning radars operating in hot and humid regions such as the eastern part of the Mediterranean and the Red sea. We have calculated and analyzed the relative percentage errors in both target heights and its ground range at very small elevation angles in both the presence and the absence of atmospheric layers. The dependence of these errors on the geometry of the path and the different atmospheric parameters has been demonstrated. The results indicate that, in the presence of elevated layers, the percentage relative error increases with the increase in layer thickness and lapse rate within it and with the decrease of the layer height and the initial ray elevation angle. In the case of absence of layers, a steep surface gradient may cause the presence of ducting resulting in range ambiguity.

Progress in Electromagnetics Research Symposium, PIERS 1997 ISBN 962-442-097-1

Non-Gaussian Properties of HF Sea Clutter

S.J.Anderson
HF Radar Division
Defence Science and Technology Organisation
Salisbury SA 5108
AUSTRALIA

Abstract

The representation of the rough sea surface as a superposition of freely propagating, dispersive, surface gravity waves is widely used in oceanography. The k-space distribution (or wave directional spectrum) for a given sea state provides a meaningful description of the surface as long as the individual Fourier components can be assumed to satisfy the appropriate dispersion relation, normally that corresponding to deep water. Strictly speaking, this is equivalent to the assumption of infinitesimal amplitude. Alternatively, the perturbations in wave profile which appear beyond the linear term in the Stokes expansion can be separately represented on other sheets of the distribution. Generally these higher-order terms contain relatively little energy and hence can often be ignored.

An important exception to this situation arises in the remote sensing of the sea surface by means of HF radio waves. By applying Barrick's extension of the Rayleigh-Rice perturbation expansion for the scattered field, it can be shown that some contributions of scattering from wave harmonics and other evanescent waves generated by nonlinear hydrodynamic interactions of the first-order sinusoidal waves can be distinguished from the contributions from the first-order waves via the selectivity of the kernel function. Power spectra computed by this method have shown excellent agreement with measured HF Doppler spectra so there is little reason to doubt the validity of the technique.

While the fundamental of one wave and the second harmonic of another longer wave may have identical wave numbers, they differ in their frequencies and in their higher order statistics as a consequence of the phase locking of the second harmonic to its fundamental carrier. To investigate these nonlinear coupling effects, a statistical analysis of bispectra and other higher-order statistics computed from time series of sea clutter recorded with an HF surface wave radar has been carried out. The results support the hypothesis that coherent nonlinear hydrodynamic contributions to the Doppler spectrum can be identified and exploited for remote sensing purposes.

Progress in Electromagnetics Research Symposium, PIERS 1997 ISBN 962-442-097-1

SESSION 6P11

Monday, January 6, PM 1330-1710, Lecture Theatre 11, City University of Hong Kong

Inverse Scattering & Polarimetry

Organizer: Ross Murch

Chairperson: Ross Murch, HK Univ. of Science & Technology
Co-Chairperson: Hsin-Chia Lu, National Taiwan University

13:30 ***Microwave Diversity Imaging Using Six-Port Reflectometer in a Compact Range Arrangement*** 79
Hsin-Chia Lu, Tah-Hsiung Chu
National Taiwan University

13:50 ***Polarimetric Borehole Radar*** 80
Moyoyuki Sato, Takashi Miwa, Hiroaki Niitsuma, Katsuto Nakatsuka
Tohoku University

14:10 ***Polarimetric and Time Series Features and Their Application to Classification Algorithms for Detection of Surface Roughness, Moisture and Ice Layers*** 81
Rolf Finkele, Andreas Schreck, Gerd Wanielik
Daimler-Benz A G, Research Center Ulm

14:30 ***Three-Dimensional Electromagnetic Inverse Scattering by Local Shape Function Method with CGFFT*** 82
Jiun-Hwa Lin, Weng Cho Chew
University of Illinois at Urbana-Champaign

14:50 ***A General Formula of UIM for the EM Inverse Scattering Problem*** 83
Weiyan Wang, Shourong Zhang
Academia Sinica

15:10 Break

15:30 ***Two-Dimensional Microwave-Imaging Approaches in the Spatial Domain Using Probabilistic Concepts*** 84
*S Caorsi, **G L Gragnani, **M Pastorino
*University of Pavia
**University of Genoa

15:50 ***Imaging of Cross-Sectional Absorption Distribution in Diffuse Medium*** 85
Koichi Shimizu, Aki Awata, Katsuyuki Yamamoto
Hokkaido University

16:10 ***Diffraction and Phase Method of the Troposphere Radiorefraction Measurement in UHF with the Help of a Satellite*** 86
D D Darizhapov, E M Khomyak, E Ch Daribazaron
Buryat Institute of Natural Sciences

16:30 ***The Ecological Monitoring in Siberia and Baikal Lake Region*** 87
D D Darizhapov, B Ch Dorzhiev, P A Shirokov
Buryat Institute of Natural Sciences

16:50 ***Radiorefraction in the Far-East Region and Its Influence VHF Propagation*** 88
D D Darizhapov, E V Batueva
Buryat Institute of Natural Sciences

Microwave Diversity Imaging using Six-port Reflectometer in a Compact Range Arrangement

Hsin-Chia Lu and Tah-Hsiung Chu

Electrical Engineering Department, National Taiwan University

Taipei, Taiwan, Republic of China

Microwave diversity imaging technique basically uses a vector network analyzer (VNA, e.g. HP8510) to measure the object scattered field (amplitude and phase) over a wide frequency range at various viewing angles, then reconstructs the scattering object characteristic function through a two-dimensional Fourier inversion. However, VNA may have two constrains in performing measurement. One is the upper frequency limit for correct phase measurement, and the other is the cost consideration in instrumentation.

It is known that using six-port reflectometer is an alternate approach in the measurement of microwave device reflection coefficient. It measures four amplitudes from a six-port circuit which is constructed to give a linear combination of the incident signal and reflecting signal of the test device. Six-port reflectometer is simple in structure, and requires only amplitude measurement. Therefore, it can be easily extended into higher frequency region which may be difficult for VNA.

In this paper, we will describe the microwave diversity imaging measurement arrangement using six-port reflectometer developed in our anechoic chamber. This arrangement consists of a compact range facility, a six-port reflectometer and a workstation. In the measurement, the workstation records the four amplitude signals from a six-port reflectometer over a wide bandwidth at various scattering object viewing angles, whereas the amplitude signals are a linear combination of the incident field and the object scattered field. Calibration procedure to acquire the range normalized object scattered field is then performed. Experimental results of two types of scattering object, a metallic cylinder and a scaled model of aircraft, will be presented using the described six-port reflectometer technique.

Polarimetric Borehole Radar

Moyoyuki Sato, Takashi Miwa, Hiroaki Niitsuma and Katsuto Nakatsuka

Faculty of Engineering, Tohoku University
Sendai 980-77 Japan
sato@earth.tohoku.ac.jp

In this paper we will discuss potential of polarimetric borehole radar measurement for geophysical applications. Borehole radar is one form of ground penetrating radar, which is used in drilled boreholes. This type of radar has been successfully used in detection of water flow in resistive rock. Frequencies lower than 100MHz is commonly used in borehole radar to have enough penetration depth. Therefore, most conventional borehole radars used axially-oriented electric dipole antennas for transmission and reception, resulting in a response only to the co-polarization at one tilt angle. Compared to the conventional co-polarization reflection measurement, polarimetric radar measurement would be useful for characterization of geological reflectors such as subsurface cracks and geological boundaries.

We have developed a network analyzer based broad-band (10MHz - 500MHz) polarimetric borehole radar system using an optical signal link. A dipole antenna and a slot antenna on a conducting cylinder are used for this system. The physical configuration of this antenna is quite suitable for borehole applications, because the antenna diameter is less than 10cm which can be used in thin boreholes.

Single-hole (reflection - monostatic) and cross-hole (transmission - bistatic) measurements using the prototype radar system were carried out in granite rock. We can not mechanically rotate antennas in boreholes, therefore we have to calibrate the antenna system by signal processing. We used an inverse filter technique to compensate the difference of dipole and slot antenna characteristics, and we developed an algorithm to estimate the scattering matrix of reflecting targets. Polarization calibration was not carried out, because we think 20dB isolation between crossed polarizations is sufficient.

Since we measure the full-components of the scattering matrix, we can synthesize any polarization state from the measured data. We observed the polarization dependency of a reflectivity of a water containing fracture, which is typical reflectors in granite. For instance, a tilt angle of an incident field effects to the cross-polarized component of the reflection coefficient, and its dependency is found to be different in each crack face. Polarization dependency of the reflection from subsurface cracks was also observed by FD-TD simulation and was compared to the measurement. It was found that a crack model which simulates actual crack generates cross-polarized component in reflection and is large enough for evaluation in measurement. The polarimetric radar information which gives us more knowledge of subsurface cracks such as surface roughness and water contaminant will be discussed in the paper.

Polarimetric and time series features and their application to classification algorithms for detection of surface roughness, moisture and ice layers

Rolf Finkele, Andreas Schreck, Gerd Wanielik

Daimler-Benz AG, Research Center Ulm
P.O. Box 2360, D-89013 Ulm,Germany
Tel.: (+49)731-505-2346 Fax: (+49)731-505-4110

To investigate the effect of roughness, moisture and ice layers on the bistatic scattering properties of surfaces, a fully polarimetric millimeter wave measurement system was realised. It works at 76 GHz and makes use of five transmitters and seven receivers of different polarisation. The system makes use of an incoherent measurement approach to allow for a perspective of cost effective mass production.

The study carried out, makes use of a set of surface samples of different degree of roughness. The thickness of water and ice layers on this surfaces can be varied. The effect of the surface parameters on the different polarisation channels are studied, and the polarisations most suitable for classification purposes can be pointed out.

For the automatic classification of different surface classes a system is realised. Special attention will be placed on the investigation in suitable features. The feature vectors used for classification will use polarimetric and time series attributes of the measured data. They will be discussed in detail and rated by their feasibility. The concept of an hierarchical classifier is introduced and classification results are presented.

The concept realised will be verified with data obtained from outdoor measurements on road surfaces under real weather and traffic conditions. The generalisation potential of the classification concept will be assessed.

Three-Dimensional Electromagnetic Inverse Scattering by Local Shape Function Method with CGFFT

JIUN-HWA LIN AND WENG CHO CHEW*
CENTER FOR COMPUTATIONAL ELECTROMAGNETICS
DEPARTMENT OF ELECTRICAL AND COMPUTER ENGINEERING
UNIVERSITY OF ILLINOIS
URBANA, IL 61801

The use of scattered electromagnetic fields to determine the parameters of unknown objects is a much-studied problem in the fields of remote sensing, nondestructive evaluation, and medical imaging. These parameters could be the location, shape and size of a metallic body, or the permittivity and conductivity of a penetrable object. Thus far, linearization approximation are widely adopted because of their numerical efficiency. For example, the Born and Rytov approximations are widely used in medical imaging, and the physical optics approximation is often used to identifying metallic objects. However, these methods suffer from nonlinearity in inverse scattering problems, limiting their range of validity.

Recently many research workers have applied nonlinear iterative methods directly in the governing equations. The advantage is the proper inclusion of all diffraction and refraction effects. But the disadvantage is the numerical complexity and higher cost of such methods. Nevertheless, the drawback can be alleviated with the advent of efficient algorithms and powerful modern computers.

To our knowledge, most nonlinear inverse scattering schemes to date are in two dimensions, while few are in three dimensions (3D) due to their higher complexity. As can be expected, the nonlinearity will be more pronounced in 3D since multiple scattering can occur with three degrees of freedom. In addition, the singularity of dyadic Green's function may exacerbate the nonlinearity if precaution is not taken in formulating the problem. In this paper, we propose the local shape function (LSF) method the solve 3D inverse scattering medium problems, whose main feature is to use the T-matrix to characterize the scatterer. Specifically, we discretize the scatterer on a grid and calculate the T-matrix for each subscatterer as a function of its constant permittivity. The forward scattering problem is then solved with the CG-FFT method. The nonlinearity in the inverse problem due to multiple scattering is accounted for in an iterative minimization scheme. Numerical examples of simulation data are given showing the capability of this algorithm.

Progress in Electromagnetics Research Symposium, PIERS 1997 ISBN 962-442-097-1

A General Formula of UIM for the EM Inverse Scattering Problem

Wang Weiyan, Zhang Shourong
(Institute of Electronics, Academia Sinica, Beijing P.R.China)

Abstract

The electromagnetic inverse scattering problem is inherently an ill-posed problem. We attribute it to failure of obtaining sufficient information of the object to be reconstructed. To overcome the difficulty, we must use more additional conditions which may be either obvious prior knowledges as described in the regularization method, or implicit relevancies involved in a certain process that will be emphasized in the paper.

We regard the considered object as a dark box, of which the inner unkowns are just the constitution parameters of the object, while the input and the output quantities are the incident and scattered fields respectively. It is obvious that the outputs of the box is not only dependent on the inputs, but also marked the signatures of the unknowns contained in the box. This implies that the information of the box is brought out through the interaction between inputs and the dark box. A different input may result in a different interaction, then the interaction will give out a different information of the box. According to this principle we proposed Unrelated Illumination Method(UIM), and proved that the transmission matrix of the considered object can be determined uniquely if a series of independent incident is exerted:

$$[T] \;=\; [E^s][e^i]^{-1} \;= -[B]([A]-[I])^{-1}\,,$$

and the unkonwn (O) of the object is then reconstructed:

$$(O) \;=\; [D_p]^{-1}(T_p)\,,$$

It is worth mentioning that to form a series of unrelated illuminations is the most important step in a practical inverse procedure. Technically, such a requirement is achievable. Some possible schemes have been suggested in our preceding work, further considerations are in progress.

Two-Dimensional Microwave-Imaging Approaches in the Spatial Domain Using Probabilistic Concepts

S. Caorsi*, G. L. Gragnani**, and M. Pastorino**

*Dept. of Electronics - University of Pavia, Via Abbiategrasso 209, 27100 Pavia, Italy
**Dept. of Biophysical and Electronic Eng. - University of Genoa,
Via Opera Pia 11A, 16145 Genova, Italy
Phone: + 39 10 353 2243, Fax: + 39 10 353 2777, e-mail: ema@dibe.unige.it

ABSTRACT

This paper deals with microwave-imaging approaches based on stochastic models. In the last few years research works have been focused on the use of monochromatic illuminations, within the first-order Born approximation [1] and for the complete inverse-scattering problem [2]. In the present paper the theory, as well as the related numerical results, are extended to the second-order Born approximation and to multi-frequency illumination (with the assumption that the scattering objects be nondispersive).

Through a Bayesian approach the quantities involved in the scattering problem (i.e., the electric fields and the dielectric properties) are considered as stochastic processes and their reconstructions are obtained by maximizing the a-posteriori probability. The unknowns of the problem (i.e., the total electric field inside the scatterer and the scattering potential) are modelled as discrete Markov Random Fields. In particular, as for the multifrequency approach, the neighbourhood system for the total electric field is extended over three or more frequencies, in order to describe a local dependence in both space and frequency. To this end, an approximate form of the Helmoltz equation is used, which, after being differentiated with respect to ω, gives the required relation for fields at neighbouring frequencies.

The results of several numerical simulations are presented. Comparisons are made among the results obtained by using the different approaches. The second-order Born approximation has shown (as compared with the first-order one) a greater capability to correctly locate a scatterer inside a fixed investigation region. The results obtained by applying the multifrequency algorithm show that, for each frequency, there is usually one of the reconstruction parameters (i.e., objects location, cross-section shape, dielectric permittivity values, etc.) which can be estimated very accurately, whereas the other ones are reconstructed with a certain error. Nevertheless, expecially for inhomogeneous scatterers, the multifrequency approach seems to provide results that are quite better than the ones obtained by a monochromatic illumination.

1. S. Caorsi, G. L. Gragnani, S. Medicina, M. Pastorino, and G. Zunino, "Microwave imaging based on a Markov Random Field Model," *IEEE Trans. Antennas Propagat.*, vol. 42, no. 3, pp. 293-303, 1994.
2. S. Caorsi, G. L. Gragnani, S. Medicina, M. Pastorino, and G. A. Pinto, "A Gibbs random field-based active electromagnetic method for noninvasive diagnostics in biomedical applications," *Radio Science*, vol. 30, no. 1, pp. 291-301, 1995.

Imaging of Cross-sectional Absorption Distribution in Diffuse Medium

Koichi Shimizu, Aki Awata and Katsuyuki Yamamoto
Department of Bioengineering, Faculty of Engineering
Hokkaido University, N13 W8, Sapporo 060, Japan

The near-infrared light of 700-1200 nm wavelength has high transmission through a human body. However, there is a strong scattering in the body tissue and it is difficult to obtain the image of the internal structure of our body. Recently there has been an increasing interest in the study of light propagation in dense random media to realize an optical CT. Using the backscattered light, we can obtain the cross-sectional image of only a certain part near the surface of the subject. However, the applicability of this technique is not restricted by the thickness of the subject. In the combination with optical fibers, it is particularly useful in the clinical applications, such as the imaging of inner walls of digestive tracts, blood vessels and heart chambers.

We have developed a new technique to reconstruct the cross-sectional image of a diffuse medium using the backscattered light. In the first process of this technique, we obtain the absorption distribution in the depth-direction of the subject. In the second process, we scan a pair of input and output optical fibers along the surface of the subject to obtain the horizontal variation.

The subject is divided into some imaginary layers. The probabilities of the photon propagation in each layers are obtained beforehand either in the Monte Carlo simulation or in the measurement with a model phantom. A short pulse of light is illuminated on the body tissue, and the output pulse shape is obtained in the time-resolved measurement. The absorption coefficient of each layer is obtained by solving linear simultaneous equations that were given from the measured pulse shape. The equations were derived in the linear approximation of the fundamental equation for the light attenuation due to the scattering and the absorption of the diffuse medium.

To examine the applicability of this technique to a diffuse medium, a computer simulation based on the Monte Carlo method was conducted. When the variation of the absorption was small among layers, the reconstructed distribution agreed well with the given distribution. However, with large variation, the error became large particularly in deep layers.

The accuracy of this technique was improved in two ways. One is the improvement of the linear approximation of the fundamental equation for light attenuation. Another one is the appropriate choice of the sampling points in the received pulse. With these improvements, the valid range of absorption was largely expanded in the reconstruction of the absorption distribution.

Progress in Electromagnetics Research Symposium, PIERS 1997 ISBN 962-442-097-1

Difraction and Phase Method of the Troposphere Radiorefraction Measurement in UHF with the Help a Satellite

D.D.Darizhapov, E.M.Khomyak, E.Ch.Daribazaron

Buryat Institute of Natural Sciences
Siberian Department of Russian Academy of Sciences
6 Sakhyanova st., Ulan-Ude, Russia 670042
Phone: +7(30122) 32841, Fax: +7(30122)32841,
E-mail: root@bien.buriatia.su

This paper deals with a new method of a study of the earth atmosphere refractional properties according to the effects occuring at the moment of the radiorise or radioset of a satellite beyond the high horizon of a mountain relief. In contrast to the other known methods based only on the characteristics of the difraction attenuation modulus here the analysis of the whole phase of this function is carried out.

The theoretical study of the difraction wave properties is carried out for the case of radiation of the earth surface horizon with a highly located source and for the case of the low height of reception aerial lifting above the earth surface. Using the known results of the solution of the radiowaves difraction problem on the spherical surface the expression of the function of field attenuation with respect to free space near the shadow boundary of a convex obstacle has been obtained. To study interference laws observed in satellite radiosets the phase of attenuation function is identified. The phase analysis can not be carried out without its correlation with geometrical parameters of the "reception aerial - point of the satellite radioset" path of the difractional obstacle, as well as with polarization of the radiowave and its frequency. The theoretical findings obtained are reduced to simple calculated formulae, permitting the calculation of the true value of the angular radiowave refraction in the earth atmosphere, taking into account all above parameters.

In experiments, the amplitude of the radio signal from the UHF source, installed in the spasecraft, was recorded during the radiorise or radioset of the satellite beyond the horizon. At the same time, precise time with the given intervals measured in steps of tens fractions of a second has been marked on the tape for radio signal records. Data on a distance, azimuth and angle of the satellite position with respect to the horizon of the stationary reception aerial are indicated by the system of the navigation tracking at different instants of time. The very moment, when the curve of the temporal dependence of the position angle takes on values equal to the angle of radio horizon screening, corresponds to the moment of the radioset. In this case the angle of the radio horizon screening is determined from the circular panorama of the screening angle with the azimuth corresponding to the radioset moment. A profile of the "reception aerial - point of the satellite radioset" path is constructed by the given azimuth. The value of the satellite position angle at the moment of the radioset is elucidated and all geometrical parameters of the path, necessary for calculation of the atmospheric refraction angle are determined from the profile of the path.

The ecological monitoring in Siberia and Baikal lake region.

D.D.Darizhapov, B.Ch.Dorzhiev, P.A.Shirokov

Buryat Institute of Natural Sciences
Siberian Department of Russian Academy of Sciences
6 Sakhyanova st., Ulan-Ude, Russia 670042
Phone:+7(30122)32841, Fax:+7(30122)32841,
E-mail: root@bien.buriatia.su

The diagnostics of the dynamics of the physical state and properties of the earth surface changes is of great importance for resolving the problem of climate-ecological monitoring. The proximity satellite sounding is the only one way to receive the main parameters of the environmental state for the whole low populated and difficult region of Siberia in real time. Within the scope of projekt "Climate and ecological monitoring of Siberia" a network of the space monitoring stations has been established in Siberian region (Krasnoyarsk, Irkutsk, Tomsk). They receive information provided by the low orbit satellites of "Meteor", "Ocean" series. The information obtained makes it possible to carry out the monitoring of the physical state and dynamics of the atmosphere with the determination of the quantitative content of main gases in it, the stream of visible and infra-red radiation, the physical state of the earth surface and climate and ecological changes in the environment.

The creation of the space monitoring station is also planning in the Institute of Natural Sciences (Ulan-Ude) to reveal laws for regional environmental changes under the influence of natural and anthropogenic processes. Nowdays, the digital information about the territory surrounding a big industrial centre has been obtained from the space platform "Almaz". The radiolocator of side scanning with the synthesized aperture has been installed on the board of the spacecraft "Almaz" working on the 10 sm wave length. On the photos, synthesized by apparatus facilities and soft ware, the changes connected with activity of a man has been clearly determined. The timely data on overflows of rivers, consequences of earthquakes, fire and other natural calamities can be obtained with the help of such synthesized photos.

The combination of radiolocational and radiometric methods makes it possible to receive uniqual data which are of great interest for agriculture and forestry, such as determination of biomass, harvest forecast, assessment of moisture content and erosion of soils and results of land-reclamation works, etc.

Radiorefraction in the Far-East region and its influence VHF propagation.

D.D.Darizhapov, E.V.Batueva

Buryat Institute of Natural Sciences
Siberian Department of Russian Academy of Sciences
6 Sakhyanova st., Ulan-Ude, Russia 670042
Phone: +7(30122) 32841, Fax +7(30122) 32841,
E-mail: root@bien.buriatia.su

Radiometeorological parameters of troposphere and average level of transhorizon VHF signals on the paths of Far-East coast are investigated. The season variation of radiometeorological parameters and average level tropospherical signals are obtained and comparisoned.

The investigations were carried ouf on two VHF radiolinks with common receiving point based on the coastal strip of Okhotsk sea. The geographical length of the first path is 201.6 km and for the second path - 415.3 km. There equivalent longhs are 167.1 km and 383.7 km correspondingly. The angles of scattering on these intervals under normal atmosphere refraction (a=8500 km) are equals 19.7 and 45.1 miliradians respectively. The both paths passed under the shurply rugged and mountainous country in the coastal strip of Okhotsk sea. The first path pass under the peninsulu; the volume of troposphere scattering moved away from the shore on the distance near 100 km and closed the mountain ridge from the ocean. The second path pass near the coastal strip.

On the intervals tested the typical tropospheric radio relay station "Horizon-M" has been used. It was provided with parabolic aerials with sizes 20x20 m on the first path and 30x30 m - on the second path and working according to the four-folded reception-transmission aerials scheme on the 1st path accounts for 41.5 dB and 42.5 dB and on the 2nd path 46 dB and 46.5 dB. Records of quick fadings were made ones at the period of three hours during from 5 to 50 minuts.

The seasonal variations of average signal on the transhorison troposphere links of Far-East coast of Russia are revealed. These variations are characterised by one maximum of summer or autumn with dependence of location of experimental links and one minimum of winter.

On the path running along the coast of the ocean the maximum of the signal is observed in autumn, and on the path far from the coast it is observed in summer this occurs due to characteristic properties of the tropospheric processes taking place near the "land-ocean" boundary.

SESSION 6P10

Monday, January 6, PM 1330-1650, Lecture Theatre 10, City University of Hong Kong

Wave Propagation in Planar Structures

Organizer: Robert Weigel

Chairperson: Robert Weigel, University of Linz
Co-Chairperson: D Jäger, Gerhard-Mercator-Universitat Duisburg

13:30 ***Wave Propagation on Nonlinear Transmission Lines*** 90
*D Jäger, **V K Mezentsev, **S L Musher, **I V Ryzhenkova, **S K Turitsyn, *R Hülsewede
*Gerhard-Mercator-Universität Duisburg
**Institute of Automation and Electrometry, Universitetskii pr.1

13:50 ***Scattering Parameters of Planar Discontinuities on Partially Doped Silicon Substrate*** 91
R Vahldieck, S Chen
University of Victoria

14:10 ***Calculation of the Coupling of Dielectric Resonators to Microstrip Circuits with a FEM/BEM-Hybrid Technique*** 92
Thomas F Eibert, Volkert Hansen
Bergische Universität / Gesamthochschule

14:30 ***A Noval Subgridding Scheme for the Distributed TLM Modeling of Thin Layers*** 93
B Isele, T Mangold, R Weigel, P Russer
Technische Universität München

14:50 ***A Contribution to the Simulation of Periodic Wave Guide Structures*** 94
Ulf Müller, Marc Walter, Adalbert Beyer
Gerhard-Mercator-Universität-GH-Duisburg

15:10 **Break**

15:30 ***Field Theory Analysis and Experimental Characterization of Wave Propagation in Microacoustic Structures*** 95
*Robert Weigel, *Andreas Holm, *Hans Meier, *Ulrike Rösler, *Ralph Schneider, *Beate Walliser, **Werner Ruile
*Technische Universität München
**Siemens A G München

15:50 ***Accurate Analysis of Ridged Circular Waveguide and its Transition to Circular Waveguide by an Integral-Equation-Mode-Matching-Technique*** 96
Severine Catreux, Smain Amari, Rüdiger Vahldieck
University of Victoria

16:10 ***Optimum Correlation Functions for GPR Data Processing by Spectral Domain Methods*** 97
Juergen Detlefsen, Dirk Felbach
Technische Universität München

16:30 ***The Method of Lines for the Simulation of Elevated Coplanar Waveguides*** 98
Dennis Kremer, Reinhold Pregla
Fern Universität

Wave Propagation on Nonlinear Transmission Lines

D. Jäger+, V. K. Mezentsev*, S.L.Musher*, I. V. Ryzhenkova*, S. K. Turitsyn*,
and R. Hülsewede+
+Fachgebiet Optoelektronik, Sonderforschungsbereich 254
Gerhard-Mercator-Universität Duisburg,
Kommandantenstrasse 60, 47048 Duisburg, Germany
*Institute of Automation and Electrometry,
Universitetskii pr.1, 630090 Novosibirsk, Russia

In recent years it has been demonstrated, that nonlinear transmission lines (NLTLs) can successfully be applied to generate picosecond electrical pulses from a sinusoidal input signal [1,2]. Experimentally, the NLTL is a coplanar waveguide loaded with hyperabrupt varactor diodes in a periodic or graded manner. Theoretically, a suitable equivalent circuit is used as the basis for a numerical simulation in the time domain. In this paper, wave propagation on various NLTLs is studied where special emphasis is laid upon technical applications in the millimeterwave region.

As a first example it is shown that specific bi-modal NLTLs consisting of a bi-periodic array of varactor diodes and fixed capacitances, can be used for efficient generation of millimeter wave power by direct second or third harmonic conversion. In case of third harmonic generation, varactors with a symmetric capacitance-voltage relations are chosen. As a further application, varactor-NLTLs are studied for mixing and parametric amplification [3].

A second example addresses NLTLs with Schottky- or pn-diodes driven into forward direction. A distributed rectifier for high-speed input signals results where a suitable design leads to a device with high power-conversion efficiency.

When resonant tunneling diodes (RTDs) are used to form a periodic NLTL, a traveling-wave active device results which is capable to be operated as a distributed oscillator. The dispersion of the structure including the resonance condition of a transmission line with a certain length, introduce filter characteristics leading to a well defined harmonic signal [4].

As a final example, a monostable RTD-NLTL is discussed which produces a spiking behavior for a given input signal. It is shown, that such a "neuristor"-type of NLTL [5] can be applied for high-speed A/D conversion.

[1] M.J.W. Rodwell, S.T. Allen, R.Y.Y. Yu, M.G. Case, U. Bhattacharya, M.Reddy, E. Carman, M. Kamegawa, Y. Konishi, J. Pusl, R. Pullela, "Active and nonlinear wave propagation devices in ultrafast electronics and optoelectronics", *IEEE Proc.*, vol. 82, no. 7, pp. 1037-1059, 1994 (invited paper)

[2] M. Dragoman, R. Kremer, and D. Jäger, "Pulse generation and compression on a travelling wave MMIC Schottky diode array", in: Ultra-Wideband, Short-Pulse Electromagnetics, H.L. Bertoni, L.Carin, and L.B.Felsen, eds., Plenum Press, New York, pp. 67-74, 1993

[3] D. Jäger, "Characteristics of travelling waves along nonlinear transmission lines for monolithic integrated circuits: A review", Int. J. Electron. 58, 649-669 (1985) (invited paper)

[4] R. Hülsewede, V. K. Mezentsev, S.L.Musher, I. V. Ryzhenkova, S. K. Turitsyn,and D. Jäger, "Millimeter Wave Generation on Nonlinear Transmission Lines", 1996 International Workshop on Millimeter Waves, April 11-12, Orvieto, Italy, 1996

[5] H.D.Crane, "Neuristor - a Novel Device and System Concept", Proc. IRE, vol.50, pp. 2048-2060, 1962.

Scattering Parameters of Planar Discontinuities on Partially Doped Silicon Substrate

R. Vahldieck and S. Chen
Laboratory for Lightwave Electronics, Microwaves and Communications (LLiMiC)
Department of Electrical and Computer Engineering
University of Victoria
Victoria, B.C., Canada V8W 3P6
Tel: (604)721-8679, Fax:(604)721-6052
E-Mail: vah@ece.UVic.ca

Abstract

A rigorous field theory analysis of discontinuities between planar transmission lines, where one part of the transmission line is printed on insulating and the other on partially doped silicon material is presented. This kind of transition has not been investigated in great detail in the open literature yet, but is of importance for implementing semiconductor-based slow-wave structures in a circuit environment. The problem when implementing slow-wave structures with other transmission line sections on normal insulating material is that the slow-wave section of the transmission line exhibits also a different characteristic impedance if the line dimensions are not changed. Hence, a 50 Ohm transmission line on an insulating substrate will show different line dimensions than the 50Ohm section in the slow-wave region. As a result, the dimensions of both transmission lines change abruptly which, in spite of the same characteristic impedance on both sides of the transition, will affect the field components of the wave and, hence, the S-parameters significantly. To investigate this effect in more detail the method of analysis is based on the frequency-domain TLM (FDTLM) method. The structures under investigation are mainly coplanar (CPW) metal-insulator-semiconductor (MIS) transmission lines on bulk silicon or semiconductor on insulator (SOI). To simulate the practical structure as closely as possible, the doping intensity distribution over the depth of the substrate was assumed to be Gaussian. Because it was found in an earlier investigation that the slow-wave factor in MIS CPW can be optimized by limiting the lateral extend of the doped region to the area under the strip and both slots, the investigation in this contribution focusses on the S-parameter calculation for the abrupt transition from a CPW to a MIS CPW with various lateral widths of the doping region. This investigation also includes the transition effect between microstrip lines.

Progress in Electromagnetics Research Symposium, PIERS 1997 ISBN 962-442-097-1

Calculation of the Coupling of Dielectric Resonators to Microstrip Circuits with a FEM/BEM–Hybrid Technique

Thomas F. Eibert and Volkert Hansen,
Lehrstuhl für Theoretische Elektrotechnik, Bergische Universität/Gesamthochschule Wuppertal,
Fuhlrottstr. 10, D-42119 Wuppertal — Germany

Analysis of the coupling of dielectric resonators of simple shapes (e. g. cylindric resonator) to microstrip lines is often performed based on approximate analytical techniques. If more complicated resonator shapes or microstrip circuits have to be considered the use of a numerical modeling technique is necessary.
Dielectric resonators itself are favorably be modeled by a local modeling technique (Finite Differences, Finite Element Method (FEM)) whereas microstrip circuits are favorably be described by Boundary Element Methods (BEM) based on an analytic formulation of the layered structure Green's function in the spectral domain. So it is straightforward to use a hybrid method combining a local technique with the BEM for layered media to deal with the coupling problem of dielectric resonators to microstrip ciruits. We use a hybrid method based on the FEM and the BEM. In this framework only the dielectric resonator has to be modelled by finite elements. The influence of the resonator onto the fields in the layered medium is included in the integral equation formulation of the BEM by the introduction of equivalent Huygens surface currents on a surface completely enclosing the resonator. The Huygens currents are directly coupled to the fields inside the resonator. Special care is necessary if the Huygens surface is situated in the interface between two different layers. In this case the singular character of the Green's functions is changed as compared to the homogeneos space case what has to be considered in the formulation of the surface integral equation. The integral equation is used in form of a mixed potential integral equation (MPIE) with a Green's functions representation in terms of Sommerfeld integrals. Due to the surface current modeling of the microstrip structures equivalent circuit parameters such as S–parameters of filter structures can easily be obtained from the calculations. Numerical results for several configurations are presented.

Progress in Electromagnetics Research Symposium, PIERS 1997 ISBN 962-442-097-1

A Novel Subgridding Scheme for the Distributed TLM Modeling of Thin Layers

B. Isele, T. Mangold, R. Weigel, P. Russer

Lehrstuhl für Hochfrequenztechnik, Technische Universität München,
Arcisstr. 21, D-80333 München 2, Germany

The present work arose from a requirement of accurate time domain modeling of interconnections in multichip modules (MCM's). As is the case with similar methods, the Transmission-Line-Matrix (TLM) method provides the feasibility to handle nearly any geometry and is not restricted to planar geometries. However, the modeling of circuits consisting of elements with strongly varying geometrical dimensions such as thin layers is not suitable for a conventional discretization due to limited computational resources. Also the use of graded meshes is very limited since the dispersion characteristic of these meshes becomes worse. For metalic layers surface-impedance models may be used which yield accurate broadband frequency characteristics [3]. In general, a local mesh refinement is required to increase the spatial resolution. Such subgridding techniques enable the mesh to carry for details, which could not be resolved by a coarse mesh. The combining of fine and coarse meshes requires for a careful investigation at the interface. In [1] the following conditions are postulated for the coarse mesh/fine mesh interface: energy conservation (i), charge conservation (ii), zero reflection (iii) and zero delay (iv). In the subgridding model, proposed by [1] the wave amplitudes incident from the coarse mesh to the fine mesh are kept constant during the time step within the coarse mesh. This introduces some lag in the interfering of the sub meshes. In contrary, we use a recursive description, in which also the incident pulses from the coarse mesh are adjusted to the updated field situation on the fine mesh. In this improved subgridding model additional transformations between the wave amplitudes and the field quantities are necessary, which can be done exactly only at the cell boundaries of the TLM nodes.
Our algorithm is completely embedded in a TLM simulation package utilizing distributed computing making best use of the available resources [2]. We use the Parallel Virtual Machine (PVM) as an environment for the distributed computing. The simulations are done within clusters of interconnected workstations and parallel computers. The subgridding model was tested for several scenarios and has been approved to satisfy the previously mentioned conditions. The method was applied to the simulation of interconnections in multichip modules, where the thickness of some intermediate layers was more than one order of magnitude smaller than the transversal dimensions of the remaining elements. The improved subgridding approach opens a wide range of applications for the TLM method and benefits inherently from the flexibility of distributed computing.

[1] J. Herring, C. Christopolous, "Solving Electromagnetic Field Problems Using a Multiple Grid Transmission-Line Modelling Method ", IEEE Trans. Ant. Prop., Vol. AP-42, No. 12, Dec. 1994.

[2] B. Isele, J. Schmöller, P. Russer, "Simulation of Coplanar Resonators with TLM Method in a Parallel Computing Environment", Proc. PIERS 1995, Seattle, July 1995, p. 733.

[3] B. Isele, P. Russer: "Improved Skin Effect Model in TLM", Proc. COMPUMAG 1993, (Miami, Florida), 31 Oct–4 Nov, 1993, pp. 450-451.

A Contribution to the Simulation of Periodic Wave Guide Structures

Ulf Müller, Marc Walter and Adalbert Beyer

Adalbert Beyer - tel.: +49 203 3789-217, fax: +49 203 379-3218, email: a.beyer@uni-duisburg.de
Ulf Müller, Marc Walter
mailing address: Gerhard-Mercator-Universität -GH- Duisburg, FB 9 / ATE, Bismarckstr. 81, D-47048 Duisburg, Germany

Periodic wave guide structures can be distinguished into two basic classes:

- Wave guide structures with continously changing, periodic, electromagnetic properties (e.g. a circular waveguide filled with a dielectric and continously and periodically changing relative permeability) as well as
- Wave guide structures with periodic boundary conditions (e.g. a rectangular waveguide loaded with reactive elements in regular intervals).

The mostly appearing forms of periodic structures are those of the class mentioned at last.

Periodic structures do all have one characteristic property in common: the appearing of different frequency bands in which a wave propagation along the periodic structure is possible, in contrast to stop bands in which the wave is strongly damped so that there is no possibility of wave propagation.

The proposed process treats the periodic wave guide structures with the help of the TLM method in time-domain. Corresponding to the Floquet theorem it is supposed that the wave propagates along the periodic structure with a proportionality according to the fundamental system $\{\exp(\gamma z), \exp(-\gamma z)\}$ whereby damping types are permitted. This statement can then be transmitted to electromagnetic fields.

The relations yielded for the TLM simulation of a periodic wave guide structure using the SCN considers not only the properties of the fundamental system but also the periodicity of the structure.

The applicability of the method proposed is verified at the example of different structures. First a capacitively loaded rectangular waveguide is treated with the TLM method for the formulation of periodic wave guide structures. Since therefore analytically evaluatable formulas are available, the accuracy of the yielded results can be easily tested.

As a further example a capacitively loaded coplanar line should be considered. Therefor independent measurement results are for comparison available. In all cases very good fittings between simulation and reference results could be achieved.

Field Theory Analysis and Experimental Characterization of Wave Propagation in Microacoustic Structures

Robert Weigel[1], Andreas Holm[1], Hans Meier[1], Ulrike Rösler[1], Ralph Schneider[1], Beate Walliser[1], Werner Ruile[2]

[1]Technische Universität München, Lehrstuhl für Hochfrequenztechnik, Arcisstr. 21, D-80290 München, Germany
[2]Siemens AG München, Corporate Research and Development, Otto-Hahn-Ring 6, D-81739 München, Germany

Microacoustic devices using surface acoustic waves (SAW's) are used in a considerable range of applications in modern electronics to carry out particular signal processing functions with great technical facility. Their advantages over concurrent techniques are their small size and cost-effective mass-production combined with high performance. The major technical applications are momentarily both front end- and IF-filtering in mobile radio transceivers and (both fixed-code and programmable) matched-filtering in spread-spectrum systems. In most cases, SAW devices consist of several basic structures such as interdigital transducers and reflectors, made up of arrays of metalic strips of finite thickness. As substrates, piezoelectric materials such as $LiNbO_3$ (lithiumniobate), $LiTaO_3$ (lithiumtantalate) and quartz are used. Upcoming applications of microacoustic devices require for new materials and new structures which must be analyzed very accurately.

We have developed a generalized full wave analysis tool for computing microacoustic modes propagating in multilayered piezoelectric media. Our analysis tool for solving the microacoustic wave equations (WMAT) consists of a combination of matrix-, partial wave-, and simplex-analysis. Each region of the layered structure is characterized by its own set of constants which are as follows: elastic stiffness, piezoelectric and dielectric tensors, and mass density. The analysis does not only solve the eigenvalue problem for the pertinent boundary problems (such as free, metalized, and periodically loaded surfaces) to yield the dispersion of the propagation. It can also deal with the propagation loss by allowing for complex elements of both the elastic and the dielectric tensor. Neglecting beam steering, diffraction and crystalline defects and impurities, the propagation loss arises from a combination of air loading (superstrate radiation) and the temperature dependent interaction with thermally excited elastic waves.

To verify the analysis results, we are able to characterize the microacoustic modes both by measuring and evaluating the S-parameters of special test chips and by using a sophisticated laser probing technique which allows for the accurate detection of the surface wave field by employing a mode-locked picosecond laser, harmonic mixing, and coherent detection. We report on the analysis and characterization of piezoelectric Rayleigh modes and leaky waves in layered structures incorporating piezoelectric, semiconducting and metalic materials by way of some illustrating examples. We present new SAW propagation data for $LiTaO_3$ and $LiNbO_3$ at room temperature.

Progress in Electromagnetics Research Symposium, PIERS 1997 ISBN 962-442-097-1

Accurate Analysis of Ridged Circular Waveguide and Its Transition to Circular Waveguide by an Integral-Equation-Mode-Matching-Technique

Severine Catreux, Smain Amari and Rüdiger Vahldieck
Laboratory for Lightwave Electronics, Microwaves and Communications (LLiMiC)
Department of Electrical and Computer Engineering
University of Victoria
Victoria, B.C., Canada V8W 3P6
Tel: (604)721-8679, Fax:(604)721-6052
E-Mail: vah@ece.UVic.ca

Abstract

Ridged circular waveguides, which constitute an essential part of dual mode filters, have been analyzed using the Mode Matching Technique (MMT), the Method of Lines (MoL), the Finite Element Method (FEM), as well as the Boundary-Integral-Equation Technique (BIET). In this work, a technique which allows the inclusion of the edge conditions in the Mode-Matching Technique is used to determine the cutoff frequencies of circular ridged waveguides. A set of coupled integral equations are derived and solved by the moment method using basis functions which include the edge conditions. A significant reduction in the size of the matrices compared to the MMT can be achieved. The scattering from a finite section of a circular ridge waveguide in a uniform circular waveguide is also analyzed. Two different approaches to determining the transmission and reflection coefficients are presented. The first one consists in cascading the generalized scattering matrices of the two coupled integral equations for the transverse electric field at the gaps of the two discontinuities. In the second approach, the normal modes in the ridge section are given a minor role in favor of the transverse electric fields at the gaps of the discontinuies to emphasize the fact that the dominant physics of the problem takes place at the discontinuities and not in the uniform sections of the structure. Results from the present work are compared with available data and measurements to demonstrate the efficiency of the technique.

Progress in Electromagnetics Research Symposium, PIERS 1997 ISBN 962-442-097-1

Optimum Correlation Functions for GPR Data Processing by Spectral Domain Methods

by Juergen Detlefsen, Dirk Felbach

Technische Universitaet Muenchen
D 80290 Muenchen, Germany

GPR data, which is obtained while the GPR system is moving along a straight track is usually processed according to SAR principles. In this case a large bandwidth is required to gain a high spacial resolution. It is wellknown that the optimum processing can be achieved by applying a correlation procedure. The correlation procedure between the signal measured along track and calculated reference signals of point scatterers in various depths become maximum, if the depth of the buried object and that of the point scatterer are identical. In this case a high resolution in depth is obtained from the synthetic aperture by only using a CW modulation. In the case of GPR, the reference signal is often determined by assuming a straight propagation path, which only takes into consideration the dielectric properties of the homogenous ground.

In the paper reference functions are presented that are calculated by using spectral domain techniques, describing the ground as a layered dielectric medium and taking into account the inevitable air gap between antenna and ground surface. By this method the transfer function can be efficiently calculated in spectral domain, while a 2-D Fourier transform gives the reference functions in spatial domain also for different lateral positions of the point scatterer. Also these reference functions may allow for a finite extension of the antenna aperture, giving the chance to optimise the configuration with respect to spacial resolution. The method of calculation and the improvements which can be obtained are discussed in the paper and related to the additional numerical effort. The gain of the advanced signal processing using correlation functions effectively obtained by spectral domain methods will be demonstrated with experimental data measured by a single frequency system.

Corresponding author:

Prof. Dr. Juergen Detlefsen
Technische Universitaet Muenchen
D 80290 Muenchen, Germany
Tel. +49 89 289 23390
Fax: +49 89 289 63390
email: det@hfs.e-Technik.tu-muenchen.de

Progress in Electromagnetics Research Symposium, PIERS 1997 ISBN 962-442-097-1

The Method of Lines for the Simulation of Elevated Coplanar Waveguides

Dennis Kremer and Reinhold Pregla
FernUniversität, Allgemeine und Theoretische Elektrotechnik,
D-58084 Hagen, Germany
e-mail: R.Pregla@fernuni-hagen.de

Nonlinear transmission lines (NLTL's) integrated with sampling circuits are commonly used in millimeter wave and submillimeter wave instruments. The elevated coplanar waveguide (ECPW) has been proposed [1] to decrease the loss and the distributed capacitance of the transmission line which leads to an increase of the circuit bandwidth.

A full vectorial analysis of such ECPW's will be presented by using the method of lines (MoL). The MoL is a semianalytical method, i.e., the wave equations are discretized only as far as necessary and in one direction the calculation is carried out analytically, which yields accurate results with less computational effort. Extreme large permittivity differences, like those which appear at the transition from dielectric to metal with finite conductivity are considered in the analysis by including complex or imaginary permittivities.

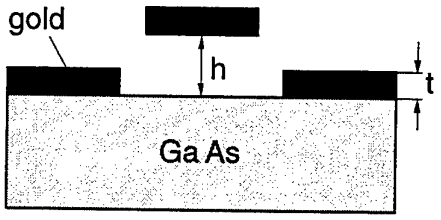


Figure 1: Elevated Coplanar Waveguide

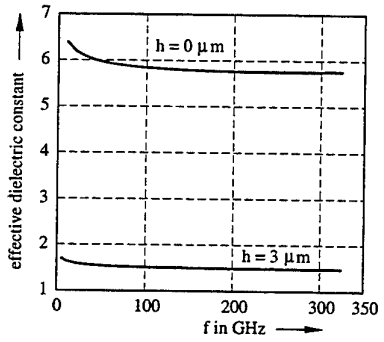


Figure 2: Effective dielectric constant for different elevation heights

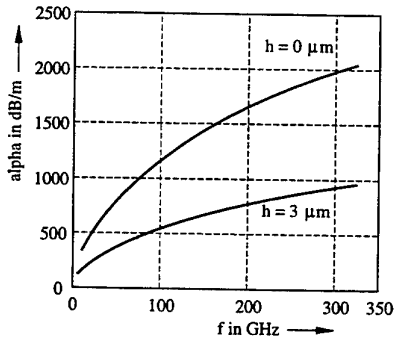


Figure 3: Loss constant for different elevation heights

The usage of the singular value decomposition in the MoL enables us to make the computation of the effective dielectric and the loss constant more efficient. The numerical results in Fig. 2 and Fig. 3 demonstrate the very strong influence of the elevation height on these constants. These results were obtained from our program MOLCAR (method of lines complex arithmetic routine) which allows the analysis of planar structures with arbitrarily shaped cross-sections.

The semianalytical determination of the power flux density in inhomogeneous layers leads to a very accurate calculation of the characteristic impedance in microwave structures. Latest numerical results will be presented at the conference.

[1] U. Bhattacharya, S. T. Allen, and M. J. W. Rodwell, "DC-725 GHz Sampling Circuits and Subpicosecond Nonlinear Transmission Lines Using Elevated Coplanar Waveguide", In: *IEEE Microw. Guid. Wave Lett.*, vol. 5, no. 2, pp. 50–52, Feb. 1995.

SESSION 6P9

Monday, January 6, PM 1330-1650, Lecture Theatre 9, City University of Hong Kong

Optical Waveguide Structures

Organizer: Reinhold Pregla

Chairperson: Reinhold Pregla, FernUniversitat
Co-Chairperson: Dennis Kremer, FernUniversitat

13:30 ***High-Order-Accurate Finite Difference Equations for Photonics Modeling***[+] 100
G Ronald Hadley
Sandia National Laboratories

14:10 ***Computer-Aided Design of Photonic Waveguide Devices*** 101
C Glingener, J-P Elbers, E Voges
Universität Dortmund

14:30 ***Mode Expansion Methods for Field Calculations in Optical Waveguides*** 102
Aasmund Sudbϕ
University of Oslo

14:50 ***Layered Media for Modal and Polarization Control in Optical Waveguides*** 103
R J Deri, S P DiJaili, F G Patterson, M A Emanuel
Lawrence Livermore National Laboratory

15:10 Break

15:30 ***Design and Analysis of Singly and Doubly Periodic Waveguides Using Time Domain Methods*** 104
*R Zengerle, **S Leonhard
* Deutsche Telekom AG, Technologiezentrum
**University of Kaiserslautern

15:50 ***A Very Stable and Accurate Algorithm for the Analysis of Periodic Structures with a Finite Number of Periods*** 105
S Helfert, R Pregla
Fern Universität

16:10 ***Modeling of VCSELs*** 106
Barry Koch, Philip Cheung, James Leger, Anand Gopinath
University of Minnesota

16:30 ***Optical Properties of A Cantor Corrugated Waveguide*** 107
M Bertolotti, P Masciulli, P Ranieri, C Sibilia
Universita' di Roma "La Sapienza"

[+] double time-slot (40 minutes)

High-Order-Accurate Finite Difference Equations for Photonics Modeling

G. Ronald Hadley
M/S 0603
Sandia National Laboratories
Albuquerque, New Mexico 87185-5800

ABSTRACT

The rapidly-growing science of photonics has depended heavily upon numerical modeling for both the analysis of data and the design of new devices. The majority of this modeling, whether beam propagation, eigenmode analysis or the analysis of reflecting structures, has been performed by numerical solution of finite-difference equations derived from the basic governing Maxwell Equations. These finite difference equations have for the most part been derived by the replacement of derivatives by their simple centered difference expressions, resulting in equations that typically display a second-order truncation error. While some attempts have been made to extend this procedure to higher order[1-3], they have been few and often restrictive in scope, with the derivations applicable only to uniform grids and with little attention payed to the accuracy of the equations at dielectric boundaries.

The reasons for this trend are, I believe, twofold. First, the derivations of the higher-order terms are difficult. Not only is the algebra tedious, but more importantly the discontinuities of the higher spatial derivatives of the fields must be accurately accounted for if the equations are to retain their high truncation order at dielectric boundaries. This latter issue has been sometimes treated incorrectly, but most often ignored completely, resulting in equations that may be fourth order within a region of constant properties, but first or second order at the interfaces. The additional error incurred by this neglect rises significantly as the number of grid points is decreased, thus robbing the approach of its real benefit. Second, there seems to be a general opinion that high-order finite difference equations are of dubious utility. Reasons for this doubt include a suspicion of reduced numerical stability and the belief that a fourth-order method is only better when the grid spacing is small, becoming actually worse than the second-order result when the grid is made coarse. Also, it is thought that the increase in accuracy (when it occurs) is of necessity accompanied by an increase in matrix bandwidth, thus incurring a sizeable penalty in numerical effort

In this talk I intend to address each of these issues using both theoretical derivations and actual numerical comparisons with standard methods. These results will demonstrate that, while the equation derivations are indeed difficult, they need only be done once, whereas the numerical benefit is realized each time the resulting code is run. The derivations will be discussed for a wide variety of photonics problems using a variable grid, with the resulting truncation error of (dx(i)-dx(i-1))*dx(i)*dx(i) shown to be achievable with only a negligible increase in matrix bandwidth. (dx(i) is the grid size associated with grid point i). These equations may be referred to as quasi-fourth-order since they reduce smoothly to fourth-order in the limit of a uniform grid. In addition, calculations for a variety of problems obtained using these high-order equations will be presented that show no loss of numerical stability or robustness, and demonstrate remarkably accurate results on grids so coarse as to appear entirely useless. This result is understandable when one realizes that the fourth-order error terms (that indeed become large as the grid size increases) are partially canceled by fifth and higher-order terms so that the resulting error is still significantly less than a second-order result.

The implications of this approach are significant for the future of photonics modeling. Using higher-order equations, the increase in accuracy with almost no increase in computational speed or memory implies that standard problems previously requiring workstations should now be solvable on personal computers, while larger (presently intractable) problems should become amenable to analysis. In addition, certain numerical methods (for example, direct matrix inversion for 3D wide-angle beam propagation) that are presently too slow and memory intensive to be of wide-spread use may now become the methods of choice.

1. B. Hermansson and D. Yevick, Optics Lett., Vol. 16, 354(1991).
2. L. Sun and G. Yip, Optics Lett., Vol. 18, 1229(1993).
3. J. Yamauchi, J. Shibayama, H. Nakano, Optics Lett. Vol. 20, 7(1995).

Computer-Aided Design of Photonic Waveguide Devices

C. Glingener, J.-P. Elbers, E. Voges
Lehrstuhl für Hochfrequenztechnik, Universität Dortmund,
D-44227 Dortmund, Germany

Photonic waveguide devices are key elements in optical communication systems and optical sensor technology providing transmitter, receiver, and network functions. Using suitable fabrication techniques, it is possible to realize a large variety of components. Due to the high degree of complexity, an accurate CAD program is essential for the development of modern photonic waveguide devices. Several commercial design packages are already available. Most of them either lack generality or are difficult to use. The analysis of the wave propagation is often restricted to the 2D case, and the vector nature of the electromagnetic field is not taken into account. Additionally, none of them includes an accurate modeling of the basic material systems.

Here, we present a complete design environment for the CAD of photonic waveguide devices, which is easy to use, flexible and extendible. We focus on the general concept, the realization of design tools, and the applicability. The basic simulation algorithms, the accurate modeling of the material parameters, and the device characterization are described. Supplementary, the realization of the program by using the benefits of object-oriented programming is illustrated.

Three databases provide an accurate characterization of the photonic device. The material database contains the complex refractive index of the materials used for the fabrication of photonic devices. The basic material systems are based on III-V semiconductors, silicon, silica glass, $LiNbO_3$ or polymers. Predefined waveguide cross sections, characterized by geometrical and material parameters are included in the profile database. The component database covers the parametric description of basic structures including scaling laws. The preprocessor is a layout editor for photonic circuits, which uses the three databases and features interfaces acting together with the fabrication and the simulation. It offers a constructive circuit generation based on the connection of basic components.

The simulation algorithms cover modal analysis techniques and two-dimensional and three-dimensional propagation algorithms, which are based on finite difference approximations. The eigenmode module is used for scalar, semivectorial or vectorial modal analysis. In addition, it provides the capability of an effective index approximation, whereby a 2D profile can be reduced to a 1D profile. Finally, it can be utilized to produce an initial field for propagation analysis. 2D and 3D propagation algorithms are included in the beam propagation module. The postprocessor is a visualization tool for reviewing and interpreting the results.

The concept was completely realized by utilizing the object-oriented programming language C++. It covers the definition of adequate data structures for materials, profiles and components, and the object-oriented implementation of the simulation algorithms, and the required mathematical operations. A graphical user interface (GUI) is provided for the interaction between program and user. Some examples show the effectiveness of our CAD package.

Mode Expansion Methods for Field Calculations in Optical Waveguides

Aasmund Sudbø, University of Oslo
Center for Technology, UNIK, P.O. Box 70, N-2007 Kjeller, Norway

For a number of methods for calculating electromagnetic field distributions in waveguiding structures, the field in a substructure is expressed as a sum of contributions from the modes of that substructure. Hence they may be called generically mode expansion (ME) methods. Examples are the Transverse Resonance Method and the Method of Lines for mode field calculations in straight and curved waveguides. Methods of this kind have been used for more than thirty years in model calculations with applications in microwave and optical devices. Recent refinements of the methods have made it possible to attack a number of design problems encountered in devices used for optical communication. Impressive results have been obtained, even with the processing power of standard desktop computers.

The talk will review the strengths of ME methods and some of their fundamental problems and limitations.

Complex structures with inhomogeneities yielding strong scattering, reflections, and interference may be analyzed. Polarization may be taken into account. For a number of waveguiding structures of great practical interest, very accurate twodimensional field distributions may be calculated quite rapidly, in a few minutes on a desktop computer. The processing time grows very rapidly with the size of the domain within which the field is calculated, however, and full threedimensional field distributions cannot reasonably be calculated on a desktop computer with these methods, except in very simple geometries.

One fundamental problem with ME methods is that the structures that can be analyzed have sharp edges and corners that are known to yield field distributions with singularities. The singularities slow the convergence of all numerical methods (including ME methods) used for calculating the distributions. Edges and corners may also be viewed as scattering centers, and a serious numerical problem is encountered with the presence of strong multiple scattering and interference, if the most straightforward analytic formulations of ME methods are used. Alternative formulations have overcome this problem.

A few recent applications of ME methods in optical waveguide device design will be presented. An attempt will also be made at discussing the relevance to microwave applications of the developments in the optical area.

Progress in Electromagnetics Research Symposium, PIERS 1997 ISBN 962-442-097-1

Layered Media for Modal and Polarization Control in Optical Waveguides

R. J. Deri, S. P. DiJaili, F. G. Patterson, and M. A. Emanuel
Lawrence Livermore National Laboratory, PO Box 808, Livermore, CA 94550, USA
Tel +1 (510) 422-1642 Fax +1 (510) 422-1066 deri1@llnl.gov

Advanced fiber-optic systems for communications and sensing employ increasingly sophisticated combinations of optical and optoelectronic devices to generate, detect, switch and multiplex optical signals. Optical waveguides fabricated on planar substrates provide a practical technology for fabricating and/or integrating such devices.[1,2] Major issues which complicate the deployment of this technology in conventional, single-mode fiber systems are the small mode size and excessive waveguide birefringence. Small mode size increases the difficulty of robust, efficient optical coupling between device and fiber.[2,3] Birefringence can cause a polarization-dependent performance which results in undesirable, time-dependent fading when devices are used with conventional (non-polarization-preserving) fiber.[3] Recently, several techniques utilizing layered media have been proposed to address these issues. This contribution reviews the application of these techniques to optical waveguides in III-V compound semiconductors.

Layered media in the form of multiple quantum wells (MQWs) are widely used in GaAs and InP waveguide devices[2] to enhance optical gain (lasers) or absorption (modulators). Layered structures based on the same epitaxial growth technology have also been used for refractive index control well below the MQW absorption edge. An early application was the use of the inherent MQW birefringence (due to both layering and quantum selection rules) to build integrated optical polarizers, in which only one polarization was guided.[4] More recently, the precise control of MQW properties via epitaxial growth techniques has enabled device designs which improve the optical mode size and minimize polarization dependence.

One such approach involves "diluted MQWs", in which very thin QWs separated by thick barriers are used to create extremely small, yet highly reproducible, refractive index changes. Such small index changes simplify the fabrication of single-mode waveguides with large mode size for improved fiber coupling.[5] It was subsequently recognized that the small index difference in diluted MQW waveguides can provide low birefringence as well.[6] Achieving low birefringence is important in certain wavelength demultiplexers, such as those based on gratings or interferometers, because the polarization-dependence of the multiplexed wavelength is proportional to the guide birefringence.

Other waveguide filters, notably those based on asymmetric directional couplers, require large index changes to achieve narrow passbands. The asymmetric coupler's polarization dependence arises from the differential birefringence of the two coupled waveguides. It has recently been shown that MQWs can be used to alter the birefringence of one coupler guide in order to eliminate the differential birefringence, and thus the polarization dependence.[7] Details of this approach will be described at the conference.

This work was performed under the auspices of the U.S. Department of Energy by Lawrence Livermore National Laboratory under contract No. W-7405-Eng-48.

References

[1] T. Tamir (ed), Integrated Optics (Springer-Verlag, Berlin) 1979.
[2] T.L. Koch and U. Koren, IEEE J. Quantum Electron. 27, 641 (1991).
[3] R.J. Deri and E. Kapon, IEEE J. Quantum Electron. 27, 626 (1991).
[4] E. Kapon, N. Stoffel, et al., Appl. Phys. Lett. 52, 351 (1988).
[5] R.J. Deri, N. Yasuoka, et al., Electron. Lett. 25, 1162 (1989).
[6] J.-M. Verdiell, M.A. Newkirk, et al., IEEE Photonics Technol. Lett. 4, 451 (1993).
[7] R.J. Deri, M.A. Emanuel, et al., Appl. Phys. Lett. 68, 1037 (1996).

Design and Analysis of Singly and Doubly Periodic Waveguides Using Time Domain Methods

R. Zengerle, S. Leonhard*

Deutsche Telekom AG, Technologiezentrum
P.O. Box 100 003, D-64276 Darmstadt
* University of Kaiserslautern, Theoretical Electrical Engineering and
Optical Communications, P.O. Box 3049, D-67653 Kaiserslautern

Electromagnetic wave propagation is governed by Maxwell's equations. The Finite Difference Time Domain method (FD-TD) takes into account all the propagation properties including reflections and transients. The main advantage of the FD-TD method is its computational ease of implementation and its ability to handle arbitrary structures. However as the FD-TD solves the Maxwell's equations directly, enormous computer resources are required. In order to reduce the memory requirements several time domain algorithms are proposed. In addition to an explicit time domain solution of Maxwell's equations using a non-equidistant grid we present a novel FD-TD algorithm based on a transformation of variables. In comparison with one of the conventional FD-TD methods only 1-2 % of the computer memory are required. As the FD-TD method is well suited for vector processors, the algorithm is implemented on a CRAY Y-MP4E/464. In order to minimize the CPU time we present the possibility to organize the structure of the programming code with regard to the optimal performance of the vector processor.

The advantage of the FD-TD algorithm is the ability to handle reflected waves in optical waveguides. For the sake of simplicity, we consider two-dimensional wave propagation. Three-dimensional structures are replaced by an equivalent slab waveguide using an effective index method. One way to obtain the reflection coefficient is to determine the standing-wave ratio. We investigate the accuracy of the method by comparing its results on strongly modulated structures with other theoretical results. Additionally we demonstrate the applicability of the FD-TD with regard to design and analysis of singly and doubly periodic structures. The characteristics of these structures are calculated and compared with the Floquet-Bloch formalism that uses the general solution of Maxwell's equations in a periodic medium. In contrast to the Floquet-Bloch formalism the FD-TD method permits a more efficient and exact analysis of the wave propagation in strongly modulated periodic structures.

A Very Stable and Accurate Algorithm for the Analysis of Periodic Structures with a Finite Number of Periods

S. Helfert and R. Pregla,
FernUniversität, Allgemeine und Theoretische Elektrotechnik,
D-58084 Hagen, Germany
e-mail: R.Pregla@FernUni-Hagen.de

Periodic structures are important optical components. An example is the Bragg grating sketched in Fig. 1. To obtain accurate results bidirectional methods including reflected modes have to be used. In [1]–[3] algorithms for the analysis of such structures are described. The numerical effort increases with the number of periods and for long distances numerical problems may occur.
In this new approach we use Floquet's theorem together with a general admittance/impedance transfer algorithm. The numerical effort does not depend on the number of periods and numerical problems can be avoided.

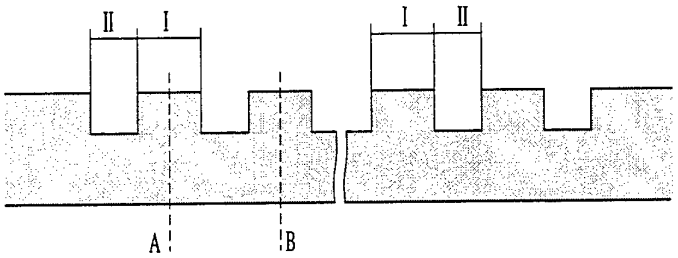


Fig. 1: Example of a periodic structure

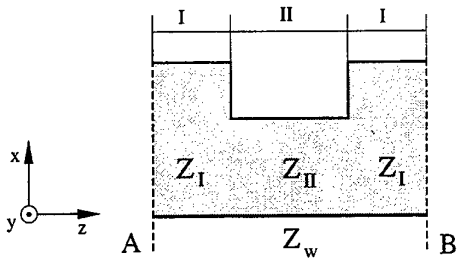


Fig. 2: One sector of the periodic structure

Periodic structures (Fig. 1) are divided in sectors (Fig. 2). The relation between the tangential field components on the two sides (A, B see Fig. 2) of each sector is calculated by a transfer matrix. By determining the eigenvalues and eigenvectors of this transfer matrix it is possible to introduce Floquet's theorem and to determine the wave impedance Z_w of such a sector.
In what follows the impedance at the end of the periodic structure is transferred to the beginning (or to any other position) by simple matrix multiplication. Supplying now a known incident field the reflected modes can be determined.
For the calculation of the whole field a division in forward and backward traveling waves is performed. Now, propagating in z-direction the backward traveling part increases exponentially. This may lead to the above mentioned numerical problems. For that reason only the forward traveling modes are propagated in this algorithm. Using these modes together with the impedance the whole field can be calculated. The impedance itself can be computed as described above.
Since all increasing terms are avoided, a very stable algorithm is guaranteed.

It should be noted that the described method can be used in the same form for the examination of 3D structures. Obviously, this algorithm is useful for the analysis of structures with an infinite number of periods, too.

[1] J. Gerdes and R. Pregla, "Bidirectional Beam-propagation Method based on the Method of Lines", in *Integr. Photo. Resear. Technic. Digest*, Washington, DC, USA, 1993, vol. 10, pp. 400–403.

[2] J. Gerdes, "Bidirectional Eigenmode Propagation Analysis of Optical Waveguides Based on Method of Lines", *Electron. Lett.*, vol. 30, no. 7, pp. 550–551, 1994.

[3] W. D. Yang and R. Pregla , "Method of Lines for the Analysis of the Waveguide Structure with Multidiscontinuities", *Electron. Lett.*, vol. 31, no. 11, pp. 892–893, 1995.

Modeling of VCSELs

Barry Koch, Philip Cheung, James Leger, Anand Gopinath
University of Minnesota
Department of Electrical Engineering
200 Union Street SE Minneapolis, MN 55455

Numerical modeling of VCSELs has received much attention, and recent papers by Hadley et al [1], and Ahlers et al [2] have provided a review of recent work. In this paper we discuss the analysis of VCSELs in the vertical plane with confining apertures. Recent work in this area has considered square section devices, and here the hybrid modes of the cylindrical VCSEL are replaced by TM (E-field in the plane of the interfaces) and hybrid modes. In this paper we investigate the properties of these square VCSELs using the finite element method. The modes of this type of VCSEL are obtained with and without apertures. These apertures may be generated either by oxidation or by means of metal deposition for modal control of the structure.

We are in the process of investigating these square and circular VCSELs defined by proton bombardment, which results in very weakly guided structure. Here, the V numbers of the circular devices often exceed 2.4 when the diameter size is greater than 8 to 10 μm, and thus make them multimode in the transverse direction. We will present results of large area VCSELs whose modes are also controlled by apertures.

Current large area VCSELs with their low mirror stack resistances tend to break up into a variety of mode combinations often termed filamenting, and do not follow the patterns of the predicted modes. Thus, the investigation in progress is to determine under what conditions such behavior is probable. The effect of thermal lensing is also of considerable importance in these devices. It is thought that the higher resistance stacks of the earlier devices were the main source of thermal lensing, and hence these earlier VCSELs showed great similarity between predicted and measured mode patterns. We are in the process of investigating the effect of thermal lensing in these devices. This requires the solution of the thermal distribution in the device, and this will be solved using the finite element method for the Poisson equation.

These and other results will be presented at the meeting.

References

[1] G. H. Hadley, K. L. Lear, M. E. Warren, K. D. Choquette, J. W. Scott, S. W. Corzine, "Comprehensive numerical modeling of vertical cavity lasers," *IEEE J. Quantum. Electron.*, Vol. 32, pp. 607-616, 1996.

[2] E. Ahlers, S. F. Helfert, R. Pregla, "Modeling of VCSELs by the Method of Lines", *1996 Integrated Photonics Research Meeting Technical Digest* , paper ITuE5-1, pp. 340-343, 1996, Boston, MA April 1996.

Progress in Electromagnetics Research Symposium, PIERS 1997 ISBN 962-442-097-1

OPTICAL PROPERTIES OF A CANTOR CORRUGATED WAVEGUIDE

M. Bertolotti, P. Masciulli, P.Ranieri, C. Sibilia

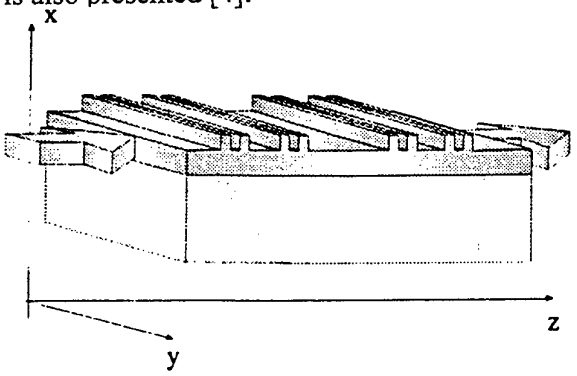
Dipartimento di Energetica- Universita' di Roma " La Sapienza "

Via Scarpa 16 , 00161 Roma, Italy,

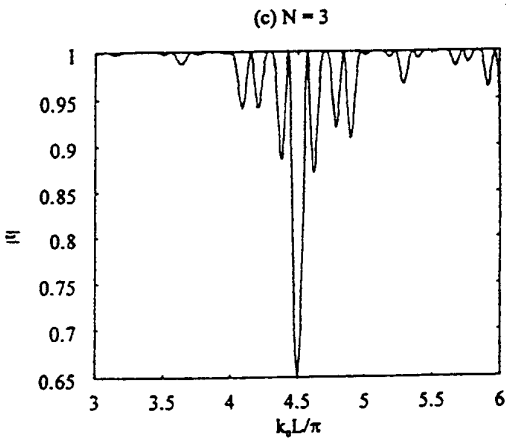
tel +39 4 49916541, fax + 39 6 442 40183

and GNEQP of C.N.R. and INFM, Italy

The spectral transmission properties of a fractal corrugated optical waveguide are theoretically studied. The considered structure can be realized by a planar waveguide with a square wave modulation of the guiding film thickness such that the thickest layers belong to a triadic Cantor set. Consider a planar dielectric waveguide with refractive indices n_s, n_f, n_c for the substrate, guiding and cladding layers, respectively. The corrugated waveguide structure is made by alternating two pieces of waveguide of different guiding layer thickness, t_1 and t_2 with $t_2 > t_1$. It is possible to choose a frequency band such that the structure supports a single guided mode everywhere. The structure can be regarded as a special kind of waveguide Bragg reflector [1] . For this configuration we obtain results very similar to the ones of a planar Cantor Fabry-Perot resonator described in [2]. Also in this case the transmission spectrum exhibits localized peaks inside forbidden frequency band gaps; the main difference is that in the present case dispersion has to be taken into account and the spectrum is not periodic as in [2, 3]. A nonlinear response of the structure, when a third order material is introduced , is also presented [4].



Cantor corrugated waveguide configuration for the level $N = 3$.



Transmission $|t|$ versus $k_0 L/\pi$

[1] M. Bertolotti, P. Masciulli, C. Sibilia, F. Wijnands, H.Hoekstra -"Transmission properties of Cantor corrugated waveguide ", In press on J.Opt. Soc. of Am. B

[2] M. Bertolotti, P. Masciulli, C. Sibilia, Optics Letters.19 (1994) 777

[3] M. Bertolotti, P. Masciulli, C. Sibilia, Proceedings of Integrated Optics Conference, Lindau (Germany), 11-15 April 1994

[4] M. Bertolotti, P. Masciulli, P.Ranieri, C. Sibilia " Optical bistability in a nonlinear Cantor corrugated waveguide , In press on J.Opt. Soc. of Am B.

SESSION 6P8

Monday, January 6, PM 1330-1730, Lecture Theatre 8, City University of Hong Kong

Semiconductor Lasers & Photonic Devices

Organizers: Weiping Huang, E Herbert Li

Chairperson: K Yokoyama, NTT Opto-electronic Laboratories
Co-Chairperson: E Herbert Li, University of Hong Kong

13:30 ***High Temperature Operation of Long-Wavelength Strained-Layer Quantum-Well Semiconductor Laser Diodes***[+] 109
Kiyoyuki Yokoyama
NTT Opto-electronics Laboratories

14:10 ***Strained Quantum Well Lasers with Non-(001) Crystal Orientations***[+] 110
Tsukuru Ohtoshi, Atsuko Niwa, Takao Kuroda
Hitachi Ltd

14:30 ***Numerical Modeling of the Optical Field in Vertical-Cavity Surface-Emitting Lasers***[+] 111
G Ronald Hadley, Kent D Choquette
Sandia National Laboratories

14:50 ***Fast and Accurate Analysis of Coated and Angled Facets Considering Two-Dimensional Beam Profiles*** 112
*T M Benson, **P C Kendall, *M Reed, *P Sewell
*University of Nottingham
**University of Sheffield

15:10 Break

15:30 ***Modeling and Measurement of Some Functional Semiconductor Laser Devices*** 113
G-H Duan
Ecole Nationale Supérieure des Télécommunications

15:50 ***Gain Coupled DFB Semiconductor Laser Monolithically Integrated with Electroabsorption Modulator*** 114
Yi Luo, Chang-Zheng Sun, Guo-Peng Wen
Tsinghua University, Beijing

16:10 ***Adiabatic Frequency Chirp Analysis in Semiconductor DFB Lasers Monolithically Integrated with Mach-Zehnder Modulators*** 115
*X Li, *W P Huang, **D M Adams, **C Rolland, **T Makino
*University of Waterloo, **Nortel Technology

16:30 ***Intermixed Quantum Well Laser*** 116
Michael C Y Chan, E Herbert Li
The University of Hong Kong

16:50 ***Modelling of Avalanche Photodiodes*** 117
M Jamal Deen
Simon Fraser University

17:10 ***Large and Small Signal Equivalent Circuit of QW Lasers*** 118
*P R Vaya, **H A Tafti
*Indian Institute of Technology, **Anna University

[+] double time-slot (40 minutes)

High Temperature Operation of Long-Wavelength Strained-Layer Quantum-Well Semiconductor Laser Diodes

Kiyoyuki Yokoyama
NTT Opto-electronics Laboratories
3-1 Morinosato Wakamiya
Atsugi, Kanagawa 243-01, Japan

Out of the various kinds of semiconductor laser diode (LD) characteristics, I will focus on high temperature LD design for telecommunication purposes in this talk. Much attention has recently been attracted to introducing cost-reduced optical subscribing systems, so called fiber-to-the-home (FTTH) and fiber-in-the-loop (FITL) systems. For system applications, long-wavelength (I will mainly talk about 1.3-μm wavelength) highly-efficient uncooled semiconductor LDs with high output power and low threshold current over a wide range of operation temperatures are required. Designing the active region, which consists of strained-layer (SL) quantum wells (QWs) and separate carrier confinement heterostructures (SCHs), so as to obtain sufficient output power while maintaining high temperature characteristics is a very important issue. For this purpose, a deep understanding of the underlying physics is indispensable. Many research institutes including universities have been engaged in this research subject.

In my talk, I will start from the band structure engineering proposed by Adams and Yablonovitch. This epoch-making proposition pretty much stimulated research activities into SL multi-quantum-well (MQW) LDs. As a result of introducing SL, the threshold current for lasing has been able to be reduced. Since the effect is sufficiently practical, SL MQW LDs are in common use in our telecommunication networks. However, improvements in high temperature characteristics have been limited (although not as much as had been expected). I am going to discuss the main reason for this discrepancy.

After extensive experimental and theoretical efforts, the factors limiting high temperature characteristics have gradually been unveiled. In the presentation, our design criteria for the highly-efficient operation of InP-based SL MQW LDs at elevated temperatures will be introduced. Not only our own experimental results but also results so far published in prestigious journals will be cited to support the criteria. Discussion will be extended a little to other materials such as Al contained AlGaInAs. In the course of my presentation, I will introduce our numerical simulation tool which incorporates various kinds of important physics. By analyzing our experimental results, we propose a critical temperature Tc for threshold current and quantum efficiency versus temperature characteristics. As the highlight of my talk, I will explain the importance of Tc. That is, there is a different temperature dependence above and below the Tc. This means that the physical mechanisms restricting high temperature characteristics are different above Tc and below Tc. Below Tc, the Auger recombination is a dominant factor determining the temperature characteristics. While above Tc, a significant increase in both the internal loss and radiative recombination in SCH plays a major role in determining temperature sensitivity. Important guidelines towards much greater high temperature performance LDs will be mentioned in the presentation based on an understanding of the underlying physics above and below Tc.

Strained Quantum Well Lasers with Non-(001) Crystal Orientations

Tsukuru Ohtoshi, Atsuko Niwa, and Takao Kuroda
Central Research Laboratory, Hitachi, Ltd.
1-280, Higashi-Koigakubo, Kokubunji, Tokyo 185, Japan

We discuss theoretically the dependence of the optical gain of quantum well (QW) lasers on strain and crystal orientations. The model that we discuss is based on the multiband effective-mass theory and takes into account the effects of anisotropy and nonparabolicity on the valence subband dispersion. The k·p Hamiltonian with strain is described in terms of a 4x4 matrix, which includes the mixing of the heavy-hole states and the light-hole states. The resulting effective-mass equation is numerically solved by means of the finite-difference scheme [1, 2].

As an example, we analyze InGaAs/InP strained QW lasers. The valence subband dispersions for (001)- and (221)-oriented QW lasers are shown in Fig. 1. The nonparabolicity and the related density of states (DOS) near the band edge for the (221) orientation are reduced in comparison with the (001) case. In addition, conventional models that assume infinite barriers (dashed lines) are shown to underestimate the DOS.

The optical gains in vertical-cavity surface-emitting lasers (VCSELs) are also calculated for various crystal orientations. Figure 2 shows the relationship between the gain and the polarization angle in the QW plane. We find that in VCSELs with non-(001) orientations, excluding (111), the polarization can be controlled and high gains are obtained [1]. This is attributed to the symmetry and the DOS in the valence subbands.

[1] T.Ohtoshi, T.Kuroda, A.Niwa, and S.Tsuji, Appl. Phys. Lett. **65**, 1886 (1994).
[2] A.Niwa, T.Ohtoshi, and T.Kuroda, IEEE J. Select. Topics Quantum Electron. **1**, 211 (1995).

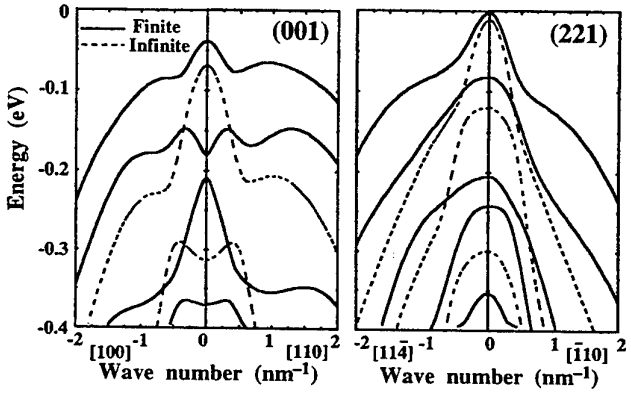


Fig.1 Valence subband structures for $In_{0.7}Ga_{0.3}As$ /InP strained QW lasers. The solid lines show the finite barrier model (this work) and the dashed lines show the infinite barrier case.

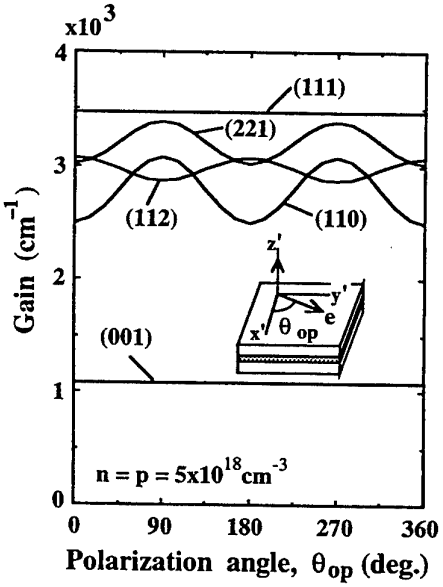


Fig.2 Optical gains for five different orientations plotted as a function of the in-plane polarization angle θ_{op}.

Numerical Modeling of the Optical Field in Vertical-Cavity Surface-Emitting Lasers

G. Ronald Hadley
Kent D. Choquette
M/S 0603
Sandia National Laboratories
Albuquerque, New Mexico 87185-5800

ABSTRACT

Vertical-cavity surface-emitting semiconductor lasers have recently become candidates for successful commercial devices with reports of 50% wall-plug efficiency[1] and 10-microAmpere thresholds[2]. However, modeling of the optical fields in these devices is difficult for all but the simplest cavity designs, due to the distributed reflectivity mirrors and the high cavity Q. In fact, the devices that are presently performing at record levels (the so-called selectively-oxidized lasers) are the hardest to model, because the oxide layers present a region of high index contrast that introduces interference fringes and scattering loss into the problem. Approximate methods such as effective index techniques or beam propagation approaches that are adequate for other geometries are clearly not sufficient to treat these new devices.

Two new methods have recently arisen that purport to accurately solve for the field in such complex devices: the method of lines[3], and the direct finite-difference method. In the former, a discretization grid is employed along one spatial axis only, with the dependence remaining analytic along the other. This method is fully vectorial. The finite-difference method, which will comprise the majority of this talk, is at present a scalar method that employs discretization on a two-dimensional grid and performs an eigenmode analysis by direct matrix techniques. The difference equations for this latter method have been derived using both the standard Crank-Nicholson differencing (second-order accurate) and a new approach that is second-order in the radial direction, but of considerably higher order in the direction perpendicular to the epi layers, becoming infinite in order (having no truncation error) as the device geometry tends to strict one-dimensionality. Comparisons between calculations performed using the method of lines and the finite-difference method for simple etched-post designs have shown good agreement.

More recently, the finite-difference method has been used to study scattering loss from selectively-oxidized lasers as a function of device radius. The scattering loss is expressed as a ratio of the imaginary part of the eigenvalue to that obtained for a similar large-radius device for which the only loss is through the mirrors (or a small free-carrier-absorption component). These calculations show the expected abrupt rise in scattering loss as the device radius decreases, and the large mode discrimination resulting from the higher scattering losses incurred by higher-order modes. We believe that this latter result explains the otherwise inexplicable single-mode operation of these lasers to several times threshold. The results also show that lasers of radius greater than about 4-5 μm experience virtually no losses owing to the presence of the oxide layer; *i.e.*, they look one-dimensional. This result agrees well with laboratory measurements of threshold current density as a function of active area for oxidized lasers. These measurements demonstrate a threshold current density nearly independent of size for devices of area > 100 μm^2, in agreement with the calculations.

The real importance of these modeling tools lies in their ability to quickly explore new designs in a parameter space that is clearly too large for purely experimental investigation. This impact will be particularly apparent as the field solvers are made faster and less memory intensive so that they can be combined with heat and charge transport and thus become an integral part of comprehensive device models.

1. K. L. Lear, K. D. Choquette, R. P. Schneider, Jr., S. P. Kilcoyne and K. M. Geib, Electron. Lett. 31,208(1995).
2.G. M. Yang, M. H. MacDougal and P. D. Dapkus, Electron. Lett. 31, 886(1995).
3. E. Ahlers, S. F. Helfert and R. Pregla, Proc. of Integrated Photonics Res. Topical Mtg, Boston, MA, April 29, 1996, paper ITuE5.

FAST AND ACCURATE ANALYSIS OF COATED AND ANGLED FACETS CONSIDERING TWO-DIMENSIONAL BEAM PROFILES

T M Benson, P C Kendall+, M Reed, P Sewell
Department of Electrical and Electronic Engineering, University of Nottingham, UK
+ Department of Electronic and Electrical Engineering, University of Sheffield, UK.

The calculation and measurement of mode reflectivity for a waveguide or laser incident upon a facet has received much attention in the literature. Recently new demands have been placed on the analysis, particularly by semiconductor travelling wave amplifiers where the reflectivity must be reduced to near zero for both polarisations by a combination of angling the waveguide to the facet and optimisation of multi-layered anti-reflection coatings on the facet. To aid the designer we extend the free-space radiation mode (FSRM) method to provide new formulae for the polarisation dependent reflectivity of a guided mode supported by a two-dimensional waveguide incident at arbitrary angle onto a multi-layered coating.

The FSRM method [1-6] has already been firmly established as an attractive semi-analytical method which possesses the benefits of speed of calculation, minimal computational resource and simplicity, yet retains high accuracy. In the method the exact guided modes are used in the calculation but the radiation modes are assumed to be propagate in a region of uniform refractive index. Whilst this restricts the method to configurations in which the refractive index variation is small in the transverse plane, the FSRM solution is self-consistent and underpinned by exact Fourier operator transform (F-OPT) methods [7-10].

The FSRM method was previously applied to the study the reflectivity of a polarised mode supported by a 1D (slab) waveguide normally incident on an arbitrary multi-layered coating in [1,2] and recently extended to the angled case [4]. Subsequent advances have shown that the FSRM method gives accurate cross-sectional analyses for the guided modes of buried waveguides (scalar [5], polarised (3 component) and fully vectorial [6]). In this paper we combine these previous investigations in order to provide novel 2D analyses for coated and angled facets. Solutions are obtained very efficiently. Results obtained provide new insight into experimental observations and demonstrate that a 2D investigation is required for a full understanding of the facet problem.

References.

1. P C Kendall et al: Semiconductor laser facet reflectivity using free-space radiation modes, IEE Proc-J, 1993, 140, 49.
2. P C Kendall et al: New formula for semiconductor laser facet reflectivity, IEEE Photonics Tech. Lett., 1993, 5, 148.
3. C J Smartt et al: Free space radiation mode method for the analysis of propagation in optical waveguide devices, IEE Proc-J, 1993, 140, 56.
4. M Reed et al: AR coated angled facet design, to appear in IEE Proc-Optoelectronics, 1996.
5. M Reed et al: Free space radiation mode analysis of rectangular dielectric waveguides, to appear in Opt. Quan. Elec, 1996.
6. P Sewell et al: Transcendental equation for the vector modes of buried rectangular and rib waveguides, submitted for publication.
7. C J Smartt et al: Exact polarised rib waveguide analysis Elec. Lett.,1994, 30, 1127.
8. G M Berry et al: Exact and variational Fourier transform methods for the analysis of multi-layered planar waveguides, IEE Proc-Optoelectronics, 1995, 142, 66.
9. C J Smartt et al: Exact analysis of waveguide discontinuities..., Elec. Lett. 1993, 29, 1352.
10. C J Smartt et al: Exact transcendental equation for scalar modes of rectangular dielectric waveguides, Opt. Quant. Elec, 1994, 26, 641.

Modeling and Measurement of Some Functional Semiconductor Laser Devices

G-H. DUAN

Laboratoire d'Optoélectronique (Unité de Recherche Associée au CNRS 820)
Ecole Nationale Supérieure des Télécommunications
46, rue Barrault, 75634 Paris cedex 13, France
Phone: 33-1-45 81 77 28, Fax: 33-1-45 89 00 20
Email: duan@com.enst.fr

Introduction

The maturity and wide-range use of optical transmission technology lead now to the development of direct optical switching and interconnection systems. In these systems, new devices are needed to perform functions such as wavelength conversion, clock recovery and signal reshaping. In this talk, we review recent progress in modeling and measurement of some functional semiconductor laser devices.

Wavelength conversion using lasers and amplifiers

Wavelength conversion is one of the key functions in future wavelength division photonic switching systems. It consists in shifting the wavelength while keeping the carried information. Potential all-optical candidates for this application include i) diode amplifiers, ii) tunable laser diodes and iii) tunable bistable laser diodes. Physical mechanisms involved in wavelength conversion are gain and/or index saturation in amplifiers or lasers, absorption saturation in bistable lasers and four-wave mixing in amplifiers.

The most remarkable result was obtained in a symmetrical interferometric configuration containing two laser amplifiers. The bit-rate obtained is as high as 20 Gbit/s with very small penality in the contrast ratio. Gain and/or index saturation in tunable laser diodes produced by a high power on/off optical sequence provides a wavelength conversion with large bandwidth. Absorption saturation in bistable lasers containing a saturable absorber allows even an improvement of the on/off ratio of an input signal. Highly efficient four-wave mixing in some laser amplifiers is also a promising way to realize wavelength conversion. In general, the modeling of a wavelength converter is based on a set of rate equations describing dynamics of photon density and carrier density. In this talk, simulation and measurement results will be summarized, and the performances of different types of wavelength converters will be compared.

Clock recovery by self-pulsating lasers

Self-pulsation (SP) in multielectrode distributed feedback (DFB) lasers has been observed previously. This effect is undesirable for applications of semiconductor lasers in optical transmission systems. However, it has been shown experimentally that self-pulsation can be locked to an intensity modulated return-to-zero signal. This property makes SP lasers good candidates for clock recovery in transmission systems. All-optical clock extraction at 18 Gbit/s was demonstrated by using a two-section DFB SP laser.

Several assumptions such as the competition between two longitudinal modes and the instability of the longitudinal mode intensity distribution have been proposed to explain the SP in DFB lasers. This talk will review recent modeling and measurement results. At last, the locking properties of self-pulsation to an optical input signal will be presented with emphasis on locking bandwidth and time jitter.

Gain-Coupled DFB Semiconductor Laser Monolithically Integrated with Electroabsorption Modulator

Yi LUO, Chang-Zheng SUN, and Guo-Peng WEN

Dept. of Electronic Engineering, Tsinghua University, Beijing 100084, China
Fax: +86-10-6256-4176; E-mail: deely@tsinghua.edu.cn

Abstract

Distributed feedback (DFB) semiconductor laser integrated with electroabsorption (EA) modulator is considered a most promising emitting source for long-haul, high-speed optical communication system. Up to now, all the photonic integrated circuits (PIC) of this kind are based on index-coupled DFB lasers with quarter-wave-phase-shift structure, which requires perfect AR coating at both facets, resulting in equal allocation of the output power to each facet and difficulties in fabrication. In this paper, we report our results on the gain-coupled DFB semiconductor laser monolithically integrated with EA modulator, both theoretically and experimentally.

By introducing gain-coupling mechanism, the single-mode selectivity of the device will be enhanced and its performance unaffected by external reflection, hence making it possible to increase the effective output power by applying asymmetric facet coating .

A novel PIC device composed of a gain-coupled DFB laser and an EA modulator is designed and fabricated for the first time. Absorptive grating is introduced to achieve gain coupling, thus the demand for facet coating procedure can be reduced very much due to the insensitivity to facet reflection of gain-coupled DFB lasers. The active layer of the laser section and the waveguide of the EA modulator are designed to use an identical MQW layer. Therefore, the fabrication process is much simplified. The design model and fabrication procedure are also given in detail.

The PIC device with cleaved facets operates at pulsed condition and shows a good static characteristics. A modulation depth of 5 dB is obtained at a reverse bias of -5 V. No mode hopping is observed during the static modulation.

Adiabatic frequency chirp analysis in semiconductor DFB lasers monolithically integrated with Mach-Zehnder modulators

X. Li, and **W. -P. Huang**
Department of Electrical and Computer Engineering
University of Waterloo
Waterloo, Ontario, Canada N2L 3G1
D. M. Adams, C. Rolland, and **T. Makino**
Advanced Technology Laboratory
Nortel Technology
Ottawa, Ontario, Canada K1Y 4H7

A gain-coupled DFB laser integrated with an external MZ modulator is an excellent candidate for long haul fiber optical communication systems with modulation speed beyond 10GBits/s[1]. An understanding of the behavior of the adiabatic chirp is required for device optimization. The transmission/reflection characteristics of the individual MZ modulator are analyzed and the influence on the lasing condition of the monolithically integrated DFB laser is obtained using the transfer matrix method. Adiabatic frequency chirps under various conditions are calculated accordingly[2]. The results show that the MZ modulator can be viewed as an equivalent FP cavity due to residual reflection from the DFB/MZ interface and the anti-reflection coated MZ output facet. The effects of MZ phase modulation on this equivalent FP cavity can be understood as the combination of two effects; i) the phase modulation causes an alteration in the optical cavity length of the equivalent FP, and ii) the modulation induces a relative phase delay between the two MZ arms, which changes the equivalent end reflection amplitude, due to the phase-sensitive power transfer characteristics of the MZ multi-mode Y-junctions[3]. For a given modulator structure, the results show that adiabatic frequency chirp can be minimized by a proper choice of DFB laser parameters.

Reference

[1] D. M. Adams, C. Rolland, N. Puetz, R. S. Moore, F. R. Shepherd, H. B. Kim, and S. Bradshaw, "Mach-Zehnder modulator integrated with a gain-coupled DFB laser for 10GBit/s, 100km NDSF transmission at 1.55μm", *Elec. Lett.*, vol. 32, no. 5, pp. 485-486, 1996.
[2] X. Li and W. -P. Huang, "Analysis of Frequency Chirp in DFB Lasers Integrated with External Modulators", *IEEE J. of Quantum Electron.*, vol. 30, no. 12, pp. 2756-2766, 1994.
[3] C. Rolland, D. M. Adams, D. Yevick and B. Hermansson, "Optimization of Strongly Guiding Semiconductor Rib Waveguide Y-Junctions", *IEEE Phot. Tech. Lett.*, vol. 2, no. 6, pp. 404-406, 1990.

Intermixed Quantum Well Laser

Michael C.Y.Chan and E. Herbert Li
Department of Electrical and Electronic Engineering
The University of Hong Kong

Abstract

The intermixed quantum well (QW) laser has been highly considered in recent years. The main advantage of applying the intermixing process in QW laser is to optimize the device's performance for large optical gain, low threshold current density and high relaxation oscillation frequency. In a conventional QW laser, enhancement of the low-threshold current density is mainly dependent on the type of QW material systems (AlGaAs/GaAs, InGaAs/GaAs, InGaAs/InP, InGaAs/AlGaAs) and laser structures (stripe width, cavity length). In the above material systems, they classify into two types of QW structures, lattice-matched (unstrained) QW and lattice mismatched (strained) QW. It has been shown that a strained QW laser has superior characteristics as compared to an unstrained one. For instance, compressive strain in QW layers can reduce the valence band density of states, which is a key to achieve high differential gain and low threshold current density. Theoretical studies indicated that the threshold current density deceases as the strain increases. For a highly strained QW material system, there is the difficulty in growing a high quality QW layered structure. This is due to their widths must be below the critical layer thickness of the particular material system. Above this thickness, the strain is relived by the formation of dislocation. This is because the stability of strained layers in the QW laser active region is important for device applications. An intermixing process will relief the strain induced between the QW layers. Under this process, atoms will diffuse into the neighboring layers obeying to Fick's law. The optical properties of QW, such as absorption coefficient, refractive index, and optical gain, are also changed by modification of the confinement potential from an as-grown square well to a diffused non-linear well. In this presentation, we report the dependency of threshold current density of InGaAs/GaAs strained QW laser as a function of well width, indium composition, and annealing conditions. We believe that the optimization of the above parameters can further reduce the threshold current density of the intermixed QW laser. The best InGaAs/GaAs intermixed-QW laser has been shown to be one of the most attractive candidates for application to optoelectronic integrated circuits.

Modelling of Avalanche Photodiodes

M. Jamal Deen

School of Engineering Science, Simon Fraser University,

Vancouver, British Columbia, V5A 1S6 Canada

Avalanche photodiodes (APDs) have been recognized as being very important and useful for long distance fiber optical transmission systems operating in the 0.95-1.65 μm wavelength region. In comparison to germanium APDs, InP/$In_{0.53}Ga_{0.47}As$ (InGaAs) APDs, offer lower dark currents and lower noise. Because of these advantages and the maturity of III-V compound semiconductor technology, InP-based APDs has attracted considerable atention from researchers in recent years. In this presentation, we concentrate on discussing planar **s**eparate **a**bsorption, **g**rading, **c**harge, and **m**ultiplication (SAGCM) InP/InGaAs avalanche photodiodes because they possess several processing and operational advantages over other APDs such as SAM APDs, and they have the highest gain-bandwidth products (122 GHz) reported to date.

The detailed modelling of the electrical (I-V) and optical (M-V) current-voltage characteristics, the breakdown voltage (V_{BR}), the leakage current will be presented and compared to experimental results. Further, these SAGCM APDs are ideal for studying the multiplication (photogain) versus bias voltage (M-V) characteristics because the self-calibrated nature of the multiplication (M) and the bias-voltage independent quantum efficiency make it possible to compare theory and experiment accurately in an InP-based APD. We will discuss the Miller empirical formula for Si and Ge and show that it is appropriate for the SAGCM InP/InGaAs APDs. Using the physics-based model, the M-V and breakdown characteristics and their temperature dependence for the SAGCM APDs with different device parameters is calculated theoretically, and the calculations are in good agreement to the experimental results. We also provide results to demonstrate that this model can be applied to SAM APDs. In addition, we will show from the detailed physical modelling and the punchthrough and breakdown voltages obtained from DC photocurrent measurements that two critical device parameters - multiplication layer thickness x_d and integrated areal charge density σ_{active}, can be accurately obtained in a simple, fast and non-destructive manner. We will also report on the noise characteristics of these APDs, and will discuss techniques for improving their gain-bandwidth products. Finally, we will compare these and other APDs with pin photodiodes for future long-haul fiber optical communication systems.

LARGE AND SMALL SIGNAL EQUIVALENT CIRCUIT OF QW LASERS

P.R.Vaya
Department of Electrical Engineering
Indian Institute of Technology,Madras-36,India.

H.A.Tafti
School of Electronics and Communication Engineering
Anna University,Madrs-25,India.

ABSTRACT

Various type of laser models and their methods of construction have been developed in parallel with the progress in laser diodes. These models are broadly classified as static and dynamic models. Traditionally,the dynamic models have been derived from analytical or numerical solution of the rate equations. However, the models derived from the above methods suffer from the limitation of non-inclusion of substrate and package parasitics and device-circuit interactions in the calculations. An alternate approach that overcomes these limitations is to transform the rate equations into a circuit model which can then be solved using standard circuit analysis techniques.

The issue of circuit modeling of semiconductor lasers has been reported in our previous work. Previously reported laser models are limited to conventional double heterostructure lasers [1,2]. More recently, attention has been focussed on quantum well (QW) lasers due to the low threshold, high modulation bandwidth, narrow spectral linewidth etc. With this approach,the large signal circuit model of QW laser diode has been derived from rate equations and implemented using the general purpose circuit analysis package PSPICE. This model in conjunction with the optical fiber and photo detector model constituting an optical link has also been simulated. In addition a small signal model of the QW laser diode has been derived from the rate equations. The model simulated and a modulation band width of about 0.1 GHz was obtained. Further, a circuit model for gain switched QW laser diode corresponding to the first, second and third quantised state transition have been developed. picosecond pulses of 7 psec and 2 psec FWHM coresponding to the second and third quantised level transition was observed by gain switching method using circuit modelling techniques.

1. H.A.Tafti et al, " Circuit modelling of multimode semiconductor lasers and study of pulse broadening effect" Electronics Letter,vol.29,1993,pp.1443-1445.

2. H.A.Tafti et al,"Analysis of laser frequency chirp using circuit modelling of semiconductor laser",Proc.of the International Conference on Telecommns, Dubai, 9-12 Jan. 1994,pp.250-253.

SESSION 6P7

Monday, January 6, PM 1330-1710, Lecture Theatre 7, City University of Hong Kong

Electromagnetics - Efficient in Cancer Treatment

Special Session to Honour the Pioneering Work of Chinese Physicians on Application of Electromagnetics in Medicine

Organizers: Hiroshi Kikuchi, Swen Alfas

Chairperson: Hiroshi Kikuchi, Nihon University
Co-Chairperson: Swen Alfas, ELKRAFT, Innovation Dept., Ballerup

13:30 ***Case Reports Showing 80% Efficiency of Defeating Various Cancer Tumours by BET in China***[+] 120
Y-L Xin, F R Zhao
China-Japan Friendship Hospital

14:10 ***Effectiveness of Bio-Electric Treatment on Hepatic Hemangioma and Carcinoma of Gall-bladder*** 121
C K Gu, X Y Chen
Affiliated Hospital of Sichuan Academy of Medical Science

14:30 ***Effects of Applied Electric Fields on Cancer Tumours*** 122
*H Kikuchi, **S Alfas, ***S Kawamata, ****Y Nagai
*Nihon University
**ELKRAFT, Innovation Dept., Ballerup
***Utsunomiya University
****Shonan Institute of Technology

14:50 ***Effect of Electric Field Penetration into a Human Body*** 123
*Y Nagai, ** S Kawamata, ***H Kikuchi
*Shonan Institute of Technology
**Utsunomiya University
***Nihon University

15:10 Break

15:30 ***Effect of Electric Field Application on Water in Living Things*** 124
Y Nagai
Shonan Institute of Technology

15:50 ***Fundamentals of Electro-Biology in Medical Applications*** 125
Swen Alfas
ELKRAFT, Innovation Dept., Ballerup

16:10 ***Panel Discussion on Future Directions***
Moderator : Swen Alfas

[+] double time-slot (40 minutes)

Case Reports Showing 80% Efficiency of Defeating Various Cancer Tumours by BET in China

Xin Yu-Ling, Zhao Feng-Rui,

China-Japan Friendship Hospital, East Yinghuayuan Street, Beijing 100029, China

Bio-Electro Therapy, BET, is relatively new method for defeating various cancer tumours. The knowledge about Biologically Closed Electric Circuits put forth by Nordenström in 1983 has Chinese physicians elaborated and worked out an efficient method for defeating cancer tumours. The results already achieved by BET have proved better than those gained by any conventional method.

There are more than 1.000 hospitals using BET in China today. At The First International Symposium on using electricity in defeating cancer in Beijing in 1992, the Chinese physicians presented short-term efficiency of 78%, based on 2516 cases of various tumours. At The Second International Symposium in Stockholm in 1993, the presented short-term efficiency concerning 4081 cases was 80% in China.

Some specific examples such as lung-, liver-, skin-, breast-cancer, metastatic tumours in lymph nodes, melanomas, facial tumours, metastatic tumours of chest-abdominal wall, thyroid carcinomas, oral cancer, rhabdomyosarcomas, will be presented and discussed.

Progress in Electromagnetics Research Symposium, PIERS 1997 ISBN 962-442-097-1

Effectiveness of Bio-Electric Treatment on Hepatic Hemangioma and Carcinoma of the Gall-bladder

Gu Chunkang, Chen Xiaoyu
Affiliated Hospital of Sichuan Academy of Medical Science
Jian Yang, 641400, P. R. China

Bio-Electric Treatment, BET, utilises the direct current flowing through a tumour and bringing about the inner and outer change of microenvironment disadvantageous for the tumour cells to survival.
This paper concerns BET used to defeat hepatic hemangioma, 13 tumours on 8 patients. Before the treatment, the diagnosis of all the patients were confirmed by B-type ultrasonography laparotomy and pathological examination. Preparation: operation done to insert electrodes into the tumours under direct vision as shown below.



Operation - preparation for the treatment.



Inserting the electrodes and BET.



Finishing up

The anode has been placed in the central part of the tumours, the cathodes at the periphery. The distance between the electrodes 2 - 2,5 cm., voltage 6 - 10 V, current 40 - 100 mA, the treatment time 60 - 100 minutes (after the hepatic hemangioma got black/violet colour).

After the treatment all tumours showed degeneration, necrosis. 8 days after the treatment B-type ultrasonography showed that the echo image of hepatic hemangioma disappeared. Follow-up after 3, 6, 12, 18 months, no recurrence. The result of the treatments according to international criterion is CR, (complete relief).

Under and after the treatment, no complications or side effects observed.

Effects of Applied Electric Fields on Cancer Tumours

Hiroshi Kikuchi
Nihon University, College of Science and Technology
8, Kanda Surugadai, 1-chome, Chiyoda-ku, Tokyo 101, Japan

Swen Alfas
ELKRAFT, Innovation Department, Ballerup, Denmark

Shuichiro Kawamata
Utsunomiya University, Utsunomiya 321, Japan

Yoji Nagai
Shonan Institute of Technology, Fujisawa 251, Japan

From electrical measurements around malignant tumours, it has recently been found that there is a potential difference between the tumour and the healthy tissue around the tumour. The centre of the tumour has a rather broad nucleus and its border possesses fine structure irregularities with sharp or gentle slope in potential to the surrounding healthy tissue. For example, its potential drop is measured to be 10 mV or so. Apart from microstructure, the healthy tissue is considered a neutral plasma with equipotential in macrostructure. The tumour with a charged nucleus is forming a spherical double layer or capacitor.

These observations are described in detail in terms of electrostatics for equilibrium. Then, the effects of an applied DC or quasi-DC electric field on cancer tumours are discussed in terms of electrodynamics and/or electrohydrodynamics. Based on these theoretical considerations and laboratory simulation of electric field penetration to a human body, the possibility of destroying cancer tissues is indicated.

Finally, a new method of remote voltage or electric field application to cancer tumours is proposed in contrast to the conventional method of direct injection of electrodes into cancer tumours.

EFFECT OF ELECTRIC FIELD PENETRATION INTO A HUMAN BODY.

Yoji Nagai,
Shonan Institute of Technology, Fujisawa 251, Japan
Tel: (+81) 466-34-4111; Fax: (+81) 466-35-8897

Shuichiro Kawamata
Utsunmomiya University, Utsunomiya 321, Japan

and

Hiroshi Kikuchi
Nihon University, College of Science and Technology, Tokyo 101, Japan

The discovery of Biologically Closed Electric Circuits (= BCEC) started with an observation of a corona structure around malignant tumours. Such observations lead to performing some electrical measurements, and it is found that there is a potential difference between the tumour and healthy tissue around the tumour. As a result, it is expected to defeat a tumour by penetrating an appropriate electric field into a human body.

While the problem of electric field penetration into a human body is thought to be most basic, practical and important for bio-electromagnetics or electrobiology, very little information is available at present. Among them, a human body is generally considered to be formed of the skin and inner tissues and therefore, to be formed electrically of a double layer with different resistivity.

Based on such a little information, a double-layer model for a human body is introduced to evaluate the potential and field distribution inside a human body by using an electrolytic bath filled with water. A theoretical study is extended based on the experiment.

EFFECT OF ELECTRIC FIELD APPLICATION ON WATER IN LIVING THINGS.

Yoji Nagai,

Shonan Institute of Technology, Fujisawa 251, Japan

Tel: (+81) 466-34-4111 ; Fax: (+81) 466-35-8897

It is very basic, practical and important to investigate the interaction of electric and magnetic field with a human body including body fluids in the human body for bio-electromagnetics or electro-biology.

Hitherto, the author has been investigated a method for activiating water by applying high (DC, AC or impulse) voltage between the electrodes inserted in water tank filled with the water.

The experimental results show that application of the electric field to water leads to activiate water, that is, tends not only
(1) to drop the ORP (= Oxidation Reduction Potential) value of the water, but also
(2) to decrease the ORP value of water with time.

From these results, it is expected that penetration of the electric field into a human body leads to possibility of activiating the body fluid in biological system surrounding the cancer.

Progress in Electromagnetics Research Symposium, PIERS 1997 ISBN 962-442-097-1

Fundamentals of Electro-Biology in Medical Applications

Swen Alfas
ELKRAFT, Innovation Dept.
Lautruphoj 5, DK-2750 Ballerup, Denmark

In 1808, Dalton introduces the atomic concept of matter, Fig. a). Chemical actions between atoms became the fundamental model of chemistry, widely applied in molecular biology and medicine today. There are hundreds of different atoms and consequently almost limitless numbers of possible chemical actions between all these atoms and their compounds. Due to these varieties, a profound understanding of biological matter is difficult (if not impossible) by applying the molecular model.

However, atoms exemplify only one state of matter. Since Dalton's time, it has been observed that the supposed ultimate pieces of matter - particles (atoms) - undergo disintegration as well as creation of their shapes. After particles' annihilation (e.g. $e^+e^- \leftrightarrow \gamma$), matter within particles' shape spreads as γ-waves throughout space until it reaches the unified state of complete homogeneity called FIELD. Illustratively, FIELD can be taken as an evaporated state of particles. The state of matter FIELD is everywhere and it is the carrier of all material phenomena [1]. In the non-stationary, wavy condition (e.g. γ-waves) FIELD is identified as electromagnetic field, [2]. Today we can conclude that the underlying nature of matter in general is electrical, c.f. [3], (and not chemical).

Biological matter emits (and absorbs) electromagnetic field of various wavelength all the time. This crucial fact showes and proves that inside biological matter there are various current loops which are the source of these radiations. Therefore, biological matter structuring and function can be modelled as a network of Bio-Electric Circuits, BECs. In Fig. b) BEC model is illustrated as loop. Moreover, in the atomic model, particles (ions) are in motion, dislocating all the time. Such displacements represent elementary BECs closed by $\mathbf{j} + \partial \mathbf{D}/\partial t$, which in electromagnetics is described as Ampere-Kozelj's law. The BECs are the basic, simple principle of electro-biology.

The main difference between molecular biology and electro-biology is that the molecular model, Fig. a) can fit a concept of inorganic matter (if there is such). The BEC model, Fig. b), fits the nature of matter in general and biological matter in particular.

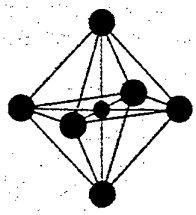


Fig. a) *The atomic model.*

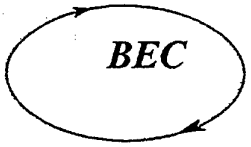


Fig. b) *The BEC model*

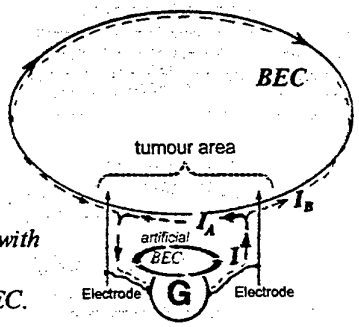


Fig. c) *Treatment with electricity - an interaction with BEC.*

When the BEC model is applied in medicine, e. g., by inserting electrodes into a selected BEC, Fig. c), we interact with biological matter in the same way as biological matter works. The ancient practise of acupuncture, and the latest results of treating cancer by electricity can corroborate the BEC model.

References: [1] W. Thirring, *Urbausteine der Materie,* Almanach der Österreichiche Akademie der Wissenshaften, Vol. 118, 1968, p. 153. [2] S. Alfas, *Einstein's Approach to Understanding Electromagnetic Fields as Part of Matter in EMC,* IEEE proceedings of 1992 regional symposium on EMC, Tel Aviv, p.3.3.2. [3] Cyril W. Smith & Simon Best, *The Electromagnetic Man,* J.M.Dent & Sons Ltd., London 1990, p. 18.

SESSION 7A18

Tuesday, January 7, AM 850-1210, Lecture Theatre 18, City University of Hong Kong

Microstrip & Printed Antennas 2

Organizers: Doris Wu, John Huang

Chairperson: Doris Wu, Boulder Microwave Technologies, Inc.
Co-Chairperson: John Huang, California Institute of Technology

8:50 ***Recent Studies of the U-Slot Patch Antenna*** 127
*K F Lee, **K M Luk, **K F Tong
*University of Missouri-Columbia
**City University of Hong Kong

9:10 ***Techniques for Easing the Fabrication Tolerances of Shorted Microstrip Patch Antennas*** 128
*R B Waterhouse, *D M Kokotoff, **J T Aberle
*Royal Melbourne Institute of Technology
**Arizona State University

9:30 ***Surface Admittance of Arbitrarily Shaped Microstrip Antenna*** 129
Takafumi Fujimoto, Mitsuo Taguchi, Kazumasa Tanaka
Nagasaki University

9:50 ***Transversely Assembled Printed-Circuit and Integrated-Circuit Antenna Arrays and Applications*** 130
Andrew J Parfitt
The University of Adelaide

10:10 ***A Retrodirective Microstrip Antenna Array*** 131
*Shyh-Jong Chung, **Kai Chang
*Chiao Tung University, Hsinchu
**Texas A&M University

10:30 Break

10:50 ***Crank-Line Array Antennas*** 132
*H Nakano, **K Hirose
*Hosei University
**Tokyo Denki University

11:10 ***Integrated Strip Gratings on Top of Microstrip Antennas and Arrays for Low and Ultra-Low Cross-Polar Radiation*** 133
N K Das, A Mohanty
Polytechnic University

11:30 ***Radiation Properties of Planar Array Composed of Ring Microstrip Antennas*** 134
M Haneishi
Saitama University

11:50 ***Design of Omnidirectional Wraparound Microstrip Antennas for Cylinders with Small Radii*** 135
Doris I Wu, Richard C Hall
Boulder Microwave Technologies, Inc.

Recent Studies of the U-Slot Patch Antenna

K. F. Lee*, K. M. Luk+, K. F. Tong+

*Department of Electrical Engineering, University of Missouri-Columbia
+Department of Electronic Engineering, City University of Hong Kong

Abstract

The basic form of the microstrip antenna, consisting of a conducting patch printed on a grounded substrate, has an impedance bandwidth of 1-2%. One way of improving the bandwidth to 10-20% is to use parasitic patches, either in another layer (stacked geometry) or in the same layer (coplanar geometry). The former has the disadvantage of increasing the thickness of the antenna while the latter has the disadvantage of increasing the lateral size of the antenna.

Recently, Huynh and Lee [Electronics Letters, Vol. 31, No. 16, pp. 1310-1312, 1995] introduced a new microstrip antenna in the form of a coaxially-fed rectangular patch with a U-shaped slot which appeared to achieve wideband characteristics without the need of parasitic elements. This antenna retains the thin profile characteristics and will not introduce grating lobe problems when used in an array environment.

In this paper, recent studies of the U-Slot Patch Antenna are reviewed. These include the coaxially-fed rectangular U-Slot patch, a two-element array of such patches, the coaxially-fed circular patch with a U-Slot, and the aperture-coupled U-slot rectangular patch. It is found that the coaxially-fed single patch and a two-element array of such patches can attain 20-30% impedance as well as gain bandwidths, with good copolar and crosspolar pattern characteristics. The gain of the single patch is 2-3 dB higher than the patch without the slot. The coaxially-fed U-slot patch can also be designed for dual-frequency operation, with 20% separation of the two frequency bands easily obtainable. The aperture-coupled U-slot patch also yielded an impedance bandwidth of some 20%. However, its improvement over that of the regular patch is much less pronounced than the coaxially-fed case. Possible future work on this antenna will be discussed.

Techniques for Easing the Fabrication Tolerances of Shorted Microstrip Patch Antennas

R.B. Waterhouse*, D.M. Kokotoff* and J.T. Aberle+

*Department of Communication & Electronic Engineering
Royal Melbourne Institute of Technology
GPO Box 2476V
Victoria, 3001
Australia

+Telecommunications Research Center
Arizona State University
Tempe, AZ 85287-7206
USA

Recently a small printed circular antenna was proposed which incorporated a single shorting post to significantly reduce the overall size of the antenna [1]. Due to the inherent small physical dimensions of the radiator (with a radius, R = 0.025 λ_g compared to R = 0.076 λ_g for a conventional circular microstrip patch mounted on the same substrate), the antenna is very suited to situations where minimum antenna real estate is a premium. Such scenarios occur for mobile communication hand-sets, for both present day and next generation mobile systems where the operating frequency is still relatively low. As is expected for electrically small antennas, the price paid for reduced antenna real estate is unfortunately reduced impedance bandwidth, as well as lower gain. However, it has been shown that by using techniques usually employed for conventional microstrip patch antennas (for example, the use of low dielectric constant substrate), these parameters can be improved [2].

A fundamental problem with the single shorting post microstrip patch antenna is the dependence of the input impedance of the antenna on the relative positioning of the probe feed with respect to the short circuited pin. This feature in itself is not unexpected; however, to achieve a 50 Ω match at the resonant frequency, typically the relative position is a small fraction of a wavelength (0.002 λ_g), thus requiring very accurate fabrication processes. This is primarily due to the small radiator relying on the physical discontinuities associated with the close proximity of the probe to the post to achieve the necessary currents on the printed antenna.

In this presentation, techniques are proposed and investigated which can alleviate the fabrication difficulties associated with shorted printed antennas. One such method incorporates the use of multiple shorting pins aligned in the same plane. Simplistically, as the number of shorting pins along this plane increases, a 'stronger' shorting plane is established on the radiator, and thus the performance of the printed antenna approaches that of a conventional quarter-wave patch. Importantly, as the number of shorting pins is increased the relative position of the probe feed with respect to the shorting plane is enlarged. This ease in fabrication tolerances is achieved at the expense of increased antenna real estate. Thus a compromise between fabrication tolerances and overall size must be considered. For example, using two shorting posts in the previously mentioned case increases the separation of the probe feed and shorting plane to 0.004 λ_g and increases the radius of the patch conductor to 0.029 λ_g. A rigorous analysis of this configuration and other shorted patch variations was achieved by generalising the analysis presented in [3], such that a multiple number of pins can be included. A thorough investigation of these shorted patches will be presented, including an investigation of the impedance performance and the far-field radiation properties.

REFERENCES

[1] R.B. Waterhouse, "Small microstrip patch antenna," *Electron. Lett.*, vol. 31, pp. 604-605, Apr. 1995.

[2] R.B. Waterhouse and S.D. Targonski, "Performance of microstrip patches incorporating a single shorting post", to be presented at *IEEE Antenn. Propagat. Symp.*, Baltimore, 1996.

[3] J.T. Aberle, D.M. Pozar and C.R. Birtcher, "Evaluation of input impedance and radar cross section of probe fed microstrip patch elements using an accurate feed model", *IEEE Trans. Antennas & Prop.*, AP-39, pp. 1691-1697, Dec. 1991.

SURFACE ADMITTANCE OF ARBITRARILY SHAPED MICROSTRIP ANTENNA

Takafumi FUJIMOTO, Mitsuo TAGUCHI and Kazumasa TANAKA

Dept. of Electrical Eng. & Computer Science, Nagasaki University
1-14 Bunkyo-machi, Nagasaki-shi, 852, Japan
E-mail : fujimoto@ec.nagasaki-u.ac.jp

The cavity model is a simple and efficient analytical method on the microstrip antenna (MSA) of any configuration, where the separation of variables is possible in the wave equation expressed in the particular coordinate system. In this method, the antenna is treated as a resonant cavity bounded above and below by the conducting plates and on the side by the admittance wall. The electromagnetic fields within the cavity are expanded in terms of the eigenfunctions and determined by the impedance boundary condition at the side aperture. The contribution from the outside region of antenna is taken into account by the surface admittance at the aperture. The accuracy of the surface admittance affects the resonant frequency and the input impedance of antenna.

In this paper, the formulation method of surface admittance of arbitrarily shaped MSA by the spectral domain analysis is proposed. The surface admittance is defined by the magnetic field produced by the equivalent magnetic current on the aperture. The magnetic field is expressed by Green's functions for the vector potential and the scalar potential due to the horizontally directed magnetic dipole. The Green's functions are determined by applying the boundary conditions at the interfaces between free space, dielectric substrate and ground plane to the solution of the wave equation in the spectral domain.

As examples of arbitrarily MSA, circular MSA for linear polarization and elliptical MSA and elliptical ring MSA with circular slot for circular polarization are calculated. In the analysis of elliptical MSA and elliptical ring MSA, the electromagnetic fields within the cavity are expanded in terms of the eignfunctions in the cylindrical coordinate system. The electromagnetic fields and determined so as to satisfy the impedance boundary condition on the aperture in the least squares sense. The calculated surface admittance of the circular MSA is constant along the aperture without depending on the equivalent magnetic current distribution on the aperture. On the other hand, the surface admittances of elliptical MSA and elliptical ring MSA vary with the observation point and the magnetic current distribution along the aperture. In the case of elliptical ring MSA, the mutual coupling between the outer aperture and the inner slot is taken into account. In order to ascertain the validity of the surface admittance of these antennas, the calculated input impedances are compared with the experimental data. Good agreement between the calculated and measured input impedances are obtained. In the cases of elliptical MSA and elliptical ring MSA, the circular polarization characteristics are also discussed.

Progress in Electromagnetics Research Symposium, PIERS 1997 ISBN 962-442-097-1

TRANSVERSELY ASSEMBLED PRINTED-CIRCUIT AND INTEGRATED-CIRCUIT ANTENNA ARRAYS AND APPLICATIONS

Andrew J. Parfitt

Department of Electrical and Electronic Engineering
The University of Adelaide
South Australia, 5005

Abstract

Microstrip antenna arrays have been developed over the past several decades into a low-cost printed-circuit planar array technology. In general, microstrip structures have been fabricated on a grounded dielectric substrate and assembled by stacking substrates longitudinally where more than one substrate is required or when connection to other circuits is necessary. An alternative approach, whereby substrates are assembled transversely to the array aperture, has a number of attractive features for some applications.

In this paper, some typical antenna structures compatible with this alternative approach are described, and their array performance outlined. Examples include substrate-supported metal-strip dipole antennas and tapered slot antennas. Particular reference is made to the bandwidth and scanning performance of such antennas in an array environment, and their compatibility with monolithic integration for millimetre wavelength operation. Since the antenna geometry itself is more complex than that of conventional microstrip antennas, the analytical and numerical techniques required for accurate design are different, and will be outlined. Emphasis here will be on computationally efficient analysis and the ability to model all of the details of a variety of geometries.

Two applications of transversely assembled arrays will be described. In the first application, a single substrate is used for a 10 element linear array and constrained lens structure intended for 35GHz imaging applications. In the second application several antennas on individual substrates are used to form a phased array wherein oscillators at individual antenna elements are synchronised by mutual coupling in a common cavity. Both examples illustrate the effectiveness of the array architecture in achieving a highly integrated system.

Progress in Electromagnetics Research Symposium, PIERS 1997 ISBN 962-442-097-1

A Retrodirective Microstrip Antenna Array

Shyh-Jong Chung
Dept. of Communication Eng., Chiao Tung Univ.
Hsinchu, Taiwan, ROC

Kai Chang
Dept. of Electrical Eng., Texas A&M Univ.
College Station, TX77843-3128, USA
Tel: (409)845-5285 Fax: (409)845-6259
E-mail: chang@eesun1.tamu.edu

Abstract

A Van Atta retrodirective reflector was designed and developed, using the aperture-coupled microstrip antenna array. This reflector possesses the advantage of returning high fields to the source point over a wide range of incident angles, and, owing to the low cost and comformability of the structure, is suitable for the applications in the future automotive collision avoidance system and the road traffic management system. A theory considering the reradiation and the scattering effects of this array reflector was introduced, which showed a good agreement with the measurement. According to this theory, the reradiated fields from the antennas are the primary contribution to the retrodirectivity property of the reflector. The lengths of the microstrip feed lines should be suitably designed so that a well-interfered pattern by the reradiated and scattered fields can be achieved.

The superiority of the new retrodirective reflector was demonstrated by comparing with a metal plate reflector. The returning-field pattern of the retrodirective reflector possesses a beamwidth larger than 120°, while that of the plate reflector is only 10°. A comparison was also made between the present reflector and a microstrip antenna array having the same elements as the retrodirective reflector but without feed structures. Although, due to the edge diffraction and self-reradiation effects, the microstrip antenna array gives extra high returning fields at angles away from the specular direction, the fields at other angles are much weaker as compared to the present retrodirective reflector. Finally, the reflector with switches in the midways of the microstrip feed lines was investigated for the possible applications in communications and remote identifications.

CRANK-LINE ARRAY ANTENNAS

H. Nakano and K. Hirose*
College of Engineering, Hosei University, Koganei, Tokyo 184, Japan
*Tokyo Denki University, Hiki-gun, Saitama 350-03, Japan

A design for a crank line array antenna (CLA) printed on a dielectric substrate based on the line electric-current source method [1] has been reported. Since this line electric-current source method does not take into account the mutual coupling between bent lines and the effects of substrate surface waves, some experimental work is needed to complete the CLA design. The purpose of this paper is to present a rigorous CLA design using the method of moments [2].

The CLA radiates a circularly polarized wave in the broadside direction when each cell of the CLA has appropriate dimensions that are expressed in terms of the guide wavelength of the current along the crank lines, λg. It is, therefore, essential to obtain the guide wavelength for CLA design.

The guide wavelength is determined in several steps. In the first step, crank lines are constructed by assuming that λg is equal to $\lambda g(1)$, where $\lambda g(1)$ is a rough estimate of the guide wavelength using conventional microstrip line theory. The CLA based on $\lambda g(1)$ is called CLA(1).

In the second step, CLA(1) is analyzed to obtain the current distribution. The guide wavelength is evaluated from the phase progression of the current distribution and designated as $\lambda g(2)$. Then, a crank line antenna called CLA(2) is constructed by assuming that λg is equal to $\lambda g(2)$.

In the third step, CLA(2) is analyzed to obtain the current distribution. This analysis yields a new guide wavelength, $\lambda g(3)$, which is compared with the previously evaluated guide wavelength, $\lambda g(2)$. If $\lambda g(3) = \lambda g(2)$, then the iterative process is terminated. $\lambda g(3)$ is the final guide wavelength of a CLA that radiates a circularly polarized wave in the broadside direction. That is, $\lambda g = \lambda g(3)$. If $\lambda g(3) \neq \lambda g(2)$, a crank line antenna called CLA(3) is constructed, and the process in the third step is repeated until $\lambda g(n) = \lambda g(n-1)$, ($n = 4, 5, \ldots$).

A dielectric substrate with a relative permittivity of $\varepsilon_r = 2.6$ and a thickness of $(\lambda_0/\sqrt{\varepsilon_r})/8$ is used for the CLA design. It is found that λg is obtained after only three steps. The CLA constructed on the basis of $\lambda g = \lambda g(3)$ radiates a circularly polarized wave with an axial ratio of 0.3 dB in the broadside direction.

Further numerical results show that the surface waves due to the presence of the dielectric substrate reduce the antenna efficiency [3]. In addition, the gain is enhanced by gradually changing the antenna height from the ground plane [4]. These two facts lead to a new CLA, where the crank lines are printed on a thin film, which has an obliquity of 1 degree with respect to the ground plane, and is supported by a foam material with a relative permittivity of $\varepsilon_r \cong 1$. It is found both numerically and experimentally that the new CLA has a gain of approximately 30 dB over a frequency range of 2.5%.

[1] J. R. James and P. S. Hall, *Hand book of microstrip antennas*, Peter Peregrinus Ltd., Chaps. 13, 14, 19, 1989.
[2] H. Nakano, et al., "The moment method solution for printed wire antennas of arbitrary configuration", *IEEE Trans. Antennas & Propagation*, Vol. 36, No. 12, pp. 1667-1674, 1988.
[3] H. Nakano, et al., "Numerical analysis of a crank-type antenna on a dielectric substrate", *Int. J. of Microwave and Millimeter-Wave Computer-Aided Engineering*, Vol. 4, No. 1, pp. 43-49, 1994.
[4] H. Nakano, et al., "A numerical analysis of crank-line antenna", ICAP'93, pp. 647-650, 1993.

Integrated Strip Gratings on Top of Microstrip Antennas and Arrays for Low and Ultra-Low Cross-Polar Radiation

N. K. Das and A. Mohanty
Weber Research Institute/ Department of Electrical Engineering
Polytechnic University, Route 110, Farmingdale, NY11735, USA

ABSTRACT: Antennas with low or ultra-low levels of cross-polar radiation are of significant interest to communication, radar and remote sensing. Printed and integrated antennas, although are becoming increasingly popular for general applications, do not often meet the low cross-polarization requirement. The cross-polar radiation may be generated due to several reasons: (i) due to orthogonal currents inherently excited on a microstrip antenna, or additionally induced in an array environment due to mutual coupling, (ii) due to basic polarization coupling effect of the antenna substrate itself, or (iii) due to spurious radiation from the feeding circuitry. One attractive solution is to integrated - either directly on top or properly spaced above - narrow strip gratings on top of microstrip antennas, which can function as a filter for the unwanted polarization. However, a successful design of such "integrated grating antennas" must account for the critical loading and resonance effects that the strip grating layer may introduce.

In this paper we will present a rigorous, general method of analysis for integrated grating antennas, and discuss critical design and analytical issues. Various basic phenomena will be explained through specific results computed for an integrated grating dipole geometry, the conclusions from which can be extended to to other antenna geometries as well. Some results to be presented include: (i) effect of strip grating layer on antenna impedance and resonant frequency, (ii) cross-polarization performance for different parameter variation, and (iii) scan blindness problems that may result in an array design due to excitation of "grating modes." Interestingly, for certain range of grating parameters it may be possible to model a strip grating as an "ideal unidirectionally conducting screen." We will also present an approximate model based on this idealization, that will be shown to be quite useful at least for initial design simplification and physical understanding. Finally, based on the computed results, we will suggest useful design guidelines in order to avoid or minimize the various problems due to strip grating effects. In conclusion, as our investigation demonstrates, suitable geometries of integrated grating antennas can be quite practical and effective for a large range of design requirements.

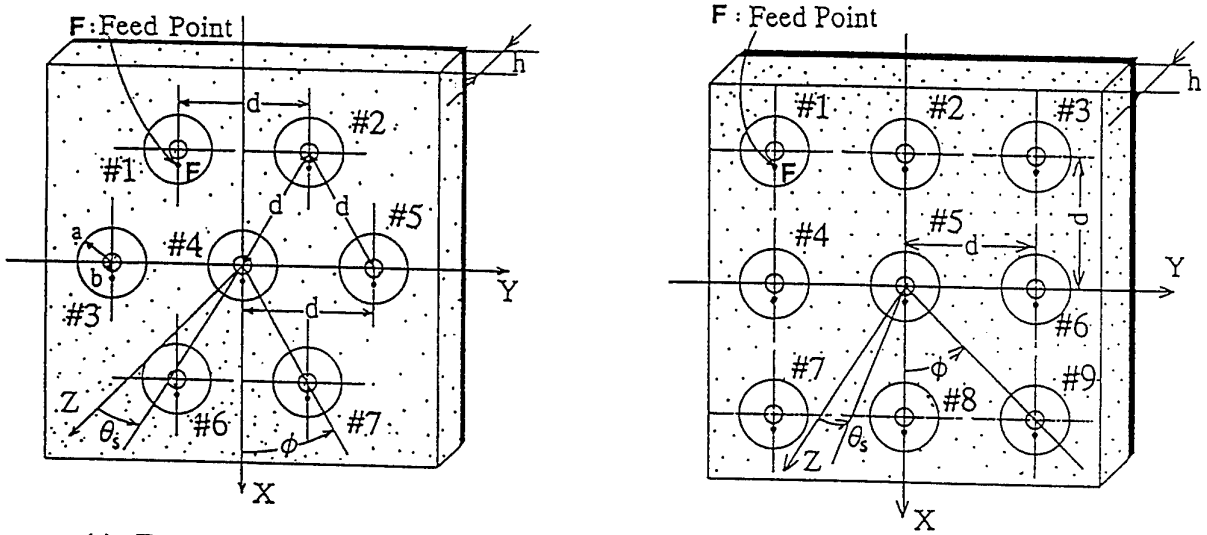
Radiation Properties of Planar Array Composed of Ring Microstrip Antennas

M. Haneishi
Department of Electrical and Electronic Systems Engineering,
Faculty of Engineering, Saitama University
255 Shimookubo, Urawa, 338, Japan

A ring microstrip antenna(R-MSA) has been studied by many researchers, since it permits reduction of antenna size and easily allows excitation of circular polarization by single feeding. As well known, in the designing of array antenna, it is important to estimate mutual coupling effect |S12|, active element pattern and active reflection coefficient |Γ|. For this reason, both active element pattern and active reflection coefficient for R-MSA planar arrays are investigated in the present contribution. Two typical arrangements, square and triangular arrangements are employed in this study, as shown in the Figure. The test samples of these R-MSA arrays are fabricated using a Teflon fibergrass substrate(ε_r=2.6, tanδ=0.0018) and tested at the C-band. A large scale planar array can be realized by integrating a large number of these subarray units.

First, the active element patterns of the array are computed by considering the mutual coupling effect of R-MSA elements and using GTD technique. The computed patterns for each element are compared with the experimental results. As a result of experiment, the computed patterns agreed well with the experimental ones.

Next, active reflection coefficient |Γ|, which is useful in the designing of a phased array antenna, is investigated. In order to obtain some useful designing data, two types of radiating element, circular MSA(β=0, where β is the ring ratio of patch element, and denoted as β = b/a) and R-MSA, are employed as elements in the arrays. The active reflection coefficient |Γ| is computed for the center element of the arrays. The results demonstrated that a lower active reflection coefficient |Γ| was achieved for the R-MSA element compared with a usual circular MSA .



(a) Triangular arrangement

(b) Square arrangement

Basic configuration of planar array

Design of Omnidirectional Wraparound Microstrip Antennas for Cylinders with Small Radii

Doris I. Wu and Richard C. Hall
Boulder Microwave Technologies, Inc.
2336 Canyon Blvd, Boulder, CO 80302
email: dwu@bmt.com

ABSTRACT

Wraparound microstrip antennas which can be wrapped around a missile or a lamp post are particularly useful in providing an inexpensive means of data transmission in applications ranging from telemetry to cellular base stations. For large mounting cylinders (radii greater than a guided wavelength), the effect of the curvature is generally small; therefore, a planar model can be used to generate an initial design. However, when the radii are small, planar models become inadequate. This is particularly true for omnidirectional and circularly-polarized arrays where the polarization purity of the array as well as the mutual coupling between the patches can be affected by the curvature. For wraparound antennas with small radii, the inclusion of the cylindrical curvature effect in the design process is crucial in attaining an optimal design. The availability of an accuracy simulation tool which can take into account the curvature effect in the design process becomes necessary.

To facilitate the design of wraparound antennas for cylinders with small radii, an accurate simulation program has been developed in-house. Based on the full-wave mixed-potential integral equation approach, the simulation tool is rigorous and applicable for arbitrarily-shaped structure. Several S-band omnidirectional circularly-polarized microstrip arrays for cylinders with radii less than one-half guided wavelength have been designed with the aid of the simulation tool. Key design issues, such as number of elements required to achieve good omnidirectionality, tradeoffs between number of elements and element spacing, matching of each array element, and the optimization of the array for circular polarization, will be presented along with sample prototypes and measured results.

SESSION 7P18

Tuesday, January 7, PM 1330-1610, Lecture Theatre 18, City University of Hong Kong

Microstrip & Printed Antennas 3

Organizers: Doris Wu, John Huang
Chairperson: John Huang, California Institute of Technology
Co-Chairperson: Doris Wu, Boulder Microwave Technology Inc.

13:30 ***A Circularly Polarized Printed Slot Array Fed by Coplanar Waveguide*** 137
Koichi Ito, Shin-ichiro Matsuzawa
Chiba University

13:50 ***A Ka-Band 0.5m Circularly Polarized Microstrip Reflectarray*** 138
J Huang
California Institute of Technology

14:10 ***Perforated Microstrip Patch Antennas*** 139
L Shafai
University of Manitoba

14:30 ***Design of Finite Array of Wideband Aperture-Coupled Microstrip Antennas*** 140
B Chen, D G Fang, F Ling
Nanjing University of Science and Technology

14:50 ***DBS Antennas : Present and Future*** 141
Qun Wu, Daoli Sun
Harbin Institute of Technology

15:10 **Break**

15:30 ***Characteristics of Single and Coupled Microstrip Antennas on Anisotropic Substrates*** 142
*A G d'Assuncao, **J R S Oliveira
*Federal University of Rio Grande do Norte
**Federal Center of Technological Education

15:50 ***The Synthetic Approach of Wideband Microstrip Antenna Design*** 143
*Bocheng Zhu, **Wenhong Chen, *Shizhi Li
*Beijing Institute of Technology
**Institute of Command and Technology, COSTIND

A Circularly Polarized Printed Slot Array Fed by Coplanar Waveguide

Koichi Ito† and Shin-ichiro Matsuzawa‡
†Faculty of Engineering
‡Graduate School of Science & Technology
Chiba University
1-33 Yayoi-cho, Inage-ku, Chiba-shi, 263 Japan

The popularity of the coplanar waveguide (CPW) has increased significantly in recent years. The advantages of CPW include wider bandwidth, smaller mutual coupling between two adjacent lines, and easier integration with solid state active devices. Patch antennas [1], loop antennas [2], and folded-slot antennas [3] fed by CPW were reported.

In this paper, we propose a new structure of a circularly polarized printed slot antenna fed by CPW. The advantages of this antenna are a simple geometry of an element, easy construction of a linear array and the capability of switching the polarization by using active devices. We have investigated the characteristics of this antenna by using the FDTD analysis with the super-absorbing first-order Mur boundary condition [4].

Some numerical results were calculated at 12 GHz band. We obtained the antenna parameters producing a good circular polarization and a minimum axial ratio (AR) of less than 1 dB was achieved at 11.8 GHz with a relative frequency bandwidth (AR $\leqq$ 3 dB) of 3.0 %. The bandwidth will be much improved by optimizing the antenna parameters. Other characteristics such as a reflection coefficient and radiation patterns will be demonstrated.

For further study, we will analyze the antenna with a reflector in order to get an unidirectional pattern and fabricate a liner array with a series feed.

References

[1] R.N.Simons and R.Q.Lee, "Coplanar waveguide aperture coupled microstrip patch antenna," *IEEE Microwave Guided Wave Lett.*, vol.2, no.4, pp.138-139, July 1991.

[2] H.C.Liu, T.S.Horng and N.G.Alexopoulous, "Radiation of Printed Antennas with a Coplanar Waveguide Feed," *IEEE Trans. Antenna Propagat.*, vol.43, no.10, pp.1143-1148, Oct. 1995.

[3] T.M.Weller, L.P.Katehi and G.M.Reiz, "Single and Double Folded-Slot Antennas on Semi-Infinite Substrates," *IEEE Trans. Antennas Propagat.*, vol. 43, no.12, pp.1423-1428, Dec. 1995.

[4] K.,K.Mei, J.,Fang, "Superabsorption - A Method to Improve Absorbing Boundary Conditions," *IEEE Trans. on Antennas and Propagat.*, vol.40, no.9, pp.1001-1010, Sep. 1992.

A Ka-Band 0.5m Circularly Polarized Microstrip Reflectarray

John Huang

Jet Propulsion Laboratory
California Institute of Technology
4800 Oak Grove Drive
Pasadena, California 91109 USA

The microstrip reflectarray antenna, being in the form of a flat reflector, has recently been investigated by several antenna researchers. This antenna, when compared to the conventional parabolic reflector, not only has the potential advantages of achieving smaller mass, smaller volume, simpler deployment mechanism, but also has the capability of scanning its main beam to larger angles from the broadside direction. Without any power divider and its associated large insertion loss, a phased reflectarray may not need the high cost T/R modules and can still remain to be an efficient array antenna.

To demonstrate that such an antenna can be developed with relative large electrical aperture at millimeter frequencies, a half-meter-diameter microstrip reflectarray has been designed and constructed at 32 GHz with circular polarization. It is believed that this is electrically the largest microstrip reflectarray has ever been build. Close to seven thousand square patches are etched on 10-mil thick Duroid substrate. All square patches have identical dimensions. Far-field phase coherence is achieved by attaching to the patches with different-length microstrip phase delay lines. A corrugated feed horn was specially designed to optimally illuminate the reflectarray aperture. Measurement results and potential applications of this microstrip reflectarray will be discussed in the symposium

Progress in Electromagnetics Research Symposium, PIERS 1997 ISBN 962-442-097-1

Perforated Microstrip Patch Antennas

L. Shafai

Department of Electrical and Computer Engineering
University of Manitoba
Winnipeg, Manitoba, Canada, R3T 5V6

Microstrip patch antennas have simple geometries and in rectangular or circular shapes have been used as primary radiators or the elements of microstrip arrays. Their main disadvantage is the narrow bandwidth that has been overcome by electromagnetic coupling to other resonant patches or slots. Multi-band operating have also been achieved by stacking several patches, and feeding them using a single or multiple feed probes, but the configuration becomes a three-dimensional structure.

In patch antennas the size controls the operating frequency and at high frequencies, or, narrow band antennas require high precision fabrications. In the present study perforated patch antennas are investigated. Perforation affects the resonance frequency and can be used in frequency tuning, where a wide range of frequencies is obtained without changing the antenna size. It also allows incorporating smaller higher frequency patches on a larger one to design for dual or multi-band operation.

The paper will review the type of microstrip patch and its perforation shape, identifying the key parameters. The performance of the antenna in bandwidth, gain and cross-polarization will then be investigated for single and stacked patch configurations.

DESIGN OF FINITE ARRAY OF WIDEBAND APERTURE-COUPLED MICROSTRIP ANTENNAS

B. Chen, D. G. Fang, and F. Ling
Department of Electronic Engineering
Nanjing University of Science and Technology
Nanjing, 210094, China

The aperture-coupled microstrip antenna has several advantages compared to the probe or transmission line fed patch antennas. In this kind of antenna, separate substrates can be used for the feed circuit and the antenna element to isolate spurious feed radiation. This is attractive for the design of low side lobe level. This kind of structure also possesses the wideband property.

In this study, for the analysis of single aperture-coupled microstrip antenna, we use the FD-TD method which may provide the wide band information. The modified Berenger PML absorbing boundary condition (MPML) is used. The MPML is more efficient in absorbing the evanescent energy and keeping the same performance for propagating modes. This good performance results in the reduction of computational region significantly. The results from FD-TD method are compared with those by using spectral domain approach. The effects and the sensitivity of the geometric parameters of the antenna element are investigated which provide the guideline of the design.

In the analysis of a practical array, a good understanding of the mutual coupling between elements in a finite array environment is necessary. We introduce the approximate treatment of involving such coupling. This treatment needs less CPU time and keeps reasonable accuracy. Under certain excitation, the current distributions and the input impedances may be obtained. Based on the analysis, for a given current distribution, the determination of the excitation may be obtained through genetic algorithm, therefore the design of both the array and the feed network will be completed.

DBS Antennas: Present and Future

Wu Qun Sun Daoli
Department of Radio Engineering
Harbin Institute of Technology
Harbin 150001,PRC

Prior to utilizing Ku-band(12GHz) for DBS(Direct Broadcast from satellites) business was recommended by the world Administrative Radio Conference in 1977. Up till now,many countries has started this business.More and More countries are planning to start DBS service,too. DBS intensively stimulated research work concerning receive equipment,especially the planner antennas.With the rapid development of low-noise amplifiers and low-loss substrate materials,researchers has concentrated their attention on high- efficiency antennas.This makes the DBS receive antennas for individul subscribers tend to smaller size and lower cost. During the past ten years,some types of antennas with new concept and novel design have been proposed.This paper reviews the progress in DBS plannar antennas for Ku- band reception, and summerizes their present status and future trends,including the early research of microstrip line,strip line and suspended line planar antennas,and recent advances in radial line slot array,leaky-wave slot waveguide array,multiple beam forming,self-steering active array planar antennas,etc.

Progress in Electromagnetics Research Symposium, PIERS 1997 ISBN 962-442-097-1

CHARACTERISTICS OF SINGLE AND COUPLED MICROSTRIP ANTENNAS ON ANISOTROPIC SUBSTRATES

Adaildo Gomes d'Assunção* and José de Ribamar Silva Oliveira**

* Federal University of Rio Grande do Norte
Electrical Engineering Department, Caixa Postal 1655
59072-970 Natal, RN, Brazil, Fax: +55-84-231-4254 E-mail: adaildo@ncc.ufrn.br

** Federal Center of Technological Education
Av. Getúlio Vargas 04, Monte Castelo, 65025-001 São Luís, MA, Brazil
Tel.: +55-098-221-3390 Fax: +55-98-232-3129

A fullwave analysis of single and coupled microstrip patch antennas on anisotropic substrates is presented. The analysis is developed in the spectral domain by combining Hertz vector potentials, Parseval's theorem, Galerkin method, and the phase stationary condition.

The structure considered is obtained by coupling two rectangular microstrip patch antennas on two uniaxial anisotropic layers (Fig. 1). From this structure, several single and coupled microstrip configurations are investigated, such as patches on single, suspended, and double anisotropic layers. The optical axes orientation in dielectric regions 1 and 2 is assumed to be along the microstrip main axes (x, y, and z), separately.

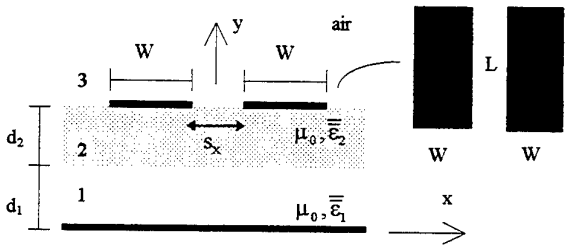


Fig. 1 - Coupled patches on anisotropic substrates.

The analysis of single microstrip patch antennas is developed to determine the effect of the anisotropy of the different dielectric layers on the antenna parameters, such as: resonant frequency, quality factor, input impedance and radiation pattern. The impedance matrix for the structure considered is obtained by using Hertz vector potentials, which are considered to be along the optical axis orientation, in each anisotropic dielectric layer.

In the study of coupled microstrip antennas, the coupling characteristics are investigated, by using the spectral domain technique. Even and odd mode resonant frequencies are determined as functions of the structural parameters.

Numerical results are presented for several configurations, such as patches on single, suspended and double uniaxial anisotropic layers, showing the effect of the anisotropy in the dielectric layers on the characteristics of the considered microstrip structures. Three different orientations for the optical axes (x, y, and z, in Fig. 1) are assumed, allowing to compare the results for these cases. The results obtained in this work are in agreement with those available in the literature, for several particular cases.

THE SYNTHETIC APPROACH OF WIDEBAND MICROSTRIP ANTENNA DESIGN

Bocheng Zhu, Wenhong Chen* and Shizhi Li
Department of Electronics Engineering
Beijing Institute of Technology
P.O.Box 327, Beijing 100081, China
*Institute of Command and Technology, COSTIND
P.O.Box 3380, Beijing 101407, China

Abstract: Wideband microstrip antennas have enjoyed increasing support for use in radar and communication systems where weight, size and conformability are critical factors. In this paper, a synthetic method of designing broadband microstrip antenna is presented, and a dual-patch configuration fed by coaxial probe is investigated by adopting new feed technique and impedance matching network to obtain broad bandwidth. The two factors restricting the bandwidth of microstrip antennas, the inductive reactance introduced by coaxial feed probe and the frequency dependence of the input impedance, are mainly studied.

The coaxial probe introduces a series inductive reactance which becomes quite significant with respect to the radiation resistance. In order to widen the bandwidth, the conventional feed technique is improved, and a small round capacitive patch fed by the coaxial probe is introduced into the dual-patch structure and used to counteract the inductive reactance caused by the feed probe.

In the designing, the lossless impedance matching network is introduced, which is applied to compensate the frequency dependence of the input impedance, thus to lower the input VSWR and broaden the input impedance bandwidth further. The impedance matching network is designed by the real frequency technique, and a low-pass circuit is employed to realize the impedance matching network.

A two-sided structure has been employed in the configuration design. The improved dual-patch structure is installed on one side of the ground plane, and the loseless impedance matching network is on the other side. The coupling between the dual-patch structure and the loseless matching network is accomplished by a probe through the ground plane.

The experimental results demonstrated that the bandwidth of microstrip antenna can be broadened significantly by adopting dual-patch configuration, developed feed technique and impedance matching network. In term of the input VSWR less than 1.5, a bandwidth of 25% of the centre frequency has been achieved, and the realized gain with a flatness of $8.2 \pm 0.4 dB$ has been obtained within the desired bandwidth.

SESSION 7A17

Tuesday, January 7, AM 850-1230, Lecture Theatre 17, City University of Hong Kong

Antenna Measurements

Organizers: Nizar Sultan, Guy Seguin

Chairperson: Nizar Sultan, Canadian Space Agency
Co-Chairperson: Guy Seguin, McGill University

8:50 ***Near-Field Measurement Deconvolution*** 145
G Seguin, T J F Pavlasek
McGill University

9:10 ***Radar Active Antenna and Complete Radar Chain Pulse Measurement in Compact Test Range*** 146
D Carbonne, J M Lopez, D Belot, J Blouvac, C Sourdois
Centre Spatial de Toulouse

9:30 ***Phase Retrieval Diagnostic in Bi-Polar Planar Near-Field Measurements*** 147
Yahya Rahmat-Samii, Robert G Yaccarino
University of California, Los Angeles

9:50 ***Fresnel to Far Field Transformation Using Least Squares Minimization and Equivalent Magnetic Sources Reconstruction*** 148
Fernando Las-Heras, Belén Galocha, José Luis Besada
Universidad Politécnica de Madrid

10:10 ***Spherical Near Field Measurements at the David Florida Lab.*** 149
*S R Mishra, *J G Dumoulin, *D Lee, **D Rensburg, *N Sultan, *G Seguin
*Canadian Space Agency
**Comdev Inc.

10:30 Break

10:50 ***Antenna Development and Evaluation Using a Compact Antenna Range*** 150
L Shafai
University of Manitoba

11:10 ***Focusing Effect of Radio Holographic Metrology in the Fresnel Region*** 151
*Hiroyuki Deguchi, *Masanori Masuda, *Norio Miyahara, **Masato Ishiguro
*Mitsubishi Electric Corporation,
**Nobeyama Radio Observatory

11:30 ***Microwave Antenna Measurements at NPL - Theory and Practice*** 152
Peter McNair, David Gentle
National Physical Laboratory

11:50 ***Antenna Measurements at the European Space Agency*** 153
John Reddy
ESTEC

12:10 ***Advance Calibration Techniques for Indoor Collimating Ranges*** 154
V J Vokurka
Eindhoven University of Technology

Near-Field measurement deconvolution

G. Séguin* and T.J.F Pavlasek

Department of Electrical Engineering
McGill University, Montréal, Canada
* Also with the Canadian Space Agency

The Far-field parameters of an antenna are obtained from Near-Field measurement with an accuracy that is limited by two main sources of errors; those that are due to the applicability of the technique and that impose limitation on our real knowledge of the field in the near zone, and those that are due to the instrumentation errors.
The first type of error refers to the truncation of the measurement surface and the sampling rate used to collect the measurement data.
These "limitations", that must be imposed to the measurement, introduce some errors on the knowledge of the Far-Field parameters. A trade-off is usually made between the limitation imposed to the measurement and the level of errors tolerable in the Far-Field.
These measurement "limitations" were usually hidden by the instrumentation errors, but the development of highly accurate Near-Field Facility to verify very accurate far-field specifications gives more importance to these "limitations" as before. This is particularly true for large radar antennas that require very accurate measurements to verify very precise performance.
A mathematical techniques based on the Fourier Transform is proposed to attempt the correction of the measurement limitations. The near-field measurement data $\mathbf{E}_m(x,y)$ is mathematicaly expressed as the convolution of two spatial functions as follow:

$$E_m(x,y) = \int\int E(u,v)\, H(x-u, y-v)\, du\, dv$$

Where E(x,y) is the true near-field tangential vector and H(x,y) the impulse response function of the measurement system. The resolution of the above equation ly in the fact that the Fourier Transform of this equation is just the product of the individual Fourier Transform.

$$f_m = f\ h$$

Where f_m is the fourier transform of the measured data, f is the fourier transform of the true near-field and h is the fourier transform of the impulse response function of the measurement system. From the measured field f_m is obtained. Therefore if we know h the spectral decomposition of the true near-field f could becomes available by simple division.

This paper will address the circonstances under which this is possible and will present some possible applications. Some schemes will also be presented to obtain the "h" function. Typical results will be shown.

Progress in Electromagnetics Research Symposium, PIERS 1997 ISBN 962-442-097-1

Mesure Impulsionnelle d'Antenne Active Radar et de Chaine complete radar en base compacte.

D.Carbonne, J.M.Lopez, D.Belot, J.Blouvac, C.Sourdois
Centre National d`Etudes Spatiales,
Centre Spatial de Toulouse
18, av. Edouard Belin, 31055 Toulouse Cedex, France

Un démonstrateur d`antenne active à 96 modules émission - réception MMIC pour radar d`observation de la terre en bande X et l`éctronique centrale associtée ont été développés pour le CNES. Des mesures de diagrammes de rayonnement en régime impulsionnel et de réponse impulsionelle radar ont été réalisées dans la base compacte de mesures d'antennes du CNES à Toulouse, France. Des dispositifs de mesure de signal impulsionnel ont été mis en oeuvre à partir de dispositifs classiques de mesure d`antennes en continu. Malgré la réduction de la dynamique de mesure, les résultats obtenus pour les diagrammes de rayonnement sont tot a fait comparables à ceux mesurables en continu.

Un disposifif d`électronique radar émission réception avec génération numérique de chirp a été associé au démonstrateur et à une ligne à retard afin de réaliser des mesures de bout en bout de la chaîne d`acquisition radar et d`évaluer l`influence de l`antenne dans cette chaîne de mesures. Le système de calibration des modules actifs émission - réception de l`antenne à partir du signal impulsionnel mesuré a été testé avec succès. Le diagramme de rayonnement composite émission - réception sure la bande utile est aussi mesurable en un nombre limité de directions à partir de la réponse implusionnelle correspondante. Ces méthodes permettent d`envisager des calibrations rapides des systèmes d`antennes actives a grand nombre de modules, une caractérisation fine de lìnfluence de l`antenne dans la chaîne instrumentale et une recette, in fine, de la chaîne d`acquisition complète.

Progress in Electromagnetics Research Symposium, PIERS 1997 ISBN 962-442-097-1

Phase Retrieval Diagnostic in Bi-Polar Planar Near-Field Measurements

Yahya Rahmat-Samii and Robert G. Yaccarino
University of California, Los Angeles
Electrical Engineering Department
Los Angeles, CA 90095-1594
e.mail: rahmat@ee.ucla.edu

Phase retrieval microwave imaging techniques are now beginning to emerge as a viable methodology in the microwave antenna measurements and diagnostic arena when phase cannot be directly measured. The attraction of phaseless near-field measurements arises due to, for example, the inability to accurately measure phase at high frequencies or the prohibitive cost of vector measurement equipment. In addition, the requirements for a practical planar near-field range implementation requires the antenna under test (AUT) to measurement plane separation to be on the order of just a few wavelengths. This presentation examines recent investigations of phaseless near-field measurements using the UCLA bi-polar planar near-field technique.

The UCLA bi-polar planar near-field scanner consists of an AUT mounted to a rotary positioner which rotates about one axis and a probe antenna mounted to a probe arm which rotates about a second axis. The concept, design , and implementation for this measurement scanner along with various inter-range measurements comparisons, may be found in previous publications by the authors. The bi-polar technique results in near-field data collected on concentric rings with data samples located at the intersection with radial arcs. An optimal sampling interpolation of the measured bi-polar data samples to a rectangulary regularized format is required in order to take advantage of fast Fourier transform (FFT) methods. The near-field to far-field transformation and microwave holographic imaging and diagnostics using the rectangulary regularized near-field samples may then be performed using an efficient FFT implementation.

Various algorithms, almost exclusively numerical in nature, have been investigated in recent years for the phase retrieval problem at microwave and millimeter wave frequencies. A number of methods have focused on iterative Fourier transform algorithms with enforcement of the measured phaseless data constraints at each step. These techniques with exception of the Plane-to-Plane algorithm, all originated in the optical regime. The Plane-to-Plane algorithm was specifically formulated for the case of near-field antenna measurements and, therefore, admits the same measurement apparatus for both required near-field antenna measurements. In recent years, an approach to the phase retrieval problem as a non-linear inverse problem has also gained some attention. These techniques, however, with few exceptions have been applied to simulations and measurements in which the near-field measurement planes are separated by a considerable electrical distance.

This presentation examines recent investigations of phaseless near-field measurements using the UCLA bi-polar planar near-field technique. A phase retrieval algorithm suitable for bi-polar planar near-field measurements, which relies on a two-plane squared amplitude optimal sampling interpolation method, will be detailed. In addition, measurement results will be presented and compared to results obtained when phase is retained in the processing.

Fresnel to Far Field Transformation using Least squares Minimization and Equivalent Magnetic Sources Reconstruction

Fernando Las-Heras, Belén Galocha, José Luis Besada
Grupo de Radiación, Dpto. Señales, Sistemas y Radiocomunicaciones, Universidad Politécnica de Madrid
E.T.S.I. Telecomunicación, Ciudad Universitaria, 28040 Madrid, Spain
Tlf: 34-1-5495700 Fax : 34-1-5432002 E-mail : fernando @gr.ssr.upm.es

A method to obtain two-dimensional far field radiation patterns of an antenna from the correspondent two-dimensional measured patterns in the Fresnel region is presented.

The method is based on the reconstruction of magnetic equivalent sources over a plane that radiate in free space. By minimizing the RMS error of the radiated field due to the equivalent sources and the measured data at every aspect angle, the value of the equivalent sources can be found and then the radiated far field can be obtained at every aspect angle. The equivalent sources are expanded using different types of basis functions.

Probe correction has been considered in the transformation process by including in the radiation integral a term related to the probe pattern and that depends on the aspect angle and the source point.
The method has been validated by calculating the far field pattern from measured Fresnel field data of antennas with separable distribution excitation.

If only two-dimensional far field patterns are desired, the advantages of using this method in an anechoic chamber measurement facility with respect to a spherical measurement system are the simplification of the mechanical instrumentation in the acquisition process, the reduction of the measurement time and the possibility of using directive probes to minimize the disturbances due to reflections on the walls.

In addition, if the equivalent sources are placed in the same surface of the original radiating elements, the method allows the diagnosis of the antenna in the measurement process, and even can be used as a synthesis tool.

Spherical Near Field Measurements at the David Florida Laboratory

S.R.Mishra, J.G.Dumoulin, D.Lee
David Florida Laboratory
Canadian Space Agency,
Ottawa, Ont. Canada K2H8S2
D. Rensburg
Comdev Inc. Kitchner Ont.
N. Sultan, G. Seguin
Canadian Space Agency, Montreal Canada.

This paper describes the instrumentation, hardware and software for data acquisition, near-field to far-field transformation and data presentation developed at the David Florida Laboratory of the Canadian Space Agency.

Antenna characteristics using spherical near field configuration can be measured at a number of ranges, Each range employs its own specific instrumentation. Traditional instrumentation from well known antenna equipment suppliers is used in some of the ranges. In other ranges custom developed positioning hardware, and control systems are used. Details of these systems will be presented. The data acquisition software originally developed for instrument controllers has been significantly modified and to benefit from low-cost PC based platforms. State of the art computer control and data acquisition permit fast measurements limited only by the speed of r.f instrumentation. A networked architectures permits high speed transport of data in order to process the data in almost real time.

The near-field to far-field transformation is carried out using CASAMS software. This software permits transformation of near field data obtained using polar or equatorial scanning schemes. Built in routines allow corrections for some of the inherent errors such as displacement of axes, polarization mismatch and data acquisition delays which are inherent in near-field measurements. The special features of CASAMS software in analyzing measured data will be discussed.

A detailed study of errors in spherical near field measurements has been carried out. The effect and contribution of various static and dynamic errors on predicted far field performance will be discussed. Using a combination of measured data and simulations it is possible to estimate of errors in measured results, The details of this scheme will be presented along with actual measured data to verify some the conclusions

Antenna Development and Evaluation Using a Compact Antenna Range

L. Shafai
Department of Electrical and Computer Engineering
University of Manitoba
Winnipeg, Manitoba, Canada, R3T 5V6
e-mail: shafai@ee.umanitoba.ca

A number of important Telecommunication and Remote Sensing programs, Satellite or Terrestrial utilize frequencies in the vicinity of 1.0 GHz band, such as the mobile satellites, GPS, personal communication system and SARS. Some of these systems, especially mobiles and GPS, utilize circularly polarized waves, while the others as SARS use dual-linear polarizations. In either case, the required antenna must generate low cross-polarization in its coverage zone, that can include the entire upper-hemisphere, or more.

The wide coverage zone of these antennas means that their size will be small, and during operation and test should not be placed on large hosts or supports. Otherwise, their radiation pattern, and thus beamwidth, will be altered. Also, the support structure, when large, will scatter sufficient power to deteriorate their cross polarization. Thus, to evaluate these antennas properly the anechoic chamber must have a suitable size quiet zone. This requires low level wall reflectivity and a sufficient test range size to prevent significant amplitude and phase deviations. In conventional far field ranges these requirements necessitate a large anechoic chamber, that often is too costly and not practical due to the space limitation.

Compact Antenna Ranges overcome some of these limitations. The range size reduces due to the phase-front generation of the reflector, and the side wall reflectivity minimizes due to the collimated beam of the reflector. The quality of the quiet zone, however, must be evaluated. At the lower frequency ends, the diffraction from the range reflector edges becomes significant and deteriorates the quiet zone field quality. This problem can be partially overcome by using an array feed to reduce the reflector edge illumination. This solution, however, decreases the quiet zone size, and is effective mostly for small antenna measurements.

This paper will present some of the antenna development candidates and show the hybrid far-field and compact range measurements to enhance the accuracy.

Progress in Electromagnetics Research Symposium, PIERS 1997 ISBN 962-442-097-1

Focusing Effect of Radio Holographic Metrology in the Fresnel Region

H. Deguchi†, M. Masuda†, N. Miyahara†, and M. Ishiguro‡
† Mitsubishi Electric Corporation
5-1-1 Ofuna, Kamakura 247, Japan
‡ Nobeyama Radio Observatory
Minamimakimura, Minamisaku, Nagano 384-13, Japan

Abstract

The radiation patterns in the Fraunhofer region can be approximately obtained from antenna measurements in the Fresnel region by a focusing technique[1]. In this paper, we apply this technique to radio holographic metrology using a signal source located in the Fresnel region, and the focusing effect is examined. The radio holographic metrology in the Fresnel region is based on the Fresnel transform between the Fresnel radiation pattern and the aperture distribution, using the fast Fourier transform(FFT). The dominant aberration due to the Fresnel region measurements is approximately compensated by adjusting the sub-reflector position in the parabola-axis, and then the residual aberration is evaluated by using Geometrical Optics.

We evaluated focusing effect of radio holographic metrology in the Fresnel region for the 10-m parabolic antennas of the Nobeyama Millimeter Array which is used for high resolution astronomical imaging at millimeter wavelengths. The main reflector surfaces of the 10-m antennas are comprised of surface panels arranged in two concentric rings. The panels have a typical size of 1m×2m. Simulations were performed by taking account of errors due to truncation of the radiation pattern measured in the Fresnel region, and phase error corresponding to a panel displacement of 5μm. The Fresnel radiation pattern is calculated by employing linear combination of FFT with the spatial resolution of 0.025m, 512×512 points, instead of its numerical integration. The simulated test distance normalized by wavelength, R, is $D^2/15$, where D is the diameter normalized by wavelength. The spatial resolution degraded by the truncation is 0.4m, 0.2m, 0.1m, and 0.05m, corresponding to 32×32, 64×64, 128×128, and 256×256 points, respectively. The values of average offset and deviation are derived from the phase error data by using the best-fit panel model method[2],[3], the results are compared both for focused at infinity and at R with displacement of the sub-reflector. In the data of 64×64 points, the values of average offset for the panels are about 80% of the actual values. For the panels arranged in the outer ring, the rms values of deviation of results focused at R are less than 50% of those focused at infinity. It was confirmed by simulations that the accuracy in estimating the surface error is improved by the focusing technique.

References

[1] T. S. Chu, *IEEE Trans Antennas Propagat.*, AP-19, pp.691–692 (1971).

[2] M. Ishiguro et al., Proc of the International Workshop on "THE HOLOGRAPHY TESTING OF LARGE RADIO TELESCOPES", pp.34–39 (1991).

[3] H. Deguchi et al., *IEICE Trans. Commun.*, E76-B, 12, pp.1492–1499 (1993).

Microwave Antenna Measurements at NPL - Theory and Practice

Peter McNair and David Gentle
Antenna Measurements Group
National Physical Laboratory
Teddington
Middlesex TW11 0LW
United Kingdom

For several years the National Physical Laboratory (NPL) has been making high quality measurements of microwave antennas using an extrapolation range. Two years ago, a near-field planar scanner facility was introduced to meet the growing demand for measurements of electrically large antennas.

This paper presents an overview of the microwave antenna measurement facilities used for gain and pattern measurement of antennas operating in the range 1 to 60 GHz at the National Physical Laboratory. An important goal of the work at NPL is the realisation of high quality measurements with proper uncertainty estimates. The measurement methods used together with methods for estimation of uncertainties will be presented.

Particular emphasis will be given to the near-field scanner as an antenna measurement method. Like all measurement methods, the near-field scanner is subject to certain limitations and care must be taken in several areas if a high quality measurement is to be realised. For example, errors in the positioning of the probe antenna will lead to errors in the far-field gain pattern obtained for the antenna under test. A thorough understanding of all such limitations is a clear prerequisite to providing a measurement with accurate uncertainty estimates. New methods have been developed at NPL for the estimation of uncertainty contributions in near-field scanners. These methods, which recognise the fact that the uncertainty associated with a measurement depends on both the characteristics of the antenna under test and the probe antenna, will be discussed.

Progress in Electromagnetics Research Symposium, PIERS 1997 ISBN 962-442-097-1

Antenna Measurements at the European Space Agency

John Reddy
ESTEC, Keplerlaan 1, 2202AG Noordwijk, The Netherlands

Since the establishment of the European Space Technology Centre (ESTEC) at Noordwijk, the European Space Agency has been involved in the development of antenna measurement techniques and associated facilities required for the development of antennas and payloads for satellites.

At ESTEC, two Compact Ranges have been established using different geometries in order to develop techniques for gain measurements, range error corrections and the measurement of complex satellite radiating payloads.
These ranges are also used in support of satellite development programmes of the European Space Agency.

Together with these developments, ESTEC has been responsible for establishing standards and reference laboratories to assist European Industry in the non space sector also - the joint facilities at the technical University of Denrnark (The Joint ESA/TUD Spherical Near Field Test Facility), which is also responsible for the maintenance and operation of the ESA Standard Gain Horn Facility, and at Ericsson Space in Sweden (The Joint Ericsson/ESTEC Planar Near Field Facility). Of particular importance in antenna measurements is the establishment of standards not only for gain measurement but also for the validation of the numerous facilities used for satellite antenna calibration.

The ESTEC VAST (VAlidation STandard Programme has been established in order to allow a quantitative assessment of the quality of a particular facility to perform measurements according to the stringent requirements associated with satellite antennas.
Special VAlidation STandard antennas have been designed and developed with specific characteristics in order to cover different frequencies and types of facility. In addition to these activities, ESTEC is actively involved with other laboratories involved not only with antenna measurements but also associated measurements such as radar cross section and microwave signatures.
The aim is to establish a network of laboratories in order to explore the benefits of synergy, collaboration, including development of standards, operational protocols, quality assurance, and inter-range comparisons.

This paper will review and summarize all of the above activities and present plans for future developments in the European Space Programmes.

Progress in Electromagnetics Research Symposium, PIERS 1997 ISBN 962-442-097-1

Advanced Calibration Techniques for Indoor Collimating Ranges

V.J. Vokurka

Eindhoven University of Technology, Department of Electrical Engineering,
P.O. Box 513, 5600 MB Eindhoven, the Netherlands

Indoor testing of antennas with dimensions up to approximately 6 meters can be realized on present generation of Compact Antenna Test Ranges (CATR) for various applications, such as testing of space qualified hardware for frequencies up to 60 GHz.

Present and future demands on the accuracy in antenna measurements make direct applications of compact ranges questionable. Accuracy in sidelobe level determination of for instance +/- 1 dB at -40 dB level is physically not realizable on most ranges. Similar requirements apply also for cross polarization measurements and determination of gain characteristics.
Furthermore, due to application of larger antenna subsystems and utilization of higher frequencies, boresight determination in order of 0.001 degrees is required in many new systems. As in the previous case this accuracy is physically not achievable. In fact, the maximum boresight accuracy which can be realized is approximately 0.02 degrees.

The limitations in pattern accuracy and boresight determination are caused by finite size of the collimating reflector(s) in terms of wavelength, by diffraction effects at the edges of the compact range, by scattering from RAM and other spurious radiation such as spill over from the feed.

Taking the previously described constrains into account, it becomes obvious that additional calibration will be needed for accurate pattern, gain and boresight determination. In order to carry out such a calibration, accurate field determination across the test zone is required. Probing the near-field or using a reference target with known scattering behaviour are two most frequently applied methods. It will be shown that the latter method has important advantages when compared to field probing. Finally, using two independent calibration methods makes a full-field characterization process possible and the most demanding accuracy requirements can be satisfied.

SESSION 7P17

Tuesday, January 7, PM 1330-1630, Lecture Theatre 17, City University of Hong Kong

Six-Port Technology

Organizer: R G Bosisio

Chairperson: R G Bosisio, Ecole Polytechnique de Montréal
Co-Chairperson: S P Yeo, National University of Singapore

13:30 ***Optimum Design of the Five-Port Circuit Used in mm-wave Digital Receiver*** 156
Ji Li, Renato G Bosisio, Ke Wu
Ecole Polytechnique de Montréal

13:50 ***Six-Port Digital Millimetric Receiver*** 157
Yansheng Xu, Renato G Bosisio
Ecole Polytechnique de Montréal

14:10 ***Nine-Port Network Analyzer Utilizing Six Power Detectors to Measure Scattering Coefficients of Two-Port Devices*** 158
S P Yeo, M Cheng, C K Ang
National University of Singapore

14:30 ***Broad Band Reflectometer Using Four Electric Probes*** 159
Jose Margineda, Juan Munoz, Marta Rojo
Universidad de Murcia

14:50 ***Power Measurements Made with the Six-Port in the Frequency Range 0.1-18 GHz*** 160
Joseph Achkar, Marcel Valon
BNM-LCIE

15:10 **Break**

15:30 ***On Wafer InP-HEMTs Transistor Evaluation for Microwave/Millimeter-wave Frequency Doublers Using Six-Port Technique*** 161
*A Rahal, **D Schreurs, *A Merza, *R G Bosisio, **B Nauwelaeres, ***M Van Rossum
*Poly-Grames
**K.U.Leuven
***IMEC

15:50 ***High Power Single Frequency Network Analyzer*** 162
Martin Caron, Cevdet Akyel, Fadhel M Ghannouchi
Ecole Polytechnique de Montréal

16:10 ***Millimeter Wave Six-Port System Using NRD-Guide*** 163
Tsukasa Yoneyama, Takahiro Tamae
Tohoku University

Optimum Design of the Five-Port Circuit Used in mm-wave Digital Receiver

Ji Li, Renato G. Bosisio and Ke Wu
Groupe de Recherches Avancées en Microondes et en Electronique Spatiale
(POLY-GRAMES), Département de Génie Electrique et de Génie Informatique
Ecole Polytechnique de Montréal, C.P. 6079, succursale centre-ville,
Montréal, Québec, Canada H3C 3A7

Abstract

It has been demonstrated that a six-port circuit can be used in a mm-wave digital receiver to perform direct demodulation of PSK and QAM signals. The new mm-wave digital receiver promises a cost effective solution for mm-wave backhaul in PCS systems.

In this paper, an optimum five-port circuit is proposed. The new planar five-port circuit is suitable for MMIC and MHMIC.

The five-port design addresses the following aspects: 1) Minimized overall circuit dimension. 2) Minimized insertion loss between the RF input port and power detector ports to increase sensitivity. The insertion loss to all the power detector ports should be even, as to prevent the noise of a single diode detector from deteriorating the overall performance before the threshold is reached. 3) Maximized isolation between the RF input port and LO port to reduce LO leakage to the antenna. 4) The LO power presented at all the detector ports should be at the same order. This is to facilitate the baseband signal conditioning and A/D conversion circuit design. 5) Similar to the six-port reflectometer design, the qi points should be equal in magnitude and 120° different from each other in phase.

Progress in Electromagnetics Research Symposium, PIERS 1997 ISBN 962-442-097-1

SIX-PORT DIGITAL MILLIMETRIC RECEIVER

Yansheng Xu and Renato G. Bosisio
Groupe de Recherches Avancées en Microondes et en Electronique Spatiale
(POLY-GRAMES), Département de Génie Electrique et de Génie Informatique
Ecole Polytechnique de Montréal, C.P. 6079, succursale centre-ville,
Montréal, Québec, Canada H3C 3A7

Abstract

Six-port junctions were developed in the seventies for automated microwave network analysis. The parameters of the devices under test are calculated by using the power readings of the four detectors of the output ports. The measurement errors introduced by hardware imperfections can be eliminated by a suitable calibration procedure. Recently a novel digital millimetric receiver (DMR) scheme was introduced in which the six-port junction is used as a frequency/phase discriminator [1,2]. DMR is essentially a homodyne type receiver which has the advantage of reduced complexity and cost in comparision with the conventional hetrodyne receiver. Another advantage of DMR lies in that the errors due to hardware inaccuracy may be compensated by the calibration procedure as in the measurement of S-parameters using conventional six-port junctions.
In this presentation the concept of DMR using six-port junction is introduced. Then our attention is concentrated on the simulation of DMR by using the software Signal Processing WorkSystem (SPW). The six-port model is built according to reference [3]. Bit error rate (BER) analysis is simulated in the presence of noise. The non-linear cross-modulation interference effects inherent to six-port junction receiver are also discussed. The methods to overcome these interference effects are studied and compared. The effects of fluctuations of the output power of the local oscillator to the signal output of the receiver are calculated and compared with the results of SPW simulations.

References

[1] Ji Li, Renato G. Bosisio and Ke Wu, "Computer and measurement simulation of a new digital receiver operating directly at millimeter-wave frequencies", IEEE Trans. Microwave Theory Tech. vol. MTT-43, pp. 2766-2771, December 1995

[2] Ji Li, Renato G. Bosisio and Ke Wu, "Dual-tone calibration of six-port junction and its application to the six-port direct digital millimetric receiver", IEEE Trans. Microwave Theory Tech. vol. MTT-44, pp. 93-99, January 1996

[3] Ji Li, Renato G. Bosisio and Ke Wu, "Modeling of the six-port discriminator used in a microwave direct digital receiver", Conference Proceedings of 1995 Canadian Conference on Electrical and Computer Engineering, Montreal, September 1995, pp. 1164-1165

NINE-PORT NETWORK ANALYZER UTILIZING SIX POWER DETECTORS TO MEASURE SCATTERING COEFFICIENTS OF TWO-PORT DEVICES

S. P. Yeo, M. Cheng and C. K. Ang

Center for Microwaves & RF
Electrical Engineering Department
National University of Singapore
Kent Ridge Campus
Singapore 119260

Abstract

It is known that the dual six-port network analyzer is able to derive the unknown scattering coefficients of a two-port device from the readings taken by eight power sensors. We propose, instead, the use of an alternative technique (based on an extension of the six-port reflectometer procedure) that requires only six power sensors for the measurement of the two-port device under test. This reduction in the requisite number of power sensors results from a change of strategy in the manner the power readings are to be processed: Whereas for the dual six-port arrangement the power readings have to be sorted into two independent groups which are then processed separately by the two six-port reflectometers, for our proposed technique we have found from analysis that all the power readings can in fact be grouped together and processed collectively. The resulting system equations are, admittedly, more complicated in form; given the ready availability nowadays of enhanced PC capabilities, however, we have found from field tests that the computations required for the solution of the various system equations are actually not that difficult to handle.

Our proposed instrument has a total of nine ports – two ports for connection to the device under test and another port for connection to the source (apart from the six ports that have to be terminated in the power sensors). Extensive tests on the two prototype instruments that we have constructed confirm that our proposed nine-port network analyzer can yield measurement accuracies of better than ± 0.01 and $\pm 2^\circ$ for the magnitudes and phases, respectively, of all the four scattering coefficients. Finally, it should also be pointed out that the theory we have developed does not require us to assume that the device under test is reciprocal and we therefore did not observe any additional complications when using either of the two prototype instruments to measure the scattering coefficients of non-reciprocal components (*e.g.* ferrite isolator).

Progress in Electromagnetics Research Symposium, PIERS 1997 ISBN 962-442-097-1

BROAD BAND REFLECTOMETER USING FOUR ELECTRIC PROBES

Jose Margineda, Juan Muñoz and Marta Rojo
Dpto. de Física, Universidad de Murcia, Apdo 4021, 30071 MURCIA, SPAIN

The use of three electric probes as a 5-port ANA has been widely reported in the literature (see, for instance, [1-3]). The main problem of this scheme is the ambiguity related to the spacing between probes, and so their application in broad band measurements is difficult. A modification based on adding a fourth probe is proposed in order to avoid ambiguities and to extend the operating band.

For a reflectometer with three electric probes located at z_i (i = 1,2,3), the reflection coefficient ($\Gamma = \rho e^{j\phi}$) is calculated from normalized readings l_i in the probes by solving the simultaneous equations [1]:

$$l_k - l_j = A_{kj}X + B_{kj}Y \qquad \text{for } k = 1, j = 2,3 \text{ or any permutation}$$

where $X = \rho\cos\phi$, $Y = \rho\sin\phi$ and $A_{kj} = 2(\cos 2\beta z_k - \cos 2\beta z_j)$, $B_{kj} = 2(\sin 2\beta z_k - \sin 2\beta z_j)$, being β the propagation constant.

Ambiguity in the solution appears when the spacing between the probes is in the order of $n\lambda_g/2$ (n integer). If a fourth probe is added, the three most suitable probes at each frequency can be selected, thus avoiding ambiguity problems.

Following this idea, we have implemented a reflectometer for 2-18 GHz with a slotted line (hp 816A) and four electric probes located as indicated in Figure 1. Using Engen's geometrical analysis, it is easy to see that any combination of three probes presents ambiguities in the band. However, measurements can be made with no ambiguity if the probes are selected according to Table I. The experimental system is similar to that described in [1]. The computer controls the measurement procedure and chooses, at each frequency, the readings of three probes according to Table I. The reflectometer is a 6-port system, but the measurement at each frequency is made under the 5-port principle [1]. The performances are therefore the same as that described In [1], except that the operating band is extended. This is limited by the slotted line. We hope to further extend the operating band by improving the reflectometer design.

REFERENCES

1.- J. Muñoz, J. Margineda, E. Martin and M. Rojo, "Dual Five-Port Analyzer Using Fixed Probes", IEEE Trans on Instrum. Meas., vol. IM-43, pp 415-420, June 1994.

2.- C. Hu, "Microwave Automatic Impedance Measuring Schemes Using Three Fixed Probes", IEEE Trans on Microwave Theory and Tech., vol. MTT-31, pp 756-762, sept. 1983

3.- S. Li and R.G. Bosisio, "The Measurement of Complex Reflection Coefficient by Means of a Five-Port Reflectometer" IEEE Trans on Microwave Theory and Tech., vol. MTT-31, pp 321-326, sept. 1983

Probe set	Operating Frequencies (in GHz)
1,2,3	2-5.3, 5.8-10.4, 11.8-16.3, 16.9-18
2,3,4	5.2-5.9, 10.3-11.2, 16-17.4
1,2,4	11-12

Table I.- Frequency bands and probe set used

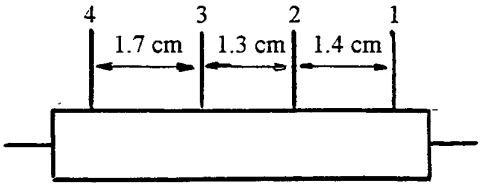


Fig. 1.- Four probes reflectometer

Power measurements made with the six-port in the frequency range 0.1-18 GHz

Joseph Achkar, Marcel Valon
BNM-LCIE
BP n° 8, 92266 Fontenay-aux-Roses, France
TEL +33 1 40 95 60 44
FAX +33 1 40 95 60 50

One of advantages in the use of the six-port system is the possibility to carry out power measurements. It means the characterization of microwave thermistor mount power detectors. This paper describes the six-port system used at BNM-LCIE which is built with five hybrid couplers and four thermistor mounts. After calibration of the system, power measurements can be made using one standard thermistor mount. The effective efficiency of an unknown thermistor mount is determined after measuring the complex reflection coefficient and the calibration factor of the mount. A comparison of measurements is made between the results obtained with the six-port system, the microcalorimeter system and the power transfer standard system. Up to 1 GHz, the deviations on the results obtained with these different systems is less than 0.005 for thermistor mounts with more than 99 % of efficiency.

Progress in Electromagnetics Research Symposium, PIERS 1997 ISBN 962-442-097-1

On wafer InP-HEMTs Transistor Evaluation for Microwave/Millimeter-wave Frequency Doublers Using Six-Port Technique.

A. Rahal, D. Schreurs*, A. Merza, R.G. Bosisio, B. Nauwelaeres* and M. Van Rossum**.

Poly-Grames ,C.P. 6079, Succ.'Centre Ville' Montreal, Quebec, Canada H3C 3A7
Tel. : (514) 340-3239, Fax. : (514) 340-5892, E-mail : alirahal@grmes.polymtl.ca
* K.U. Leuven, Div. ESAT-TELEMIC, Kard. Mercierlaan 94, B-3001 Heverlee, Belgium
** IMEC, Div. ASP/CSP, Kapeldreef 75, B-3001 Heverlee, Belgium

Abstract :

The fast growing market of personal communication systems urged the development of new integrated, reliable and cost effective components. The HEMTs devices have been proved to have superior performances for low-noise and high gain millimeter-wave applications. The success of non-linear design, such as frequency doublers, rely greatly on the fidelity and precision of the transistor model used in the simulations. Most of the actual models are based on small signal S parameters measurements and so are not so accurate in non-linear simulations. To predict the optimal loading of the frequency doubler, active load-pull measurements have been performed on wafer samples at the fundamental and the second harmonic. Both T-gate and multi-finger gate devices have been measured. The T-gate devices are on InP substrate while the multi-finger devices are on GaAs. The effect of the fundamental loading on the performance of the frequency doubler has been investigated, an offset short is found to be optimal. The T-gate transistors shows 6.5 dB of conversion gain with 12.5% power added efficiency at 24 GHz. In order to validate the obtained results, a frequency doubler will be built and tested. The obtained results has been already compared with Harmonic balance simulation results based on a new non-linear model and shows good agreement. The active multi-harmonic Six-port based load-pull measurement setup and the measurement results will be presented at the conference.

HIGH POWER SINGLE FREQUENCY NETWORK ANALYZER

Martin Caron, Cevdet Akyel,
Fadhel M. Ghannouchi

Abstract

The proposed high-power network analyzer is made up with two high-power six-port reflectometers using two hybrid microstrip/waveguides couplers. The first prototype is band limited (2,45 Ghz) and has been used 200W for measurements of full S-parameter set (S_{11} , S_{12}, S_{21}, S_{22}).

We already reported [1], [2], the techniques of construction for a high power reflectometer based on the design of two special hybrid directional couplers (waveguide/stripline) which provide the unique opportunity to use all six-port calibration and measurement techniques at high power microwave signal levels.

This approach permits the obtention of reflection coefficient with module and phase angle at a frequency of interest (usually an ISM frequency for industrial scientific and medical applications). The new combination of such a two way reflectometers enables us to design for the first time a complete six-port high power network analyzer (SPHPNA) at 2,45 Ghz capable of measuring simultaneously the four complex S-parameters of a two-port device (active or passive). The power level reached for practical measurements was 200 watts in S band. This was due to the power limitation of the TWA used during the measurements. The technique is not limited by the power level as far as high power and stable sources (regarding frequency) are available. The complete system is automated using a personal computer. All transmission and reflection information about the two-port device is transferred to the lower power six-port circuits via the hybride microstrip/waveguide directional couplers (see figure 1).

The only limitation on frequency is imposed by the construction of these two hybrid directional couplers which are band limited. As far as one can find high quality, high power directional couplers (high directivity, low coupling, large band, etc) the proposed SPHPNA can operate over a large band of frequency.

Millimeter Wave Six-Port System Using NRD-guide

Tsukasa Yoneyama and Takahiro Tamae

Research Institute of Electrical Communication
Tohoku University
Katahira 2-1-1, Aoba-ku
Sendai 980-77, Japan

The NRD-guide technology was applied to build a six-port network at 60GHz. NRD-guide is known as a low loss dielectric waveguide operating at millimeter-wavelengths without any unwanted radiation at curved sections and truncations of circuits. This nature of NRD-guide is particularly useful for constructing compact as well as high-performance six-port networks for millimeter-wave applications. The Engen's topology was used with beam-lead detectors installed in it as shown in Fig.1.

A unique calibration technique is proposed based on the method of least mean square in which power measurement is repeated at more than 100 positions over one-wavelength portion of a short plunger connected to the DUT-port of the six-port network. Complex reflection coefficients are also found by means of the method of least mean square. Fig.2 shows reflection coefficients obtained at 60GHz by using the constructed NRD-guide six-port network for several DUT's in comparison with vector network analyzer measurements. Excellent agreement can be found between them. A comment will be given for expanding the operation bandwidth of the NRD-guide six-port network.

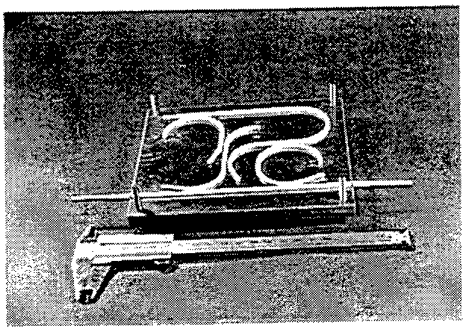


Fig.1 NRD-guide six-port network

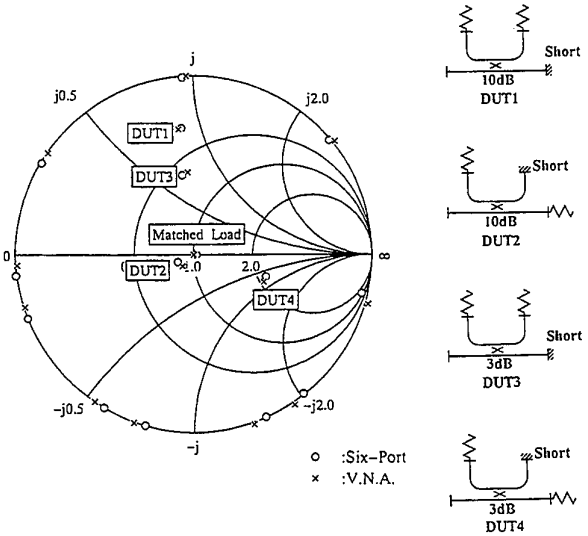


Fig.2 Complex reflection coefficients for DUT's shown right in comparison with V.N.A. measurements

SESSION 7A16

Tuesday, January 7, AM 850-1130, Lecture Theatre 16, City University of Hong Kong

Computational Techniques 2

Organizers: Wolfgang J R Hoefer, Poman So

Chairperson: Wolfgang J R Hoefer, University of Victoria
Co-Chairperson: Poman So, University of Victoria

8:50 ***The PPS-Method for the FD-Calculation of Inductances of Unrestricted Lossless 3D-Structures Using a Scalar Magnetic Potential*** 165
*Stefan Lindenmeier, **Peter Russer
*Ferdinand-Braun-Institut fuer Hoechstfrequenztechnik
**Lehrstuhl fuer Hochfrequenztechnik

9:10 ***Hybrid Mode Matching Multiple Multipole Method for the Analysis of the Radiation Characteristics of Elliptically Corrugated Horns*** 166
*E Kühn, **A S Omar
*German TELEKOM
**Arbeitsbereich Hochfrequenztechnik

9:30 ***Design of Electromagnetic Structures with TLM*** 167
P P M So, J Herring, W J R Hoefer
University of Victoria

9:50 ***A Simple Analytical Approach to Construction of Absorbing Boundary Condition for Modeling Unbounded Electromagnetic Structures*** 168
Ke Wu
Ecole Polytechnique de Montréal

10:10 ***Formulas for the Local Characterization of the Field Lines*** 169
I R Ciric
The University of Manitoba

10:30 **Break**

10:50 ***Analysis of a Folded Wire of Arbitrary Dimension Enclosed in an Electromagnetic Cavity*** 170
H Rahman
Saint Louis University

11:10 ***Generalized Treatment of Dielectric Waveguide Analysis in a Normalized Space*** 171
Yoshihiro Emori, Tetsuya Mizumoto, Yoshiyuki Naito
Tokyo Institute of Technology

The PPS-Method for the FD-Calculation of Inductances of Unrestricted Lossless 3D-Structures Using a Scalar Magnetic Potential

Stefan Lindenmeier[1] and Peter Russer[2]

[1] Ferdinand-Braun-Institut fuer Hoechstfrequenztechnik
Rudower Chaussee 5, D-12489 Berlin / Germany
[2] Lehrstuhl fuer Hochfrequenztechnik, TU-Muenchen
Arcisstr. 21, D-80333 Munich / Germany

For the design of MMIC-devices the calculation of the capacitances and inductances of three-dimensional structures can be done by static field calculations. With the Finite Difference Method the field-problems can be solved for nearly unrestricted threedimensional structures. In the electrostatic case this is done efficiently by the fast calculation of a scalar potential. The calculation of the magnetic field couldn't be done in that simple way because the field is not free of rotation in every point of the structure. While the calculation in values of three components makes the computational effort increase there is the need to find a way how to derivate the magnetic field by a scalar potential. In Ref.[2] the magnetostatic field has been calculated by the scalar magnetic potential with a Finite Difference-algorithm for special structures. The application of the calculation method is restricted to structures with symmetrical properties. The magnetostatic field in unsymmetrical structures with mainly one plane of metallization like a planar spiral conductor can be calculated approximately with only considering the space below the metallization plane and assuming different constant magnetic potentials in the non-metallized areas of the plane.

In this contribution we present the method of potential parting surfaces (PPS-method) for the numerical calculation of a scalar magnetic potential in unrestricted lossless threedimensional structures. For solving the magnetic field problem the structure of the circuits is discretized due to Yee's scheme [1]. Into the discretization mesh potential parting surfaces (PPS) are inserted connecting every conductor with the structures boundary in a way that every integration path around the conducting material will cross its potential parting surface. The further choice of the exact position and form of the surfaces is arbitrary. Assuming the case of a lossless three-dimensional structure, the consideration of the field is reduced on the field in the space around the conducting material. This space is cut by the PPS so that the resulting space is bordered by two more surfaces which are the both sides of the PPS. In this new defined space the magnetic field is free of rotation and so it can be described by a scalar magnetic potential, analogue to the electrostatic case. At the PPS there are defined new boundary conditions. Between the two sides of the PPS, there is a difference in potential of the value of the current in its conductor. So this difference has to be added as a source to the finite difference term of the derivative of the potential between two discretization-points which are separated by a PPS. With that kind of field-source the magnetic potential can be calculated in a FD-algorithm analoguous to the electric potential. So the computation effort of thePPS-method is not higher as the one of the FD-calculation of the electrostatic field. The versatility of the PPS-method is shown in excemples of the calculation of inductances in several MMIC-structures.

References:

[1] K.S. Yee, "Numerical solution of initial boundary value problems involving Maxwell's equations in isotropic media," IEEE Trans. Antenna Propagat., Vol.14, pp.302-307, May 1966.

[2] M. Abdo-Tuko, M. Naghed, I. Wolff, "Novel 18/36 GHz (M)MIC GaAs FET frequency doublers in CPW-techniques under the consideration of the effects of coplanar discontinuities", IEEE Trans. Microwave Theory Tech., Band 41, NO. 8, S. 1307-1315, Aug. 1993

Hybrid „Mode Matching"-„Multiple Multipole"-Method for the Analysis of the Radiation Characteristics of Corrugated Horns

By

E. Kühn and A.S. Omar

ABSTRACT

A hybrid „Mode Matching" -„Multiple Multipole"- Method for the analysis of both the internal and the external characteristics of corrugated horns is presented. The method is based on expanding the electromagnetic field inside the horn with respect to the eigenmodes corresponding to the different waveguide sections comprising the corrugated horn. The external (radiation) field on the other hand is expressed as a multiple-multipole-expansion. The continuity of the field at the aperture as well as the boundary conditions at the horn metallic surface are enforced using a point matching procedure. This results in two systems of linear equations. The first system, which describes the matching of the tangential electric field at both the radiating aperture and the horn surface, relates the modal coefficients of the aperture electric field (generalized voltages) to the amplitudes of the multipoles. The second one, which represents the matching of the tangential magnetic field at the aperture only, relates the modal coefficients of the aperture magnetic field (generalized currents) to the amplitudes of the multipoles. Eliminating the latter results in the aperture generalized admittance matrix.

Two point matching algorithms are presented. In the first one, the number of matching points on the horn surface and the radiating aperture is chosen in such a way that the above described systems of linear equations are determined. Perfect matching is achieved in this case only at the matching points. between these points the mismatching cannot be controlled. The second algorithm is featured by over determined systems of equations, which can be obtained by accounting for more matching points than it is necessary and/or considering the matching of the normal field components. In this case no perfect matching can be achieved at any point on the antenna surface. On the other hand, the mismatching allover the surface is minimized in a mean square sense.

To validate the method, the field distribution on the aperture plane as well as on the horn surface is plotted in a 3D presentation. Comparison of co- and cross-polarization to measured data is also presented.

Progress in Electromagnetics Research Symposium, PIERS 1997 ISBN 962-442-097-1

Design of Electromagnetic Structures with TLM

P.P.M. So, J. Herring, and W.J.R. Hoefer

NSERC/MPR TELTECH Research Chair in RF-Engineering
Department of Electrical and Computer Engineering
University of Victoria
Victoria, British Columbia, Canada, V8W 3P6

Home Page: http://www.wjrh.ece.uvic.ca/

To design high frequency electromagnetic structures with the transmission line matrix (TLM) method is not trivial in spite of the simplicity of the fundamental TLM algorithm. This is because TLM is a time and space discretization method in which the entire computational domain must be filled with nodes. In three-dimensional cases, the computational effort to solve realistic problems would soon become intractable unless special techniques are used. To be attractive to the design engineer, field simulation tools must include these advanced techniques automatically in the models.

New theory for special nodes and meshes for the representation of fine geometrical features through local modification have been developed. This improves the efficiency, accuracy and versatility of the TLM method. Therefore, unnecessary fine TLM mesh does not have to be used to model structures with small details. In addition to that, new algorithms based on parallel and distributed computing as well as signal processing techniques have also been developed to improve the computational efficiency of TLM. Many of these features have been incorporated in a state-of-the-art multipurpose electromagnetic field simulator developed by our researchers. Also, the simulator has automatic mesh generation and engineering parameter extraction capabilities; it can also be integrated with external programs so that TLM can be used strategically in conjunction with traditional linear circuit simulators to perform analysis and optimization.

The theoretical foundations of the above mentioned contributions will be presented; their capabilities will be demonstrated during the presentation by using the field simulator.

A Simple Analytical Approach to Construction of Absorbing Boundary Condition for Modeling Unbounded Electromagnetic Structures

Ke WU

Poly-Grames Research Center
Dept. de genie electrique et de genie informatique
Ecole Polytechnique
C. P. 6079, Succ. Centre-Ville
Montreal, Quebec, Canada H3C 3A7
Tel: 514-340-5991, Fax: 514-340-5892, E-mail: wuke@grmes.polymtl.ca

The use of an appropriate absorbing boundary condition is the corestone for a successful field modeling and design of unbounded electromagnetic structure such as antennas, wave diffractions and scatterings, and high-frequency circuits under open environment. There have been a number of formalisms proposed for constructing absorbing boundary conditions or mesh-truncation algorithms. They include, to name a few examples, wave factorization, transmission line technique, PML scheme, and MEI approach. These methods have been applied to simulate various structures. In this paper, an alternative formalism of absorbing boundary condition is proposed and developed for modeling unbounded electromagnetic structures. The present algorithm is derived from the framework of the well-known method of lines, and is in particular suitable for use in conjunction with finite-element and finite-difference methods. With the proposed technique, a class of simple analytical absorbing boundary conditions under three principal coordinates are developed, which are field-theoretically rigorous. Numerical results will be presented to demonstrate its usefulness. In addition, the proposed formalism allows to use direct mesh-truncation which may involve both in-bound and out-bound propagations if a scattering problem or other similar situation is considered. The formulation of the absorbing boundary conditions may provide an alternative way to the existing techniques for both finite-element and finite-difference schemes.

Progress in Electromagnetics Research Symposium, PIERS 1997 ISBN 962-442-097-1

Formulas for the Local Characterization of the Field Lines

I.R. Ciric

Department of Electrical and Computer Engineering
The University of Manitoba, Winnipeg, MB R3T 5V6, Canada

Except for a small number of simple geometries, where closed analytical expressions are available, the shape of the field lines for vector fields is determined by numerical computation or by graphical means. Even when the fields are given analytically, exact expressions for the field lines can rarely be obtained. In this paper, we derive parametric equations for the field lines valid in the neighbourhood of any point at which the field and its derivatives are defined. The parameter used in these equations can be particularized to be either a field potential or the arc length of the field line. The equations presented are not available in the published literature.

The parametric representation of a field line in a given interval of the parameter u is

$$x_1 = x_1(u), \quad x_2 = x_2(u), \quad x_3 = x_3(u) \tag{1}$$

where x_1, x_2, x_3 are the Cartesian coordinates and the functions $x_i(u)$, $i = 1, 2, 3$, are single-valued and continuously differentiable as needed, and at least one of the first derivatives $x_i'(u)$ is different from zero in the interval considered. Using Taylor's formula, the expansion of the coordinates in (1) near the point $u = u_0$ is written as

$$x_i(u) = x_i(u_0) + (u-u_0)\,x_i'(u_0) + \frac{(u-u_0)^2}{2!}x_i''(u_0) + \frac{(u-u_0)^3}{3!}x_i'''(u_0) + o\left((u-u_0)^3\right) \tag{2}$$

where o is the *small o* Landau symbol. The calculation of the first three derivatives of the coordinates in (1) is presented in the paper, with the parameter u defined directly in terms of the field components and also when the parameter is chosen to be the arc length of the field line measured from the point considered. As well, for vector fields which are derived from scalar potential functions, local parametric equations are presented with the parameter being the potential itself. When the field components or the potential functions are determined in closed analytical form, the terms in the expansions (2) are also calculated in closed analytical form. In the case the field or the potential is determined numerically, the derivatives in (2) are computed numerically according to the presented formulas. By taking into account the terms containing the third derivatives the range of validity of the expressions (2) in the neighbourhood of the field points is correspondingly increased. This is illustrated in the paper for a test example involving a family of ellipsoids as equipotential surfaces.

The formulas presented are useful in the field analysis for the local characterization of the field lines and for developing field visualization techniques. The expressions derived in this paper can readily be used for fields in n -dimensional (Euclidean) spaces. Derivation of local parametric equations of the field lines can be extended to orthogonal curvilinear coordinates and to vector fields which are derived from combinations of scalar and vector potentials.

Analysis of a Folded Wire of Arbitrary Dimension Enclosed in an Electromagnetic Cavity

H. Rahman
Saint Louis University
Parks College
Department of Electrical Engineering
Cahokia IL 62206, USA

Abstract: A computationally simple and efficient approach to the analysis of a folded wire of arbitrary dimension enclosed in a rectangular cavity is presented. The wire penetrating through the top face of the cavity is folded at right angle within it. Any electromagnetic source exterior to the cavity may excite the wire which may assume any arbitrary load conditions.

This boundary value problem may be viewed as an idealization of a folded wire or cable in some metal enclosure. The formulation is based on the Fourier Series Method developed previously by the author. The electromagnetic behavior of the wire, in terms of the current induced on it, is examined. The unknown current is approximated by a truncated Fourier series. The current on the wire, in turn, results in an electromagnetic field within the cavity which is associated with a triply infinite sum. The expression describing the prescribed cavity environment is reduced from a triply infinite sum into doubly infinite one by using the Fourier series representation and orthogonality properties. In case of a wire with arbitrary dimension the current is still assumed to reside on the wire axis, but the boundary condition is enforced on four generatrices equally spaced around the circumference of the wire. A testing function encompassing the assumed four generatrices is considered for satisfying the boundary condition on the surface of the wire, and finally a matrix equation for the unknown Fourier coefficients are determined. Once the Fourier coefficients are determined, one can easily compute the field existing within the cavity and the current distribution on the wire. Other information pertaining to cable-metal enclosure problems can easily be derived from the current and field distribution. Numerical results are presented to illustrate the effects of wire diameters on currents induced on the folded wire. A threshold value of the wire diameter is identified below which the wire behaves like a thin-wire.

Generalized Treatment of Dielectric Waveguide Analysis in a Normalized Space

Yoshihiro Emori, Tetsuya Mizumoto and Yoshiyuki Naito

Department of Physical Electronics, Faculty of Engineering,
Tokyo Institute of Technology, 2-12-1 Ookayama Meguro-ku Tokyo 152 Japan

All waveguide parameters such as a wavelength, refractive indices and geometrical sizes are to be specified to analyze waveguide characteristics using numerical techniques, e.g. a finite element method (FEM), an effective index method and a beam propagation method (BPM). Numerical calculation must be carried out for every set of waveguide parameters in designing waveguide structures for device applications.

On the other hand, if the sets of waveguide parameters stand in a special relation, the characteristics of waveguide systems with different structure could be identical. This is called device equivalence. In this work, we propose generalized treatment of dielectric waveguide analysis based on device equivalence. By virtue of this treatment, each value of wavelength and refractive indices does not need specifying when we analyze waveguide characteristics using ordinary numerical techniques.

First, we define a normalized coordinate system (X, Y, Z) in terms of the following conversion from the ordinary coordinate system (x, y, z).

$$X = k_0 n_0 x \ , \quad Y = k_0 n_0 y \ , \quad Z = k_0 n_0 z \qquad \left(k_0 = \frac{2\pi}{\lambda} = \omega\sqrt{\mu_0 \varepsilon_0} \right)$$

, where the refractive index n_0 is arbitrarily chosen as the reference refractive index. And we define a new parameter R in the following manner,

$$\frac{n^2(x,y,z)}{n_0^2} = r(x,y,z) = r(\frac{X}{k_0 n_0}, \frac{Y}{k_0 n_0}, \frac{Z}{k_0 n_0}) = R(X,Y,Z)$$

, where $n(x, y, z)$ represents the refractive index distribution. Then we define a normalized space constituted of the coordinate system (X, Y, Z) and the parameter R. Thus the structure of a waveguide system in the normalized space can be defined by the function $R(X, Y, Z)$.

It will be shown that, in a waveguide system consisting of isotropic lossless media, the wave equation and a coupled mode equation in the normalized coordinate system are characterized only by the function R. It means that the dielectric waveguide analysis requires only the function R in the normalized space. It is concluded that all the waveguide systems represented as ~~an~~ identical structure in the normalized space show equivalent characteristics of lightwave propagation.

SESSION 7P16

Tuesday, January 7, PM 1330-1630, Lecture Theatre 16, City University of Hong Kong

Measured Equation of Invariance

Organizer: K K Mei

Chairperson: K K Mei, City University of Hong Kong
Co-Chairperson: Y L Chow, City University of Hong Kong

13:30 ***Application of Fast Discrete Periodic Wavelets to Measured Equation of Invariance for 2-D Conducting Scatterings*** 173
Y W Liu, K K Mei, K M Luk, K N Yung
City University of Hong Kong

13:50 ***Measured Equation of Invariance for FD-TD Computations*** 174
Alexander Heldring
Joint Research Institute of the European Commission, Ispra

14:10 ***Electromagnetic Scattering and Radiation From Sub-Reflector by the Method of MEI*** 175
Y L Luo, K M Luk, Y W Liu, K K Mei, Edward K N Yung
City University of Hong Kong

14:30 ***The MEI Method - A Theoretical Justification*** 176
Y L Chow, Y W Liu, K K Mei, K M Luk, K N Yung
City University of Hong Kong

14:50 ***Recent Advances on the Integral Formulation of the Measured Equation of Invariance*** 177
Juan M Rius
Universitat Politecnica de Catalunya (UPC)

15:10 **Break**

15:30 ***Application of a Matrix Decomposition Algorithm to Speedup Computation of MEI Method*** 178
R M M Chen, Yaowu Liu, Shirley S K Ng
City University of Hong Kong

15:50 ***Measured Equation Invariance Method in Time Domain*** 179
Y W Liu, K K Mei, K N Yung
City University of Hong Kong

16:10 ***A PVM Based Parallel Sparse Matrix Equation Solver*** 180
G F Niu, R M M Chen, S S K Ng, Y W Liu
City University of Hong Kong

Application of Fast Discrete Periodic Wavelets to Measured Equation of Invariance for 2-D Conducting Scatterings

Y. W. Liu, K. K. Mei, K. M. Luk, and K. N. Yung
Department of Electronic Engineering
City University of Hong Kong

SUMMARY

Recently, hybrid wavelet expansion boundary element method (HWBM) [1] was introduced into the area of electromagnetic scattering computations for 2-D conducting circular cylinder. The HWBM shows success in converting an integral equation of electromagnetic scatterings into a sparse matrix equation. Unfortunately, the HWBM needs to establish the map between the contour length of a scatterer surface and a fixed interval [0,1] where periodic wavelets are supported. The HWBM also needs to select a threshold to set smaller elements to zeros in order to form a sparse matrix. Therefore, the value of the selected threshold will greatly affects the accuracy of the numerical results [1]. On the contrary, measured equation of invariance (MEI) method [2], which was introduced to the area of electromagnetic field computations as a fast computation method, generates a mush more compact sparse matrix equation by either using MEI equations combined with finite difference FD) equations or using MEI equations alone [3]. In the MEI method, we usually choose a set of sinusoidal functions as 'metrons', which represent the possible existed induced electric or magnetic currents along a scatterer surface. We put the 'metrons' into integral equations to find the potential produced by the possible electric or magnetic currents, and then find MEI's coefficients in the MEI equations that stand for the local relationship between neighbour nodes on a artificially truncated boundary. Although the sinusoidal functions are orthogonal and complete basis functions, they are supported over infinite length. In contrast to infinite length support, the periodic wavelets are compactly localized in both position and scale over finite length support. In this paper we use a number of the periodic wavelets as 'metrons' in stead of the sinusoidal functions to find the MEI's coefficients, combine with one layer finite difference (FD) to generate a sparse matrix for solving electromagnetic scattering problems of 2-D conducting circular and rectangular cylinders under both TM and TE plane wave incidences. So, we refer to such a method as hybrid wavelets and measured equation of invariance (HWMEI) method. Compared to the HWBM, the HWMEI method directly matches the length of discrete periodic wavelets to the contour length of the scatterer surface. It does not require maps between the contour length of scatterer surface and a fixed interval [0,1] where periodic wavelets are supported. Meanwhile, the HWMEI method does not require to select a threshold to eliminate smaller elements to form an approximate sparse matrix because the MEI method itself guarantees generating a sparse matrix. Numerical examples of the conducting circular and rectangular cylinder scattrings for TM and TE plane wave incidences show that the results obtained by the HWMEI agree well to those obtained by method of moment (MoM).

REFERENCES

[1] G. Wang, "A hybrid wavelet expansion and boundary element analysis of electromagnetic scattering from conducting objects," IEEE Trans. on Antennas and Propagation, Vol. 43, No. 2, pp. 170-178, February 1995.

[2] K. K. Mei, R. Pous, Z. Q. Chen, Y. W. Liu, and M. Prouty , "The measured equation of invariance: A new concept in field computation," IEEE Trans. on Antennas and Propagation, Vol. 42, No. 3, pp. 202-214, March 1994.

[3] R. Pous, J. M. Rius, "Recent advances in the measured equation of invariance," PIERS, p. 1086, Seattle, Washington, USA, June, 1995.

Measured Equation of Invariance for FD-TD computations

Alexander Heldring

Joint Research Institute of the European Commission, Ispra, Italy

A new Absorbing Boundary Condition for FDTD computations, based on the Measured Equation of Invariance is presented. The coefficients that appear in the finite difference equation which links neighbouring nodes on the edges of the FDTD grid, are determined through 'measurement' as the target is illuminated with a particular incident field or 'metron'. The choice of which metron to use being a critical issue in the implementation of the method, a superposition of plane waves at three different frequencies is proposed. This does lead to a very efficient ABC, quite superior to a traditional ABC like second order Mur, but the resulting time-stepping scheme is in general unstable. To solve this problem, an approximative stability analysis is derived, resulting in a set of stabilizing requirements to be imposed on the coefficients. Some results obtained using this procedure, are presented.

Electromagnetic Scattering and Radiation From Sub-Reflector by the Method of MEI

Y. L. Luo, K. M. Luk, Y. W. Liu, K. K. Mei and Edward K. N. Yung
Department of Electronic Engineering, City University of Hong Kong
83 Tat Chee Avenue, Kowloon, HongKong

Summary

The sub-reflector, which is the key part of a dual-reflector antenna system (for example, the Carsegrain Antenna), is traditionally analyzed by optical-ray techniques. For numerical methods, the MoM seems to be a hopeful way if it is not limitted by the computing time and computer memory. By MoM, the unknowns encountered in problem are limited to the objects surface and so the number of unknowns is small. The integral equation is converted into a full matrix equation system. To solve the full matrix equation, which is the dominant part of MoM, large mount of time and computer memory is needed in case of electrically large dimension objects. This makes MoM less efficient.

In this paper, we try to use the method of Measured Equation of Invariance (MEI) to numerically analysis the radiation characteristics of sub-reflector in a dual-reflector antenna system.

The MEI method was introduced by Mei et al. [2] in 1992, as a mesh truncation condition for the finite difference (FD) method. This method allows the termination of the mesh very close to the scatterer surface, usually only two or three layers above the object's surface. This approach has been proved to be more robust than the absorbing or radiation boundary condition applied close to the scatterer surface and, in contrast to the hybrid FE-BEM method, the interrelation between the field points is sparse. Thus, it has the advantages of the two popular methods: the sparse matrix in the FD method and small number of unknowns in MoM.

Based on its advantages, the method of MEI is applied to analysis the induced current of a sub-reflector in a dual-reflector antenna system. From the induced surface current distribution, the radiation characteristics of the sub-reflector will be obtained by integration the current over the sub-reflector surface. The results will be given in the form of induced currents distributions and the radiation field patterns, accompanied with corresponding Physic-Optics (PO) solutions or GTD solution.

The MEI Method - A Theoretical Justification

Y.L. Chow, Y.W. Liu, K.K. Mei, K.M. Luk and K.N. Yung
City University of Hong Kong

In electromagnetics, there are two popular but quite different numerical methods, namely: i. the finite difference (FD, kin to finite element) method, and ii. the moment method (MoM). The former has a very large but sparse matrix, and the latter has a much smaller but filled matrix. The recently invented MEI method appears to have combined the advantages of the two, that is: it has a matrix that is both small and sparse.

The MEI method, however, requires an additional step of learning from a number of solved examples. Despite this addition, the MEI method has been found to be still *very fast and accurate* for many examples, in both static and dynamic cases.

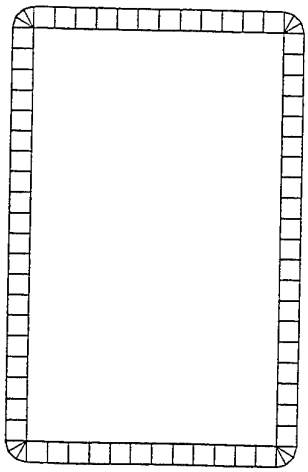
While numerically demonstrated for many specific cases, the MEI method is still to be theoretically justified for the general cases. This is necessary for completeness, and also to gain a better physical insight on the method on its limitations and on its future extension. Given below is a brief discussion on the theoretical justification, from the familiar MoM to the fast new method of MEI.

The Moment Method (MoM) Solution

We begin the justification with simple case of a 2D conductor with V=0 subjected to an exciting voltage distribution V_i. This causes an induced charge Q_s on the cylinder S. Then the MoM matrix becomes

$$-(V_i) = [G_{is}](Q_s)$$

where G_{is} is the Green's function. The above is usually solved for Q_s.



The Conversion to the MEI Solution

Let V_t be the voltage on nodes on cell away from the boundary. With Q_s known, V_t can be found by a direct matrix multiplication as below

$$(V_t) = [G_{ts}](Q_s)$$

The two equations above combine into

$$(V_t) = [G_{ts}][G_{is}]^{-1}(-V_i) = [A](-V_i)$$

The resulted matrix [A] is actually the sparse matrix of EMI. This is evident if we make the above mentioned cell width away from the boundary to reduce to zero. Then $[G_{t.}]$ becomes $[G_{ts}]$ and thus [A] becomes a unity matrix. A unity matrix is the sparest matrix possible. The above conversion can easily be extended to the dynamic cases. For example, in the 2D TAM case, this is done by replacing the static V, Q and G by the dynamic E_z, J_z and G_{dym}. This means that MEI is faster but is as justified theoretically as MoM.

To complement the theory, this paper also gives several numerical examples of [A].

RECENT ADVANCES ON THE INTEGRAL FORMULATION OF THE MEASURED EQUATION OF INVARIANCE

Juan M. Rius
Dpt. TSC, Universitat Politècnica de Catalunya (UPC)
Campus Nord, Edifici D-3, Gran Capitán, s/n
08034 BARCELONA - Spain

The Measured Equation of Invariance (MEI) was presented by Prof. K.Mei as a mesh truncation condition for the finite difference and finite element methods in the frequency domain. Later, J.M.Rius presented a new conception of the MEI as a weighted residual integral equation method (IE-MEI) that produces an sparse impedance matrix with the same number of unknowns as the method of moments (BEM-MoM). However, in contrast with the most usual formulations of method of moments, the IE-MEI uses both EFIE and MFIE operators for the computation of the matrix coefficients. Results for two-dimensional PEC objects with convex shape have been obtained showing enormous CPU and memory savings compared to method of moments.

Recent advances in the integral formulation of the MEI include:

- ☐ Extrapolation of matrix coefficients for higher frequencies, which allows the numerical analysis of electrically very large objects. In order to obtain accurate results for all kinds or convex shapes, coefficients corresponding to nodes located near edges are computed differently than coefficients corresponding to nodes located on a smooth part of the surface.

- ☐ Three-dimensional formulation using triangular surface elements, for perfectly conducting objects.

- ☐ Advances in the analysis of non-convex shapes (cavities, etc.).

- ☐ Applications.

In this communication we will also discuss the MEI as a very general method for numerical derivation of coefficients in the discretization of differential or integral operators. The IE-MEI method will be compared to methods that derive the numerical coefficients analytically, in special EFIE, MFIE and CFIE formulations of method of moments. In fact, we will show that the numerical error of the MEI in the computation of induced surface current can be derived from the error in the computation of EFIE and MFIE operators.

Application of a Matrix Decomposition Algorithm to Speedup Computation of MEI Method

Richard M M Chen, Yaowu Liu, and Shirley S K Ng
Dept of Electronic Engineering
City University of Hong Kong

A matrix decomposition algorithm developed by the first author is applied to solve the linear simultaneous equations resulted from MEI (Measured Equation of Invariance) method in solving electromagnetic filed problems.

The Algorithm decomposes the overall matrix equation into a number of sets of smaller submatrix equations, which are related to each other by a set of small number of unknowns, called interconnection unknowns. This set of interconnection unknowns is a subset of the unknowns of the overall linear equations. The key of the algorithm is the formulation of an interconnection level matrix equation which must be solved first. Once the interconnection unknowns are solved, each of the submatrix equations can be solved independently. Thus parallel processing can be used to solve the submatrix equations concurrently.

The speedup can be contributed by two factors: (1) A larger computational problem of dimension n with computational complexity $O(n^a)$ is decomposed into a number of r sub-problems of smaller dimension n_1, n_2, ..., n_r, where $n_1 + n_2 + \ldots + n_r = n$. Since $a > 1$ even if a sparse matrix routine is used. Therefore, there will be a speedup if the overhead of the decomposition is smaller than the speed gain of such technique. (2) A speedup contributed by parallel processing of the submatrix equations.

A numerical example is given to show the effect of the speedup in computation when this algorithm is applied to solve the linear simultaneous equations resulted from the application of MEI method.

Measured Equation Invariance Method in Time Domain

Y. W. Liu, K. K. Mei, and K. N. Yung
Department of Electronic Engineering
City University of Hong Kong

SUMMARY

Since the Measured Equation of Invariance (MEI) method has been applied in computational electromagnetic fields, the most of efforts is to focus on frequency domain problems [1]-[3]. One question people always ask is whether the principle of the MEI can be used in time domain or not. The answer is very positive. Except of initial results reported in 1994 [4], we have further investigated and developed the Time Domain MEI (TDMEI) method. The most important discovery is we use time domain Green's functions in the MEI method to find the TDMEI coefficients that are unchanged with time. This characteristic permits us to truncate computational boundaries much closer to scattering objects than any absorbing boundary conditions. Additionally, the TDMEI method can be implemented to other disciplines, such as acoustics, fluid mechanics, and elastics, etc..

REFERENCES

[1] K. K. Mei, R. Pous, Z. Q. Chen, Y. W. Liu, and M. Prouty , "The measured equation of invariance: A new concept in field computation," IEEE Trans. on Antennas and Propagation, Vol. 42, No. 3, pp. 202-214, March 1994.

[2] R. Pous, J. M. Rius, "Recent advances in the measured equation of invariance," PIERS, p. 1086, Seattle, Washington, USA, June, 1995.

[3] Y. W. Liu et al, " Large circular scattering computation by MEI coefficient extrapolation," Proceedings of 1995 International Conference on Radio Science, pp.106-109, Aug.10-12, 1995, Beijing, China.

[4]. K. K. Mei and Y. W. Liu, "On time domain measured equation of invariance," URSI Meeting, Seattle, Washington State, June 20 - June 24, 1994.

A PVM Based Parallel Sparse Matrix Equation Solver

G.F. Niu, R.M.M. Chen, S.S.K. Ng, and Y.W. Liu

Department of Electronic Engineering, City University of Hong Kong
83 Tat Chee Avenue, Kowloon, Hong Kong

Key words: Sparse (UC Berkeley), Parallel Virtual Machine (PVM), Memory Hierarchy

A PVM (Parallel Virtual Machine) based general purpose parallel sparse matrix equation solver capable of handling both real and complex numbers has been developed to speed up the solution process of existing large problems and to solve larger problems which are computationally infeasible on a single computer. Decomposition of the matrix to a number of smaller sub-matrices which can be solved inside the physical memory of a single computer significantly speeds up the solution by reducing and/or avoiding the expensive virtual memory access. Each sub-matrix and the interconnection matrix resulting from the decomposition algorithm are solved by using routines in the UC Berkeley sparse matrix package *Sparse*, and self-scheduling is used to allocate tasks to processors. Experiments with a 204832 by 204832 complex matrix from the MEI method (Figure 1) show encouraging results: the matrix computationally infeasible on a single Pentium (P5-133MHz) can be solved on a network of 3 Pentiums running Linux in 641 seconds which is 8 times faster than the solution using *Sparse* directly on a Sun Sparc-20 running Solaris. Speedup is contributed by 3 factors: 1) easier to solve sub-matrices from the decomposition algorithm; 2) parallel multiprocessor processing; and 3) distributed memory hierarchy which reduces the time-consuming access to virtual memory for large problems. Since memory is at a premium, specially for the master processor, items are copied out of memory directly in message passing, and sent to target processor in small chunks. The code is written in a way portable to either MPP or heterogeneous network of PCs and workstations.

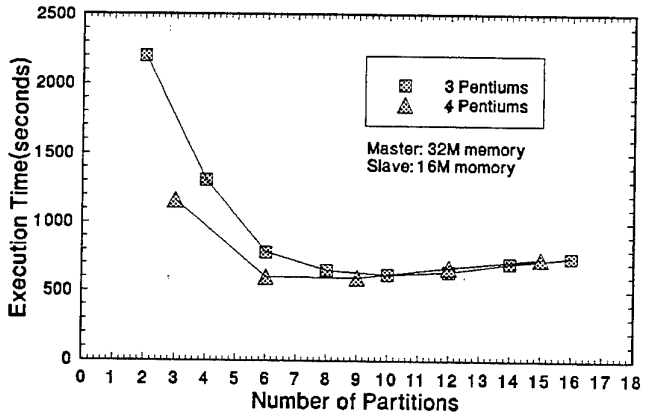


Figure 1 Experimental result with a 204832 by 204832 matrix from MEI method.

SESSION 7A15

Tuesday, January 7, AM 850-1210, Lecture Theatre 15, City University of Hong Kong

Scattering & Diffraction 2

Organizer: Wen Xun Zhang

Chairperson: Wen Xun Zhang, Southeast University
Co-Chairperson: Jhin- Fang Huang, National Taiwan Institute of Technology

8:50 ***Scattering Analysis of Radar Targets*** 182
D. X. Jin, D. G. Fang, S. M. Cui
Nanjing University of Science and Technology

9:10 ***Numerical Diffraction Coefficients of Partly Coated Conducting Wedge*** 183
Wen Xun Zhang, Ming Zhong
Southeast University

9:30 ***The Over-Modes Propagation in Millimeter Waves V-Groove Guide*** 184
*Kai Kang, *Wen Xun Zhang, **K F Tsang, **Wei Min Shi
*Southeast University
**City University of Hong Kong

9:50 ***Analysis of Groove Guides by Using the Method of Lines*** 185
*K F Tsang, *W M Shi, **W X Zhang, **K Kang
*City University of Hong Kong
**Southeast University

10:10 ***Microwave Simulation of HF Ground Wave Back-Scattering from Ocean Waves*** 186
Haipin Song, Tongyi An, Jinming Pei, Manshu Wang
East China Normal University

10:30 **Break**

10:50 ***EMI Analysis of Transient Electromagnetic Wave to Multilayered Dielectric-Multiconductor Bus System*** 187
Shouzheng Zhu, Jinming Pei, Tongyi An
East China Normal University

11:10 ***Geometrical Modeling and Graphical RCS Computing Simulation for Complex Objects*** 188
Tiejun Liu, Yong Chou, Dacai Shen
Beijing Institute of Environment Feature

11:30 ***EMP Reflection and Diffraction Incident on A Small Circular Conductor*** 189
Ying-Wem Su, Jhin-Fang Huang
National Taiwan Institute of Technology

11:50 ***On the Radiation from Terrain Medium with Nonuniform Dielectric Profile*** 190
Ying Lu, Shijie Lin, Wei Guo, Zuyin Zhang
Huazhong University of Science & Technology

SCATTERING ANALYSIS OF RADAR TARGETS

D. X. Jin, D. G. Fang and S. M. Cui
Department Electronic Engineering
Nanjing University of Science and Technology
Nanjing, 210094, China

Many radar targets can be well approximated as consisting of a set of discrete scattering centers. By understanding how these centers process the transmitted waveform, scattering center information is stored instead of the response. Thus, the data storage is reduced significantly. The scattering center information is closely related to the radar target discrimination and the radar cross section modeling both for the near field and far field.

In this study, the obtaining of the scattering center information is carried out through the near scattering field from both the measurement and the numerical computation. The maximum likelihood (ML) algorithm is used to yield high resolution of the centers for wideband data. To obtain the initial estimates of ML algorithm, the matrix enhancement and TLS-ESPRIT technique are repeatedly employed to provide the position and amplitude of scattering centers for each segment narrow-band data. The initialization of the discrete geometry parameters is obtained by approximation based on the amplitude variations at different frequency segments. The computer simulation shows the validity of this technique.

The joint time-frequency techniques are very effective means of visualizing and interpreting scattering mechanisms in radar echo for such applications as radar target identification. These techniques including the multiresolution wavelet transform, Wigner distribution (WD), super-resolution such as matrix enhancement and matrix pencil or ESPRIT algorithm, and adaptive cone-kernel distribution (CKD) in the scattering analysis of radar target are introduced and the radar target identification scheme based on the scattering centers, target resonances, and dispersive phenomena information is also proposed in this study. The results under different signal noise ratio are also given.

NUMERICAL DIFFRACTION COEFFICIENTS OF PARTLY COATED CONDUCTING WADGE

Wen Xun ZHANG & Ming ZHONG

State key Laboratory of Millimeter Waves
Southeast University
Nanjing,210096,CHINA

A hybrid generalized multipole technique-physical optics(GTD-PO) iteration approach was developed by the authors for calculating the numerical diffraction coefficients (*NDC*) of irregular conducting wedge with complex geometry of the edge. Where the current sources of the total scattered fields consist of the physical optics term distributing on the wedge surface zone far from the edge, and the term of generalized multipoles placed inside the edge zone, their complex amplitudes are determined respectively by means of the boundary conditions on whole surface. An appropriate overlapping of those two zones forms an iterative procedure for smooth continuity of the currents on wedge surface. Finally the difference between total scattered field calculated from the determined currents and reflected field of the geometric optics is just the diffracted field, which corresponds to the *NDC* for each specific direction of diffraction.

An important law was concluded from a great number of examples calculated, theat only the *NDC* in reflectionless illuminated range are obviously influenced by the gemetry of irregular wedge, and where only the contributions of the multpoles in edge zone are effective. In additin, a Herrmann Windowing technique can be employed for suppressing the errors due the current truncation. Based on the above experiences, the *NDC*, especially the backward *RCS* of partly coated conducting wedges with verious lossy materials under different incident and diffracted angles are systematically calculated and compared with each other in this article.

Progress in Electromagnetics Research Symposium, PIERS 1997 ISBN 962-442-097-1

THE OVER-MODES PROPAGATION IN MILLIMETER WAVES V- GROOVE GUIDE

KANG Kai & Wen Xun ZHANG

State Key Laboratory of Millimeter Waves
Southeast University, 210096
2 Si Pai Lou, Nanjing, China

K. F. TSANG & Wei Min SHI

Department of Electronic Engineering
City University of Hong Kong
83 Tat Chee Avenue, Kowlon, Hong Kong

Groove guide is a proper transmission line for use at short millimeter wave bands above 100 *GHz*. It is shown experimentally that the V-groove guide (VGG) has the lowest attenuation and most effective rejection of higher modes in all kinds of shapes of groove guides. VGG has electrically large cross section resulting in over-modes propagation in the guide, whose propagation properties have not been known very well.

Since we could not find the analytical closed form of the modes' functions satisfying the boundary conditions of the V shaped groove, the eigenfunction sequences of the wave equation in Cartesian coordinates are employed to constitute the mode functions of the VGG by linear combination. According to the concept of weighted residuals, the boundary residual least square method is used to set up for analyzing the propagation and modal characteristics. The characteristics of dominant-mode obtained by this method coincide with those obtained by experiments and other analyses. The validity of this method is verified.

The properties of high order modes of the VGG are calculated by the same method as well as the dominant-mode. Their propagation characteristics are analyzed too. It is shown that single-mode propagation can be realized when the size of guide is small, the propagation in the guide is over-modes when the size is larger. When VGG is excited by a rectangular aperture tapered from a standard rectangular waveguide (WR8) transmitting TE_{10} mode, the energy distribution between the high order modes and the dominant-mode are also calculated.

TABLE. High-order modes magnitudes in rectangular V-groove guide excited by a rectangular aperture (λ_0 =3.117 *mm*)

The sizes of VGG (*mm*) (groove angle 90°)		Magnitudes of high-order modes						
		dominant mode	Propagation				Non propagation	
Width of parallel plates	Width and depth of VGG		1st order	2nd order	3rd order	4th order	1st order	2nd order
10	2	1.000	0.139	0.117	0.119	0.071	0.009	0.001
10	4	1.000	0.230	0.092	0.078	0.011	0.011	0.010
10	6	1.000	0.314	0.131	0.131	0.125	0.099	0.054
12	2	1.000	0.200	0.157	0.126	0.098	0.024	0.001
12	4	1.000	0.287	0.162	0.141	0.108	0.045	0.034
12	6	1.000	0.361	0.198	0.189	0.124	0.066	0.057

Analysis of Groove Guides by Using the Method of Lines

K. F. TSANG & W. M. SHI
Department of Electronic Engineering,
City University of Hong Kong, Kowloon, Hong Kong

W. X. ZHANG & K. KANG
State Key Laboratory of Millimeter Waves,
Southeast University, Nanjing, P R China

Abstract

Groove guide is potentially attractive for millimetric and sub-millimetric wave bands because of its low losses (compared to rectangular waveguide), low dispersion, and high power handling capability (large cross-section). Several methods including the Mode Matching method (MM), Conformal Mapping method, and Transverse Resonance method were used for the analysis of the dominant mode of groove guides. The Mode Matching method itself is very accurate provided complete waveguide modes are used. Because incomplete waveguide modes were employed, the MM used in groove guide analysis is usually not accurate. However the complete solutions require extensive computer resources. In this paper, the Method of Lines(MoL), a special kind of FDM method, is used to analyze the transmission characteristics of the rectangular-, trapezoidal- and V-groove guides. The dominant mode of the groove guides has been analyzed. The cutoff wavelengths λ_c of several groove guides were calculated and compared with measured data in literature. It was found that the difference between calculated and measured λ_c were within 1%. The field distributions, current distributions and power density distributions were calculated and presented which can assist designer in groove guide component's design. Comparison with the attenuation figures in literature showed that the present method is efficient and promising. The reasons are two-fold: First, the MoL is simple and efficient. Second, MoL is suitable to analyze groove guides of different shapes and sizes.

Progress in Electromagnetics Research Symposium, PIERS 1997 ISBN 962-442-097-1

Microwave Simulation of HF Ground Wave Back-Scattering from Ocean Waves

Haipin Song ,Tongyi An , Jinming Pei and Manshu Wang
Microwave Institute of East China Normal University
3663 North Zhong Shan Road, Shanghai, 200062, China

Coastal ocean surface feature (ocean waves, surface currents, and sea winds) measurement using high frequency ground wave radar has got considerable progresses. The potential applications include ocean dynamics, fishery, transportation, under sea petroleum recovering, etc. However, people are still waiting for more verifications of this method.

Field observation takes too much time and money, and it is difficult to make the ocean situation recur. The simulation technique is to make the natural phenomena recur in the laboratory according to some similar conditions.

In this paper, taking advantage of the microwave scaling-down simulation technique, we show that the radio wave back-scattered by ocean waves, which looks complex and random, follows the Bragg scattering principle. In other words, only the radio wave, whose wavelength is two times longer than that of the ocean wave, will produce considerable back-scattering. This is the basis for ocean surface feature measurement with high frequency ground wave radar. In simulation, some metallic models were made as scaling-down ocean waves, while the incident microwave was vertical polarized to the model. The HP8408S automatic network analyzer system was used for measuring reflection coefficient and transmission coefficient. The experimental results do verify the Bragg scattering principle and also suggest the posible relationship between ocean wave height and high frequency reflection coefficient intensity.

EMI Analysis of Transient Electromagnetic Wave to Multilayered Dielectric-Multiconductor Bus System

Shouzheng Zhu, Jinming Pei, and Tongyi An
Microwave Institute of East China Normal University
3663 North Zhong Shan Road, Shanghai, 200062, China

Multilayered Dielectric-Multiconductor(MDMC) Bus Systems are now widely used in computers and electronic devices. Therefore, the electromagnetic compatibility(EMC) and interference(EMI) problems of MDMC buses must be considered, as they will directly affect the working reliability of these devices. The modeling of crosstalk between multiconductors has received considerable attention since early 80's. However, little research work was found in literature on the EMI of external electromagnetic fields to MDMC bus system.

In this paper a modeling of EMI for MDMC bus system is presented. It is based on a quasi-static solution. The incident electromagnetic field is a double exponential plane wave, which can come from arbitrary direction. The MDMC bus is modeled as inhomogeneous multiconductor transmission lines, the signal sources with internal resistance at the left ends and the terminal loads at the right ends. The coupling of incident wave is treated as distributed voltage and current sources along the transmission lines. The total response of the terminal loads caused by the source signals and external field is then calculated to find the interference influence of external field on the signal transmission. The modeling is carried out in the frequency domain first, and then the obtained results are transformed to the time domain. The numerical results for a few examples are provided. It was found for a three line printed board bus, the induced voltage on a load reached a value of the order of volt when the magnitude of incident pulse wave was of several thousands volts per meter.

Geometrical modeling and Graphical RCS Computing Simulation for complex objects

Liu-Tiejun Chouyong Shen-Dacai
(Beijing Institute of Environment Feature , Branch 207, POB 142, Beijing 100854, China)

This paper presents a computational method of RCS of complex object using Computer Graphics. A real-time, general, animated RCS computing system is developed. Geometrical modeling method is based on Computer-Aided Geometric Design(CAGD). Geometrical shape of the complex object is reconstructed from three-view drawing by the software RVCAD we developed. Mathematical principle of the RVCAD and the electromagnetic model of graphical RCS as well as system constitution are introduced. The correctness of the method is verified by the canonical scattering data of a sphere, cylinder and dihedral. RCS of scale models of several military targets such as missiles, aircrafts, tanks and vessels are computed and compared with the measured ones in the chamber. Results indicates the RCS of a complex object could be obtained in real time as soon as the 3D graphics of the object could be seen on the computer screen using this system.

Comparing our system with GRECO (GRaphical Electromagnetic COmputing) developed by Doctor Rius, a spanish scientist, there are some advantages as follow:

· Hardware platform on which our system works can be a PC computer such as Pentium or 486. But a workstation with 3D Graphical accelerator is necessary for GRECO to work ordinarily .

· Reconstruction of geometrical shape of a complex object whose RCS need to calculate can be completed from three-view drawing in our system. In ordinary system the reconstruction need the cross-section data of the object.

· Data format of the graphical files which represents geometrical shape of the complex object can be more wide-ranging received by our system than GRECO.

In this paper, the effects of the graphical size on RCS are also considered.

EMP Reflection and Diffraction Incident on A Small Circular Conductor

Ying-Wem Su*, Jhin-Fang Huang**
*Graduate student,**Associate Professor
National Taiwan Institute of Technology
No.43, Kee-lung Rd. Sec.4, Taipei,Taiwan 10772, R.O.C.

The reflection and the diffraction of an EMP (Electromagnetic Pulse) incident on a small circular cylindrical conductor are of interest because the scatterer may be simulated as a missile and the backscattered fields are useful for radar applications. The EMP response can be regarded as the function of time which describes the field scattered by a radar target illuminated by a short pulse plane wave. A variety of techniques have been proposed for analyzing scattered problems, such FDTD (Finite Difference Time Domain) method, finite element method, the method of moment and others. The main charactereistics of the preceding approaches are based on finite scatterer configurations and account for a big amount of calculation if the region becomes large. Numerical calculations are somewhat accurate but terious by the above mentioned methods.

In this study, starting from Maxwell's equations, we present theoretical analysis of EMP response from a small circular cylindrical conductor. Generally mathematical formulas of EMP impinging on the scatterer for evaluating time domain responses are developed by Fourier transform techniques. The transmitted and reflected EMP waves in all regions are then determined from those developed formula for an arbitrary angle of incidence. The resulting expressions are linked to a double exponential pulse which is simulated as an EMP source and is first transformed to frequency domain. The induced surface current on the conductor versus time is also evaluated and plotted. The Multiplication of the source and the previous transfer function yields the results in the frequency domain. After taking the inverse Fourier tranform, the corresponding EMP time domain responses in the far region are then readily found. The resultant equation is expressed as the integral form of Bessel functions. The plots of backscattered electric field versus time for an EMP incidence are shown to illustrate the theoretical discussions. The results satisfy the expected phenomena. The present development may be useful for a missile simulated as a circular conductor cylinder, encounting for an electromagnetic interference or detecting its presence.

A numerical modeling technique is also provided to compute the EMP reflected and diffracted fields for both TE (Tranverse Electric) and TM (Transverse Magnetic) polarizations in the near region. The calculated time waveforms indicate the wave propagation properties. Three dimensional plots illustrate the field configuration properties. From the surface plots, the significant effect is that one can clearly understand the wave expansion. It expands out circurlarly and continuously to external space. This phenomenon is in agreement with our electromagnetic features. The results may be highly helpful for equpment design considerations of shielding on lightning EMP strikes and nuclear EMP effects.

On the Radiation from Terrain Medium with Nonuniform Dielectric Profile

Lu Ying Lin Shijie Guo Wei Zhang Zuyin
(Dept. of Electronics & Information Engineering,
Huazhong University of Science & Technology, Wuhan 430074, P.R. China)

Abstract

Literature [1] gives two approaches to compute the radiation from terrain medium with nonuniform dielectric profile (Subsection 4-14). For the isothermal case, $T_2 = T_3 = T_g$, the brightness temperatures calculated through the incoherent approach and the coherent approach respectively are given below,

$$T_{Bin}(\theta_1; p) = \frac{(1-\Gamma_1)(1-\Gamma_2/L_2^2)}{1-\Gamma_1\Gamma_2/L_2^2} T_g, \qquad T_{Bco}(\theta_1; p) = \frac{(1-\Gamma_1)(1-\Gamma_2/L_2^2)}{\left|1+R_1R_2\exp(-2\gamma_2 d\sec\theta_2)\right|^2} T_g,$$

where

$$\gamma_2 = \alpha_2 + j\beta_2, \quad L_2 = \exp(2\alpha_2 d\sec\theta_2).$$

Pay attention to the procedure deriving equation (4.163), especially Figure 4.25. Each component transmitted into layer 1 moves a distance of $2d\tan\theta_2$ along the boundary from the previous one. However all of them are added directly in (4.158) and (4.160). Also notice equations (4.135)--(4.138) and Figure 4.22. According to the equivalent transmission-line theory, it is the transverse field components that are equivalent to the scalar modal functions. Solving Maxwell's equations in layered media [2], we get

$$E_{y2} = (A_2 e^{-jk_{2z}z\cos\theta_2} + C_2 e^{jk_{2z}z\cos\theta_2}) e^{-jk_1 x\sin\theta_1} \qquad \text{for TE case,} \quad (1.a)$$

$$E_{x2} = -\frac{k_2\cos\theta_2}{w\varepsilon_2}(A_2 e^{-jk_{2z}z\cos\theta_2} - C_2 e^{jk_{2z}z\cos\theta_2}) e^{-jk_1 x\sin\theta_1} \qquad \text{for TM case,} \quad (1.b)$$

where the unit vector $\bar{x}$ is along the interface between medium 1 and 2. From (1) it is easy to derive that γ_2' in equation (4.135) of [1] should be

$$\gamma_2' = \gamma_2\cos\theta_2.$$

Based on the analyses above, we believe that the radiation from three-layer terrain media computed through the coherent method should be

$$T_{Bco}(\theta_1; p) = \frac{(1-\Gamma_1)(1-\Gamma_2/(\exp(2\alpha_2 d\cos\theta_2))^2)}{\left|1+R_1R_2\exp(-2\gamma_2 d\cos\theta_2)\right|^2} T_g,$$

and which is the exact result obtained by directly analyzing the electromagnetic fields among the layered media using Wilheit's method [3].

References

1 ULABY. F.T., MOORE. R.K., and FUNG. A.K.: Microwave Remote Sensing: Active and Passive, Volume 1, Reading, MA: Addison-Wesley, 1981

2 KONG. J. A.: Electromagnetic Wave Theory, John Wiley & Sons, USA, 1986

3 WILHEIT. T.T.: 'Radiative Transfer in a Plane Stratified Dielectric', *IEEE Trans. Geosci. Elec.*, April 1978, GE-16, pp.138-143

SESSION 7P15

Tuesday, January 7, PM 1330-1650, Lecture Theatre 15, City University of Hong Kong

Scattering & Diffraction 3

Chairperson: H M Lee, Naval Postgraduate School
Co-Chairperson: Y Hwang, City University of Hong

13:30	***UTD Prediction on Propagation Characteristics in Tunnels*** Y Hwang, Y P Zhang City University of Hong Kong	192
13:50	***Calculating the RCS of a Coated Arbitrary Cavity by SBR*** Minggui Zhao, Changqing Xu Nanjing	193
14:10	***Zero On-Axis Backscattering of An Anisotropic Impedance Coated Body of Revolution*** Hung-Mou Lee, Chen-Kuo Yu Naval Postgraduate School	194
14:30	***Diffraction of Electromagnetic Wave by Circular Disk with Surface Impedance*** Kohei Hongo Toho University	195
14:50	***Scattering of An Off-Axis 2D Gaussian Beam by A Multilayered Cylinder*** Zhensen Wu, Lixin Guo Xidian University	196
15:10	**Break**	
15:30	***Reconsturction of An Embedded 2-D Perfectly Conducting Object Within Dielectric Region*** S Y Shi, D B Ge Xidian University	197
15:50	***Stimulated Scattering in Aerosol Nonlinear Optics*** A A Zemlyanov, Yu E Geints Russian Academy of Sciences	198
16:10	***Electromagnetic Scattering from Conducting Rectangle : Fourier Series Entire Domain Formulation*** Yifan Gao Xian Highway University	199
16:30	***Polygonal Model of RCS for Complex Targets*** Shunlian Chai, Demiao Yao, Zhunjie Mao National University of Defence Technology	200

UTD Prediction on Propagation Characteristics in Tunnels

Y.P. Zhang and Y. Hwang
Department of Electronic Engineering
City University of Hong Kong
Tat Chee Avenue
Kowloon, Hong Kong

Tunnels are common in metropolitan cities, mountain areas, or under the sea. This paper is to propose to study the propagation characteristics of tunnels by the uniform geometrical theory of diffraction (UTD). A tunnel was modelled as congregates of walls. The wall was approximated by uniform impedance surface. The problem was reduced to solve a canonical problem of a wedge with uniform impedance surface. We first considered the diffraction by a right-angle wedge with different impedance boundary conditions at its two surfaces. A functional transformation was used to simplify the boundary conditions. The eigen-function solutions for the transformed functions were replaced by integral representations, which were then evaluated asymptotically by the modified Paulie-Clemmow method of steepest descent. We have interpreted the solution ray-optically to obtain the diffraction coefficient for the uniform geometrical theory of diffraction. The obtained diffraction coefficients are related directly to Keller diffraction coefficients in uniform version. The total field is continuous across the shadow of the geometrical optics fields. The formulation can be extended in an approximated way to an arbitrary-angle wedge.

We used the developed diffraction coefficients to compute the propagation characteristics in both empty and obstructed tunnels. The propagation characteristics were computed for both narrow-band and wide-band. Narrow-band propagation was characterized in spatial domain, and wide-band propagation in time domain. The experiments were conducted at 900 and 1800 MHz frequency bands. The computed results are in excellent agreement with measurements.

Calculating the RCS of a Coated Arbitrary Cavity by SBR

Minggui Zhao Changqing Xu
PO BOX 447 29 YUDAO STREET NANJING 210016 CHINA

Traditionally, the problem of calculating the RCS of a cavity structure is treated by the modal analysis. In this paper, a different method for analyzing the electromagnetic scattering character of a Coated Arbitrary Cavity , named Shooting and Bouncing Rays(SBR), is provided. A dense grid of geometric optics (GO) rays representing an incident wave is "shot" into the cavity through the front aperture and followed as the rays bounce from coated conductors, penetrate through materials, and eventually return to the opening of the cavity. A new scheme is then used to integrate the aperture field to abtain the scattered field. This method has the two following traits. First, this is the first attempt at solving partially open structures using the ray technique. This method is different from the traditional ray-tracing or ray-mode hybrid methods. Second, a real physical problem can be modeled closely, taking into account the noncircular opening of the cavity, the wall coating , the long bending or twisting and the large electrical size of the cavity. To be brief, this approach is so simple in concept that there is virtually no restriction on the shape ,the size or material coating of the cavity. The problem is formulated based on geometrical optics. The path of each ray is firstly determined by Snell's law. The field amplitudes associated with each ray are computed by taking into consideration (1) geometrical divergence factor, (2) polarization, and (3) material coating of the cavity walls. Then, the contributions to the backscattered field from individual rays are summed up to arrive at the total RCS due to the interior irradiation of the cavity. In the last part of this paper, results of the SBR method are compared to the existing modal results for the case of a straight circular cylinder with a perfect electric conducting (PEC) termination ,where radius=10 λ depth=40 λ.And, good agreement is observed between the SBR method and modal analysis method.

Minggui Zhao was born in Nanjing , People's Republic of China. Director of Antenna and Electromagnetic Scattering Lab, Nanjing University of Aeronautics and Astronautics, a professor of Electrical Engineering. His research interests include antenna design ,numerical computing of electromagnetic scattering and microwave circuit design.

Changqing Xu was born in Jiangxi, People's Republic of China on Jan. 1, 1973. He received the B.S. degree from the Department of Electrical Engineering , Nanjing University of Aeronautics and Astronautics., Nanjing , China, in 1994, and is now working toward the M.S. degree. His research interests are in numerical computing of electromagnetic scattering and microwave imaging.

Zero on-axis backscattering of an anisotropic impedance coated body of revolution

Hung-Mou Lee and Chen-Kuo Yu

Department of Electrical and Computer Engineering
Naval Postgraduate School, Monterey, California 94943-5121, U. S. A.

A sufficient condition for eliminating the on-axis backscattering of an anisotropic impedance coated shell of revolution has been deduced. The outside and inside normalized surface impedances Z^+ and Z^- with which this sufficient condition can be satisfied have all been found. One exceptional situation is when the impedance matrices are equal and skew-symmetric with their determinants equal to -1. All other cases require that the two matrices be symmetric, their determinants be unity, and the determinant of their difference be zero.

Based on the duality of Maxwell equations, Weston argued that an object coated with a unit normalized surface impedance will have zero on-axis backscattering if the object is invariant under a 90° rotation around its axis of symmetry. This duality property has also played a crucial roll in this work. Therefore results of this work should not be limited to shells of revolution only. This aspect of the problem is being completed and will be published shortly.

The shell under consideration can be a closed one. A body of revolution coated on the outside with an anisotropic surface impedance Z^+ can be modeled as a shell having $Z^+ = Z^-$. Since the impedance boundary condition separates completely the exterior of the body from its interior, only the conditions on Z^+ need to apply, i.e., Z^+ must be either symmetric or skew-symmetric, with $\det[Z^+] = \pm 1$. This is an extension of Weston's result to anisotropically coated bodies.

It should be noted that a properly shaped and coated body can always be carefully deformed into a shell without generating any on-axis backscattering. This procedure yields the condition $Z^- = Z^+$. By beginning with a shell, we are able to relax this condition to $\det[Z^+ - Z^-] = 0$ for the symmetric case.

Results of this work make available a wide class of models which must have zero on-axis backscattering cross section. All general purpose numerical codes for computing the scattering cross sections of anisotropic impedance coated objects should be checked for their accuracy against a selected group of such models. Such comparisons should provide indications of an error bound of the particular algorithm.

Diffraction of Electromagnetic Wave by Circular Disk with Surface Impedance

Kohei HONGO

Faculty of Science , Toho University, 2-2-1, Miyama, Funabashi 274, Japan

The diffraction of electromagnetic wave by circular disk and circular hole has been studied as the boundary value problems using eigen-function (spheroidal function) expansion and Weber-Schafheitlin's discontinuous integral (WSI)[1] when the radius of the disk or hole is not very large compared to wavelength. The method using WSI is also referred to Kobayashi potential. In the original work on this problem by Kobayashi potential, Nomura and Katsura imposed the boundary conditions and edge condition separately. The procedure needed a lot of analysis and its applicability to more complex related geometries seems to be restricted. Recently present author has proposed a new method for deriving the solution of this kind of problem [2]. In this analysis we devised to find the solution which satisfies the boundary conditions and edge condition simultaneously. The process of the application of this analysis to the diffraction of plane wave by the circular disk (radius a) with surface impedance is described as follows. (1) We introduce cylindrical coordinates (ρ, ϕ, z) and the disk is assumed to be located on the plane $z = 0$. (2) $z-$components of electric and magnetic vector potentials are introduced in the forms of Hankel transform. The integrands consist of the elementary solutions of Helmholtz equation of circular cylindrical coordinates and weighting functions which are to be determined so as to satisfy the required conditions. (3) On the plane $z = 0$, tangential components of the magnetic fields must be continuous for $\rho > a$ and tangential components of the electromagnetic fields must satisfy the specified impedance boundary conditions for $\rho < a$. Imposition of these conditions yields the dual integral equations. (4) According to the method of Kobayashi potential, the weighting functions of the Hankel transform may assume the functions which include the Bessel functions. The indices of the Bessel functions must satisfy some condition to meet the required boundary condition for $\rho > a$. Since the choice of the indices of the Bessel functions has some freedom, we can choose the indices so that the resulting potential functions satisfy the edge condition for conducting disk as well as the boundary conditions on the plane $z = 0$, $\rho > a$. Therefore, the general solutions for the vector potential may be expressed as the linear combination of the functions whose integrands satisfy the above mentioned conditions. This is the key point of this method. The expansion coefficients are determined from the rest of the boundary conditions by taking the inner product with respect to Jacobi's polynomials. The main reasons of using Jacobi's polynomials for the projection functions are that the expansion formulae of Bessel functions are available and they constitute orthogonal set. It is worthwhile to note that, although the edge condition for impedance disk is different from that of conducting edge, the effect of this difference can be taken into account by the expansion coefficients. (5) The matrix elements are given by infinite integrals which may be expressed by power series of the parameter associated with normalized radius of the disk. (6) The expressions for the current distribution and the far diffracted field may be derived readily.

REFERENCES

[1] J.J.Bowman, T. B. A. Senior and P.L.E. Uslenghi, Electromagnetic and Acoustic Scattering from Simple Shapes, North-Holland,1969:

[2] K. Hongo, Diffraction of electromagnetic wave by circular disk and cicular hole, EMT meeting, Oct., 1994, Wkayama, Japan

Scattering of an off–axis 2D Gaussian beam by a multilayered cylinder

Wu Zhensen and Guo Lixin
Department of Physics, Xidian University, Xi'an, Shannxi Province 710071, P.R.China

ABSTRACT

In this paper, we investigate the problem of a cylindrical Gaussian beam incident perpendicular on an infinitely long multilayered cylinder. Our approach is based on the exact solution of the Helmholtz equation in circular cylindrical coordinates. The incident Gaussian beam (TEM_{00}) is expanded in terms of plane wave spectrum and vector cylindrical harmonics. The theory of the interaction between a 2D Gaussian beam and an infinite multilayered cylinder is presented. The electric and the magnetic fields based on the Helmholtz equation in circular cylindrical coordinates are derived. At the first–order approximation, The modified algorithm for beam–shape coefficients C_n are determined more accurately. An iterative algorithm and the computing procedure to calculate the scattering coefficients $a_{n\mathrm{II}}$ and $b_{n\mathrm{I}}$ for TE and TM modes are proposed, the scattering widths of a Gaussian beam by a multilayered cylinder is obtained. These results provide an extension of our previous paper. Our recursive formulae overcome the difficulties in computing Bessel functions when the size parameter of the multilayered cylinder becomes large. The numerical results show good agreement with the limit cases when the multilayered cylinder is reduced to a homogeneous cylinder or when the Gaussian beam is reduced to the plane wave. Our algorithms can also be applicable to the microwave, milimeter range. Some numerical results including scattering fields and scattering widths are given for several kinds of cylinders, especially for a glass fiber.

Reconstruction of an Embedded 2-D Perfectly Conducting Object within Dielectric Region

S. Y. Shi and D. B. Ge
Department of Physics, Xidian University
Xi'an, 710071, P.R.China

The reconstruction problem dealing with either a PEC target or a dielectric object has been widely studied. We now consider a 2-D composed object. In free space there exists a PEC target embedded in a dielectric region whose outer contour is known, its dielectric constant is, however, not known. Suppose that the object is illuminated by a TM plane wave and the scattered fields are measured on a circle outside the composed object. First the boundary integral equations concerning the equivalent electric and magnetic current are derived based on the Green's representation theorem and the boundary condition. The scattered fields can be evaluated through the equivalent current. These are in fact the nonlinear integral equations relating the scattered fields with the object function consisting of the shape of PEC target and the dielectric constant of surrounding medium. We then apply the Newton- Kantorovitch method to convert the nonlinear integral equations into a linear equaiton which relates the incremental scattered field with the incremental object function. The incremental means the difference of successive approximation of object function or the difference of measured data and the computed scattered fields in each iterative step. Starting from an initial guess of the object function, the appropriate scattered fields and the incremental scattered fields can be computed. Correspondingly, the Frechet derivative of the scattering operator with respect to the object function in each iterative step can also be evaluated. Inversion of this linear integral equation yields the incremental object function and the successive approximation of object function. The iterative procedure continues until the termination rule is satisfied. To find the numerical solution we use the MoM to discretize the intergal equations. To overcome the ill-posedness in the reconstruction procedure, the abundant scattered data are collected on the measurement circle by using a succession of plane waves illuminating the object and an iterative method is implemented to solve the discretized linear integral equation. Some examples show the feasibility of this reconstruction scheme and also demonstrate the robustness to the noise in measured scattered data.

STIMULATED SCATTERING IN AEROSOL NONLINEAR OPTICS

A.A. Zemlyanov, Yu.E. Geints*

Institute of Atmospheric Optics, Russian Academy of Sciences,
1 Akademitcheski av., Tomsk, Russia, 634055
fax: (3822)-25-90-86, e-mail: zuev@iao.tomsk.su

The physical basis of four basic nonlinear stimulated scattering processes in transparent droplets (SRS, SBS, lasing, scattering on droplet surface vibrations) caused by intensive pumping radiation is considered. The vector Maxwell equations, where the nonlinear polarization is the source for nonlinear harmonics origin, are used as a starting point for theoretical analysis of stimulated processes in a droplet. The solution of this system of equations is written in the form of series through droplet resonance eigenmodes. The main attraction is devoted to the energetic thresholds of nonlinear scattering processes to be considered. The chain (double resonance) generation of SBS-SRS waves is investigated. The threshold values of the stimulated scattering in droplets are evaluated depending on the droplets radius.

The paper presents the results of theoretical investigations of the task on droplet surface deformations and vibrations under the pressure of the ponderomotive forces caused by intensive laser field also. It is pointed out that for small particles (less or compared to laser radiation wavelength) the surface deformations are initiated in perpendicular direction to laser beam axis, while large droplets begin to vibrate along the laser beam. This fact is the consequence of the inhomogenouty of internal electromagnetic field distribution in large droplets, that can lead to strong local surface deformations and even droplet destruction. The induced surface deformations cause the intensive nonlinear scattering of primary electromagnetic field at the combined frequency. The spectral characteristics of this scattering are considered.

Progress in Electromagnetics Research Symposium, PIERS 1997 ISBN 962-442-097-1

Electromagnetic Scattering from Conducting Rectangle: Fourier Series Entire Domain Formulation

Gao Yifan

XIAN HIGHWAY UNIVERSITY
329 mailbox
XIAN
SHAANXI
P. R. CHINA

Abstract : A efficient numerical solution is presented for electromagnetic scattering for conducting rectangle. The formulation is based on the solution of electric-field integral equations using the method of moments (MM). Fourier series entire domain representations for the currents are used on the surface of conducting rectangle. The solution is well behaved , rapid weakened and high accuracy. Using the microcomputer, main processor is 80386DX, numeric processor is 80387, it needs only several minutes to calculate the scattering field of $1\lambda \times 1\lambda$ square and achieve a satisfactory result. For $3\lambda \times 3\lambda$ square , it needs less than an hour to achieve a satisfactory result.

Polygonal Model of RCS for Complex Targets

Shunlian Chai , Demiao Yao , Zhunjie Mao

Institute of Electronic Engineering, National University of Defence Technology
Changsha, Hunan, 410073, P.R. China

Abstract---This paper presents the prediction method of radar cross section (RCS) for complex targets using the polygonal model. The calculation of RCS for complex targets involves two steps: modeling and calculation. The target is described in terms of polygons, which provides the following capabilities: 1) No limitation on target geometry and shape; 2) Better account for phase calculations than the component method; 3) Easier account for shadowing and detailed multiple scattering; 4) May be applied to the target coated dielectric materials completely or partly. 5) Explicit formulas for RCS calculation for polygonal flat plate and straight-line edge and so reduction largely of CPU time. This polygonal model is more powerful than the previous components technique using primitives. High-frequency RCS is calculated through physical optics (PO), method of equivalent currents (MEC), physical theory of diffraction (PTD) and Impedance boundary condition (IBC). Shadowing effects, discontinuities effects and multiple scattering (including surface-surface, surface-edge interactions) are considered. The results for the cone, the cylinder, the ogive-cylinder are agreed with the measurement, which shows that the method here is valid. The complex targets of genetic missile and aircraft are then calculated in both horizontal and vertical polarization. The polygonal model method is an accurate and powerful approach for calculating the RCS of complex targets.

Keywords---radar cross section, polygonal model, high frequency method, complex target

SESSION 7A14

Tuesday, January 7, AM 850-1230, Lecture Theatre 14, City University of Hong Kong

Non-Radiative Dielectric Waveguide and Its Millimeter-Wave Applications

Organizer: Ke Wu

Chairperson: Ke Wu, Ecole Polytechnique de Montréal
Co-Chairperson: Tsukasa Yoneyama, Tohoku University

8:50	***Introduction to NRD-Guide*** Tsukasa Yoneyama Tohoku University	202
9:10	***Studies of NRD Waveguide in China*** Jing-Feng Miao Southeast University	203
9:30	***The Hybrid Planar/NRD Integration Technology : A New Concept*** Ke Wu Ecole Polytechnique de Montréal	204
9:50	***NRD Guide Technologies and Their Applications at 60 GHz Band*** Futoshi Kuroki Kure National College of Technology	205
10:10	***Power Combining Techniques in NRD-Guide*** Tsukasa Yoneyama Tohoku University	206
10:30	**Break**	
10:50	***Uniaxial Anisotropy Effect on the Non-Radiative Dielectric (NRD) Waveguide Performance*** *Amilcar Careli César, **Rui Fragassi Souza, *University of Sao Paulo (USP) **State University of Campinas (UNICAMP)	207
11:10	***Modeling and Design of NRD Tunable Circuits Using Ferrite Materials*** *Jifu Huang, *Philip Mambo, **Ke Wu *Harris Farinon Canada **Ecole Polytechnique de Montréal	208
11:30	***Fabrication of 60 GHz NRD-Guide FM-CW Radar for Motor Vehicle*** Hiroyuki Ishizaka Hino Motors, Ltd.	209
11:50	***Design and Optimization of NRD-guide Components*** Francois Boone, Ke Wu Ecole Polytechnique de Montréal	210
12:10	***High Performance Millimeter-Wave Module Using Single Mode NRD Guide Coupled with Planar Circuit*** Yohei Ishikawa, Toru Tanizaki, Hiroshi Nishida, Atsushi Saito Murata Mfg.Co. Ltd.	211

Introduction to NRD-Guide

Tsukasa Yoneyama

Research Institute of Electrical Communication
Tohoku University
Katahira 2-1-1, Aoba-ku
Sendai 980-77, Japan

Although inherent losses of dielectric waveguides are reasonably small, additional radiation losses at curved sections and discontinuities are often above the tolerable level. Use of the nonradiative dielectric waveguide or NRD-guide has been proposed to overcome such difficulty. The NRD-guide resembles the H-guide in structure and field configuration, but the metal plate separation is less than half a wavelength. As is well known, if two parallel metal plates are separated by a distance smaller than half a wavelength, electromagnetic waves with the electric field parallel to the metal plates cannot propagate between them because of the below cutoff nature. However, if a dielectric strip is inserted, the cutoff is eliminated and waves are able to propagate along the strip without any radiation, whether it is straight or curved.

The NRD-guide is usually used in a horizontal configuration as shown in Fig.1. Since the outer surfaces of the top and bottom plates can be the ground planes of microstripline circuits for IF and lower frequency stages, a complete millimeter wave subsystem can be assembled in a planar structure. Fig.2, for instance, shows an NRD-guide digital transceiver which operates at bit rate more than 100 Mbps at 60 GHz.

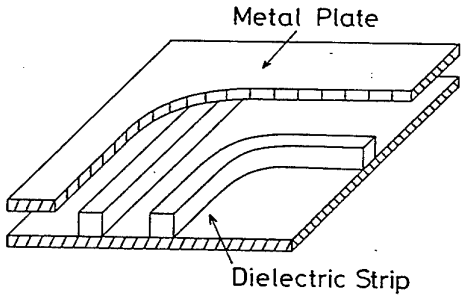


Fig.1 Geometry of NRD-guide

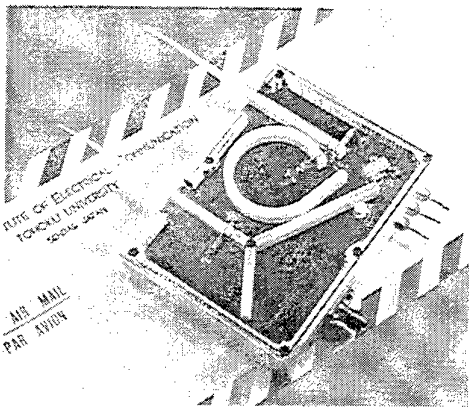


Fig.2 NRD-guide transceiver operating at bit rate more than 100 Mbps at 60GHz

Studies of NRD Waveguide in China

Jing-Feng Miao
Dept. of Radio Engineering
Southeast University
Nanjing, 210096, P. R. of China

ABSTRACT: A brief survey on studies of MMW NRD and improved structure — GNRD、MGNRD and applications in china is reported. for conveience, the report is described under following subheadings: 1. GUIDANCE CHARACTERISTICS The characteristic of propagation mode, mode exciting and suppression, scattering characteristics, impedance characteristic in the NRD waveguide have been analyzed by chinese researcheres. In order to fix the relative position of dielectric strips, chinese researchers proposed a groove NRD waveguide (GNRD) and mono-groove NRD waveguide (MGNRD). It has been shown that the new GNRD guide configuration can be better applied to MMW. 2. PASSIVE COMPONENTS The components made of NRD waveguide are essential in forming MMW integrated system in conjunction with active devices. The NRD guide periodic structure and periodic metallic strips are proposed for millimeter wave bandstop filters. These two structures have been analyzed by effective network approach and the method of lines, respectively. 8mm branched NRD guide directional coupler, impendance transformer, resonator and NRD circulator are made and tested by researchers in chinese universities. 3. ACTIVE COMPONENTS The NRD waveguide Gunn oscillator is developed in 8mm and 6mm waveband. The measured output power is 49 mw in 36. 02 GHz, 28. 2 mw in 53. 2 GHz. The small metal piece is used to mount Gunn diode and the bias is supplied through a coaxal loss-pass filter and metal resonant cap. Another oscillator is operation at LSE°_{11} mode as a local source of mixer. The NRD-guide crossbar balanced mixer has been recently developed in china, the conversion loss (SSB) of the NRD-guide receiving frond-end in Ka-band is about 7. 33dB. 4. LEAKY-WAVE ANTENNA The NRD waveguide antenna has the characteristics of frequency scanning and very narrow beam. At the frequency of 94 GHz, the half-power beamwidth of 0.14^{0} of the antenna is made, and the frequency scanning is about $\pm 7^{\circ}$ relating to the beam angle. the MGNRD leaky-wave antenna keeps the similar performance of symmetrical GNRD antenna and it is more suitable for MMW applications.

The Hybrid Planar/NRD Integration Technology: A New Concept

Ke Wu

The Center for Advanced Research of Microwave and Space Electronics (Poly-Grames), Dept. of Electrical and Computer Engineering, École Polytechnique, Montréal, Québec, Canada
Tel: 514-340-5991, Fax: 514-340-5892, E-mail: wuke@grmes.polymtl.ca

Abstract

There are two fundamental classes of technology used for microwave and millimeter-wave circuits: planar and nonplanar structures. The planar circuits are mainly related to MICs and M(H)MICs while the nonplanar counterpart essentially consists of coaxial, metallic and dielectric waveguides. Generally speaking, the planar technology presents a number of advantages such as easy integration with active devices, light weight and low-profile as well as relatively low-cost at RF and microwave frequencies. However, it has some serious problems such as ohmic loss, possible leakage and fabrication cost at millimeter-wave frequencies. Among the nonplanar structures, the dielectric waveguide technique is much less used and matured compared to the coaxial and metallic waveguides. Nevertheless, this cost-effective waveguide may offer low-loss transmission for millimeter-wave circuits.

In particular, the nonradiative dielectric (NRD) waveguide proposed by T. Yoneyama presents both mechanical and electric features which are attractive for practical applications, namely, radiationless even at sharp bends/discontinuities and easy fabrication as well as low cost. The principal limitation is that the NRD geometry is difficult to integrate with active devices although the insertion technique of active devices has been proposed to solve this problem to some extent. Still, a matching circuit (high-permittivity dielectric sheet) is usually required and mechanical assembling may be complicated. On the other hand, the operating principle of NRD circuits demands that the spacing between two metallic plates be smaller than half free-space wavelength. This restricts further the size of active devices to be inserted at millimeter-wave frequencies. To overcome this obstacle in use of the NRD technology, an alternative hybrid integration has been proposed, making use of an aperture through which the NRD waveguide and planar circuits are coupled to each other. In this way, the advantages of both technologies can be benefited while the shortcomings may effectively be eliminated. With a number of practical examples and experimental results, it is shown that the proposed hybrid technology promises to be one of the leading figures among the state-of-the-art technologies.

To begin with, this presentation will talk about the newly proposed hybrid integration of planar/NRD-guide and its potential applications for wireless technology. Future development and potential problems will be indicated. Examples of circuits built based on this hybrid technology will be also presented.

Progress in Electromagnetics Research Symposium, PIERS 1997 ISBN 962-442-097-1

NRD Guide Technologies and Their Applications at 60 GHz Band

Futoshi KUROKI
Department of Electrical Engineering, Kure National College of Technology
2-2-11 Aga-Minami Kure 737, Japan
Phone:+81-823-73-8466, Fax:+81-823-73-8474, E-mail:kuroki@kure-nct.ac.jp

Introduction

Because 60GHz frequency band has been allotted for the research and development purpose of millimeter wave systems in Japan, various circuit components and systems have been fabricated by using printed transmission lines. The NRD guide[1] can be another candidate of a transmission medium for millimeter wave integrated circuit applications since it has been proven to be excellent in performance at those wavelengths. This paper concerns with the NRD guide technologies at 60 GHz band.

NRD Guide Circuit Components and Their Applications

The NRD guide consists of a rectangular dielectric strip sandwiched in a bellow-cutoff parallel metal plate waveguide. The metal plate separation is decided to be 2.25mm so as to be less than half a free space wavelength at 60GHz. The material of the dielectric strip is chosen to be teflon because of its low loss nature in the millimeter wavelength. Its height is the same as the metal plate separation of 2.25mm and its width is 2.5mm to obtain the maximum single mode operation bandwidth from 55GHz to 65.5GHz. Various millimeter wave integrated circuit components and RF front ends have been fabricated by using the NRD guide. For example, a 60GHz digital transceiver, which has been applied in wireless LAN systems, is shown in Fig.1. The transceiver consists of frequency stabilized Gunn oscillator, circulator, PIN pulse modulator, directional coupler and transmitting and receiving pyramidal horn antennas. Remarkable advantages of the circuit components are high reliability of Gunn oscillator, wide bandwidth of the circulator and high speed operation of the PIN pulse modulator beyond 100 Mbps. Other millimeter wave integrated circuits such as car collision avoidance radar and FM transmitter/receiver for video transmission have been developed successfully at 60 GHz.

Conclusion

Advantages of the NRD guide are low loss, no unwanted radiation and easy circuit integration. The highly reliable performance of the NRD guide has been confirmed.

Reference

(1)T.Yoneyama and S.Nishida, IEEE Trans., MTT-29, 11 (Nov. 1981)

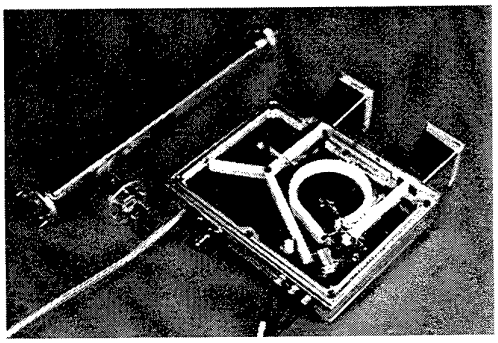


Fig.1 Fabricated LAN Transceiver at 60GHz

Power Combining Techniques in NRD-Guide

Tsukasa Yoneyama

Research Institute of Electrical Communication
Tohoku University
Katahira 2-1-1, Aoba-ku
Sendai 980-77, Japan

The NRD-guide technology is very promissing for the use of millimeter wave circuits and even competitive with MMICs. A variety of circuit components have been built based on this technique. NRD-guide gunn oscillators, for instance, can produce the same amount of power as waveguide counterparts. In order to enhance power capability of NRD-guide gunn oscillators, three types of power combining techniques have been developed. Fig.1 shows the circuit configuration for one of them. A multielement oscillator is constructed by installing gunn diodes in a metallic block so as to produce the electric field polarized horizontally. Power of oscillation is led to a dielectric strip in NRD-guide via a strip line created on a Teflon substrate of 0.26 mm in thickness. Fig.2 shows power and frequency characteristics of the multielement oscillator against length of the strip line. Power performance is satisfactory considering power level of 20mW for each single diode, and frequency is kept unchanged over a wide range of strip line length. This frequency behavior is quite peculiar and remains to be studied. It is challenging to try to further increase the number of gunn diodes to obtain millimeter-wave power around 1W or more. Other two types of power combining techniques will be presented at the conference.

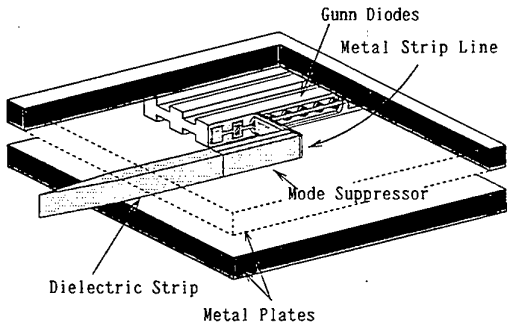


Fig.1 Structure of NRD-guide multielement oscillator

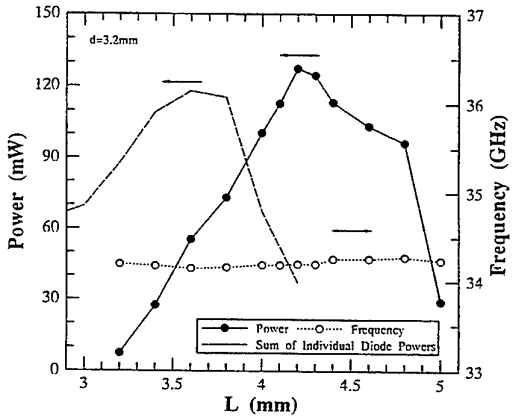


Fig.2 Power and frequency characteristics of NRD-guide multielement oscillator

Uniaxial Anisotropy Effect on The Non-Radiative Dielectric (NRD) Waveguide Performance

Amílcar Careli César
University of São Paulo (USP), EESC, Department of Electrical Engineering
C.P. 359, 13560-250 São Carlos, SP, BRAZIL
e-mail: amilcar@peterpan.sel.eesc.sc.usp.br

Rui Fragassi Souza
State University of Campinas (UNICAMP), FEE, Department of Microwave and Optics
C.P. 6101, 13081-970, Campinas, SP, BRAZIL
e-mail: rui@dmo.fee.unicamp.br

Abstract

In recent years there has been a growing interest in the investigation of the anisotropy effects on the propagation characteristics of waveguiding structures. Depending on the media involved such effects can be large and its accurate knowledge is important, specially at high frequencies, like millimeter waves. The non-radiative dielectric (NRD) waveguide proposed for millimeter wave applications is nowadays an available technology. Most of the devices proposed in this technology use isotropic [1] or ferrite [2]-[4] materials.

In this paper, the simultaneous effect of the uniaxial dielectric and magnetic anisotropies on the propagation characteristics of single and coupled NRD waveguides is investigated.

The isotropic slabs of the single and coupled conventional NRD waveguides are replaced by another material that is lossless and has uniaxial permittivity and permeability tensors. The components of the electromagnetic field are written in terms of the electric (LSM modes) and magnetic (LSE modes) field components normal to the dielectric interfaces. The boundary conditions at the dielectric interfaces lead to the characteristic equations for the propagating modes. The coupled slabs are investigated using even and odd modes analysis. The characteristic impedances of single and coupled slabs are also obtained using a power-voltage relation.

Numerical results of the dispersion for three materials that exhibit uniaxial dielectric anisotropy are shown. Those materials are sapphire, Epsilam-10 and boron nitride.

The analysis performed shows that, depending on the media involved, the anisotropy effect on the propagating single slab modes can be large. The coupled slabs propagating modes are strongly influenced by anisotropy. The appropriate choice of the anisotropic dielectric material can enhance directional coupler performance. Dielectric anisotropy of some materials increases the useful bandwidth wherein the even and odd mode impedances are equalized.

References

1. T. Yoneyama, "Nonradiative Dielectric Waveguide", in Infrared and Millimeter Waves, vol. 11, K.J. Button, Ed. New York: Academic Press, 1984.
2. H. Yoshinaga and T. Yoneyama, IEEE Trans. Microwave Theory Tech., vol. MTT-36, pp. 1526-1529, November 1988.
3. S. Zhongxiang, Int. J. Inf. Millimeter Waves, vol. 12, pp. 1399-1408, 1991.
4. A. C. César and R. F. Souza, IEEE Trans. Microwave Theory Tech., vol. MTT-41, pp. 647-651, April 1993.

Modeling and Design of NRD Tunable Circuits Using Ferrite Materials

Jifu Huang*, Philip Mambo*, and Ke Wu**

* Harris Farinon Canada
3 Hotel De Ville, DDO
Montreal, Canada H9B 3G4

** POLY-GRAMES Research Center
École Polytechnique de Montréal,
C.P. 6079, Succ. Centre Ville
Montréal, Québec, Canada H3C 3A7

Tunable microwave and millimeter-wave circuits such as filters and phase shifters can be realized in many techniques. The ferrimagnetic resonance is the most common technique. Recently, a novel hybrid integrated planar/NRD-guide architecture becomes an attractive way of exploiting inherent advantages of planar structures and NRD waveguide for low-cost wireless applications. Therefore, the tunable passive NRD-guide component is possible to offer the tuning circuit for integrating planar active circuits through microstrip-slot aperture interconnection. In this paper, we are thus motivated to study the non-reciprocal propagation and scattering characteristics of electromagnetic waves in the NRD-guide structure where the isotropic dielectric slab is replaced by ferrite slabs. The dispersion curves and S-parameters will be investigated by using the generalized TLM algorithm, which has been well established for arbitrary anisotropy. The possible non-reciprocal effect associated with the operating mode of the ferrite NRD-guide can be used to realize to tunable NRD-guide circuits. Espercially, the accurate non-reciprocal S-parameter calculations of NRD-guide discontinuties will lead to effective design of new tunable NRD filters. Moreover, the influence of the both biasing dc-magnetic field and NRD structure sizes to non-reciprocal effect (differential phase shift) of the ferrite NRD-guide structure will be discussed to determine the relative bandwidth of monomode operation.

Progress in Electromagnetics Research Symposium, PIERS 1997 ISBN 962-442-097-1

Fabrication of 60GHz NRD-guide FM-CW Radar for Motor Vehicle

Hiroyuki ISHIZAKA

HINO MOTORS, LTD. TECHNICAL RESEARCH LABORATORY

1-1, HINODAI 3-CHOME, HINO-SHI,TOKYO 191 JAPAN

TEL:+81-425-86-5991 FAX:+81-425-86-5124

Abstract: Recently, infrared collision warning systems has been put into market in Japan. Because there are many rear-end accident which is a serious problem in Japan. However, laser systems do not operate adverse weather, such as rain, snow and fog. Millimeter wave CWS's (Collision Warning System) are expected to eliminate such difficulty.

If try to think about CWS system design, what is best way to make millimeter wave CWS. Waveguide based CWSs are likely to be bulky, even at millimeter wavelength. On the other hand, microstrip lines can offer devices small enough in size, but transmission losses are above a tolerable level. The NRD-guide (Nonradiative Dielectric Waveguide) is moderate in size and low in transmission loss as well. A newly developed NRD-guide is promising for millimeter wavelength applications. A frequency modulator and a mixer has to be fabricated here. Frequency modulator was developed by newer method and mixer's S/N ratio was improver by novel method in this study. Also FM-CW radar was cleated by those components. Necessary, NRD-guide circuit components have been already fabricated.

Finally on this study, the FM-CW radar was fabricated with 7dBm output power. The radar detected targets at 30m and 47m ahead. A performance of the radar is good enough for the first prototype. Because this fabricated FM-CW radar's antenna has a single beam which is grater than 16 degree beam width. Further study of improvement in the manufacturing process, cost reduction and etc. will be required as a next step of this study.

Design and Optimization of NRD-guide components

François BOONE, Ke WU

Poly-Grames Research Center
Dept. de genie electrique et de genie informatique, Ecole Polytechnique
C. P. 6079, Succ. Centre-Ville,
Montreal, Quebec, Canada H3C 3A7
Tel: 514-340-5991, Fax: 514-340-5892, E-mail: wuke@grmes.polymtl.ca

Abstract

The NonRadiative Dielectric (NRD) guide becomes a well established transmission line for millimeter wave application due to its very attractive features such as radiationless even at sharp discontinuities, low loss of transmission, and potentially low cost. However, most of the commercial modeling and design packages are not suitable or even impossible for use in the design of NRD-guide based microwave and millimeter-wave circuits because of the dispersive and hybrid-mode nature of the NRD-guide. To this end, the development of a CAD algorithm that is able to predict, design and optimize NRD circuits is indispensable for any further commercial application of this technology.

Considering the particularity of this NRD geometry, we have formulated and developed an efficient algorithm based on the mode-matching method together with the concept of equivalent network model. In this way, the hybrid-mode characteristics and discontinuity effects can be accurately described under this field-theoretical framework. With a transverse resonance technique, the propagation constant of a mode of single or layered NRD guide can be calculated and leads to the knowledge of its field profile. A generalized scattering matrix is used to determine the S-parameters of a NRD discontinuity or a NRD circuit consisting of multiple discontinuities. This CAD package with a build-in optimization procedure is designed such that the frequency response of a designated NRD circuit can be obtained within a very short CPU time on a workstation environment. As the first example of its application, a transition from rectangular waveguide to NRD-guide has been designed, optimized and a comparison has been made between the theoretical prediction and experimental results. Such an optimization has been done in terms of both metallic and dielectric geometrical profiles with constraints on related S-parameters over a large frequency band. The second example is concerned with the design of multiple-strip NRD filter. A complete equivalent model using inductance and/or capacitance derived from the S-parameters of relevant NRD-guide circuits has been developed for fast optimization using a curve-fitting technique.

High Performance Millimeter-Wave Module using Single Mode NRD Guide coupled with Planar Circuit.

Yohei Ishikawa Toru Tanizaki Hiroshi Nishida Atsushi Saito
Murata Mfg. Co.,Ltd.
Address: 26-10, 2-CHOME, TENJIN,
NAGAOKAKYO-SHI, KYOTO 617, JAPAN
TEL: 81-75-951-9111
FAX: 81-75-956-5724
E-mail: ishikawa@murata.co.jp

Abstract

A new technology of millimeter-wave NRD module is proposed. Each NRD components has some input-output NRD ports and is made to be satisfied specifications and measured. The module is obtained easily by mounting them to the base plate from the surface direction without tight connection like the waveguide flange.

The new performance NRD guide with the new structures is developed.
(1)The planar circuit board with circuit patterns and some mounted devices is inserted horizontally in the center of the dielectric strips. NRD guide can easily coupled to the planar circuit. So the components like oscillator can be realized by using this structure.
(2)The separation of the metal plates is made to be less than the height of the dielectric strips. So the cutoff frequencies of fundamental NRD guide modes (LSM01 mode and LSE01 mode) can be changed. By optimizing each mechanical parameters, the structure in which only the operating LSM01 mode propagates in the band width is realized. As the result, the small size bends and circuits are obtained.

By using this module technology and this new NRD guide, some high performance millimeter-wave module like the compact size radar front end can be expected.

SESSION 7P14

Tuesday, January 7, PM 1330-1650, Lecture Theatre 14, City University of Hong Kong

Millimeter, Submillimeter & Lightwaves 2

Organizer: Weigan Lin

Chairperson: Weigan Lin, Univ. of Electronic Science and Technology of China
Co-Chairperson: W B Dou, Southeast University

13:30	***Progress of MMW Ferrite Devices Research at SKL of MMWs of China*** W B Dou, Z L Sun Southeast University	213
13:50	***Discontinuities in Millimeterwave Phase Shifter*** Liquan He, Zhaofeng Zhang, Yong Li Southeast University	214
14:10	***Microwave Power Transmission Simulated at Millimeter-Waves by its Scale Model Systems*** Hongwei Liu, Weigan Lin, Zhendong Shi University of Electronic Science and Technology of China	215
14:30	***Experimental Diffraction Radiation Oscillator*** Jiayu Chen, Yongchuan Zhang, Yuxiang Duan University of Electronic Science and Technology	216
14:50	***Realization of Optical Wavelet Filter by Binary Optics*** Ming Ni, Zhi Ping Jiang, Qi Sheng Lu National University of Defence Technology	217
15:10	**Break**	
15:30	***Real-Time Closed-Loop Correction on Nonlinearity of MMW Wideband FM Generator*** Zhuming Chen, Yiyuan Ding University of Electronic Science & Technology of China	218
15:50	***An Analysis of Far-Field Pattern of a Focal-Plane Array Antenna with Coma-free Lens*** W B Dou, Z L Sun Southeast University	219
16:10	***94GHz Imaging Radar for Detecting Shape of Burden Distribution in Blast Furnace*** Yiyuan Ding, Jianyu Yang, Xiaobo Yang, Zhuming Chen University of Electronic Science & Technology of China	220
16:30	***Typical Elliptic Curves as Boundaries of Static Fields*** Weigan Lin, Jianhua Zhu University of Electronic Science & Technology of China	221

Progress of MMW Ferrite Devices Research at SKL of MMWs of China

W.B. Dou Z.L. Sun
State Key Lab. of Millimeter Waves
Southeast University, Nanjing 210096
P.R. China

SUMMARY

The research work on millimeter wave ferrite devices including (1) waveguide junction circulators; (2) microstrip junction circulators; (3) Faraday rotation devices are described.

Because of the limitation of the available ferrite materials which has about 5300 Gauss of saturation magnetization, conventional design way at microwave band can not get broadband performance at 3mm band. An attempt for expanding the bandwidth of waveguide junction circulators is carried out. Working modes of junction circulators is researched. The electromagnetic field eigenmodes are described and classed into two kinds: volume modes and surface modes. The properties of the junction resonant modes which are the superimposition of eigenmodes are stated. There are two kinds of junction resonant modes: lowest modes and higher order modes. Dual higher order modes have been used to get dual frequency circulators at 3mm band. And the dual higher order modes are staggered to expand the bandwidth of 3mm band circulator.

Ka band microstrip circulator using hybrid integrated techniques are developed. RT/duroid substrate and NiZn ferrite are used. Isolation of 17 dB over 4 GHz is achieved for which insertion loss is about 1.0dB.

Research on Faraday rotation devices contains: (1) quadruply-ridged circular waveguide Faraday rotation devices and (2) quasi-optical Faraday rotation devices. Quadruply-ridged circular waveguide partially filled with longitudinally magnetized ferrite rod is solved. The approach is a combination of the mode expansion method and the boundary element method. Examples of kind of waveguide are presented to show the validity and usefulness of this approach. General field theory treatment of quasioptical Faraday rotator for use as either an isolator or circulator is presented. The use of matrix methods in conjunction with Fourier-transformation techniques greatly facilitates the formation of the boundary-value problem, and provides a closed- form representation of the electromagnetic field over the anisotropic region. Numerical results are presented and compared with those of other authors, and they agree with experiments.

REFERENCES

[1] W. Holpp, 19th EMCP, pp.633-638,1989.
[2] W.B. Dou , Science in China (A), Vol.32, No.9, pp.1915-1923, 1989.
[3] Y. Rong, W.B. Dou, S.F. Li IEE Proc.-H, Vol.138, No.5, 412-416, 1991.
[4] W.B. Dou, Z.L. Sun, Microwave & Optical Tech. Lett., Vol.9, No.5, 274-278,1995.

Discontinuities in Millimeterwave Phase Shifter

HE Liquan ZHANG Zhaofeng LI Yong

State Key Laboratory of Millimeter Waves
Department of Radio Engineering
Southeast University
Nanjing 210096, P.R.China

Abstract

Three kinds of discontinuities are analyzed in this paper. The discontinuity of DC isolation slot is analyzed with FDTD method and S parameter is obtained. The numerical result indicates that resonance at certain frequency will be introduced if the shape and size of slot are not correctly selected. In the experiment, the reasonance phenomenon is observed. SDA method is utilized to analyze the discontinuity of full-height fin-line short end. As a discontinuity, the short end equals a supplementary fin-line at the end of the fin-line. The effective transmission length are obtained. The discontinuity problem of tuning post in a fin-line side is analyzed based on the full-wave mode-matching method and perturbational techniques. The equivalent *T*-parameter is given out and its phase-shift characteristic in electromagnetic propagation is also obtained. Based on the numerical results, low insertion loss reflection-type phase shifters at 38GHz and 94GHz are successfully achieved. A phase shifter is connected with a circulator in series to compose a BPSK modulator. The 90° BPSK modulator at 94Ghz was achieved with its insertion loss lower than 3.8dB. Its bandwidth is 2.5Ghz with a phase error of $\pm 5^0$. At 38Ghz band, the insertion loss of 90° BPSK is lower than 1.9dB and that of 180^0 BPSK is 2.4dB. The bandwidths of them are about 1.0Ghz.

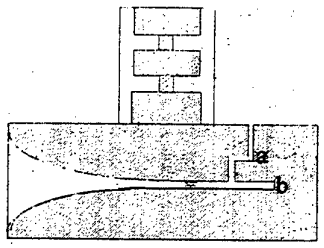


Fig 1 Phase shifter circuit layout
a--DC isolation slot b--fin-line short end

Microwave Power Transmission Simulated at Millimeter-waves by Its Scale Model Systems

Hongwei Liu, Weigan Lin, Zhendong Shi

Faculty of Electronic Engineering
University of Electronic Science and Technology of China
Chengdu, 610054, People's Republic of China

ABSTRACT

Scale model Technique has been used extensively in electromagnetic systems for a number of years. By this method, the very large or small systems can be studied by scaling their geometrical size down or up, if the wavelengths used are also scaling down or up proportionally. According to the physical similarity of electromagnetic system, a physical scale factor between the model and the prototype is presented. Therefore, the system used to transmit microwave power at microwave band(2450.0 MHz) can be studied by its scale model system worked at millimeter-waves(26.5 to 40.0 GHz) in the much smaller size.

In this paper, emphasis is firstly placed on the theory of the physical similarity between the model and the prototype, that is, which factors play a key role between model and prototype. And secondly, the beam focusing of the antenna, according to the complex ray tracing technique(CRT), for the microwave power transmission is to be found out by the theoretical analysis and the experimental study. Finally, the photograph of the millimeter-wave scale model system and the measured results of the beam focusing are both given.

Progress in Electromagnetics Research Symposium, PIERS 1997 ISBN 962-442-097-1

EXPERIMENTAL DIFFRACTION RADIATION OSCILLATOR

Chen Jiayu, Zhang Yongchuan, Duan Yuxiang
Inst. of High Energy Electronics
University of Electronic Science and Technology
Chengdu, 610054
China

Abstract: In this paper, researching on 3mm; 4mm band device in our laboratory, design method of diffraction radiation oscillator (DRO) are reported in brief ; Theoretical and test results of DRO have been introduced. The main experimental results are; from 2400v to 4000v , the 3mm tube operates in 84 GHz— 104 GHz range, the maximum output power is about 200 mW. In 60 GHz—86 GHz, the maximum output power of 4mm tube is up to 1.3W. [2-4]

For researching millimeter waves spectrum, in the medium power range, the conventional periodic circuit devices such as BWO, TWT Klystorn, and Magnetron need a smaller interaction structure for higher operating frequencies, and usually require higher magnetic field, and higher beam density. Therefore, medium or high power source on short millimeter waves becomes increasingly difficult because of fabrication difficulties and the decrease in the heat-dissipation capability of smaller circuits. So DRO that combines aspect of microwave and optical techniques has several of the desirable features with sufficient tunable bandwidth, medium output power, and frequency stability. [1]

The diffraction radiation oscillator, called DRO for short or Orotron, is a sort of new vacuum electronic device with an open resonator and a reflecting grating. This device is based on the Smith-Purcell effect. In a sense, DRO is also called a Smith-Purcell effect free electron laser . This is the excellent program of produced source of band width tunable on sub millimeter band.

The design parameters of the device on 3mm, 4mm band are given; the radius of curvature of upper sphere mirror is $R_{1x}=R_{1y}=80mm$, the radius of curvature of lower cylindrical mirror is $R_{2x}=\infty$, $R_{2y}=110mm$, $q=7-12$. For 4mm device the grating period is 0.4 mm; h=0.88 mm; On 3mm band, the grating period is 0,3 mm; h=0.6 mm. The main experimental results are : from 2400v to 4000v, the 3mm tube operates in 84 GHz-104 GHz band, and the maximum output power is about 200 mW; from 60 Ghz to 87 GHZ (4mm tube) the maximum output power is up to 1.3 W. The design method of the device、linear theory and 3 dimension numerical simulation are reported in brief. many applications of DRO on science and technology are introduced.

Realization of Optical wavelet Filter by binary optics

Ming Ni Zhi-ping Jiang Qi-sheng Lu

(Graduate Group,Department of Applied Physics,National University of Defense Technology ,Changsha,Hunan, 410073 China)

Abstract

The wavelet transform(WT) provides an efficient representation for signal processing applications such as multi-resolution image analysis, data compression and pattern recognization, subband coding, fractal aggregation analysis,etc. Much attention has been paid to the WT in the signal processing due to their capability of multiple-resolution. The WT is a convolution operation and can be optically implemented in the space domain using the shadow-casting system and in the spatial frequency domain using optical filtering system.As we know, many popular wavelets are real and symmetric function[1]. Furthemore, the Fourier transform of those wavelets is positive,which favors the realization of optical wavelet filter. The WT filters can be optically recorded by holographic or computer generated by photographic[2].

In this paper,we propose a novel way to make the WT filters. The Gerchberg-Saxton algorithms[3]is effective in solving the general amplitude-phase retrieval problem in any linear unitary transform system. We suppose that a uniform intensity distribution lies on the input plane,the output is an intensity distribution which is an Fourier spectrum of an optical wavelet.We calculate the phases at the input plane by use of the iterative algorithm(GS algorithm) starting with the intensity distributions of input and output plane.Only if a binary optical element,which makes the plane wave into the calculated phase distribution,is put at the position of input plane,we will have the Fourier spectrum intensity distribution of a wavelet at the position of output plane. At last, we can make the wavelet filter by photograph[4].

We choose the Mexican-hat wavelet and improve it(we named it improved Mexican-hat wavelet) to process signals in a $4f$ optical setup. The computer simulations for edge extraction are given using this system.

In summary,we propose a way to make an optical wavelet filter by binary optics.The computer simmulation tests its reliability.

References

[1] Y.Sheng,J.Chen,and H.Szu, " Wavelet transform and its optical implementations " Proc.SPIE 1705(1992)

[2] Yunlong Sheng,Danny Roberge and H.John Caulfield, " Optical N^4 implementation of a two-dimensional wavelet transform " Opt.Eng. 1859 (1992)

[3] R.W.Gerchberg and W.O.Saxton, " A Practical Algorithm for the Determination of Phase from Image and Diffraction Plane Pictures " OPTIK 35:237(1972)

[4] Zhang Jingfang and Wang Xiaoli, " Using a complex filter for uniform distribution of Gaussan beam " Optical Technique(Chinse) 2:29(1995)

Real-Time Closed-Loop Correction on Nonlinearity of MMW Wideband FM Generator

Chen Zhuming Ding Yiyuan

(University of Electronic Science and Technology of China)

LFMCW (linear frequency-modulation continuous wave) imaging radars working at millimeter wave (MMW) band need high linearity frequency-sweep Generator. Because of the nonlinear varactor-tuned characteristic of MMW Gunn oscillator, its original nonlinearity error is about 5%, and can't by far satisfy the requirements of MMW imaging radars. Therefore, outside nonlinearity correction is used for decreasing the frequency-sweep nonlinearity error. The correcting system described by this paper is as shown in figure 1.

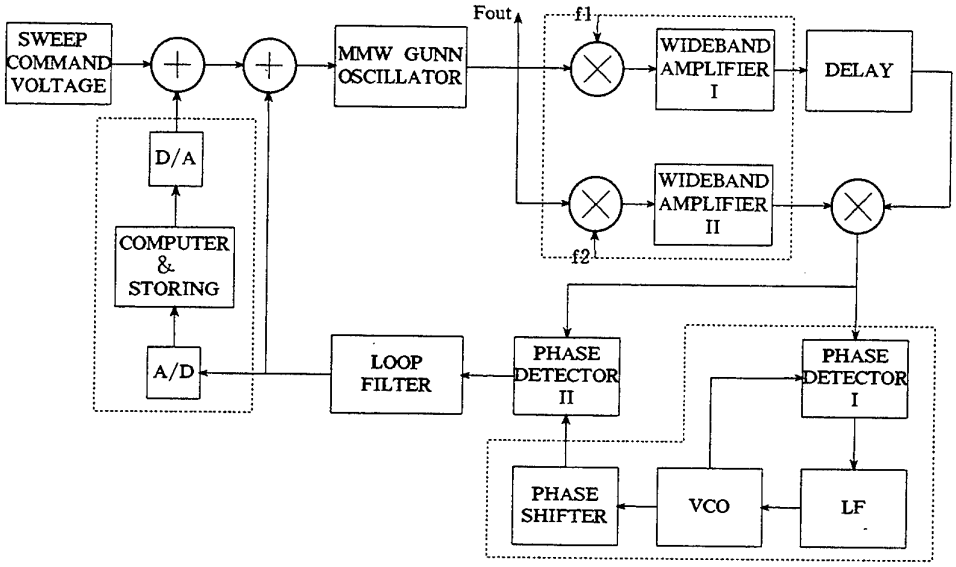


Figure 1 The practical system used for real—time closed—loop nonlinearity correction

A delay-mixing method easy to realize is employed and three specific structures are adopted in the system. First, the system uses balanced mix-amplifying structure in RF channels to decrease the system error created by the nonlinear phase-frequency characteristic of the wideband RF channels, and increase the IF frequency to avoid that its direct leakage reduce the loop performance. Second, the system uses IF phase-locked tracking method to remove automatically the system DC error and slowly varying error created by environment's effect, such as the drift of the initial sweep frequency in the Gunn oscillator. Third, the system uses period-storing precorrecting method in a few initial frequency-sweep periods in order to correct the larger error to acceptable level. Storing the corrected command voltage wave makes the nonlinearity error period-convergent and contributes to decreasing the instantaneous transition process, widening the effective bandwidth and decreasing the remanent nonlinearity error of the system.

The system in this paper can improve the nonlinearity error from 10% to the order of 0.01% theoretically. However, because of some hardwares' limit, the practical correcting precision is about 0.1%, and can satisfy the requirements of many MMW imaging radars. The system has been applyed to the 3mm burden distribution imaging radar operating at the top of the blast furnace in metallurgical industry.

An Analysis of Far-Field Pattern of A Focal-Plane Array Antenna with Coma-free Lens

W.B. Dou Z.L. Sun
State Key Lab. Millimeter Waves,
Southeast University,
Jiangsu, Nanjing, 210096, P. R. China

SUMMARY

A very common focal-plane array antenna configuration consists of a collimating device illuminated by an array of feeds. The collimating device is a coma-free lens. The feeds are horn antennas with a circular aperture located on the focal plane of the lens. This antenna may be used in focal-plane array imaging system. Imaging can be considered to be the process of measuring the radiation arriving from different directions. The millimeter wavelength region of the electromagnetic spectrum is situated between microwave frequencies, in which range coherent signal processing techniques are well developed, and the infrared region, in which incoherent technology has predominated. It is indicative of the position of the technological frontier to compare the lack of imaging arrays at millimeter wavelengths with infrared cameras which already employ focal plane arrays with thousands of elements, and sophisticated microwave phase array systems. Now as a result of many developments, focal plane array technology has been adopted as design approach for imaging systems in 2 mm to 3 mm wavelength range. The critical parameters of the focal plane array include maintaining antenna gain, beam size, and beam quality over the range of angles scanned; achieving these goals is made difficult by a combination of factors including the following:

1) Focal plane arrays with $\approx 10^4$ pixels are been seriously considered, with the result that scan angles $\approx$ 100 beam widths off boresight must be considered.

2) System aperture diameters are relatively small , typically only a few hundred wavelengths for commercial systems, and often less. Blockage loss for symmetric reflector systems of limited size is generally excessive.

3) The limited volume available restricts f/D for lens systems to values $\leqslant 1.25$, which seriously restricts imaging capability. For this same reason, off-axis optical systems are generally not acceptable.

In this paper the far field pattern of a focal plane array with a coma-free lens is calculated with a hybrid approach that uses ray tracing through the lens and diffraction calculation of propagation to the far- field. The coma-free lens is designed by step integration. It is adopted for keeping the beam size and beam quality from the aberration. The field pattern calculated is presented. With a lens of 200 mm diameter over 100 pixels may be achieved for difference of beam gain less than 1.8dB and approximate same beam size and beam quality crosses the lens surface.

REFERENCES

[1] P.F. Goldsmith, *et al*, "Focal Plane Imaging Systems for Millimeter Wavelength", IEEE MTT-41, 1993(10),pp.1664-1675.

94GHz Imaging Radar for Detecting Shape of Burden Distribution in Blast Furnace

Ding Yiyuan Yang Jianyu Yang Xiaobo Chen Zhuming
(Dept. of Electronic Eng. UEST of China, Chengdu, Sichuan)
(Chengdu 610054)

A new method for detecting the shape of burden distribution in blast furnace using a millimeter wave imaging radar has been developed. As well known, a reasonable shape is very important for decreasing coking ratio, increasing pig iron and extending service life of blast furnace. It is common in traditional blast furnace that the mechanical ruler method is utilized to detect charging level in blast furnace. But this kind of method is not imaging and is impossible to get a real shape of burder distribution. In recent years, many new techniques detecting shape have been developed. But, most of them are indirect methods and bound to worsen the accuracy of final results. So, it is expected to find a more efficient method for detecting the shape of burden distribution and distance location of charging level. A series of potential superierties of millimeter wave allow to implement a perfectly new method for realizing this purpose.

The installing configuration is an optimum choice for our purpose, because it can satisfactorily meet the requirements of fixing poient outside blast furnace, tracking charging center, scanning continuously in horizontal polar coordinate of antenna.

The block diagram of system as shown in figure 1 consists of following basic parts: (1)Transmitter, 3mm varactor-tuned Gunn-oscillator and high linearity saw-toothed wave function generator; (2)Receiver and signal preprocessing unit; (3)Cassegrain antenna unit, scanning mechanism and controller; (4)Signal processing and CRT; (5)sealling window system and its controller PLC; (6)Circulater.

The parameters of system are as follows:

Operating Freq. Band	93.5—94.5GHz
Freq. Sweeping Bandwidth	1GHz
Freq. Sweeping Period	2ms
Transmission Power	40mW
Antenna Beam Width	1.7°×1.7°
Number of Resolution Elements in One Scanning Frame	800
Time for 1024 Points FFT	0.5ms
imaging period	20 seconds.

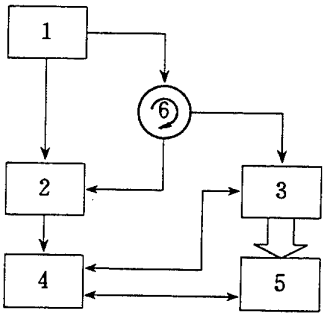


Figure 1 The System Diagram

The system has been undergone the extremely bad conditions of high temperature, large moisture, thick dust and disturbing by another equipments inside blast furnace. The applicational results indicated a very high stability and clarity of imaging are obtained.

Typical Elliptic Curves as Boundaries of Static Fields

Weigan Lin Jianhua Zhu
University of Electronic Science and
Technolgy of China, Chengdu 610054, China

We should make good use of the fraitful theory on elliptic curves. Let us look at typical but simple equations of elliptic curves

$$y^2 = x^3, y^3 = x^3 + x^2, y^2 = x^3 \pm x, y^2 = x^3 - 3x + 3$$

giving nice curves.

First, take $y^2=x^3$, then in polar coordinates, it is $\rho=tan^2\theta sec\theta$, so that, in paramentric equation, it is $x=tan^2\theta$, $y=tan^3\theta$, so we now set the equation for a complex potential function $w=u+jv$

$$z = x + jy = tan^2 mw + jtan^3 mw = (1 + jtanmw)tan^2 mw \tag{1}$$

where m is a contant to be determined by charactristics of the field. Differentiating we find

$$(m\frac{dw}{dz})^{-1} = (2tanmw + j3tan^2 mw)sec^2 mw \tag{2}$$

In (1), $z\to 0$ or -2 as $z\to\infty$ or $-\infty$, as $tan(mu+jmv)\to -j$ or j respectively, independent of m. We take $m=-j$, so $mw=v-ju$ and we make $v=\theta$ as the flux function and u the potential function, we have then the field intensity

$$|\frac{dw}{dz}|^{-1} = |2 + j3tan(\theta - ju)| \cdot |tan(\theta - ju)| \cdot |sec^2(\theta - ju)| \tag{3}$$

while

$$z = x + jy = tan^2(\theta - ju) + jtan^3(\theta - ju)$$

To find the potential and field intensity at any place, we solve for θ and u for given x and y, from (4) and then find the field intensity by (3), at $u=0$, $|\frac{dw}{dz}|$ can be found from

$$|\frac{dw}{dz}| = (\frac{dz}{dw})^{-1}|_{u=0} = \{(\frac{dx}{dt})^2 + (\frac{dy}{dt})^2\}^{-1/2} = \{\rho^2 + \rho'^2\}^{-1/2} \tag{5}$$

and for the curve $y^2=x^3$, we have

$$|\frac{dw}{dz}| = \frac{y}{(x^2 + y^2)(4 + 9x)^{1/2}}$$

Progress in Electromagnetics Research Symposium, PIERS 1997 ISBN 962-442-097-1

SESSION 7A13

Tuesday, January 7, AM 850-1250, Lecture Theatre 13, City University of Hong Kong

RF & Microwave Circuits 2

Organizer: Shanjia Xu

Chairperson: Shanjia Xu, University of Science and Technology of China
Co-Chiarperson: K C Li, The Hong Kong Polytechnic University

8:50	***The Miniature Probe Coupled Evanescent Mode Waveguide Bandpass Filters*** Lin Li, Xiaohua Yun Nanjing University of Science and Technology	223
9:10	***Combination of Edge-Element and Mode-Matching for Multi-Step Dielectric Discontinuity in Guiding Structures*** Shanjia Xu, Xinqing Sheng University of Science and Technology of China	224
9:30	***Novel Optical Nonlinear Phenomenon in Dye Polymeric Gel*** *Xianmin Zhang, *Kangsheng Chen, **Yoshiharu Kagami, **Gu Bum Park, **Jianping Gong, **Yoshihito Osada *Zhejiang University, **Hokkaido University	225
9:50	***Multiresolution Analysis in the Microwave Components and Circuits*** Y M Song, D G Fang, C F Wang Nanjing University of Science and Technology	226
10:10	***Finite Element Analysis of Non-Reciprocal Microwave Circuits*** J D Wen, Y X Huang Nanjing University of Science and Technology	227
10:30	**Break**	
10:50	***Dyadic Green's Functions for the Cylindrical Chirowaveguide*** H T Hui, Edward K N Yung City University of Hong Kong	228
11:10	***Filter Synthesis with Genetic Algorithm and Constraints*** *S Peik, **Y L Chow *University of Waterloo, Waterloo, Ontario **City University of Hong Kong	229
11:30	***Improved Slotted-Filter for Over-Mode Rectangular Waveguide*** Yaokun Qin, Yexin Yang Shanghai Transmission Lines Research Institute	230
11:50	***Researches on Millimeter Wave Low Loss Coaxial Cables*** Qing Wan Shanghai Transmission Lines Research Institute	231
12:10	***The Analysis of a Curved Coupler Structure Using Beam Propagation Method*** Ayhan Altintas, Erdem Ofli Bilkent University	232
12:30	***New Approach to the Nonlinear Biharmonic Mixer Characteristics Analysis*** S V Melichov Tomsk State Academy of Control Systems and Electonics	233

THE MINIATURE PROBE COUPLED EVANESCENT MODE WAVEGUIDE BANDPASS FILTERS

LIN LI AND XIAOHUA YUN

Microwave Engineering Research Center
Box 493 , Nanjing Univ. of Sci. & Tech.
200 Xiao-ling-wei Street
Nanjing 210094 , P. R. China

(ABSTRACT)

A design theory for miniature probe coupled Evanescent Mode Waveguide band-pass filters is presented . This type of filters differes from the orthodox waveguide filters in that it uses waveguide below its cutoff frequency . In analysing the filters , the theory based on equivalent circuits that represents the Evanescent Mode Waveguide and its obstacles is used . It is shown that cutoff dominant mode waveguide can be represented by equivalent π -sections of lumped inductance which , with appropriate capacitive elements , form resonators of very high unloaded Q-factor . The connecting lengths between obstacles are elements in the associated filters . A correction factor is introduced to allow for the added frequency sensitivity of the evanescent mode resonator . The theory derives the equivalent ladder network from the low-pass prototype . A Evanescent Mode Waveguide band-pass filter working in Ku-band designed using the derived expression yields results which are in agreement with computed values . Its center frequency is 16.5 GHz , it has a bandwidth equal to 2.2 GHz , and its insertion loss is less than 0.6 dB . The volume of this filter is $45 \times 10 \times 7$ mm^3 (the coaxial connector not involved) .

The whole unit of the filters is built in a single waveguide . With coupling probe the coxial terminations are used , thereby dispensing with the connecting flanges . Because the resonators of high Q-factor are used , low insertion loss can be achieved in the Evanescent Mode Waveguide band-pass filters . Performance , competive with orthodox waveguide band-pass filters , is achieved in greatly reduced volume (one fifth to one tenth) and weight . Another important advantage of this type of filters is that it is simple and cheap to manufacture and convenient to tune .

Combination of Edge-Element and Mode-Matching for Multi-Step Dielectric Discontinuity in Guiding Structures

Shanjia Xu and Xinqing Sheng

Department of Electronic Engineering and Information Science
University of Science and Technology of China
Hefei, Anhui, 230027, P.R.China

Summary

Dielectric discontinuity problem is one of most basic pratical problems in microwave engineering. Of various discontinuity problems, multi-step discontinuity has been recongnized as a basic one in guiding stuctures. It is because not only most discontinuities in planar circuit belong to this kind of problem, but also many discontinuity problems can be approximated to this category with staircase approximation.

A lot of methods, such as mode-matching method, multi-mode network method and 3-D finite element method have been developed to treat this kind of discontinuity problem . It is well known that mode-matching method is accurate, but it becomes very cumbersome for complicated discontinuity problem, especially it often suffers from the convergence problem due to truncate modal expansions. To overcome this difficulty, an approach combining multi-mode network theory with mode-matching method has been developed. However, searching roots of complex transcendental equation makes it inconvenient for solving lossy dielectric discontinuity problems. In recent years, 3-D finite element method has been successfully used for solving discontinuity problems in guiding structures, but long computer time and large storage required limit its application.

A new approach is proposed in this paper for multi-step dielectric discontinuity in guiding structures, which combines edge-element analysis with mode-matching method and multi-mode network theory. It is demonstrated that the approach has the generality of the edge-element analysis and the simplity of the multi-mode network treatment while retaining the high accuracy of the mode-matching method. The calculations of the scattering characteristics for lossy dielectric block partially filled in the waveguide and the semiconductor sample inserted in the waveguide verify the effectiveness and suitability of the present approach.

Progress in Electromagnetics Research Symposium, PIERS 1997 ISBN 962-442-097-1

Novel Optical Nonlinear Phenomenon in Dye Polymeric Gel

Xianmin Zhang and Kangsheng chen
Department of Information and Electronic Engineering
Zhejiang University, Hangzhou 310027, China

Yoshiharu Kagami, Gu Bum Park, Jianping Gong and Yoshihito Osada
Division of Biological Sciences, Graduate School of Science
Hokkaido University, Sapporo 060, Japan

Polymer hydrogel has been receiving much attention in recent years. Polymer gel consists of an elastic cross-linked network and a fluid filling the interstitial space of the network. It is wet and soft and look like a solid material but is capcble of undergoing large deformation. It can easily change in size and shape in response to environmental change, and this is the one of the intrinsic characteristics of a polymer gel. This is in contract with most of industrial materials such as metal, ceramics and plastics that are dry and hard. The recent research has focused on the chemical, electric and machine characteristics of polymer gel, but the optical properties have not been studied so far. Here we discuss, for the first time to our knowledge, a novel reversible optical recording phenomenon occurring in dye polumer gel.

The dye polymeric gel was fabricated in Osada Laboratory, Hokkaido University, Japan. The PAMPS gel was prepared by polymerization of AMPS solution in the presence of methylene bis(acrylamide) (MBAA) as a cross-linking agent and $K_2S_2O_8$ as an initiator. The 4-nitroaniline (dye) doped gel was obtained by immersing the PAMPS gel in a large amount of dye solution for a prolonged time. After the doping, the gel was slowly dried in the air until it became glassiness. About 20% of water was contained in the space of its network.

In the experiments, a cw He-Cd laser beam at 441.6 nm illuminated the gel film and a He-Ne laser beam with the power of 2mW was sent as a probe, copropagating with the He-Cd laser beam. First, the dye gel sample was only illuminated by He-Ne laser beam, no self-phase modulation effects could be observed. Then the He-Cd laser was turned on, the sample was simultaneously illuminated by two laser beams, an induced spatial self-phase modulation pattern of the He-Ne laser beam formed on the screen through a 632.8 nm narrow-band filter. After that the He-Cd laser beam was blocked, the He-Ne laser beam also showed the spatial self-phase modulation pattern which could be maintained for more than one hour in the gel. This experimental results showed that the grating created by the He-Cd laser beam was recorded in the gel film.

In this paper, the origin of this phenomenon has been discussed. This phenomenon can be explained as the result of the dye photochromic optical recording. Because the gel is easy to change its shape caused by thermal effects, the phenomenon may be also induced by the thermation deformation of gel. So we suppose that the optical nonlinear phenomenon in dye polymer gel is mainly due to the combination effects of dye photochromic property and gel deformation caused by thermal force. The further research is been carrying on.

MULTIRESOLUTION ANALYSIS IN THE MICROWAVE COMPONENTS AND CIRCUITS*

Y.M.Song, D.G.Fang, and C.F.Wang
Department of Electronic Engineering
Nanjing University of Science and Technology
Nanjing, 210094, China

The recent developed multiresolution analysis (MRA) has demonstrated its capability to impact electromagnetics in many aspects. Among the application areas, one of the most perspective parts is the computational electromagnetics. The use of MRA has led to dramatic savings in CPU time for complicated EM simulation of microwave components and circuits.

In this study, we observe the multiresolution properties of the basis functions in weighted residue method. According to the versatility of the transform of basis functions, we give the uniform presentation to the different methods, such as diakoptic method, multigrid method, different kinds of multilevel moment method.

Wavelets have been found to be good candidates as basis functions because of its multiresolution properties. We present the possible applications of wavelet transform in solving the operator equation both for the function and for the residue through diagram which shows the relationship between different methods and gives a clue to the establishing of new method.

Based upon the above frame of MRA, we introduce some novel methods. In wavelet-based multigrid method, the scaling spaces in wavelet theory serve as the grids in the multigrid method, and the wavelet transform transfers the information between grids; in the multi-level recursive algorithm, the sparse matrix equation resulted from the wavelet expansion method is converted into a set of equations with smaller size; the adaptive wavelet-based multigrid method in constructed by making use of an adaptive technique, the transfer between the finer and coarser level in done automatically. Numerical examples including the microwave circuit parameter extraction show the validity of the proposed methods.

* This work is supported by the National Natural Science Foundation and the Doctor Degree-Conferring Unit Foundation of China.

FINITE ELEMENT ANALYSIS OF NON-RECIPROCAL MICROWAVE CIRCUITS

J.D.Wen and Y.X.Huang
Department of Electronic Engineering
Nanjing University of Science and Technology, Nanjing , 210094 ,P.R.China

Recently , the dispersion characteristics of microwave and millimeter wave integrated circuits (MIC's) involving anisotropic materials interest in the field of applications for non-reciprocal devices . Technological advances enable the integration of different materials into composite MIC structures which results in non-reciprocal transmission effects . Dielectric loaded waveguides which employ anisotropic materials play an important role as fundamental components of microwave circuits . As a result of this situation , the development of methods to solve the associated electromagnetic field problems has attracted the attention of many researchers . The finite element (FE) method , which enables to compute accurately the mode spectrum of a waveguide with arbitrary cross section , has been known to be efficient solver for this kind of waveguide problems .

In this paper , the authors give a finite element analysis of the closed waveguide filled with several kinds of ferrite materials . Considering the permeability $[\mu]$ of ferrite material is a tensor under the direct current magnetic field , the vector variational formulation of electric field is applied to get the equation of vector finite element for electric field. In order to reduce the number of unknowns of the equation of vector finite element for electric field , the finite element equation of transverse electric field component is established by using the divergence-free constraint $\nabla \cdot \varepsilon_r \bar{H}$ and Galerkin procedure to eliminate E_z component of vector finite element equation.

As a example , the ferrite phase shifter in back-ridged waveguide is analyzed by using the finite element method . In order to analyze the ferrite phase shifter in back-ridged waveguide accurately, the triangular element is employed to divide the cross section of ferrite phase shifter . The relations of the differential phase shift with frequency and geometry parameter of the ferrite phase shifter in back-ridged waveguide are simulated . The numerical simulations agree well with the experimental results .

Dyadic Green's Functions for the Cylindrical Chirowaveguide

H. T. Hui, and Edward K. N. Yung

Electronic Engineering Department

City University of Hong Kong

83 Tat Chee Avenue, Kowloon, Hong Kong

Recently, the study of interaction of electromagnetic waves with chiral media has attracted much attention. This indicates the potential applications of such materials in the areas of antennas, microwave devices and waveguides, etc. The propagation characteristics of electromagnetic waves in chiral media have been extensively investigated, e.g., by Engheta *et al*. Dyadic Green's function (DGF) technique represents the beauty of solution to electromagnetic boundary-value problems. Dyadic Green's functions in an unbounded chiral medium as well as in the presence of a chiral sphere have been formulated. Dyadic Green's functions for a multilayered chiral cylinder and a multilayered chiral sphere have also been obtained by Yin *et al* and Li *et al*, respectively. In our present effort, DGF's for a cylindrical chirowaveguide is rigorously formulated. Bohren's decomposition of the electromagnetic field is used to obtain the vector wave functions, which are only linear linear combinations of the commonly known **M**, **N** vector wave functions. We first derive the magnetic type DGF and the electric type DGF is then generated from the magnetic DGF. The advantage to do so is that the solenoidal magnetic DGF can be completely expanded by the linear combinations of the **M**, **N** vector wave functions when they combine to satisfy the boundary condition. This enable us to derive the magnetic DGF readily by following standard procedures. The expansion of the electric DGF, on the other hand, must in general include the **L** vector wave function. However, when the magnetic DGF is known, the electric DGF can be easily obtained from it through a differential operation. In addition, the singular term in the electric DGF accounting for the electric field in the source point can be shown to be established through such a manipulation on the magnetic DGF.

Progress in Electromagnetics Research Symposium, PIERS 1997 ISBN 962-442-097-1

Filter Synthesis with Genetic Algorithm and Constraints

Soeren Peik, University of Waterloo
and
Y. Leonard Chow, City University of Hong Kong

Generic algorithm is a popular optimizer since it nearly always gets to the global minimum. To reach the minimum, it mimics the biological natural selection rule of genetics, that is, the survival of the fittest.

Genetic algorithm has been used to lumped circuit parameter designs, distributed line, circuit and antenna designs with field theory but *not* with field theory with constraints. Without constraints one may get a design that has the required electrical characteristics but that is mechanically very difficult or even impossible to build. This paper gives four filter design examples based on field theory and the genetic algorithm with constraints. One of the example is briefly discussed below.

Given in Fig. 1 are two designs of a filter that has a bandpass at 29.5 GHz for transmission and a bandstop at 20 GHz and at least -70 dB to avoid interference with the receiving radiometer. The grey circuit is the initial design by the circuit theory software Touchstone™. The black circuit is the finally design with field theory and the genetic algorithm with constraints. The frequency response of the initial and final filter design is shown in the presentation. Without the constraints, the narrow portions of the stubs are around 25 microns (1 mil) which has high resistive loss, and are no possible to fabricate with the equipment in the laboratory that we have access to. With the constraints set to 50 microns, the narrow portions become around 75 microns (3 mils) which can be fabricated with good accuracy and with low loss.

This paper will demonstrate that for the same electrical response, there can be two or more different design layouts for a filter. The design is therefore is not unique. With a proper insight, the non-uniqueness can become an advantage to select a set of good constraints to get a filter that has the desired response but is lower in loss, more inexpensive to build and is more compact for circuit packaging. The insights to the above and other examples will be discussed.

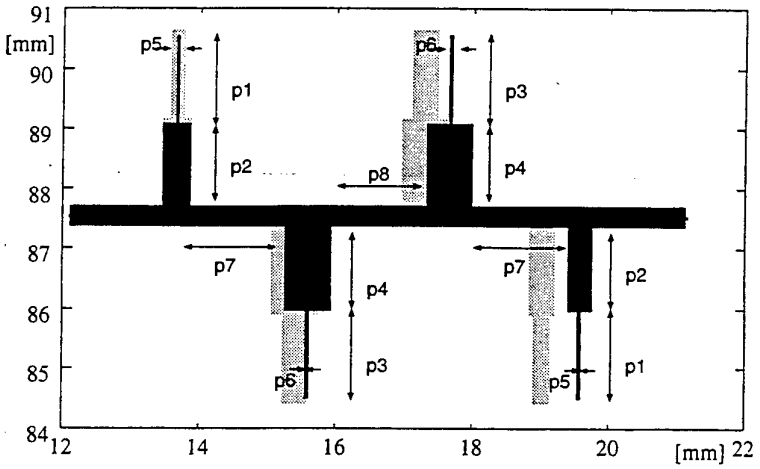


Fig. 1 Draft (grey) and the optimized (black) layouts of the KA-band filter.

Improved Slotted-Filter for Over-Mode Rectangular Waveguide

Yaokun Qin Yexin Yang

Shanghai Transmission Lines Research Institute, Shanghai, P.R. China, 200437

The power carrying of the normal rectangular waveguide at millimeter wave band is very small. There are many advantages by using the over-mode rectangular waveguide as a millimeter wave transmission line with high handling power. For example, their production cost is very low, because the waveguide blank can choose from the normal waveguide series in the microwave bands. Besides, its features are satisfactory and stable.

However, a lot of unwanted modes (or spurious modes) must excite in a closed over-mode system. Furthermore, some resonance effects can arise from these modes. The transmission properties may be deteriorated severely.

Thus, it is very important to restrain these unwanted effects by adding some mode filter or mode absorber in the over-mode system.

At the low power carrying situation, the resistive sheets filter is most in use early. Obviously, it can not use in millimeter wave transmission system with high handling power.

There are several authors developed some slotted-mode filter (SMF) or leaky wall's mode filter. That is suitable in use of the transmission line's system with high handling power, it is cut a series of slots along certain direction at the walls of the waveguide. These slots may only somewhat influence to the dominant at propagate in the waveguide; but can restrain strongly most of unwanted modes, due to their current along the walls of the waveguide is cut off.

We found that the ordinary SMF have some deficient nevertheless, it can not fully absorb the TE_{mn}/ TM_{mn} mode pairs, because they are degenerate in common over-mode rectangular waveguide, and each such mode pair can maintain balance without flowing any current. Therefore, the transverse slots can only absorb one-half full power of the degenerated TE_{mn} /TM_{mn} mode pairs. That is to say, this filter can not completely restrain the degenerated TE_{mn}/ TM_{mn} mode pairs.

We improved the design of SMF by slightly deforming the shape of the inner walls of the wavegguide. In other words, we cut some arc-shape longitudinal groove at the central parts of the transverse walls. Then the TE_{mn}/ TM_{mn} mode pairs is no longer degenerate, because of their wavelengths in it is no more equal each other, or their degeneracy is split.

For our experimental over-mode rectangular waveguide system in Ka-band, the results shows that the trapped-mode resonance effect can be restrained effectively with improved SMF, which can restrain the unwanted modes to below − 30 dB; The handling power of the system can exceed 80 kW

RESEARCHES ON MILLIMETER WAVE LOW LOSS COAXIAL CABLES

Wan Qing

Shanghai Transmission Lines Research Institute

25 Yixian Road, Shanghai 200437, P.R.China

With the rapid development of millimeter wave technology, the low loss millimeter wave coaxial cables up to 40 Ghz have found wide use in radar, communication, EW systems. The development of millimeter wave cables make the electronic equipment small and light.

Very good characteristics have been achieved as broad band, low loss, low VSWR, small size and convenient use. New method of using microporous PTFE Tape dielectric material and special technique for improving the characteristics of cable is presented. A stranded of copper wires was used as inner conductor that makes the cable ultra-soft, microporous PTFE Tape material was used as insulator. a parallel strand of silver covered round wires as outer conductor, polyester elastomer jacket was used as protection. Specifications of millimeter wave cables from both domestic and foreign manufactories are compared.

Progress in Electromagnetics Research Symposium, PIERS 1997 ISBN 962-442-097-1

THE ANALYSIS OF A CURVED COUPLER STRUCTURE USING BEAM PROPAGATION METHOD

Ayhan Altıntaş and Erdem Ofli
Bilkent University, Department of Electrical and Electronics Eng.,
Bilkent, 06533, Ankara, Turkey
e-mail : altintas@ee.bilkent.edu.tr

The analysis of guided-wave structures such as coupled waveguides is essential for the development of photonic integrated circuits. Various theoretical approaches for the analysis of single-mode couplers were investigated in the past. Almost all of these are restricted to parallel or tapered couplers. The structure considered in this study is composed of two circularly-curved single-mode waveguides. This kind of structure is also useful as a model for curved interconnections in integrated circuits as well as being a coupler. Investigation of bent losses and variation of power transfer ratios from the input waveguide to the output waveguide are important parameters in the design of such structures.

The branches of the structure are separated by a minimum distance d and are symmetric with respect to the origin [Fig.1]. We have implemented the finite difference beam propagation method (FD-BPM) based on the Crank-Nicholson discretization procedure and have applied to the analysis of propagation of optical beams in the curved structure. To confirm the accuracy, we have numerically validated the power conservation and symmetry considerations. For different values of d, the variation of power transfer ratios is calculated. Fig.2. demonstrates the variation for a specific value of d. The results are also compared with asymptotic solutions which are valid for large values of R.

The same procedure will be applied to other interconnection configurations such as sharp bends and crosses in integrated circuits.

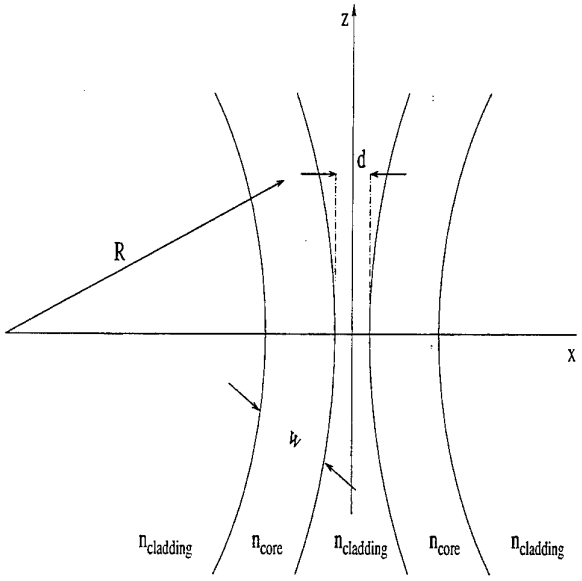


Figure 1: The schematic of the curved coupler structure. $n_{core} = 3.38$, $n_{cladding} = 3.377$, $\lambda = 1.15\mu m$,$R = 4000\mu m$, $w = 4\mu m$, $d = 0.5\mu m$.

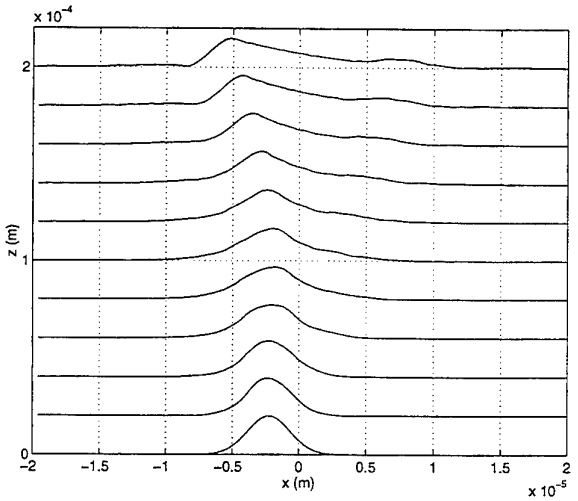


Figure 2: Gaussian Beam Propagation in the Curved Coupler Structure.

NEW APPROACH TO THE NONLINEAR BIHARMONIC MIXER CHARACTERISTICS ANALYSIS

Dr. S.V. Melichov

Tomsk State Academy of Control Systems and Electronics
40 Lenin av., Tomsk, 634050, Russia
Fax: +7 (3822) 22-32-62 E-mail: gssh@tiasur.tomsk.su

The method of linear mixer characteristics analysis and calculation when the mixer is built on the mutual mixing device is known [1]. The method is based on representation the mixer as *2 (1+2N)*-device and its description by matrix equation depending on δ-increments of currents and voltages with intermodulation frequency $\omega_{1+n} = \omega_1 + n\omega_0$, where ω_1 - signal frequency, ω_0 - heterodyne frequency, n = 0, ±1, ±2,..., ±N. Using of the method is limited by condition $V_1 << V_0$,where V_1 - signal amplitude, V_0 - heterodyne amplitude.

The linear matrix equation describing nonlinear mutual mixing de-vice (NMD) at arbitrary currents and voltages relationship with in-termodulation frequencies $\omega_{m+n} = m\omega_1 + n\omega_0$ where m=0, ±1, ±2,..., ±M; m≠n=0, n≠m=0 (1), was derived.

The performed analysis is based on representation Δ-increments of NMD currents with frequencies of (1) kind as the sum of real time increments differentials of corresponding voltages at the NMD outputs when NMD conductance's and capacitance's changes in time are described by Fourier serials. Complex amplitudes of currents and voltages are combined by term-by-term integration in time of the received differential sums' components. According to the author's opinion it was done for the first time.

While doing the analysis it was proved that NMD could be represented as *2[(1+2M)(1+2N)-1]*-device depending on intermodulation frequencies of (1) kind and descibed by linear matrix equation. The equation takes into consideration the matrix of coductances which elements are NMD complex conductance's coefficients of Fourier serials with corresponding multipliers. Magnitude and sign (plus and minus) of each multiplier is determined by the frequency of current and voltage, which are connected in the matrix equation by the particular Fourier coefficients. There are currents and voltages of both positive and negative frequencies in the matrix equation. When one takes into consideration these last frequencies it allows to analyse and calculate the NMD characteristics when $V_1 > 0.05V_0$.

The way of the received matrix equation solution by the methods known for linear networks is shown, including graphoanalitical method of conform transformation.

The analysis and calculation results were proved by experiments with secondary parameters of intermediate frequency, their dynamic range on intermodulation products with frequencies ω_{1+2}, ω_{1+3}, ω_{2+1} .

Reference:

1. D.N.Held, A.R.Kerr . Conversion loss and noise of microwave and millimeter-wave mixers. Part 1- Theory, Part 2 - Experiment//IEEE trans, vol.MTT-26, N2, 1978, p.49-61.

SESSION 7P13

Tuesday, January 7, PM 1330-1710, Lecture Theatre 13, City University of Hong Kong

RF & Microwave Circuits 3

Organizer: Masami Akaike

Chairperson: Masami Akaike, Science Univ. of Tokyo
Co-Chairperson: D Polifko, CIENA Corporation

13:30 ***Microwave Filtering Devices Using Stripline Dual-Mode Ring Resonators*** 235
Hiroyuki Yabuki, Michiaki Matsuo, Morikazu Sagawa, Mitsuo Makimoto
Matsushita Research Institute Tokyo, Inc.

13:50 ***V Band Planar Type Dielectric Resonator Filter*** 236
Yohei Ishikawa, Toshiro Hiratuka, Sadao Yamashita, Kenichi Iio
Murata Mfg. Co. Ltd.

14:10 ***100 Gigabit per Second, Long Haul Fiber Optic Communication Systems*** 237
David Polifko, Mike Fagen
CIENA Corporation

14:30 ***Leaky-Mode Emission from Planar Circuits*** 238
C-K C Tzuang, Kuo-Cheng Chen
National Chiao Tung University

14:50 ***Microwave and Millimeter-Wave Planar Filters Based on Coplanar Waveguide and Slot-line*** 239
*Y Noguchi, **K Wada, **I Awai, *J Ishii
*Kinki University
**Yamaguchi University

15:10 **Break**

15:30 ***CAD Program Using a Modified Time-Domain Method and its Applications for Design and Analysis of Nonlinear Microwave Active Circuits*** 240
*El-S A El-Badawy, **H A El-Motaafy, ***H M El-Hennawy, ****S H Ibrahim
*International Islamic University Malaysia(IIUM),
**HTI - Ramadan Tenth City,
*** Ain-Shams University,
****MTC

15:50 ***Chaos in Phase-Locked Loops*** 241
David B Levey, Paul D Smith
University of Dundee

16:10 ***Phase Noise Analysis of a 15-GHz-HFET-Oscillator*** 242
G R Olbrich
Technische Universität München

16:30 ***High Efficiency Power Amplifier with Travelling Wave Combiner and Divider*** 243
Yu-On Yam, Chi-Wai Cheung
City University of Hong Kong

16:50 ***Nanosecond Pulse Microwave Generator*** 244
V P Gubanov, A I Klimov, S D Korovin
Siberian Division of Russian Academy of Sciences

Microwave Filtering Devices Using Stripline Dual-Mode Ring Resonators

Hiroyuki YABUKI, Michiaki MATSUO, Morikazu SAGAWA, and Mitsuo MAKIMOTO

MATSUSHITA RESEARCH INSTITUTE TOKYO, INC.

3-10-1 Higashimita, Tama-ku, Kawasaki 214, JAPAN

ABSTRACT

In this presentation, we will demonstrate the fundamental properties of two orthogonal resonant modes within stripline ring resonators, as well as their application to microwave filtering devices.

Ring resonators have two principal application methods ; the first is by using two-port devices and the second four-port devices. In the two-port configuration, use of a dual-mode filter employing a coupling between two degenerate orthogonal modes was studied. Various coupling structures are proposed, and an analysis method and results of coupling coefficients obtained via simulation are presented. Based on the above discussion, an experimental dual-mode filter, developed to confirm the new structures, is demonstrated.

Four-port configurations, which make use of two resonant modes acting independently or having no coupling between them, have a wider range of applications to microwave devices. Microwave filtering circuits such as tuned amplifier with novel structure is proposed as one of the applications of four-port devices, and its excellent characteristics are demonstrated.

The experimental results obtained in this study of two and four-port devices show that dual-mode ring resonators have great potential for application to various RF and microwave filtering devices, such as filters or duplexers of mobile communication equipment.

Progress in Electromagnetics Research Symposium, PIERS 1997 ISBN 962-442-097-1

V Band Planar Type Dielectric Resonator Filter

Yohei Ishikawa, Toshiro Hiratuka, Sadao Yamashita, and Kenichi Iio

Murata Mfg. Co., Ltd.

26-10, 2-chome, Tenjin
Nagaokakyo-shi, Kyoto 617, Japan
Tel: +81 75 951 9111
Fax: +81 75 956 5724
E-mail: ishikawa@murata.co.jp

Abstract

A new planar type resonator filter, named TE_{010} mode dielectric filter, is proposed for millimeter-wave applications.

The resonator, an element of the filter, was fabricated using photolithographic technique, and high unloaded-Q of 1610 was obtained at 60 GHz. A narrow-band two-stage filter was designed and fabricated with 100 MHz pass-bandwidth at 60 GHz. NRD guide was used for input and output port. The measured filter response agreed well with the calculated values. The insertion loss within the passband was 2.6 dB and the attenuation at 1 GHz separation from the center frequency was 35 dB.

The filter has several advantages as follows.

1) Low dissipation characteristic is obtained in millimeter-wave frequency.
2) Electric and magnetic energy are concentrated in the dielectric substrate, compared to other mode resonators. Thus, mutual interferences with other devices are reduced and highly integrated circuit layout can be expected.
3) Since plural resonators can be fabricated on the same dielectric substrate for a filter, the advantage of photolithographic technology is fully utilized to realize a high precision process and a highly accurate relative position between adjacent resonators.
4) Lots of filters can be produced on a single substrate simultaneously and high productivity is readily available.
5) The filter can be easily connected to a planar circuit as MIC, MMIC or MCM.

In conclusion, TE_{010} mode dielectric filters can be applicable to future millimeter-wave communications systems.

100 Gigabit per Second, Long Haul Fiber Optic Communication Systems

David Polifko, Mike Fagen CIENA Corporation
8530 Corridor Road, Savage, Maryland 20763 USA

The joint utilization of both Time Division Multiplexing (TDM) and Wavelength Division Multiplexing (WDM) techniques has recently unlocked the bandwidth of conventional fiber. Neither methodology alone can provide sufficient capacity within a single fiber to meet the burgeoning needs of telephony and data communications network providers. TDM applications are limited by the electronics' speed as well as by optical fiber nonlinearities. WDM is usually limited by available components, especially laser diodes and optical filters. Recently, substantial progress in WDM technologies has been made. Subsequently, a combination of both TDM and WDM techniques have been used to realize the full bandwidth capacity of existing optical fibers.

The key to the success of these high capacity transmission systems are the enabling technologies in electronics and fiber optic components. Cost and performance have both substantially improved to make their widespread deployment a reality. Of these technologies, Erbium Doped Fiber Amplifiers (EDFA), In-fiber Bragg Gratings and electro-optic modulators are those which make high capacity transmission over long distances possible.

EDFAs must be designed to provide flat gain performance over a variety of input powers as well as for multiple optical carriers. They must also have a low Noise Figure to allow the successful concatenation in long-haul fiber optic links. Reliability and modularity are two additional factors which are important in field deployment. Built-in functionality and diagnostics for bias current, temperature and gain control are also necessary for remote operation.

To achieve dense optical carrier spacing, a mature filter technology must be employed which is temperature and time stable, of compact size and easily integrated into fiber optic packaging. In-fiber Bragg gratings provide such features in addition to being highly cost effective and elegant in design. Fiber Bragg gratings, being made of single mode fiber, are easily spliced into existing optical circuits, provide a high degree of in-band flatness, have extremely steep slopes and have reflectivities approaching 100%. Optical carrier spacings of 50 GHz are achievable with the use of fiber Bragg gratings.

To reduce fiber nonlinearities from impairing transmitted bit patterns, external modulation techniques are employed. These techniques maintain the narrow line width of the optical carrier and permit transmission distances of up to 600km over standard non-dispersion shifted fiber. In addition, optical carrier stabilization through the use of fiber Bragg gratings is also utilized to provide system level carrier assurance.

All of these technologies are used within a fully optimized system solution to provide up to 100 Gb/sec of data over a single optical fiber for distances up to 600km. This presentation will provide an overview of the progress of these systems. In addition system level considerations will also be addressed in relation to performance and design techniques.

Leaky-Mode Emission From Planar Circuits

Ching-Kuang C. TZUANG and Kuo-Cheng CHEN
Institute of Electrical Communication Engineering
Microelectronics and Information Systems Research Center
National Chiao Tung University
Hsinchu, Taiwan, ROC

abstract

Leaky modes' propagation in planar or quasi-planar uniform waveguides has been studied extensively in the past decade. This leads to many successful new microwave circuit designs, e.g. active integrated circuit antennas. This paper reports for the first time, to authors' best knowledge, that the leakage can occur from a two-dimensional planar circuit in the form of leaky modes, thereby the conventional understanding of the leaky mode excitation is no longer restricted in the one-dimensional line source assumed before.

One sample example of a microstrip line feed square patch antenna, of dimension 16mm by 16mm built on a 30-mil thick substrate of $\varepsilon_r = 2.55$, was fabricated, tested, and analyzed by the full-wave integral equation method. While both theoretical and experimental results for |S11| seen from the input port agreed well for greater than two octaves frequency band, no typical sharp resonant dips as normally expected in antenna had been found. Instead, these slowly varying dips of much broader bandwidth one-to-one map to the leaky modes of the first, second and third higher orders, respectively, when the patch-shaped two-dimensional circuit is elongated and viewed as a one dimensional microstrip line.

The theoretical radiation pattern shows that the directivity of the antenna is about 10 dBi at 22.5 GHz with a fan-shaped main beam and two smaller side lobes. As increasing the operating frequency, we may find an additional back lobe at the same elevation angle with the main beam. The back lobe behaves as the direct result of the reflected leaky wave from the opposite side of the antenna input port. The E-plane radiation pattern resembles that of a short one-dimensional leaky-wave antenna. The new design also retains all the frequency scan characteristics of the well-known leaky wave antenna. It scans from $\theta \doteqdot 40^0$ to $\theta \doteqdot 30^0$ when the operating frequency decreases from 23.75 GHz to 22.5 GHz. During the frequency scan toward lower frequency, the main beam width becomes broader as what a typical leaky mode does when the leaky mode's attenuation constant is getting larger.

We conclude that the radiation zones of our particular patch antenna design are predominantly leaky waves' emission. It would be not surprising that many two-dimensional planar circuits might support the leaky modes that could be applied for new microwave design.

MICROWAVE AND MILLIMETER-WAVE PLANAR FILTERS BASED ON COPLANAR WAVEGUIDE AND SLOT-LINE

Yasumasa NOGUCHI *, Kouji WADA **, Ikuo AWAI ** and Junya ISHII ***

* Department of Electronic Engineering, Kinki University, 3-4-1 Kowakae, Higashi-Osaka City, Osaka 577, Japan. TEL : +81-6-721-2332 ex.4554 / FAX : +81-6-727-2024

** Department of Electrical and Electronic Engineering, Yamaguchi University, 2557 Tokiwadai, Ube City, Yamaguchi 755, Japan. TEL : +81-836-35-9111 ex.8419 / FAX : +81-836-35-9449

*** Department of Electronic System Information Engineering, Kinki University, 930 Nishi-mitani, Uchida-cyo, Wakayama 649-64, Japan. TEL : +81-736-77-7011 ex.4206 / FAX : +81-736-77-4754

Abstract

Microwave and millimeter-wave integrated circuits (MICs) have made rapid advancement in multi-media age. Both the hybrid and monolithic MICs (HMICs and MMICs) make extensive use of what has come to be popularly known as "planar components". For development of recent mobile, satellite and microwave radio communication technologies, specifications of high frequency devices are changed following. For instance, the reduction of a circuit size for lower profile of the equipment for the above systems, compatibility to MICs and applicability to millimeter-wave systems are required. The proposals of novel devices based on "planar transmission lines" in microwave and millimeter-wave spectra are strongly expected because of the suitability to above purposes.

To date, we have investigated a number of bandpass filters (BPFs) based on planar transmission lines. Now, we present new types of BPFs using coplanar waveguides (CPWs) and slot-lines. These planar transmission-line structures are suitable for MICs, HMICs and MMICs, because the reduction of a printed circuit board size, lower profile of a component, fabricating short-circuit without via holes and mounting of elements are easily realized.

First, we propose two types of novel BPFs using a half wavelength CPW resonator with short-circuit ends. Feeding structures of conventional BPFs have been practically used the configurations such as transformers using a quarter wavelength coupled-line, a capacitor I/O coupling and a tap-feed configuration. These filters are adopted new feeding structures based on short-length combline-like coupled-lines (less than a quarter wavelength at a center frequency) and tap-feed configurations.

Secondly, we present an air-bridge-like tap-feed BPF fabricating slot-line resonators with short-ends and a BPF having dual mode resonance caused by a CPW with short-ends or a coupled slot-line. The coupled slot-line modes are existed in the CPW as an unbalanced mode. We explain in details of the duality between a CPW resonator with short-ends and a coupled slot-line resonator.

Finally, it is well known that the insertion-loss of the BPFs made of resonating sections are increased because of the decrement of the Q-factor at high frequency range. We make proposals of two types of transversal BPFs using (1) CPW directional couplers and (2) CPW branch-line couplers. As an illustration, the transmission characteristics of these transversal filters are summarized as follows : a case of (1) fabricating by 20 elements and cascaded 4 stages, a center frequency f_0 is 40 GHz, a fractional bandwidth is 28 %, an out-of-band rejection is more than -60 dB and an insertion-loss is -1.48 dB, and a case of (2) fabricating by 14 elements and multi-layered 5 stages, a center frequency f_0 is 10 GHz, a fractional bandwidth is 18 %, an out-of-band rejection is more than -40 dB and an insertion-loss is -1.74 dB.

It would be profitable to use the above-mentioned novel planar BPFs for the microwave and millimeter-wave communication systems.

CAD PROGRAM USING A MODIFIED TIME-DOMAIN METHOD AND ITS APPLICATIONS FOR DESIGN AND ANALYSIS OF NONLINEAR MICROWAVE ACTIVE CIRCUITS

El-S. A. El-Badawy[1], H. A. El-Motaafy[2], H. M. El-Hennawy[3], and S. H. Ibrahim[4]

[1] ECED, Fac. of Engineering, International Islamic University Malaysia(IIUM), 59200 KL, Malaysia, E-mail: < sayed @ eng.iiu.my>, Fax: 603-282 6957. Memmber of the Optical Society of America.
[2] EED, HTI-Ramadan Tenth City, Cairo, Egypt.
[3] EED, Fac. of Engineering, Ain-Shams University, Cairo, Egypt.
[4] EED, MTC, Cairo, Egypt.

ABSTRACT:

Microwave (MW) circuits have found wide applications in many important military and civil electronic systems. In order to design successfully a MW component or circuit, a computer aided design (CAD) approach becomes necessary. When the CAD approach is used, experimental modifications of the circuit can be replaced by a computer-based simulation and optimization of the initial design. This is important when taken into account the fact that these experimental modifications are unavoidable in the conventional design procedure. CAD procedures becomes still more essential when MW-integrated circuit techniques are used for circuit fabrication. For monolithic MW integrated circuits, many experimental iterations of a design becomes prohibitively costly.

In this paper, we describe our developed CAD program that can be used for the design, analysis, and investigation of any nonlinear microwave active circuit. Accurate models for both the active and passive microwave components and devices are incorporated in the CAD program. This program comprises essentially two main parts, a computer-aided design (CAD) procedure, and a computer-aided analysis (CAA) procedure. The CAA procedure is based on a modified time domain analysis method in which the state , output, and nonlinear equations are formulated for the microwave circuit. This results in a system of nonlinear differential, difference, and algebraic equations which are solved at each time step as the solution advances. When the change of the time response from cycle to cycle is within a prescribed acceptable tolerance the steady state is declared to be reached. Then the final microwave period is to be detected and analyzed using a discrete Fourier transform algorithm in order to determine the frequency response of the circuit together with all its other important parameters.

In order to indicate the generality of the developed program, some applications for MW circuits are presented. The analysis of a rate-race hybrid-balanced mixer, for different frequencies and voltage amplitudes of both the local oscillator and signal, is firstly performed and depicted in figures.Then the transient response, final period,and nonlinearity content of a MW amplifier designed to operate at 17 GHz are analyzed and displayed in figures. Finally the effect of the drain bias voltage on the output power, the time response and the steady state solution of a microwave oscillator is discussed and shown in figures from which one could conclude that the output frequency is not sensitive to variations in the drain bias voltage .

Chaos in Phase-Locked Loops

David B. Levey and Paul D. Smith
Department of Mathematics and Computer Science
University of Dundee
Dundee DD1 4HN
Scotland, UK.

ABSTRACT

Electronic systems provide an ideal means for investigating the theory and phenomenology of nonlinear dynamics. Many electronic circuits capable of exhibiting chaotic behaviour have already been reported but almost without exception such circuits are of a somewhat artificial nature designed for academic interest rather than for practical value. In this paper, the chaotic dynamics of a widely used *practical* circuit are investigated: the second-order phase-locked loop (PLL).

The investigation is both theoretical *and* experimental and generalises a previous study of this system. In particular, the method of Melnikov is used to *prove* the existence of chaos in the PLL. This method (one of the few purely analytical techniques currently at our disposal) measures the distance between the stable and unstable manifolds of the system as a function of the phase of the Poincaré map. It can be shown that the intersection of the stable and unstable manifolds of the Poincaré map leads to a horseshoe-type map which is the fundamental hallmark of a chaotic system.

Our analysis provides an algorithm for predicting the conditions under which an *arbitrary* given signal will drive the PLL chaotically. Previous work by Endo and Chua (IEEE Trans. Circuits and Systems, **35**, 987, (1988)) examined single frequency modulation. Specifically, we demonstrate that chaos can occur when the PLL is driven by a chirp signal (wherein the frequency changes linearly in time) using realistic circuit parameters and with a greater economy in power than previously reported by Endo and Chua.

The results are tested theoretically both by constructing the Poincaré maps and phase portaits of the system and by numerical simulation of the sytem's response to the injected signal. Specific predictions to be tested experimentally will be identified and discussed. Some conclusions can be drawn about the susceptibility to electromagnetic interference (EMI) of communications and other systems incorporating PLL's.

Progress in Electromagnetics Research Symposium, PIERS 1997 ISBN 962-442-097-1

Phase Noise Analysis of a 15-GHz-HFET-Oscillator

G.R. Olbrich

Technische Universitaet Muenchen, Lehrstuhl fuer Hochfrequenztechnik
Arcisstraße 21, 80290 Muenchen, Germany
Phone: +49 (89) 2105 8390, Fax: +49 (89) 2105 3365
e-mail: olbrich@hft.e-technik.tu-muenchen.de

In this paper the noise behavior of a HFET oscillator is analyzed theoretically and experimentally. We present a physical based large signal HFET model, which describes the signal and noise properties of the device in the frequency range from 1 Hz to 40 GHz. Calculations of oscillator output power and phase noise are compared with results of measurements.

The model is based on S-parameter measurements up to 40 GHz. The linear and not bias dependent extrinsic elements in the model (L_g, L_d, L_s and R_g, R_d, R_s) are extracted from small signal S-parameter measurements using hot and cold modeling techniques. To determine the nonlinear elements of the inner transistor (R_{gs}, R_{gd}, C_{gs}, C_{gd}, C_{ds}, G_m, G_{ds}, τ) we apply a deembedding procedure to the measured small signal S-parameter data of 200 different bias points. This has to be done for all interesting frequencies. The nonlinear diode admittances G_{gs} and G_{gd} are given by their I/V-characteristics whereas the parameters have been determined by DC measurements. To model the channel current I_{ds} we use the DC I/V-characteristic and the dynamic output I/V characteristic we get by an integration of the differential small signal RF admittances G_m and G_{ds}. So dispersion effects of G_{ds} are included.
Low frequency noise sources for the $f^{-\alpha}$-noise and the g-r noise are implemented as noise current sources $In_{1/f}$ and In_{gr} in the channel of the HEMT resulting from low frequency noise measurements of the spectral power densities at about 100 different bias points in the frequency range from 1 Hz to 10 MHz.
Noise parameter (F_{min}, Y_{opt}, R_N) measurements in the frequency range from 2 GHz to 18 GHz allow the characterisation of three intrinsic thermal noise sources. For this evaluation we use deembedding procedures based on the correlation matrix representation.

For the phase noise calculation we use a simulation method in time domain. The oscillator circuit is approximated by a lumped element circuit model. The Langevin equations - a set of ordinary first order nonlinear differential equations - describe the deterministic and stochastic behavior of the oscillator. A perturbation formulation allows the consideration of the noise contributions. As a result of the calculation we we get the phase noise spectrum $L(f_m)$ of the oscillator.

The result of the investigations demonstrates in a clear manner the influence of the different noise sources on the phase noise behavior of the oscillator. Calculated data agree with measurement results within the measurement accuracy of ±2 dB.

High Efficiency Power Amplifier with Travelling Wave Combiner and Divider

Mr. Chi-Wai Cheung , *Dr. Yu-On Yam

*Department of Electronic Engineering, City University of Hong Kong,
83 Tat Chee Avenue, Kowloon, Hong Kong.
Fax: (852)2788-7791
E-mail: "EE23AYOY@CITYU.EDU.HK"

A novel approach to achieve a high output power and high efficiency amplifier was explored. It consists of four identical Class E Power Amplifiers and a Travelling Wave power Divider/Combiner (TWPD/C). The design and implementation of 1-4-1 TVVPD/C by using lumped LC π-networks was introduced. For the application around the upper VHF and the lower UHF bands, microstrip line is not suitable as the physical quarter-wave length is too long. Analytical method with finite loaded Q of the series tuned circuit was applied on the design of the class E power amplifier. A 45O MHz and 5W output class E power amplifier was designedand constructed. The experimental results showed that it can provide a high collector efficiency viz. 89.4%. A higher output power and high efficiency amplifier with 14.96 watts output, 89.5% collector efficiency and operated at 450 MHz was then built. It is a combination of the class E power amplifiers and the TWPD/C.

NANOSECOND PULSE MICROWAVE GENERATOR

V.P. Gubanov, A.I. Klimov, and S.D. Korovin

High Current Electronics Institute,
Siberian Division of Russian Academy of Sciences

Nanosecond pulse duration sources of coherent microwave radiation are necessary for new applications such as calibration of high power microwave detectors and checking of nanosecond radar receivers, antennas and waveguides. Last time, there is an interest in transmission of nanosecond microwave pulses to investigate their propagation in open space and near a surface. Thus, the sources may be used as transmitters in nanosecond radar systems.

To meet these needs we developed a three-centimeter Gunn generator. The scheme of the generator includes a forming line, which is charged by a pulsed charging circuits, and the S-diode trigger to apply the forming line voltage to the 3A 726 Gunn diode. The latter is placed inside a standard 23×10 mm rectangular waveguide resonant cavity. The generator is capable of producing of up to 30 W power amplitude, 7 ns halfwidth microwave pulses. The waveform of pulses generated is like a trapezium with 1-2 ns slopes. The generator frequency may be tuned from 9.7 to 10.3 Hz by moving the resonator plunger. External triggering of the generator allows to tune the repetition rate of the pulses in the range of up to 1 kHz. The waveform of pulses generated is in good accordance with the pulse spectrum measured. The waveform instability (amplitude, halfwidth) doesn't exceed 1%.

Preliminary experiment was carried out to study the possibility of using this Gunn generator as a transmitter in radar system. Experimental setup included a 36 dB, parabolic antenna and a receiver whose gain coefficient and bandwidth are 90 dB and 300 MHz, respectively. It was found that this system is capable of locating natural subjects about 1 m^2 size in the range of 3 km.

The Gunn generator described was used to calibrate nanosecond pulsed power microwave detectors at up to 30 W power level as well as to check parameters of nanosecond radar antennas and receivers.

SESSION 7A12

Tuesday, January 7, AM 850-1230, Lecture Theatre 12, City University of Hong Kong

Microwave-to-Optical Polarimetry : Basic Concepts

Organizers: Wolfgang M Boerner, Ernst Lüneburg

Chairperson: Karl-Jörg Langenberg, University of Kassel
Co-Chairperson: Ernst Lüneburg, Institute for Radio Frequency Technology

8:50 ***Homogeneous and Inhomogeneous Sinclair Matrices*** 246
*E Lüneburg, **W-M Boerner
*German Aerospace Research Establishment,
**University of Illinois at Chicago

9:10 ***An Entropy Based Unsupervized Classification Scheme for Full Polarimetric Sar Data*** 247
*E Pottier, **S R Cloude
*IRESTE, **Applied Electromagnetics Ltd.

9:30 ***Detection of the Radar-Tracking Targets on Coefficients of Polarizable Anisotropy*** 248
A I Logvin, V G Vorobiev, A I Kozlov
Moscow State Technical University of Civil Aviation

9:50 ***Some Techniques for Obtaining a Stable Description of Backscattering Matrices' Polarization Invariants of Complex Radar Objects*** 249
V N Tatarinov, S V Tatarinov, V I Karnychev
Tomsk State Academy of Control Systems and Radioelectronics

10:10 ***Polarization Invariants of Plane Waves' Space Spectrum Under Scattering on Complex Radar Objects*** 250
V N Tatarinov
Tomsk State Academy of Control Systems and Radioelectronics

10:30 **Break**

10:50 ***On the Importance of Polarimetry in Modern Radar*** 251
*E Krogager, **W M Boerner
*Danish Defence Research Establishment, **Uni. of Illinois at Chicago

11:10 ***Studies of Interferometric Penetration into Vegetation Canopies Using Multifrequency Interferometry Data at JPL*** 252
Scott Hensley, Ernesto Rodriguez, Bob Truehafft, Jakob Van Zyl, Paul Rosen, Charles Werner, Søren Madsen, Elaine Chapin
Jet Propulsion Laboratory

11:30 ***Statistical Polarimetry for HF Skywave Radar*** 253
*Stuart J Anderson, **W M Boerner
*Defence Sci. and Tech. Organisaton, **Uni. of Illinois at Chicago

11:50 ***Polarization Structure of Antennas Near-Field*** 254
V A Sarytchev,G B Katchalova
Holding Company "Leninez"

12:10 ***Markov's Filtration of Radar's Polarized Signals*** 255
E A Loutin
The Moscow State Technical University of Civil Aviation

HOMOGENEOUS AND INHOMOGENEOUS SINCLAIR MATRICES

E. Lüneburg[1] and W.-M. Boerner[2]

[1]Institute for Radio Frequency Technology
German Aerospace Research Establishment (DLR)
D-82234 Oberpfaffenhofen, Germany;
Tübitak–Marmara Research Center
Department of Basic Sciences
41470 Gebze-Kocaeli, Turkey

[2]University of Illinois at Chicago
UIC-EECS Communications, Sensing and Navigation Laboratory
840 W. Taylor Str.; SEL 4210
Chicago, IL 60607-7018

The classification of Jones matrices and corresponding optical polarizations elements due to Shurcliff [3] is based on the relative orientation and the number of eigenvectors (eigenpolarizations) of the complex 2-by-2 Jones matrix $J \in M_2$. A Jones matrix is said to be homogeneous if the eigenvectors are orthogonal, otherwise it is said to be inhomogeneous. It has recently proposed by Lu and Chipman [2] to measure the degree of inhomogeneity by the absolute value of the scalar or innner product of the normalized eigenvectors:

$$\eta = |\hat{E}_1^{\dagger}\hat{E}_2|, \quad 0 \leq \eta \leq 1 \quad \text{(inhomogeneity parameter)} \tag{1}$$

where $\hat{E}_i$ $(i = 1, 2)$ are the normalized eigenvectors of the Jones matrix J. For a homogeneous Jones matrix $\eta = 0$ by definition since the eigenvectors are orthogonal. The class of homogeneous Jones matrices coincides with the class of normal matrices mathematically defined by $J^{\dagger}J = JJ^{\dagger}$. This classification relies on the existence of two eigenvectors and had to be supplemented for the case when the matrix is defective and there exists only one eigenvector/generalized eigenvector Jordain pair [2].

This classification scheme cannot be applied directly to the case of general Sinclair matrices S for the radar backscatter case. The reason is the fundamental fact that in this case the scattering properties of the radar target are determined by the coneigenvectors rather than by ordinary eigenvectors of the matrix S: $Sx = \lambda x^*$ (λ coneigenvalue, x coneigenvector), [1]. Homogeneous Sinclair matrices would be charcterized not as normal but as symmetric matrices $S = S^T$ since in this case only there exist two orthogonal coneigenvectors. For nonsymmetrical or inhomogeneous Sinclair matrices, however, there either exist two independent coneigenvectors, one or none. The matrix S is contriangularizable and, hence, has one coneigenvector if and only if all the eigenvalues of the matrix JJ^* are real and nonnegative. For instance the matrix $J = \begin{pmatrix} 0 & -1 \\ 1 & 0 \end{pmatrix}$ with $SS^* = -2I$ has no coneigenvalues and coneigenvectors at all.

The paper presents some analytical details of the application of Eq. (1) to the backscatter coneigenvector case and possible extensions. Special emphasis is paid to the comparison of backscatter and optical polarimetry.

References

[1] Lüneburg, E (1995) *Principles of radar polarimetry,* IEICE Transactions on Electronics, Special Issue on Electromagnetic Theory, **E78-C**, No. 10, 1339–1345

[2] Shih-Yau Lu and Russel A. Chipman, *Homogeneous and inhomogeneous Jones matrices,* J. Opt. Soc.Am. A **11**, 766–773, 1994

[3] W. A. Shurcliff, *Polarized Light,* Harvard Univ. Press, Cambridge, Mass., 1962

AN ENTROPY BASED UNSUPERVIZED CLASSIFICATION SCHEME FOR FULL POLARIMETRIC SAR DATA.

E. POTTIER (*), S.R. CLOUDE (**)

(*) Laboratoire SEI EP CNRS 63, IRESTE
La Chantrerie - CP 3003, 44087 Nantes Cedex 03, France.
epottier@ireste.fr

(**) Applied Electromagnetics Ltd.
5a Alexandra Place, St Andrews, Scotland, KY16 9XD.
scloude@fges.demon.co.uk

ABSTRACT

Classification of Earth terrain components within a full polarimetric SAR image is one of the many important applications of Radar Polarimetry. In this paper we consider the use of multi-polarisation data for quantitative remote sensing applications and the role polarimetric observables play in relating the two key elements of measurement and physical modelling in polarimetric systems.

We propose a method for extracting average parameters from experimental data using a smoothing algorithm based on second order statistics. This method does not rely on the assumption of a particular underlying statistical distribution and so is free of the physical constraints imposed by such multivariate models. For example, the multivariate Gaussian distribution is popular because of the ease of analytical development of moments and marginal distributions and is physically supported on the basis of the central limit theorem, which dictates that within each image cell we have a large number of polarimetric scattering elements, with no one element being a dominant scatterer.

There have recently been developed several algorithms for the classification of land features based on their polarimetric microwave signatures. These methods exploit observed similarities and correlations in feature vectors derived mainly from complete coherent scattering matrix data. Most such techniques are supervised, in the sense that the feature vector is derived from measurements over known terrain classes. Unknown terrain is then compared with the training set and a statistical decision made as to class membership. Several unsupervised techniques have also been developed. They tend to be more physically based and have the advantage that their performance is not data specific, as often arises with supervised methods. One novel group of classification techniques which has recently received attention, is a set of methods based on the use of unsupervized neural networks.

As classifiers, unsupervized neural networks have shown greater flexibility than conventional algorithms, adapting themselves more easily to distributions possessing a high degree of complexity, and providing the most relevant clustering feature vectors, without any a priori assumption on scattering properties or on specific statistical distributions.

The linear feature vector used during the classification procedure is defined from a new scheme for parameterising polarimetric scattering problems, which has application in the quantitative analysis of polarimetric SAR data. The method relies on an eigenvalue analysis of the coherency matrix and employs a 3-level Bernoulli statistical model to generate estimates of the average target scattering matrix parameters from the data. This alternative statistical model sets out with the assumption that there is always a dominant 'average' scattering mechanism in each cell and then undertakes the task of finding the parameters of this average component. The scattering entropy is a key parameter in determining the randomness in this model and is seen as a fundamental parameter in assessing the importance of polarimetry in remote sensing problems.

We show application of the method to some important classical random media scattering problems and apply it to POLSAR data from the NASA/JPL AIRSAR data base.

DETECTION OF THE RADAR-TRACKING TARGETS ON COEFFICIENTS OF POLARIZABLE ANISOTROPY.

Prof. Dr.Sc. Logvin A.I., Prof. Dr.Sc. Vorobiev V.G., Prof. Dr.Sc. Kozlov A.I.
Moscow State Technical University of Civil Aviation. Russia.

The coefficient of polarizable anisotropy of the radar-tracking target can be used for the decision of problems of detection of these targets on a background of interfering reflections from laying surfaces. For the decision of this problem it is necessary to know the statistical characteristics of a coefficient of polarizable anisotropy. In work appropriate density of distribution of a coefficient of polarizable anisotropy is received, the analysis of which has shown, that this density essentially depends on a correlation coefficient of orthogonal components and degree of asymmetry of a background. Thus the mathematical expectation of a polarizable anisotropy coefficient does not practically depend on a correlation coefficient of R at small significances of a asymmetry coefficient of a background ($r < 0,25$). The specified dependence begins self to display at the significances $r>0,5$.

Leaning on knowledge of probabilities distribution density of polarizable anisotropy coefficient, in work calculate probabilities of correct detection for various significances of parameters r and R for two cases of construction of radar-tracking station: single-channel and two-channel on polarization.

For radar-tracking station single-channel on polarization the probability of correct detection of the target is determined only by the relation a signal/background on a input of a radar-tracking receiver. For radar-tracking station two-channel on polarization the relation signal/background essentially depends on the polarizable characteristics of the target and background, i.e. on their polarizable anisotropy coefficients. And, as it follows from received results, method of detection of the targets on is the most effective to a polarizable anisotropy coefficient at the small relations a signal/background. If at a background of characteristic $r=1$, $R=0$, more expediently to use classical method single-channel on polarization of detection of the target on a background of a earthly surface.

Some Techniques for Obtaining a Stable Description of Backscattering Matrices' Polarization Invariants of Complex Radar Objects

V.N.Tatarinov, S.V.Tatarinov, V.I.Karnychev

Tomsk State Academy of Control Systems and Radioelectronics
40, Lenin Ave., Tomsk, 634050, Russia
Tel.& Fax: + 7 (3822) 232 184 E-mail: vnt@tiasur.tomsk.su

With investigating of radar characteristics of real objects and distributed surfaces by use of X-band polarization radars, temporal dependences of backscattering matrices' polarization invariants have extremely complicated and, in some cases, non-stationary character. This fact confirmed, specifically, by the Radioelectronic Systems Laboratory (TACSR, Tomsk) employees in series of experimental investigations can be connected with availability of radiated radar signal's space coherence. The space coherence leads to appearance of speckle-effect both in diffraction picture of intensities of the backscattering field's orthogonal components and in angular dependence of polarization invariants of the backscattering matrix (BM). Existence of distributed objects classes having phase range considerably exceeding 360 degrees results in simultaneous availability of the speckle-effect both in diffraction picture of full intensity and in the angular dependence of the BM's polarization invariants.

The number of experiments carried out by the authors has allowed to establish a "transitive" class of complex artificial objects, which phase range of elementary scatterers is unsufficient one that the speckle-effect develops in the diffraction picture of intensity. However, the angular dependence of the BM's polarization invariants, for example, module of complex degree of polarization anisotropy (CDPA), for such objects is developed in a kind of a complex picture of the speckle.

Considering that the statistical characteristics of the CDPA's speckle are determined by probabilistic behaviour of elementary scatterers set, which can be unknown apriori, it is necessary to investigate possible ways for obtaining of stable description of the CDPA's angular dependences for complex radar objects case.

In the given paper the following two ways of such description are considered: the first one assumes a regular space filtering of speckle; the second way of the stable characteristics obtaining is based on use of frequency averaging. In the first way, a range of filtering window or number of the CDPA samples with the speckle-effect to be averaged depends on possible quantity of elementary scatterers. In the second way, an averaging function form is chosen taking account of frequency averaging operation. In this case, one can prove that the characteristic function can be factorized in a product of one-dimensional characteristic functions at multi-frequency sensing. It permits to ensure a statistical independence of the parameters by the frequency averaging. The main theoretical statements of the paper are illustrated by experimental measurements data obtained with using of single-frequency and multi-frequency X-band radars.

Progress in Electromagnetics Research Symposium, PIERS 1997 ISBN 962-442-097-1

Polarization Invariants of Plane Waves' Space Spectrum under Scattering on Complex Radar Objects

V.N.Tatarinov

Tomsk State Academy of Control Systems and Radioelectronics
40, Lenin Ave., Tomsk, 634050, Russia
Tel.& Fax: + 7 (3822) 232 184 E-mail: vnt@tiasur.tomsk.su

In the nearest future, the concept of the scattering matrix of radar objects being a cornerstone of the modern radar polarimetry may transform into the factor which will constrain development of polarization radars' theory and techniques. It follows from the fact that this concept is based on representation of a radar object as a "point" object. In this case, the backscattering matrix itself is treated as a characteristic corresponding to isolated plane electromagnetic (EM) wave.

However, the basis of backscattering fields formation for extended and complex radar objects case is the phenomenon of diffraction. Therefore, these fields can be characterized by a space spectrum of plane waves. In this case it is impossible to determine a direct relation between elements of the operator, which is considered to be the backscattering matrix (BM) referred to an isolated plane wave, and parameters of a radar object, since these elements are Fourier coefficients (matrix space spectral density) of distribution of principal and cross-components of EM fields excited on the object by incident wave. Unfortunately, polarization parameters of the EM field have not wave properties. It does not permit directly use the diffraction methods for evaluation of these parameters.

Thus, there is an urgent necessity to carry out an analysis, which would allow to expand the area of application of the BM's theory on case of space spectrum of plane waves, to establish relation between the spectrum's polarization parameters and fields excited on the object by sounding radar signals. Naturally, that a "payment" for more adequate representation of radar objects will be a loss of simplicity provided by the BM's mathematical tools.

Using geometrical and optical methods and also wave methods of diffraction, the author investigates space spectra of plane waves scattered by complex objects and these spectra's angular distributions of the polarization invariants corresponding to the objects. As a result of the analysis, it is shown that the main integral transformations of the diffraction theory, Fourier-optics and Hilbert-optics can be effectively applied to the radar polarimetry problems.

In particular, it is proven that the concept of phase objects' contrasting, which is used in optics through the space Hilbert-transformation, permits to explain a high efficiency of the radar polarimetry methods in the problem of small-sized objects detection against distributed background.

Results of the theoretical analysis are illustrated by experimental measurements data of polarization invariants of plane waves' space spectrum for case of radar sensing of artificial complex objects.

Progress in Electromagnetics Research Symposium, PIERS 1997 ISBN 962-442-097-1

ON THE IMPORTANCE OF POLARIMETRY IN MODERN RADAR

E. Krogager
Danish Defence Research Establishment
Ryvangs Allé 1, DK-2100 Copenhagen, Denmark
T: +45 39272233 F: +45 31203315 E-mail: ek@ddre.dk

W.-M. Boerner
University of Illinois at Chicago, UIC-EECS/CSL, M/C 154
840 W. Taylor St., SEL-4210, Chicago, Illinois 60607-7018, USA
T: +1 (312) 996-5480 F: +1 (312) 996-5480 E-mail: wolfgang.m.boerner@uic.edu

This paper is dealing with one of the special topics which have become important in modern radar, namely, polarimetric imaging techniques. Although the fundamental capabilities of polarimetric radar, that is, radar utilizing the polarization of the transmitted and received waves, have been known since the early days of radar back in the fifties, it is only in recent years that such techniques have actually been implemented for practical utilization. There are a variety of reasons for that, some major reasons being the cost and complexity of polarimetric radars, but also an apparent lack of appreciation of what polarization can actually be used for. Not least in operational systems, information carried with the polarization of electromagnetic waves is only utilized to a very limited extent.

Our goal with this paper is to try to point to the necessity of utilizing polarimetric information in order to optimize the use of radar for military as well as civilian applications. The outline of the paper is as follows. First, the basics of traditional single polarization radar will be briefly recalled, and a few examples of single polarization imagery will be shown. Then some basic polarization phenomenology and terminology, as well as the radar target scattering matrix, will be explained. Some significant advances of polarimetric radar over single polarization radar will be pointed out by considering the response, i.e., the scattering matrix, for a set of significantly different elementary scatterers.

The handling of polarimetric radar data requires special techniques. Examples of such techniques will be explained in some detail, before we will turn to demonstrating the actual application of the techniques with simulated as well as measured data.

Studies of Interferometric Penetration into Vegetation Canopies using Multifrequency Interferometry Data at JPL

by

by Scott Hensley, Ernesto Rodriguez, Bob Truehafft, Jakob Van Zyl, Paul Rosen, Charles Werner, Søren Madsen and Elaine Chapin

Jet Propulsion Laboratory
Radar Science and Engineering Section
4800 Oak Grove Dr.
Pasadena, California 91109
Phone: (818)-354-3322, email: sh@kaitak.jpl.nasa.gov

Radar interferometric observations both from space borne and airborne platforms have been used to generate accurate topographic maps, measure millimeter level displacements from earthquakes and volcanoes, and for making land cover classification and land cover change maps. Interferometric observations have two basic measurements, interferometric phase, which depends upon the path difference between the two antennas and the correlation. One of the key questions concerning interferometric observations of vegetated regions is where in the canopy does the interferometric phase measure the height. TOPSAR simultaneous dual C and L-band interferometer and repeat pass AIRSAR P-band and P-3 UHF data have been studied to determine the amount of differential penetration into various types of vegetation. Our results show that the L, P and UHF frequency interferometric data can penetrate 10-20m deeper into the canopy than C-band measurements. By operating the TOPSAR instrument in the ping-pong mode (alternately transmitting and receiving on each antenna) dual baseline multifrequecy C and L-band data have been obtained and used for baseline decorrelation and vegetation parameter extraction. Results for two methods of extracting tree heights and other vegetation parameters based upon the amount of volumetric decorrelation will also be presented.

STATISTICAL POLARIMETRY FOR HF SKYWAVE RADAR

Stuart J. Anderson[1] and Wolfgang-M. Boerner[2]

(1) HF Radar Division
Defence Science and Technology Organisation
PO Box 1500
Salisbury SA 5180
AUSTRALIA
T/F : [61] (8) 259 6416 / [61] (8) 259 6673

(2) University of Illinois at Chicago
UIC-EECS/CSN, m/c 154
900 W.Taylor St., SELW-4210
Chicago ILL. 60062-3541
USA
T&F : [1] (312) 996 5480

Polarimetric analysis of echoes received by conventional line-of-sight radars has greatly enhanced the reliability and echo interpretability of target detection and classification systems; more recently, these benefits have been extended to synthetic aperture radar. A simplifying factor in many cases is that the intervening medium has no effect on the wave polarisation and hence the propagation state of the wave incident upon the target is the same as that of the transmitted wave, with a corresponding invariance along the target-receiver path.

In the case of HF skywave ('over-the-horizon') radars, the intervening ionosphere transforms the signal polarization in a stochastic time-varying manner, on both transmitter-target and target-receiver paths, so that is is not evident that useful polarimetric information about the target can be obtained. This paper examines the issue of polarimetric analysis after two-way propagation through a medium which imparts stochastic polarisation transformations belonging to the class of transformations characteristic of oblique skywave propagation. The problem is formulated in the context of a modern HF skywave radar system and the results demonstrate that is is indeed possible to make statistical inferences about certain properties of the target scattering matrix.

POLARIZATION STRUCTURE OF ANTENNAS NEAR-FIELD.

Sarytchev V.A.,Katchalova G.B.

"Holding Company "Leninez",
212, Moskovscy Pr., St-Petersburg,
196066, Russia.

At the present time different methods of the analysis of antennas near-field are developed for the scalar case and monochromatic signals. The vector case, associated with the analysis of polarization structure causes serious difficulties. These difficulties are caused by greater numbers of field components and unmatched temporary dependence of these components, that complicates the use of polarization structure . The polarization bases are proposed which are invariant to temporal structure, i.e. appropriated for analysis of any antenna. The main relation for such bases with references to various antennas and commonly used signals are presented. Besides, the result of calculations for arrays and reflector antennas , as usual, as monopulse are given. The specific role of the signal regularization procedure in the analysis of the antenna near-field and corresponding relations are discussed.

Progress in Electromagnetics Research Symposium, PIERS 1997 ISBN 962-442-097-1

MARKOV'S FILTRATION OF RADAR'S POLARIZED SIGNALS.

Dr. prof. LOUTIN E.A.
THE MOSCOW STATE TECHNICAL UNIVERSITY OF CIVIL AVIATION, RUSSIA
20 Kronshtadskij blvd., Moscow, 125838, Russia.
Phone: (095) 457-1207, Fax: (095) 457-1202.

ABSTRACT

In the present paper the synthesis of radiolocation system transmitting an unspecified elliptical polarized signal has been carriedout. It is carried out by the methods of nonlinear optimal Marcov's filtration. In addition,it is assumed that the receiving signal is partially polarized. The random character of polirized ellipse parameters is caused by the necessity for using two-component vector of state. On the assumption of covariation matrix diagonality,ellipsis differentional stochastic equations of polarization ellipsis parameters have been solved. The analysis of cumulatives of aposteriori distributions determine necessary signal-noise correlation for determining of error in parameters of polarization ellipsis. We also found the influence of stray intensity of polirizes parameters on the filtration process. The equation of optimal filtration made it possible to synthesi-
ze the optimal receiver system. In fuct the system consists of two tracking systems leading in the difference between the operating parameter value and its parameter estimation to the zero value that actually means the transformation of polarized basis.

The case of polarization ellipsis parameters correlation has been considered separately. In thus case, the synthesized structural scheme of the radar receiver has additional crossing connections. Using the method of time averaging the system of equations for cumulatives aposteriory distribution has been obtained.

Its solution by numerical methods made it possible to determine now radiolocation parameters needed in this case.

It is shown that the change of polarising parameters has substantial influence, on the filtration error which is redused when the radar potential increases. The comparison of filtration errors showed that correlation of polarization parameters increases tracking accuracy.

SESSION 7P12

Tuesday, January 7, PM 1330-1630, Lecture Theatre 12, City University of Hong Kong

Microwave-to-Optical Polarimetry : Applied Concepts

Organizers: Wolfgang M Boerner, Ernst Lüneburg

Chairperson: Viktor N Tatarinov, Tomsk State Academy of Control Systems and Radioelectronic
Co-Chairperson: W M Boerner, University of Illinois at Chicago

13:30 ***Application of the Electromagnetic Vector Fourier Diffraction Slice Theorem to Concrete Probing with Radar*** 257
K J Langenberg, M Brandfass, A Pitsch, K Mayer
University of Kassel

13:50 ***Simulation of SAR Imaging of Ship Turbulent Wake*** 258
K Oumansour, Y Wang, J Saillard
Laboratoire SEI - IRESTE

14:10 ***High Resolution Method with Polarization Diversity*** 259
Y Wang, J Saillard
IRESTE-Laboratory S.E.I.

14:30 ***Polarizable Measurements on Determination of the Characteristics of Detection of the Radar-Tracking Targets on a Background of Forestry Files*** 260
V G Vorobiev, A I Kozlov, A I Logvin
Moscow State Technical University of Civil Aviation

14:50 ***Space Spectra of Polarization Parameters of Electromagnetic Waves on Beyond-the-Horizon Propagation Paths*** 261
V N Tatarinov, G S Sharygin
Tomsk State Academy of Control Systems and Radioelectronic

15:10 **Break**

15:30 ***The Statistical Characteristics of Scattering Matrix Elements of Little Dimensions Targets on a Background of a Laying Surface*** 262
A I Kozlov, A I Logvin, V G Vorobiev
Moscow State Technical University of Civil Aviation

15:50 ***Radar Target Indentification Without Polarimetry?*** 263
*Ernst Krogager, **William A Holm
*Danish Defence Research Establishment,
**Georgia Tech. Research Institute

16:10 ***Subterrain Object Mapping Using Polarimetric Scattered Fields*** 264
P Luneau, G Y Delisle, V Sampath
INRS-Telecommunications

Application of the Electromagnetic Vector Fourier Diffraction Slice Theorem to Concrete Probing with Radar

K.J. Langenberg M. Brandfass A. Pitsch K. Mayer
Dept. Electrical Engineering
University of Kassel
34109 Kassel, Germany

An important problem in civil engineering comprises the location of metallic tendon ducts in concrete. Of course, conventional ground probing radar techniques can be applied, but they require remote sensing of a metallic object below metallic rebars which shade the penetrating electromagnetic waves.

Suitable means to assess the capabilities of a concrete probing imaging system are experiments and/or simulations. In this contribution we will supply results in both fields applying standard diffraction tomographic inverse scattering algorithms to experimental data, and a new polarimetric vector inversion algorithm to simulated data. This new algorithm is an extension of the Fourier Diffraction Slice Theorem to electromagnetic vector waves thus including polarization effects.

In Germany, the Bundesanstalt für Materialforschung und -prüfung has made experiments with a commercial ground probing radar in a monostatic operational mode on several concrete test pieces containing aluminum tendon ducts partially shaded by steel rebars and partially not. We have processed these time domain data with the scalar inverse scattering scheme, which is well-known as the Fourier Diffraction Slice Theorem in the frequency diversity version. As a result, a proper image of the duct could only be obtained without the rebars. Modifying the imaging algorithm slightly in order to include the dipole moment of the operating butterfly antenna we could increase the lateral resolution somehow, but beneath the steel reinforcement, the duct was invisible.

Having developed a linearized vector inverse scattering algorithm based on the dyadic backpropagation of electromagnetic scattering data quite recently, which proved considerably superior to scalar imaging, we evaluated a new version of this scheme which does no longer utilize a nearfield-farfield transform but operates on the nearfield data immediately. This algorithm can be considered to be the polarimetric vector version of the Fourier Diffraction Slice Theorem. Applying appropriate transition conditions we can even account for the surface of the concrete: In a first step we backpropagate the data to that surface, and then we apply the Theorem.

The polarimetric data necessary for the vector Fourier Diffraction Slice Theorem were obtained using the electromagnetic CAD program MAFIA. Scattering data were computed for a variety of different geometries with and without rebars and accounting for the concrete surface or not. Two orthogonal polarizations of the incident plane wave were applied. It turns out, that concise and proper radar images of the duct below the rebars can be obtained together with the rebars when the permittivity of the concrete is set to free space. Once the surface of the specimen is properly accounted for, this is still true but the lateral resolution is considerably reduced.

SIMULATION OF SAR IMAGING OF SHIP TURBULENT WAKE

K. OUMANSOUR, Y. WANG, J. SAILLARD
Laboratoire SEI- IRESTE
La Chantrerie - CP 3003, 44087 Nantes Cedex 03
France
phone:40683074, fax:40683233
e-mail: koumanso@ireste.fr

Ship wake patterns exhibiting a wide diversity of appearance have been noted on synthetic aperture radar (SAR). One particular type of feature, a bright narrow V wake extending aft of the ship, with a small angle of few degrees, noted firstly on the Seasat images, aroused considerable interest. Since then, attention has been focused on ship wake radar signatures as a means of detecting and classifying ships.

The appearance of a ship wake pattern is extremely variable and seems to fall into four categories: The Kelvin wake, the turbulent wake, wake from internal waves, and narrow V wake. In this study, we deal only with the turbulent wake, which is the most frequently observed ship wake, with a dark narrow line along the ship track. This line is sometimes accompanied by a bright line of one or both edges of the dark area. The surface current is assumed to be consisting of a pair of lateral vortex induced by the ship hull. The radar Bragg scattering is assumed to be the dominant mechanism in the range of incidence from 20 to 60°. So the interaction of the induced surface current with the Bragg train of waves is formalized by the kinematical and dynamical conservation equations. We simulate the behaviour of the spectral perturbations of Bragg waves function of ship parameters and the environmental conditions. The contrast of the maximum of positive and negative backscattering deviation with respect to the ambient backscattering level is evaluated function of the SAR parameters (frequency, incidence, direction of observation with respect to the ship track) for two ships. We also perform the calculations iteratively along several transversal sections of the ship track in order to show the visible SAR signature of the turbulent wake and evaluate the decay in the scattering level function of the distance aft of the ship (several kilometres). Improvements to this model will be discussed.

High Resolution Method with Polarization Diversity

Y. WANG, J. Saillard

IRESTE-Laboratory S.E.I. (Systèmes Electroniques et Informatiques)
La Chantrerie. CP3003, 44087 NANTES Cedex 03, FRANCE
Telephone: 33 40 68 32 30
Fax number: 33 40 68 32 33
E-mail address: wyide@ireste.fr

In a typical stepped-frequency radar system, when pulses are processed coherently by the radar receiver, the returned signal contains amplitude, phase and polarization information; the amplitude being related to the size and reflectivity of the target, i.e Radar Cross section (RCS), and the phase related to the target range. With the amplitude, the phase, the polarization is also a characteristic of the target. The classical system works with a single polarization. It is shown that the consideration of the polarization diversity can improve the system performance.

The RCS can not be derived analytically for complex targets, but under high frequency hypothesis, a such target can be modelled as an array of discrete scattering centers occurring principally at specular points and geometrical discontinuities of the body. Each scattering center is characterized by its range and its complex amplitude. It is shown that the characterization of the scattering centers is equivalent to the parameters estimation of a signal composed of the sum of sinusoids embedded in white noise.

The conventional method for characterization of scattering centers is based upon the fast Fourier transform (FFT). It is well known that this method has several inherent performance limitations. The most important limitation is that of frequency resolution which is inversely proportional to the observation period. A second one is due to the implicit windowing of the data that occurs when processing with FFT. In order to alleviate such limitations, many alternative procedures have been proposed in recent years. Theses methods provide a way of extracting the locations and coefficients of scattering centers from the backscattered field. It has been found to be superior to the conventional Fourier transform technique in resolution and in dynamic range.

But these methods use only a single polarization, they do not exploit the additional information provided by the polarization diversity, so it is not possible to estimate the polarization parameters in order to gain more information about the target. In this paper, we will present a method based on the high resolution concept with consideration of the polarization diversity of the signal. We use the so called transient polarization response to characterize the polarization properties of the target. The proposed high resolution method combines all information obtainable in the received signal, uses the full polarization data simultaneously and optimally in order to enhance the performance of the system. We will show that this method can not only allow a fully characterization of the target with its amplitude, phase, distance and polarization, but also provide a better performance in terms of resolution of the target.

Simulation results will be presented in order to give some ideas about the performance of the proposed method comparing with the classical FFT based method and the scalar case high resolution method.

POLARIZABLE MEASUREMENTS ON DETERMINATION OF THE CHARACTERISTICS OF DETECTION OF THE RADAR-TRACKING TARGETS ON A BACKGROUND OF FORESTRY FILES.

Prof. Dr.Sc. Vorobiev V.G., Prof. Dr.Sc. Kozlov A.I., Prof. Dr.Sc. Logvin A.I.
Moscow State Technical University Of Civil Aviation. Russia.

Variety of kinds and complexity of a structure of earthly cover largely hinder analytical determination of a scattering matrix elements and its invariant. Therefore along side with theoretical researches the important significance is acquired by experimental researches. In this connectionmeasurements of a scattering matrix elements of earthly cover and of little dimensions the targets on their background. Comparison of efficiency of detection of the radar-tracking targets on their polarizable anisotropy coefficients with a classical method of detection on a square of a module of a diagonal element of a scattering matrix was here in after conducted.

The experimental installation represented radar-tracking station two-channel on polarization. It worked in a decimeter range of waves and was intended for serial radiation and reception of radiowave vertical and horizontal polarization. After appropriate processing in a receiving device there were modules and squares of modules of a scattering matrixes diagonal elements.

The measurements were conducted in a forestry file, where it was necessary to conduct detection of three various types radar-tracking as a result of measurements a numerous statistical material was received, which has given a opportunity to determine the statistical characteristics of modules of a scattering matrix diagonal elements and of polarizable anisotropy degree of a deciduous forest in cases, when in this wood the mentioned above radar-tracking targets were or away.

Comparison of efficiency of detection of the of little dimensions targets on a background of a wood on a polarizable anisotropy degree and on a square of a module of a scattering matrix diagonal element has shown, that for reception of identical probability of correct detection it is necessary for the second case to increase the relationa signal/noise in limits from 4 up to 9 dB (depending on a kind of the target).

Progress in Electromagnetics Research Symposium, PIERS 1997 ISBN 962-442-097-1

Space Spectra of Polarization Parameters of Electromagnetic Waves on Beyond-the-Horizon Propagation Paths

V.N.Tatarinov, G.S.Sharygin

Tomsk State Academy of Control Systems and Radioelectronics
40, Lenin Ave., Tomsk, 634050, Russia
Tel.& Fax: + 7 (3822) 232 184 E-mail: vnt@tiasur.tomsk.su

The concept of plane electromagnetic (EM) wave is not always fair for all cases of spatial and temporal fluctuations' investigations of HF signal propagating on beyond-the-horizon tropospheric scattering paths. A reason is that for these paths use of transmit-receive antennas, which aperture sizes are, as a rule, considerably more than spatial correlation's radius of scattered signal fluctuations, is the most characteristic. Investigations of signals' polarization parameters (PP) on beyond-the-horizon tropospheric paths include usually measurements of temporal fluctuations of polarization ratio in certain polarization basis connected with receiving antenna. But using such measurements results, one can not characterize a polarization structure of scattered signal completely, since field of the EM wave in receiving antenna aperture situated beyond the radio-horizon is a random function both time and space coordinates. Such dependence results in incorrectness in case of interpreting experimental results of EM fields' polarization structure, when data of temporal fluctuations of signal's PP on the output of a 'large stationary receiving antenna' are only used. In such a case, it is possible to speak about effect of spatial fluctuations averaging. It makes impossible to get information about PP's spatial spectrum which is connected with spatial coherence functions of the orthogonal components of scattered fields by means of pair of the Fourier transformations.

Since far-zone antenna pattern is the Fourier transformation of the field excited on its aperture, then the antenna diffraction response ('instant pattern') will be a space spectrum of the random field investigated, if the aperture sizes are much more than spatial correlation's radius. The simultaneous recording of spatial spectra of the orthogonal components' amplitudes and their phase difference permits to determine the spatial spectra of beyond-the-horizon propagated field' PP.

In the paper, results of experimental measurements of scattered UHF-field's polarization parameters are given for more than 100 km trans-horizon paths. In these experiments, the instant patterns of the 10-m aperture antenna (wavelength of radiated and received signal was equal to 10 cm) were recorded. Considering that the angular speed of the antenna rotation was 36 degrees per second, and interval of temporal correlation was equal to 0.2 - 0.3 seconds, it is possible to consider the registered patterns as identical to instant spatial spectra in azimuth angle range about 4 degrees.

As a result of the analysis, sufficient statistics for averaged spatial spectra forms of polarization parameters have been obtained. Also their variations and appropriate probability distributions were found and investigated.

THE STATISTICAL CHARACTERISTICS OF SCATTERING MATRIX ELEMENTS OF LITTLE DIMENSIONS TARGETS ON A BACKGROUND OF A LAYING SURFACE.

Prof. Dr.Sc. Kozlov A.I., Prof. Dr.Sc. Logvin A.I., Prof. Dr.Sc. Vorobiev V.G.
Moscow State Technical University Of Civil Aviation. Russia.

At detection of the of little dimensions radar-tracking targets on a background of laying cover on a output of a antenna there is a signal, formation of which the target, but also the environmental its district within the limits of a element of the sanction of radar-tracking station participates not only. The reflection from interfering objects hinders detection of the target and results in essential change of the statistical characteristics of parameters of a reflected wave in comparison with case, when supervision of the target in free free the space. Such changes can be discounted, if for the observer the polarizable characteristics of that site districts, on which found out target is located.

For the account of interfering reflections the statistical characteristics of parameters of a signal, representing total signal (target+background) are considered. It is supposed, that a signal on a output of orthogonal channels represent a mix of two statistically independent signals, the occurrence of which is called by availability of the target and background.

In work dependences of a asymmetry coefficient of a structure, representing mix of target and background, from the relation (signal/background) are received at various significances of a asymmetry coefficient of the target, as well as dependence of a module of a generalized coefficient of correlation orthogonal making from the relation (signal/background) at various significances of a asymmetry coefficient of the target.

If the statistical characteristics of a scattering matrix district are beforehand known, on which is of little dimensions is whole at given polarization of a irradiating wave it is possible to receive the appropriate numerical characteristics for a reflected signal from a background. It enables to determine density of distribution of probabilities of modules of main and cross of a scattering matrix elements of a background. The knowledge of these characteristics enables to adjust results of on location measurements at a reception of reflected signals from the target, located on earthly surface.

Progress in Electromagnetics Research Symposium, PIERS 1997 ISBN 962-442-097-1

RADAR TARGET IDENTIFICATION WITHOUT POLARIMETRY?

Ernst Krogager
Danish Defence Research Establishment
Ryvangs Allé 1, DK-2100 Copenhagen, Denmark
T: +45 39272233 F: +45 31203315 E-mail: ek@ddre.dk

William A. Holm
Georgia Tech Research Institute
7220 Richardson Road, Smyrna, GA 30080, USA
T: +1 (770) 528-7748 F: +1 (770) 528-7728 E-mail: bill.holm@gtri.gatech.edu

One of the great challenges for modern radar is to classify and identify targets of all kinds, for military as well as for civilian purposes. A variety of different techniques have been considered and investigated over the years, and some have proven sufficiently viable for actual operational implementation.

In remote sensing, radar polarimetry seems to have been generally accepted as an indispensable tool, and convincing results have been obtained for such applications as classification of vegetation and other natural as well as man-made targets. However, most investigations related more specifically to military applications, like battlefield IFF (Identification Friend or Foe), seem to be based on traditional single polarization radar systems.

A main point is, that no matter which particular polarization is transmitted towards a given target, the polarization of the reflected wave will almost always be elliptically polarized. This means that when a radar uses the same, fixed polarization for transmission and reception, only a fraction of the potentially available information contained in the reflected signal will be acquired. Not least in military applications, this could mean a critical lack of information which might otherwise be available.

In the paper some recent progress concerning polarimetric analysis and feature extraction methods will be presented, and their application to real, measured data will be demonstrated, so as to emphasize the extra information revealed by fully polarimetric data.

Subterrain object mapping using polarimetric scattered fields

Patrick Luneau, Gilles Y. Delisle, Venkatesh Sampath
INRS-Télécommunications
16, Place du Commerce,
Ile-des-Soeurs, Verdun
Québec, Canada, H3E 1H6
Tel:(514) 765-8670, Fax:(514)761-8501, email:luneau@inrs-telecom.uquebec.ca

Introduction

In this paper, a polarimetric approach to the characterization and interpretation of the field scattered by underground targets will by presented. The problem is of great significance in the search for unexploded munltions especially when the target is made of low contrast materials.

Modelling

The model used for simulations is based upon the FDTD approach [1]. A "problem space" is defined, containing the target, the ground in which it is buried, the free space above the ground and the interface between the two media. A UHF dipole detector, containing two transmitters (fed in opposite directions) and a receiver in the middle (corresponding to the null position of the transmitted field) is mounted in the free space very close to the interface [2]. Thus, the target is the near field of the detector. The FDTD approach requires that Maxwell's equations be expanded in a scalar form and the derivatives replaced by centered difference. Mur's first and second order boundary conditions are then used to simulate the propagation of the scattered waves. Complications arise from different sources: the target may be made of low contrast dilectric, the ground may be inhomogeneous or contain secondary scatterers. Conditions at the boundary may also constitute a difficulty.

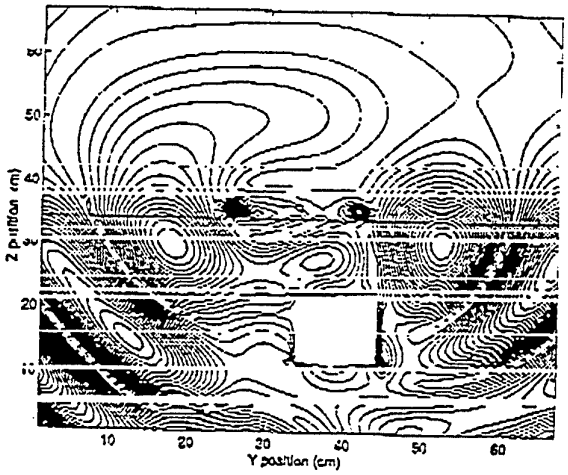


Figure 1

Results

A typical result is shown in figure 1 where the field distribution around a metallic cube located 5 cm off the detector center. As it can be noticed, a clear mapping of the field diffracted by the cube can be obtained. Of course many others results, including comparison with some experimental results obtained using a ground penetrating radar will be reported and fully discussed.

References

[1] K.S.Kunz. R.J. Lubbers, The Finite Difference Time Domain Method for Electromagnetics, chapter 1-3, Boca Raton: CRC Press, 1993
[2] Hill,D.A., "Near-Field Detection of Buried Dielectric Objects", IEEE Transactions on Geoscience and Remote Sensing, vol.27, no.4, pp.364-368, July 1989.

SESSION 7A11

Tuesday, January 7, AM 850-1130, Lecture Theatre 11, City University of Hong Kong

Remote Sensing of Precipitation

Organizer: Alfred T C Chang

Chairperson: Alfred T C Chang, NASA/Goddard Space Flight Centre
Co-Chairperson: Gin-Rong Liu, National Central University

8:50 ***Monitioring Freezing/ Thawing Terrain over Qinghai - Tibet Plateau Using Microwave Remote Sensing*** 266
*M S Cao, **Alfred T C Chang
*Lanzhou Institute of Glaciology and Geocryology
**NASA/ Goddard Space Flight Center

9:10 ***Evaluation of Non-Uniform Beam Filling Effect on TRMM Precipitation Radar Measurements*** 267
Toshio Iguchi, Toshiaki Kozu
Communications Research Laboratory

9:30 ***Spatial and Temporal Variability of Monthly Rainfall derived from SSM/I Data*** 268
Alfred T C Chang, Long S Chiu
NASA/Goddard Space Flight Center

9:50 ***Estimation of Mean Rain Rates from Instantaneous Rain Rates versus Histograms of Microwave Brightness Temperature*** 269
Long S Chiu, Alfred T C Chang
NASA/Goddard Space Flight Center

10:10 ***Applying the Ground-Based Microwave Radiometers to Estimate the Rainfall Rate in Taiwan Area*** 270
Gin-Rong Liu, Chuen-Chen Day, Tsung-Hua Kuo
National Central University

10:30 Break

10:50 ***Algorithms for Retrieval of Monthly Rainfall Totals for TRMM and Eos AMSR*** 271
*T Wilheit, *J Huang, *D Redmond, **A Chang, ***L Chiu, ****Y Hong
*Texas A&M University
**NASA/ Goddard Space Flight Center
***SAIC/ General Sciences Corporation
****Caelum Research Corporation

11:10 ***Improvement of Passive Microwave Rainfall Retrievals by Visible/Infrared Radiometry*** 272
Peter Bauer, Lars Schanz
Deutsche Forschungsanstalt für Luft- und Raumfahrt

Monitioring Freezing / Thawing Terrain over Qinhai—Tibet Plateau Using Macrowave Remote Sensing

M. S. Cao
(Lanzhou Institute of Glaciology and Geocryology, Lanzhou 730000, China)
A. T. C. Chang
(NASA / Goddard Flight Center, Greenbelt, Maryland MD 20771, U. S. A.)

The decrease in brightness temperatures with macrowave frequencies can be used as a signature of freezed ground and a combination of low 37 GHz brightness temperature and negative 10.7,18 and 37 GHz spectral gradient from Scanning Multichannel Macrowave Radiometer (SMMR) records was used to effectively map freezing / thawing boundaries at a northern Great Plains in autumn 1984. Since the difference between soil moisture in spring and autumn is large over some regions and the radiometric properties in macrowave frequencies measured in laboratory revealed that moisture can significanily influence on the magnitude of increasing effective depth of emission and emissivity for soil, while thawing soil tranforms to freeze, a modified algorithm including moisture effect is presented to discriminate freeze / thaw terrain over Qinhai—Tibet Plateau in this paper.

The 37 GHz brightness temperature partly contains the information on soil moisture and the negative spectral gradient in freezing condition will varify with it. In the text temperatures less 0(℃) measured at depth 5 cm in station are compared with the records of horizontal polarized brightness temperature at 37 GHz and spectral gradient at 18 and 37 GHz from the SMMR over this area in 1983. The correction analysis is used to determine a statistical expression of modified algorithm based on 73 freezeing and 70 thawing samples during freeze / thaw transformed seasons. The accuracy of discrimination reaches 74%. Testing to other 66 samples for check, it is 81%. Then the algorithm applies to whole Qinhai—Tibet Plateau (27 ° −40 ° N, 75 ° −100 ° E). The results show that a half area of Plateau was still in freezeing condition on May 7−11, later the thawing wider in summer and once again a half area in freezing on October 22−26. The variation along 89 ° E profile in spring and autumn shows that how the freezing / thawing terrain codition changes with altitude, aspect of slope and lantitude.

Evaluation of Non-Uniform Beam Filling Effect on TRMM Precipitation Radar Measurements

Toshio Iguchi and Toshiaki Kozu

Communications Research Laboratory
4-2-1 Nukui Kita-machi
Koganei, Tokyo 184, Japan
PHONE: +81-423-27-7551, +81-423-27-7543
FAX: +81-423-27-6666
E-mail: iguchi@crl.go.jp, kozu@crl.go.jp

It is well-known that the non-uniform distribution of rain within the radar scattering volume alters the apparent Z-R relationship and that if this effect is ignored, the estimated rainfall rate R may be positively biased. In a similar way, the relationship between the apparent attenuation coefficient (k) and the radar reflectivity factor (Z) also changes with the non-uniformity of rain. When attenuation is large, the true Z must be estimated from the measured Z by applying the attenuation correction. If the standard k-Z relationship is used in the correction formula, however, the correction may be largely biased because of the non-uniformity of rain within the angular resolution of the radar.

In the range profiling algorithm for the TRMM Precipitation Radar, a surface reference technique is used to estimate the total path integrated attenuation from the rain top to the surface. Since the footprint size of the TRMM radar is about 4 km, however, the horizontal uniformity of rain in the field of view may not be assumed for some active convective rain cells.

In this paper, the effect of non-uniform distribution of rain within the field of view on the k-Z and Z-R relationships is first examined theoretically for several types of rain distributions such as log-normal and uniform distributions. The non-uniformity of rain field and the extent of its effect are also analyzed by using the low-resolution synthetic data that are created from high-resolution radar data taken in the tropical Pacific during the TOGA/COARE. From the latter analysis, the probability distribution of rain in a scale less than approximately 10 km is investigated and the results are fed back in the theoretical model. Finally, the non-uniform beam filling effect on the TRMM PR measurements is discussed.

Spatial and Temporal Variability of Monthly Rainfall derived from SSM/I Data

Alfred T. C. Chang and Long S. Chiu
Hydrological Sciences Branch
NASA/Goddard Space flight Center
Greenbelt Maryland 20771

Abstract

Eight and half years of monthly oceanic rainfall rates derived from the Defense Meteorological Satellite Program (DMSP) Special Sensor Microwave/Imager (SSM/I) data have been produced using the brightness temperature histogram technique and with improved land mask file. Monthly rain rates have been generated for both the 5 x 5 degree and 2.5 x 2.5 degree grid boxes.

The spatial and temporal characteristics of the monthly rain fall are examined. Space and time autocorrelation functions are computed both for the 5 x 5 and 2.5 x 2.5 degree grid data sets. A comparison will be made between the 5 x 5 and 2.5 x 2.5 degree data sets using t-tests. Missing data in the 2.5 x 2.5 degree data set due to insufficient sampling will be filled using results from the 5 x 5 degree data set.

An Empirical Orthogonal Function (EOF) analysis performed on the data sets showed the El Nino-Southern Oscillation (ENSO) contributed to the dominant mode of interannual variability. A paired t-test will be performed on the two data sets to elucidate the effect of spatial resolution on detecting the climate signal.

Progress in Electromagnetics Research Symposium, PIERS 1997 ISBN 962-442-097-1

Estimation of Mean Rain Rates from Instantaneous Rain Rates versus Histograms of Microwave Brightness Temperature

Long S. Chiu and Alfred T. C. Chang
Hydrological Sciences Branch
NASA/Goddard Space Flight Center
Greenbelt, MD 20771 USA

Abstract

A technique for estimating instantaneous rain rates over oceans from passive microwave measurements has been developed and validated against shipboard radar rain rate data collected during TOGA-COARE. The techniques uses a combination of the 19 and 22 GHz for the low to moderate rain rates, and the 85 GHz for the high rain rates. The height of the rain column for each pixel is estimated using an empirical relationship between the freezing height and the total columnar water vapor. A constant beam-filling correction factor is applied. The estimated rain rates are binned to 0.5 x 0.5 degree boxes and compared with radar rain rates. The results showed a small bias for the retrieved rain rates and a fairly high probability of detection, after adjustments were made for the non-detection at light rain.

Monthly mean rain rates were estimated using a truncated mixed log-normal rain rate distribution. The truncation allows for the non-discrimination of non-raining and light rain rate pixels. The technique was applied to estimating oceanic monthly rainfall for 2.5 x 2.5 and 5 x 5 degree latitude/longitude boxes. The results were compared with monthly rain rates derived from histograms of microwave brightness temperature histograms.

Progress in Electromagnetics Research Symposium, PIERS 1997 ISBN 962-442-097-1

Applying the Ground-based Microwave Radiometers to Estimate the Rainfall Rate in Taiwan Area

Gin-Rong Liu, Chuen-Chen Day and Tsung-Hua Kuo
Center for Space and Remote Sensing Research
National Central University, Chung-Li 320, Taiwan, ROC

Abstract

The aim of this study is to figure out the physical properties and mechanism between the rainfall rate and microwave attenuation, and to establish practicable processes for rainfall estimation in Taiwan area.

This study employed two ground-based microwave radiometers, 19.35 and 22.235 GHz, respectively, to record the atmospheric brightness temperature upwards with a 45 degree azimuth angle. Meanwhile, the rainfall rate was measured by rain gauge. Then, the relationships between rainfall rate and the brightness temperature influenced by the liquid water content were analyzed. In this study, both physical models and statistical models were applied to estimate the rainfall rate, respectively. In the physical part, the Rose model proposed by Kummerow that based on the RTE in the microwave bands was used. In the statistical part, two different algorithms proposed by this research team were used. One is a traditional statistical model and another is a differential model. The basic concept of the differential model was to calculate the differentiation of rainfall or brightness temperature in time series to enhance the rainfall variation. Finally, the verification using the observed data was investigated.

The verified results based on our observed data showed that the physical models were better than the statistical models, the dual-channel mode was more accurate than the single channel mode, and the 19.35 GHz was better than the 22.235 GHz channel. The best result was 0.57 mm/h RMSE estimated by the physical model and was 0.63 mm/h RMSE estimated by the traditional statistical model. Intrinsically, the differential model should have better accuracy than the traditional one. It seems to be that the smaller rainfall rate could induced larger errors and weaken the differential one's accuracy. This point should be investigated when larger rainfall rate observed data are available.

Algorithms for Retrieval of Monthly Rainfall Totals for TRMM and Eos AMSR.

T. Wilheit, J. Huang, and D. Redmond
Department of Meteorology, Texas A&M University, College Station, TX 77845-3150

A. Chang
Hydrological Sciences branch, NASA/Goddard Space Flight Center
Greenbelt, MD 20771-0001

L. Chiu
SAIC/General Sciences Corporation, Laurel, MD 20754

Y. Hong
Caelum Research Corporation, Silver Spring, MD 20901

Abstract

The probability of rainfall intensities has been found to be well described by a mixed Log-Normal distribution. The space and time variations in rainfall are then expressed as changes in the three parameters needed to specify the distribution: the probability of non-zero rain rate, the mean of the logarithm of the rain rate, and the variance of the logarithm of the rain rate.

Estimation of rainfall totals from spaceborne observations is fraught with difficulties. Even if the measurements were perfect, significant error would result from the intermittent sampling of the rainfall. The contributions from high rain rates are particularly subject to this sampling error. The fact that the measurements are significantly less than perfect exacerbates the problems. In particular, each measurement technique is only valid over a limited dynamic range. Passive microwave measurements are limited on the low end by variability in non-precipitating contributions to the brightness temperature and on the high end by saturation. However, the lower and upper limits of the dynamic range depend on the observation channel roughly as the frequency squared.

By accumulating multiple histograms of rain rate retrieved using various measurement channels, and using a maximum-likelihood estimator to determine the Log-normal parameters for the set of histograms, these dynamic range and sampling problems can be mitigated. The current planning is to use three rain rate retrievals based on frequencies of approximately 11, 19, and 37 GHz for the estimates of monthly totals over the oceans. The challenge in this effort lies in the observation that the spatial resolution of the instruments varies from channel to channel so that the Log-normal parameters are not the same for each of the histograms, although they are related.

IMPROVEMENT OF PASSIVE MICROWAVE RAINFALL RETRIEVALS BY VISIBLE / INFRARED RADIOMETRY

Peter Bauer & Lars Schanz

Deutsche Forschungsanstalt für Luft- und Raumfahrt

Linder Höhe, 51140 Köln, Germany

phone: (+49) 2203 - 601 - 2995, fax: (+49) 2203 - 68309, e-mail: peterb@dv.kp.dlr.de

Since passive microwave radiometers suffer from low spatial resolution, retrieval errors associated with beam-filling prevail uncertainties due to insufficient knowledge of vertical cloud structures. Merging microwave and visible/infrared imager data available on the same satellite such as the TRMM Micowave Imager (TMI) and the Visible Infrared Scanner (VIRS) provides potential for the improvement of instantaneous retrievals, in particular in those cases where the spatial distribution of the desired quantity is highly variable.

Case studies are shown which demonstrate the stepwise degradation of information contained in the microwave signals when three-dimensional cloud effects and realistic antenna patterns of current and near-future sensors are simulated. Input data of convective and stratiform cloud systems were obtained from Doppler-Polarization-Radar soundings. Three-dimensional and plane-parallel radiative transfer simulations indicate the importance of geometry effects which are supressed when horizontal homogeneity is assumed. Measurements at those microwave frequencies best suited for surface rainfall estimations are most degraded due to decreasing ground resolution with decreasing frequency.

Thus spectral and spatial informations at higher frequencies as well as visible/infrared wavelengths are to be added in order to retrieve better quantitative estimates at lower frequencies. Simultaneous visible/infrared data were found to contribute mainly to better rain regime classification, in particular when cloud identification techniques and cloud parameter retrievals are incorporated. Although beam-filling problems are not solved by sensor combinations such as TMI-VIRS alone even when precipitation radar data is available, it offers great potential when transferred to systems which are already operational as well as for combining data from geosynchronous and polar orbiting satellites.

SESSION 7P11

Tuesday, January 7, PM 1330-1610, Lecture Theatre 11, City University of Hong Kong

Advanced Image and Signal Processing for Remote Sensing

Organizer: Sadao Fujimura

Chairperson: Sadao Fujimura, The University of Tokyo
Co-Chairperson: Y Eric Yang, MIT

13:30 ***Significance-Weighted Feature Extraction from Hyperspectral Data and Its Application to Sensor Design*** 274
Sadao Fujimura, Senya Kiyasu
University of Tokyo

13:50 ***An Automated Method for Accurate Registration of Remotely Sensed Images*** 275
*Hiroshi Hanaizumi, *Yutaka Kanemoto, **Sadao Fujimura
*Hosei University
**The University of Tokyo

14:10 ***Evaluation of Interferometric SAR Unwrapping Algorithms*** 276
*Masafumi Iwamoto, *Chiaki Satoh, *Kyosuke Kawabata, *Yoshihisa Hara,
**Eric Yang, **Jin Au Kong
*Mitsubishi Electric Corporation
**Massachusetts Institute of Technology

14:30 ***Estimation of Adjacent Effects Over the Coastal Zone by Reflectance and Polarization Analysis of Airborne Polder Images*** 277
T Kusaka, S Sado, Y Kawata
Kanazawa Institute of Technology

14:50 ***Ozone Layer Gas Profile Retrieval by a Satellite Sensor "ILAS" Aboard "ADEOS"*** 278
Tatsuya Yokota, Yasuhiro Sasano
National Institute for Environmental Studies

15:10 **Break**

15:30 ***SCANSAR Interferometry Simulation with EMSARS*** 279
*C C Hsu, *Y E Yang, *J J Akerson, *L F Wang, *Y Zhang, *K H Ding, *J A Kong,
**Y Hara, ***C R Kohler, ***T H Nguyen
*Massachusetts Institute of Technology ,
**Mitsubishi Electric Corporation-Kamakura Works
***Army Research Laboratory

15:50 ***An Optical SAR Processor With Digital Input/Output For Quick-Look Applications*** 280
Konstantin Litovchenko, Philippe Lemaire, Christian Barbier
Université de Liège

Significance-Weighted Feature Extraction from Hyperspectral Data and its Application to Sensor Design

Sadao Fujimura and Senya Kiyasu

Department of Mathematical Engineering and Information Physics
Graduate School of Engineering, University of Tokyo

7-3-1 Hongo, Bunkyo-ku, Tokyo 113, JAPAN
Phone: +81-3-3812-2111, Fax: +81-3-5689-7354
E-mail: fuji@k2.t.u-tokyo.ac.jp

The dimension of remotely sensed data is becoming higher and higher because of higher spectral resolution, increasing number of platforms or sensors, and multi-temporal observations. Airborne Visible Infrared Imaging Spectrometer (AVIRIS), for example, has 224 spectral bands in the 0.2-2.5μm region. Extracting significant features is essential for processing and transmission of vast volume of hyperspectral data.

We present here a feature extraction method designed for significance-weighted supervised classification. In classification of data we have some kind of objectives or intention, and we are interested in classification of a particular set of classes. Thus we introduce subjective significance explicitly into feature extraction. The evaluation to be used is the accuracy for the particular classes, though conventional feature extraction methods pay attention to the average accuracy for many classes. Our method extracts a set of features which optimally separate one class from another among a particular set of important classes as linear combinations of orthogonalized and reduced components which are obtained by principal component analysis.

We applied the results of feature extraction to evaluating the performance of current sensors and to designing the spectral bands of new sensors. The results of feature extraction indicate the informative spectral region for classifying significant classes. Bands of new sensors were designed considering the highly weighted wavelength of extracted features.

We applied this method to hyperspectral data obtained by a ground-based imaging spectrometer. Relative reflectance of 8 classes (soil, stone, concrete and five plants) were obtained as 411 dimensional hyperspectral data for experiments, assuming that two of the plant classes are significant to be classified. We extracted several features and used for evaluating the performance of current sensors and for designing the spectral bands of new sensors.

The classification accuracy of significant classes achieved by the three bands (band 2, 3 and 4) of the Coastal Zone Color Scanner (CZCS) were compared with the accuracy by the extracted features. The former was lower than the latter by about 6%.

Spectral bands of new sensors were designed by allocating them considering the highly weighted wavelength of extracted features. Classification accuracy was improved by 3% compared to the bands of CZCS. This means that the designed bands are more appropriate for the specific purpose.

An automated method for accurate registration of remotely sensed images

Hiroshi Hanaizumi, Yutaka Kanemoto,
College of Engineering, Hosei University
3-7-2 Kajino-cho, Koganei, Tokyo 184, Japan
Phone +81-423-87-6354 Fax +81-423-87-6126
E-mail hana@hana.is.hosei.ac.jp
and
Sadao Fujimura
Graduate School of Engineering, The University of Tokyo
7-3-1 Bunkyo-ku, Tokyo 113, Japan
Phone +81-3-3812-2111 ext.6900 Fax +81-3-5689-7354
E-mail fuji@k2.t.u-tokyo.ac.jp

Abstract

In order to get higher performance in various application fields, such as change detection or production of digital terrain model, accurate registration methods have been required. Here, we propose an automated method for registration of remotely sensed images with higher accuracy. The method was expanded from our former method ARTSIM (Automated Registration meThod for Satellite IMages) which automatically generates many pairs of corresponding points and register the images using piecewise Affine transformation after dividing the images into many triangles whose vertices are the corresponding points generated. In the proposed method, we control the position of corresponding point pairs (we generate them at the position where the maximum disparity is detected). As the corresponding point pair removes disparity around it, we can ensure registration accuracy by repeating the generation of corresponding point pairs until the maximum disparity falls below a threshold.

In the procedure, essential is to detect disparities. We regard the images to be registered as sequential shots of a video image, and detect the disparity by obtaining optical flow vector between them. As differentiation tends to have larger error for images having severe disparities, we adopt hierarchical processing in the estimation of optical flow. A pyramidal structure of an image is made by merging neighboring 4 pixels into one. On the top layer, severe disparities are reduced into slighter ones with reduction of number of pixels. From the top layer to the bottom one, we estimate optical flow and register them. The maximum length of the flow vector is decreased by repeating the process. We shift to the lower layer when the maximum falls below a threshold in the current layer. On the lower layer, the length of the flow vector is enlarged twice. We stop the process after the maximum of the length falls below the threshold in the bottom layer.

The validity of the proposed method was confirmed by applying the method to registration between a LANDSAT/TM image and an artificially distorted one. The former method ARTSIM generated 345 pairs of corresponding point and produced 703 triangles. The proposed method newly generated only two pairs except the initially selected 4 pairs and produced 6 triangles. We evaluated goodness of registration by the coefficient of spatial correlation between pixel densities in the same region. The former gave 0.894 and the latter 0.889. The proposed method has almost the same performance as ARTSIM in accuracy using less pairs of corresponding points.

In this paper, we will describe the principle and the procedures of the proposed method. The details of the simulation and results of the method applied to real remotely sensed images will be also described.

Evaluation of Interferometric SAR Unwrapping Algorithms

Masafumi Iwamoto
Information Technology R&D Center
Mitsubishi Electric Corporation

Chiaki Satoh, Kyosuke Kawabata, and Yoshihisa Hara
Kamakura Works
Mitsubishi Electric Corporation

Eric Yang and Jin Au Kong
Research Laboratory of Electronics
Massachusetts Institute of Technology

In spaceborne SAR interferometry, the terrain elevation information is obtained from the phase difference of two SAR images gathered by the same sensor in repeated passes. In the processing of interferometric SAR data, a number of experiences have been reported in the literature and various methods for the processing are available. Among the factors crucial to the accuracy of altitude mapping is the phase unwrapping process, which recovers the absolute phase value from the wrapped phase image. Major contribution to errors in phase unwrapping noise is in the wrapped phase measurements.

In this paper, sensitivity studies of the unwrapped phase error and the height inversion error are described using the simulated interferometric SAR images first. We adopted two phase unwrapping algorithms, the branch-cut method which is carried out by successive comparisons of neighboring pixels phases, and the least squares technique, which was first developed in the area of adaptive optics. The results of the studies show that branch cut method gives better performance when the phase noise is small (less than 40 deg), but implementation is very difficult when the phase noise is larger. Then, two phase unwrapping algorithms are applied to the real SAR data (EERS-1 SAR Alaska Toolik Lake data), and the inverted height data obtained by two different algorithms are compared with the DEM (Digital Elevation Model) of USGS. It is found that the accuracy of branch-cut algorithm is comparable to the accuracy of DEM, and there is a great possibility that the interferometric SAR gives much better accuracy.

ESTIMATION OF ADJACENT EFFECTS OVER THE COASTAL ZONE BYREFLECTANCE AND POLARIZATION ANALYSIS OF AIRBORNE POLDER IMAGES

T. KUSAKA, S.SADO AND Y. KAWATA
Kanazawa Institute of Technology
Nonoichi-machi Ishikawa 921, JAPAN
Tel.81-762-48-1100, Fax.81-762-94-6711
E-mail: kusaka@manage.kanazawa-it.ac.jp

ABSTRACT

In this study, we estimate adjacent effects arising from the land surface by analysing the 2-dimensional spatial patterns of the reflectance and polarization in the coastal zone measured by the airborne POLDER sensor over Mediterrenean Sea in 1991. The POLDER (POLarization and Directionality of Earth Reflectances) sensor will be flown on board NASDA's ADEOS satellite scheduled for launch in 1996.

The reflectance and polarization measurements by the airborne POLDER sensor were performed at wavelengths 450 nm and 850 nm.

We first estimated the total radiance and linear polarization in the coastal zone by the single scattering radiative transfer model including Stokes parameters. In this case, we assumed that the sea surface is the specular reflector given by Fresnel's formula and the land surface is the diffuse reflector given by Lambert's law. As a result, it is shown that at 850 nm, the contour line of equi-polarization over sea surface adjacent to the land surface is considerably distored, as compared with that of the polarization over the sea surface distant from the land. This indicates that the radiation reflected by the land surface has significantly effects on the degree of polarization over sea surface adjacent to the land surface.

We next investigated the difference of polarization patterns between the observed POLDER data over the coastal zone and POLDER data over sea surface distant from the land. We obtained the following results :

(1) At the wavelength 450 nm, the polarization pattern over the coastal zone is almost similar to that over the sea surface distant from the land.

(2) At 850 nm the contour of equi-polarizations over the coastal zone is significantly different from that of the polarization over the sea surface distant from the land.

Finally, adjacent effects over coastal zone were estimated, by comparing with the observed polarization patterns and theoretical ones. Consequently, it is shown that at the wavelength 850nm, the total intensity and the polarized intensity of the sea surface in the range 200m to 300m from the land can be affected by the radiation reflected by the land surface and that at 450nm, adjacent effects are not significant in the data received by the airborne sensor.

OZONE LAYER GAS PROFILE RETRIEVAL BY A SATELLITE SENSOR "ILAS" ABOARD "ADEOS"

Tatsuya Yokota and Yasuhiro Sasano

National Institute for Environmental Studies
16-2 Onogawa, Tsukuba, Ibaraki 305 Japan
Phone:+81-298-50-2550, 2444, FAX: +81-298-51-4732
E-mail: yoko@nies.go.jp, sasano@nies.go.jp

The Improved Limb Atmospheric Spectrometer (ILAS) is a sensor onboard the ADEOS satellite which will be launched in August 1996 by National Space Development Agency of Japan (NASDA). Measurements by the ILAS instrument are based on infrared absorption spectroscopy using the solar occultation technique. ILAS has two grating spectrometers to measure vertical profiles of high latitude stratospheric constituents, pressure, and temperature.

ILAS will provide vertical profile data of volume mixing ratios of O3, CH4, N2O, HNO3, H2O, NO2, and CFC-11, and aerosol extinction from infrared (IR) channels. The ILAS also has visible channels to detect absorption due to oxygen molecules, which will be used for deriving pressure (P) and temperature (T) profiles as well as aerosol extinction in visible wavelength. Precise P & T profile data are necessary to obtain the IR retrieval results with high precision. Self-measurement of P & T profiles is one of the great advantages of the ILAS measurement system.

The IR channel consists of 44 pyro-electric detector elements which cover the spectral range of 6.2 ~ 11.8 μm, and the visible channel is composed of 1,024 pixels MOS diode array that covers 753 ~ 784 nm. Measurement data are obtained as 11-bits integer signals by 12 Hz (517 Kbps) data sampling.

The ILAS level 1 to level 2 data retrieval scheme is as follows. In the ILAS visible channel, the ILAS signals are theoretically simulated by assuming initial vertical profiles of P & T after determining extinction caused by aerosol and air molecule scattering. Then the assumed profiles are iteratively adjusted to minimize a sum of squares of the differences between the computed values and the measured values. The final profiles of P & T are the retrieved results. This method is called "non-linear least squares (NLSQ) fit" computation technique. ILAS instrument function and all other non-linear factors involved in the measurement are also considered in this computation. Therefore, the best solutions are expected to be obtained by this method. Profiles of aerosol extinction coefficients from the visible channel will be retrieved by a vertical inversion method. For the IR channel data, vertical profiles of gas mixing ratios are derived in the same way as those of P & T retrieval from the visible channel. Major difference between the visible and IR retrieval method is that the unknown parameters are the gas mixing ratios for the IR channel and the P & T are given values. Aerosol profiles in the volcano oriented strong extinction layers will be also estimated from the IR channel. Contribution of these aerosols to the IR transmission is considered in the gas retrieval procedure.

According to the results of numerical simulation tests with noises for ILAS retrieval performance estimation, it was verified that the ILAS target gases will be retrieved almost within the required precision for each gas. For instance, overall estimation errors of ozone are ±5% at the altitude of 10 km, ±3% at 20 km, ±4% at 30 km, ±5% at 40 km, and ±10% at 50 km. Some examples of the preliminary retrieval results by using the actual ILAS measurement data would be reported in the PIERS presentation.

SCANSAR Interferometry Simulation with EMSARS

C. C. Hsu, Y. E. Yang, J. J. Akerson, L.-F. Wang, Y. Zhang, K.-H. Ding, and J. A. Kong
Massachusetts Institute of Technology, Cambridge, MA 02139, U. S. A.

Y. Hara
Mitsubishi Electric Corporation-Kamakura Works, Kamakura, Kanagawa 247, Japan

C. R. Kohler, and T. H. Nguyen
Army Research Laboratory, Ft. Belvoir, VA 22060, U. S. A.

In spaceborne synthetic aperture radar (SAR) interferometry, the terrain elevation information is obtained from the phase difference of two SAR images gathered by the same sensor in repeated passes. With the advantage of large swath width associated with the SCANSAR, it would cover wider area with the tradeoff of coarse azimuthal resolution. However, when the SCANSAR mode is used to derive interferometry, decorrelation due to the misalignment in the scanning cycle of two pass would be serious. In order to compare various processing methods systematically, SAR simulator can be used to analyze the performance of various SCANSAR processing algorithms.

In this paper, a SAR interferometry simulator has been developed and implemented based on the EMSARS (Electromagnetic Modeling of Scattering Applied to Remote Sensing) model. GIS database-including DEM (digital elevation map) and feature map- is used to create synthesized SAR images. The real SAR simulation involves calculation of received field for each time step and frequency component, a very time consuming process. We choose instead to start from the simulated range compressed data, in which the scattered field for each azimuthal step is calculated by summing up scattering field from individual cells that are within the specified azimuthal beamwidth and range resolution. K-distribution statistics is used to simulate the speckle inherent to the radar data. The scattering fields obtained from two repeat passes are combined to form the interferogram. The Doppler part of the commonly used range-Doppler algorithm is used to synthesize images under various misalignment conditions. Using the simulator, decorrelation effect due to the angular difference can be studied. It is found that the correlation coefficient of two image is decreased with increasing misalignment. This decorrelation effect can be shown to improve with the proper azimuthal filtering.

An Optical SAR Processor With Digital Input/Output For Quick-Look Applications

Konstantin LITOVCHENKO, Philippe LEMAIRE, Christian BARBIER
Centre Spatial de Liège, Université de Liège
Parc Scientifique du Sart-Tilman, Avenue du Pré-Aily,
Angleur-Liège, B-4031 BELGIUM
Phone 32-41-676668
Fax 32-41-675613
E-mail CSLULG@VM1.ULG.AC.BE

There exist many applications where real time quick-look lower resolution SAR images are more desirable than off-line full resolution images. Such systems could be implemented as on-board processors of airborne or spaceborne SAR as well as compact ground-based (or shipborne) processors intended for direct utilisation by SAR imagery users. The optical integration of large array of data seems to be very competitive with respect to digital one as far as the processing speed is concerned. The development of modern optical SAR processor provides an alternative and attractive way to satisfy these demands.

The optical quick-look SAR processor is developed and experimentally tested. The processor is realised as a laboratory mock-up capable to simulate all processing features. The optical configuration is based on transparent elements only (spherical and cylindrical lenses) and thus the spatial filtering is performed by means of purely phase processing. Due to the absence of semi-transparent masks such a system is energetically effective as there is no light absorption along optical path and in addition no parasitic diffracted waves are generated. However such a system is suitable only for SAR with either chirp-modulated or non-modulated pulse. The tilted plane 4-lens configuration of processor gives the most effective way to obtain uniformly scaled image. The needed in some cases correction of range migration is also realised in processor by means of cylindrical lenses. The simplified 2-lens configuration is also considered. It was demonstrated that such a configuration is generally suitable for quick-look applications.

The input of raw-data is done by means of light valve - the liquid crystal VGA display with a pixel size of 24 microns. The image is registered by CCD-camera connected with PC.

The processor is tested by simulated point targets raw data and by real raw data of ERS-1 and ALMAZ-1 satellites. The image quality in terms of radiometric and geometric resolution can be considered as sufficient for quick-look imagery.

SESSION 7A10

Tuesday, January 7, AM 850-1230, Lecture Theatre 10, City University of Hong Kong

International Workshop "Related Correlation Effects in Optics and Condensed Matter Physics 1"

(Sponsored by U.S. Army Research Office)

Organizers: Zu-Han Gu, Mikael Ciftan

Chairperson: Zu-Han Gu
Co-Chairperson:Mikael Ciftan, A Maradudin, E Wolf

Presider : Zu-Han Gu, Surface Optics Corporation

8:50 ***Speckle Correlations in Light Scattering From 1-D and 2-D Randomly Rough Metal Surfaces and Thin Films*** 282
*Alexei A Maradudin, **Arthur R McGurn
*University of California , Irvine
**Western Michigan University

9:40 ***Angular, Frequency, Time and Polarization Correlations of Scattered Waves*** 283
Akira Ishimaru, Yasuo Kuga, Charlie T C Le, Tsz King Chan
University of Washington

10:30 **Break**

10:50 ***Angular Correlation Function of Speckle Patterns Scattered from a One-Dimensional Rough Dielectric Film on a Glass Substrate*** 284
Zu Han Gu, Jun Q Lu
Surface Optics Corporation

11:40 ***Sensitivity of Far-field Speckle Pattern to the Small local Changes of the Rough Surface Geometry*** 285
*M Josse, **Zu-Han Gu, ***Alexei A Maradudin
*CEA/CESTA
**Surface Optics Corporation
***University of California, Irvine

Speckle Correlations in Light Scattering From 1-d and 2-d Randomly Rough Metal Surfaces and Thin Films

Alexei A. Maradudin
Department of Physics and Astronomy and Institute for Surface and Interface Science
University of California, Irvine, CA 92717

Arthur R. McGurn
Department of Physics, Western Michigan University, Kalamazoo, MI 49008

A perturbation theory study of the angular and frequency correlations present in the speckle pattern of light scattered from weakly rough, one- and two-dimensional, random metal surfaces is carried out. The corresponding surface profile functions are assumed to constitute zero-mean, stationary, Gaussian random processes. The power spectra defining these surfaces are assumed to have either a Gaussian form, or the form introduced recently by West and O'Donnell,[1] which is nonzero only in the vicinity of the wave numbers of the surface electromagnetic waves (surface plasmon polaritons) supported by the vacuum-metal interface in the one-dimensional case, or its two-dimensional generalizations[2]. We employ the perturbative approaches to scattering from one- and two-dimensional random surfaces presented in Refs. 3 and 2, respectively. The correlation function we calculate is given in the one-dimensional case by

$$C(q,q';k,k') = \langle [I(q|k) - \langle I(q|k)\rangle][I(q'|k') - \langle I(q'|k')\rangle]\rangle,$$

where the angle brackets denote an average over the ensemble of realizations of the surface profile function, and $I(q|k)$ is the intensity of the light scattered into a direction defined by a vector $\vec{q}$ whose component along the mean scattering surface is q, when p-polarized light of unit intensity is incident on the surface along a direction defined by a vector $\vec{k}$ whose component along the mean scattering surface is k. For each incident wave the plane of incidence is perpendicular to the generators of the surface. The correlation function $C(q,q';k,k')$ can be represented as a sum of four parts $C^{(1)}, C^{(2)}, C^{(3)}$, and $C^{(R)}$. $C^{(1)}$ is a "memory effect" part which vanishes unless $q-k = q'-k'$. $C^{(2)}$ is a long range component, which is nonzero for general q, k, q', and k', but goes to zero as $q-q' \to \infty$ and/or $k-k' \to \infty$. $C^{(3)}$ is an infinite range component, which is nonzero for general q, k, q', and k', but is relatively independent of the differences $q-q'$ and $k-k'$. $C^{(R)}$ consists of additional terms which arise in surface as opposed to volume scattering. They include contributions from resonant scattering processes involving surface plasmon polaritons, which are specific to surface scattering. Results for $C^{(1)}, C^{(2)}, C^{(3)}$, and $C^{(R)}$ are presented for both one- and two-dimensional surfaces. We also present results of calculations of the correlation function $C(q,q';k,k')$ for p-polarized light scattered from and transmitted through a thin metal film whose illuminated surface is randomly rough, while its back surface is planar.

1. C. S. West and K. A. O'Donnell, J. Opt. Soc. Am. A**32**, 397 (1995).

2. A. R. McGurn and A. A. Maradudin, Waves in Random Media (to appear).

3. A. R. McGurn, A. A. Maradudin, and V. Celli, Phys. Rev. B**31**, 4866 (1985).

Angular, Frequency, Time and Polarization Correlations of Scattered Waves

Akira Ishimaru, Yasuo Kuga, Charlie T. C. Le, and Tsz-King Chan
Department of Electrical Engineering
University of Washington
Box 352500
Seattle, Washington 98195-2500 USA
Telephone: 206-543-2169, Fax: 206-543-3842, E-mail: ishimaru@ee.washington.edu

This paper presents our recent study of the correlation effects of waves scattered by random media. The angular correlation, called the "memory effect," has been studied extensively in the past. The memory effect is applied to the determination of the average height profile of rough surfaces. This is the topographic mapping problem addressed by InSAR, and therefore, our approach is a generalization of conventional InSAR to include four antenna elements. The theory is based on the Kirchhoff approximation applied to surfaces with large radii of curvature. Unlike conventional scattering cross sections per unit area of the rough surface, we consider two incident waves at different incident angles and the corresponding scattered waves at two different directions. The correlation function of these two scattered waves, called the mutual coherence function, is then calculated. The surface consists of the slowly varying deterministic average profile and the randomly varying height. It is shown that the phase of the mutual coherence function is directly related to the average surface profile, and therefore, the topographic map of the height profile can be determined by the measurement of the mutual coherence function. The relative positions of the four antennas affect the sensitivities of the determination of the height profile, and this is studied by examining the memory signature diagram which shows the amplitude and phase of the mutual coherence function as functions of the incident and scattering angles.

The memory effect is also used to detect an object buried in random media. It is shown that the memory effects are drastically different depending on whether the medium is deterministic or random. This difference can be effectively used to separate the object and the surrounding random medium. Millimeter wave experiments are conducted to show that a conducting cylinder buried in a random medium can be detected using this technique.

The angular correlation is also extended to include the frequency correlation using the two-frequency mutual coherence function. The Fourier transform to the two-frequency mutual coherence function gives the pulse response and it shows the relationship between the pulse arrival time and the surface height profile.

If the polarization state of the incident wave changes, the polarization of the corresponding scattered wave changes. Polarization responses or signatures are one useful example of this polarization correlation. We have generalized this idea to include two different polarization states for incident waves and two different observed polarization states for scattered waves. The polarization response diagram is then generalized to show the characteristic signatures for deterministic and random media.

Progress in Electromagnetics Research Symposium
City University of Hong Kong, Kowloon, Hong Kong
January 6-9, 1997

Angular Correlation Function of Speckle Patterns Scattered from a One-dimensional Rough Dielectric Film on a Glass Substrate

Zu-Han Gu and Jun Q. Lu
Surface Optics Corporation
P.O. BOX 261602, San Diego, CA 92126, U.S.A.
E-mail: gu@physics.ucla.edu

ABSTRACT

Experimental results are presented for the angular correlation function of the far field speckle patterns scattered by a one-dimensional random rough surface of a thin dielectric film on a glass substrate when a polarized beam of light is incident on the rough surface from vacuum. This surface, which separates vacuum from dielectric, is rough enough that only the diffused speckles are observed. The experiment for the correlation measurement was set-up to use a CCD camera to obtain the image of the speckle pattern in the specular direction for each given angle of incidence, the cross correlation function is then calculated from the digitized images. It is found that the intensity correlation functions exhibit two distinct maxima, one arises from the auto-correlation and the other from the reciprocity condition. It is also found that different scattering processes give rise to quite different correlation functions, where multiple scattering processes produce narrow peaks with secondary maxima, while single scattering processes produce relatively broader peaks.

Submitted to PIES 1997

Sensitivity of Far-field Speckle Pattern to the Small Local Changes of the Rough Surface Geometry

Michel Josse
CEA/CESTA, BP2-33114, Le Barp, France

Zu-Han Gu
Surface Optics Corporation, P.O. BOX 261602, San Diego, CA 92126, U.S.A.

A.A. Maradudin
University of California, Irvine, CA 92717, U.S.A.

ABSTRACT

It is well known that the conductance of a mesoscopic disordered metal is extremely sensitive to the motion of a single impurity, or more generally, to any local change in the scattering potential that the electron wavefunction sees. There is also the analogous effect in the context of scattering from randomly rough surface.

When a coherent light is reflected from a rough surface, a complex speckle pattern is formed. This is the result of the interference among the scattered wavelets, each arising from a different microscopic element of the rough surface. Imagine now a small defect is placed onto the surface, such that the new random surface is given by a slightly different height profile $\zeta(z) = \zeta(z) + \delta(z-z_0)$, where the difference function $\delta(z)$ is localized at the origin. The far-field speckle pattern will now be slightly modified due to this local change in the scattering potential. Numerical and experimental results are presented for the angular cross-correlation function of the far field speckle patterns scattered by one-dimensional random rough surfaces, when a polarized beam of light is incident on the rough surface from vacuum. One sample is a thin dielectric film deposited on a glass substrate and the other sample is identical to the first one except for a localized defect on it.

We envision this property can be applied to inspection of a sample with defect by speckle mappings.

Submitted to PIES 1997

SESSION 7P10

Tuesday, January 7, PM 1330-1710, Lecture Theatre 10, City University of Hong Kong

International Workshop "Related Correlation Effects in Optics and Condensed Matter Physics 2"

(Sponsored by U.S. Army Research Office)

Organizer: Zu-Han Gu, Mikael Ciftan

Chairperson: Zu-Han Gu
Co-Chairperson:Mikael Ciftan, A Maradudin, E Wolf

Presider : E Wolf, Univ. of Rochester

13:30 ***Effects of Coherence on the Spatial and Spectral Distribution of Energy in Radiation Fields*** 287
Emil Wolf
University of Rochester

14:20 ***Microscopic Models for Correlation Effects in Optical Physics*** 288
G S Agarwal
Physical Research Laboratory, Ahmedabad

15:10 **Break**

15:30 ***Source Size Evaluation by Spectral Measurements*** 289
*F Gori, *M Santarsiero, *S Vicalvi, **D Paoletti, **G Schirripa Spagnolo
*Università "La Sapienza"
**Università dell'Aquila

16:20 ***Spectrum Shaping Using Three-Dimensional Antennas*** 290
Anthony J Devaney
Northeastern University

Effects of coherence on the spatial and spectral distribution of energy in radiation fields

Emil Wolf

Department of Physics and Astronomy
University of Rochester
Rochester, NY 14627, USA

Abstract

It is now well established that the coherence properties of a source have a considerable influence on the spatial and the spectral distribution of energy throughout the field generated by the source. In this talk a review will be presented of some of the main researches relating to these phenomena. Among the topics which will be discussed are the following: The possibility of generating the same distribution of radiant intensity throughout the far zone by sources with different distributions of intensity and different states of spatial coherence; and also the possibility that two such sources will generate far fields which have the same coherence properties. Researches will also be reviewed regarding developments which followed the discovery made some years ago that the spectrum of light may change on propagation, even in free space. This effect has also its origin in the spatial coherence properties of the source. The possibility of utilizing this effect to develop a new technique for remote sensing and for determining field correlations from spectral analysis will be discussed.

Both theoretical and experimental investigations will be reviewed.

Progress in Electromagnetics Research Symposium, PIERS 1997 ISBN 962-442-097-1

Microscopic Models for Correlation Effects in Optical Physics

G.S. Agarwal, Physical Research Laboratory, Ahmedabad-380009, India

Almost all the previous works on the spatial correlation induced effects and, in particular, on Wolf shifts assume phenomenological models for spatial correlations. In this review talk, I will describe various approaches towards developing models for spatial correlations starting from the basic principles of physics. I will describe several different classes of possible experiments which depend on spatial correlations.

I first consider a system of radiating atoms. I demonstrate that due to virtual exchange of photons, the atoms get correlated. This virtual exchange in turn determines various spectral characteristics and, in particular, Wolf shifts. I further demonstrate the dependence of the degree of correlation on the average distance between atoms. I present explicit results for Wolf shifts from first principles.

Wolf and coworkers had also demonstrated the possibility of splitting a single line spectrum into a multiplet. I present a microscopic model which can lead to this result.

I further show that the spatial correlation is directly related to the spatial coherence of the environment in which atoms are radiating. A control of the spatial coherence of the environment will change correlations and hence other spectral characteristics. I present several examples of this, such as radiation from a system in the presence of a metallic boundary.

I next discuss Wolf effect in the *near field optics*.

Finally I describe the extension of Wolf's ideas in several directions (i) to higher order radiative processes as well as those problems which depend on higher order correlation functions of the source. Higher order radiative processes turn out to exhibit new types of spectral features which vanish if there are no source correlations (ii) to the effect of temporal correlations on pulse propagation problems.

Progress in Electromagnetics Research Symposium, PIERS 1997 ISBN 962-442-097-1

Source size evaluation by spectral measurements

F. Gori, M. Santarsiero, S. Vicalvi

Dipartimento di Fisica, Università "La Sapienza"
Piazzale A. Moro, 2; 00185 Roma - Italy

D. Paoletti, G. Schirripa Spagnolo

Dipartimento di Energetica Università dell'Aquila
Località Monteluco di Roio; 67040 Roio Poggio (AQ) - Italy

Abstract

Recently, great interest has been paid to the spectral changes of partially coherent wave fields under propagation [1]. In particular, the effects of spatial correlations of the light illuminating a Young's interferometer on the spectrum observed in the output region was studied both theoretically and experimentally [2-5]. It was also shown that information on geometrical characteristics of the source could be derived from spectral measurements in the output plane of the interferometer, for a fixed distance between Young's apertures.

In this paper, we report results obtained by use of this method, concerning the determination of the size of a one-dimensional source (a slit illuminated by a tungsten halogen lamp). It is remarkable the fact that such a simple experiment can furnish good results, as far as sensitivity and accuracy of the measurements are concerned.

A drawback of this method in practical cases is that the power actully available is utilized with a very low efficiency. First, a very small fraction of the power arriving at the interferomer is collected by the Young's apertures. In addition, the entrance slit of the spectrometer must be much smaller than the fringe spacing. As a consequence, the power utilized by the spectrometer is a very small fraction of the initial one.

In order to overcome this problem, we introduce here an interferometric scheme, with high throughput, which seems to be very promising even in hard experimental situations, thus increasing the practical interest of the spectral method as compared to other conventional tecniques . This applies in particular to the determination of the angular size of stars.

References

1. L. Mandel and E. Wolf, Optical Coherence and Quantum Optics (Cambridge University Press, Cambridge, 1995)

2. D. F. V. James and E. Wolf, Opt. Commun. **81**, 150 (1991)

3. M. Santarsiero and F. Gori, Phys. Lett. A **167**, 123 (1992)

4. A. T. Friberg and D. G. Fisher, Appl. Opt. **33**, 5426 (1994)

5. H. C. Kandpal, J. S. Vaishya, K. Saxena, D. S. Metha, and K. C. Joshi, J. Mod. Opt. 42, 455 (1995)

Spectrum Shaping Using Three-dimensional Antennas

Anthony J. Devaney
Department of Electrical and Computer Engineering
Northeastern University
Boston, MA 02115
email: devaney@cdsp.neu.edu

E. Wolf [1] has shown that the far field spectrum of partially coherent radiators is, in general, not equal to the near field spectrum and, in particular, depends on the degree of spatial coherence of the radiator. This spectrum modification occurs because the far field spectrum of a spatially distributed source is a function of the spatial correlation function of the source rather than just the source spectrum and, hence, is influenced by spatial structure of the source. Wolf has shown that spectrum modification via source coherence can be quite pronounced and has proposed this effect as a possible cause for the observed red shifts of spectral lines of star systems [2].

In this paper the underlying concepts of Wolf's theory are employed to investigate the possibility of shaping the spectrum of an antenna array as a function of angle by controlling the spatial coherence function of the array. Three classes of radiators (antenna arrays) are considered: (i) spatially incoherent, (ii) partially coherent, and (iii) perfectly coherent. It is shown that far field spectrum shaping is possible for both partially and fully spatially coherent radiators and expressions for the far field spectrums for these classes of radiators are obtained.

Specific attention is devoted to three-dimensional arrays of identical radiators such as dipoles having prescribed radiation patterns. The far field spectrum of such arrays are found to factor into the product of the spectrum of the individual antenna elements with a modulation factor that is simply the well known antenna array factor regarded as a function of frequency and parameterized by the observation direction. A simple example of a linear array is presented illustrating the general theory outlined in the paper. Computer simulations are presented for this and related simple examples illustrating that both center frequency shifting and bandwidth modification are possible even for simple linear arrays of the type considered here.

References

[1] E. Wolf, "Influence of source correlations on spectra of radiated fields," *International Trends in Optics*, ed. J.W. Goodman, (Academic Press, San Diego, 1991), p.221.

[2] E. Wolf, "Non-cosmological redshifts of spectral lines," *Nature*, **326**, 1987.

SESSION 7A9

Tuesday, January 7, AM 850-1210, Lecture Theatre 9, City University of Hong Kong

Analytical and Numerical Techniques in Photonics 1

Organizers: Kiyotoshi Yasumoto, Hung-chun Chang

Chairperson: Kiyotoshi Yasumoto, Kyushu University
Co-Chairperson: Hung-chun Chang, National Taiwan University

8:50 ***Boundary Integral Analysis of Form Birefringence and Polarization Beam-splitting Characteristics of Fused Biconical Optical Fiber Coupling Devices*** 292
*Hung-chun Chang, *Szu-Wen Yang, **Cheng-Wen Wu
*National Taiwan University
**Chung Cheng Institute of Technology

9:10 ***Full-Wave Coupled-Mode Theory of Nonlinear Fiber Coupler*** 293
Kiyotoshi Yasumoto, Hiroshi Maeda, Naohiro Mitsunaga
Kyushu University

9:30 ***FD-TD Method Based on the Principle of the Wave Digital Filters and Its Application to Analysis of Optical Waveguide Devices*** 294
*H Ikuno, *Y Naka, **A Yata, **M Nishimoto
*Kumamoto University
**Kumamoto University College of Medical Science

9:50 ***3D BEM Analysis of Light-Beam Scattering from Pit and Emboss Mark Models of Optical Disks*** 295
Toshitaka Kojima, Kenji Wakabayashi
Osaka Electro-Communication University

10:10 ***Coordinate Transformation Approach to the Problem of Three Collinear Symmetrical Fibers*** 296
Jian Hau Zhu, Weigan Lin
University of Electronic Science and Technology of China

10:30 **Break**

10:50 ***Directional Wave Field Decomposition in Integrated Optics*** 297
Hans Blok, Mathe Van Stralen
Delft University of Technology

11:10 ***Degenerate Points and Guided Modes in Magnetooptical Waveguides*** 298
Jaromir Pistora, Dalibor Ciprian, Roman Kantor, Romana Anyzova, Jaromir Seidl, Kamil Postava, Petr Nencka
Technical University Ostrava

11:30 ***Multiple Scale Technique in Photonics*** 299
Yijiang Chen
Australian National University

11:50 ***Design Optimization of a Widened X-Branch Demultiplexer by Ion-Exchange in Glass at 1.31 and 1.523 μm*** 300
G L Yip, L J M Babin
McGill University

BOUNDARY INTEGRAL ANALYSIS OF FORM BIREFRINGENCE AND POLARIZATION BEAMSPLITTING CHARACTERISTICS OF FUSED BICONICAL OPTICAL FIBER COUPLING DEVICES

Hung-chun Chang* and Szu-Wen Yang

Department of Electrical Engineering, National Taiwan University
Taipei, Taiwan 106-17, Republic of China

Cheng Wen Wu

Department of Physics, Chung Cheng Institute of Technology
Tahsi, Taoyuan, Taiwan 335-10, Republic of China

*also with the Graduate Institute of Electro-Optical Engineering, National Taiwan University

Polarization beamsplitting function can be achieved by properly designing the fused biconical 2 × 2 optical fiber coupler structure. We have successfully fabricated such couplers based on an extremely weakly fused structure in our laboratory. In the neck region of the fused coupler the light is guided by the boundary between the (reduced) fiber cladding and the external medium which is air in our case, and the fused structure becomes a strongly guiding composite waveguide. The cross-sectional structure in the coupling region has the dumbbell shape for strongly fused condition and touching circular shape for the extremely weakly fused condition. Because the tapered structure is slowly varying, it is an appropriate assumption that only the lowest-order even and odd modes are excited. The coupling coefficient which is defined as half the difference between the even and odd supermode propagation constants depends on the polarization state. The difference in the coupling coefficient between orthogonal polarization states is usually called the form birefringence. It is the form birefringence that causes the polarization splitting in the coupler. However, the form birefringence is small, and accurate calculation of such small quantity is the main concern of this paper.

Since the reduced fiber cladding, which is now the waveguiding region of the coupler, is essentially a homogeneous medium, the boundary integral method is a suitable technique for solving the modes on the coupler. Vectorial modes are calculated in our model and polarization-dependent coupling coefficients and the corresponding form birefringence are determined accurately. We have found that the coupler performance depends critically on the detailed shape of the cross-section. Such dependences on the degree of fusion and the normalized frequency have been studied thoroughly. We have also established a three-dimensional computer model, based on the vectorial modal calculation and by properly modeling the tapered structure, which can simulate the power transfer characteristics of the fused coupler during the tapering process. The coupled power versus the drawn length at different wavelengths, the dependence on the polarization of the input wave, and the polarization extinction ratio versus wavelength response can then be predicted. The sensitive dependence on the degree of fusion of the coupled power versus drawn length curve has been observed. Measured performances of our fabricated polarization beamsplitters have been found to agree very well with the simulation results. In summary, we have performed detailed analysis of the form birefringence of fused biconical 2 × 2 optical fiber coupling devices based on full-wave boundary integral method. Polarization beamsplitting characteristics are simulated using a 3-D vectorial model and agreement with experimental results is shown.

FULL-WAVE COUPLED-MODE THEORY OF NONLINEAR FIBER COUPLER

Kiyotoshi YASUMOTO, Hiroshi MAEDA, and Naohiro MITSUNAGA
Department of Computer Science and Communication Engineering
Kyushu University 36, Fukuoka 812, Japan

Nonlinear guided wave devices are currently the topic of major interest for ultra-high-speed optical signal processing. One of the promising devices is nonlinear fiber couplers that consists of two closely spaced, parallel, single mode optical fibers with cores of Kerr-like nonlinear materials as shown in Fig.1. During the past decade, the power-dependent transfer characteristics in nonlinear fiber couplers have been extensively investigated by using the coupled-mode theory. It is now well-known that a nonlinear fiber coupler with a suitable length behaves as an optical switch. The output channel is changed from one core to the other when the input powers exceed some critical level. However those studies are based on the scalar wave approximation for optical fibers, and hence the polarization effect in the coupler has been ignored.

In this paper, we present a more rigorous coupled-mode theory for a nonlinear fiber coupler with use of the full-wave formulation. The theory is an extension of the approach developed recently by authors for the analysis of a linear fiber coupler and nonlinear planar waveguide couplers. There exist two orthogonally polarized modes for an isolated single-mode fiber in the linear limit, which are the degenerate E_z-sin θ and E_z-cos θ modes. When two optical fibers are in close proximity and the refractive index of each core is perturbed by a nonlinear modification depending on the optical powers, the orthogonally polarized modes couple to each other through the linear cross-coupling between two fibers and the nonlinear self-phase and cross-phase modulations in each of fibers. Using the singular perturbation technique[1], the coupled-mode equations to describe such a coupling in nonlinear optical fibers are obtained in closed form. The numerical results show that the coupling length, the critical power for optical switching, and the polarization of output light depend on the polarization state as well as the powers of input light.

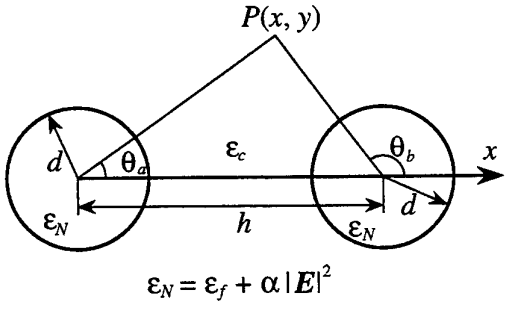


Fig. 1 Cross section of a nonlinear optical fiber coupler composed of a linear cladding with ε_c and Kerr-like nonlinear cores with $\varepsilon_N = \varepsilon_f + \alpha |E|^2$.

[1] K. Yasumoto, J. Lightwave Technol., Vol.12, No.1, pp.74-81, Jan. 1994.

FD-TD METHOD BASED ON THE PRINCIPLE OF THE WAVE DIGITAL FILTERS AND ITS APPLICATION TO ANALYSIS OF OPTICAL WAVEGUIDE DEVICES

H. Ikuno, Y.Naka, A.Yata*, and M.Nishimoto
Department of Electrical and Computer Engineering
Kumamoto University, Kurokami 2-39-1, Kumamoto 860, Japan
*Kumamoto University College of Medical Science, Kumamoto 862, Japan

In order to model the wave interaction on complicated devices in the area of ultrafast optical technology, we need to process ultra wideband signals on such structures, that is, to evaluate reflected and/or radiated fields in optical waveguides [1,2]. For such purposes many researchers have been studying on the development Maxwell solvers. One of the most promising techniques for the Maxwell solver is the finite-difference time-domain (FD-TD) method [3], because this method can be easily implemented to the problems mentioned above and its algorithm is simple and massively parallel and it has an ideal ABC called a 'perfectly matched layer' (PML) [4]. The schemes employed on the FD-TD method [3,4], however, are restricted to the central difference one. For the discretization of the Maxwell equation based on the principle of the wave digital filters (WDFs), we use the trapezoidal rule [5].

From the numerical point of view, the trapezoidal rule has several advantages over the central difference scheme, such as numerical stability, robustness and so on [5]. Since we have a WDFs representation of the Maxwell equation in the physical region [5], here we show a WDFs representation of the Maxwell equation in the PML which can be realized by using current controlled voltage sources [6]. By using the PML whose loss increases gracefully with depth, we check how the PML suppresses reflected waves from the interfaces between the computational zone and the PML. Then we calculate the wave interaction in optical waveguide devices. Finally we show numerically that we can evaluate radiation fields and reflected fields on waveguide discontinuities, tapered wave-guides, and waveguides with quantum well structures. We can conclude that the FD-TD method presented here is one of the Maxwell solvers.

References

[1] R.W.Ziolkowski and J.B.Judkins, J.Opt.Soc.Am., B, vol.10, pp.186-198, 1993.
[2] M.P.-May, A.Taflove, and J.Baron, IEEE Trans.,vol.MTT-42, pp.1514-1523,
[3] K.S.Yee, IEEE Trans., vol.AP-14, pp.302-307, 1966.
[4] J.P.Berenger, J. Computational Phys., vol.114, pp.185-200, 1994.
[5] A.Fettweis and G.Nitsche, J.VLSI Signal Processing, vol.3, pp.7-24,1991.
[6] D.E.Johnson et al., Basic electric circuit analysis, Prentice-Hall, Chap.3, 1984.

3D BEM Analysis of Light-Beam Scattering from Pit and Emboss Mark Models of Optical Disks

Toshitaka Kojima and Kenji Wakabayashi
Department of Electro-Communication Engineering
Osaka Electro-Communication University
Hatsu-cho, Neyagawa-Shi 572, Japan

Various types of optical disks have been proposed and put to practical use as a medium with which to realize high-density and high-speed recording of information. In order to realize a higher-density version of the conventional CD ROM type of optical disks such as digital video disk (DVD), it is required to reduce the size of pit and emboss marks recorded on a disk surface suitably as well as the reduction of the spot size of read-out laser beams.

In the present paper, we treat two different shapes of pit and emboss as the marks of recorded signal,i.e., cylinder type and conical trapezoid type. By using three dimensional boundary element method(3D BEM), the readout characteristics of sum and differential signals are obtained and the dependence of them on the size of the pit and emboss marks is examined.

It is clearly shown that the results predicted by the scalar theory can not be used for the present models. For scalar analysis, it is well known that the minimum output of the sum signal is obtained for the case where the depth of cylindrical pit and the height of cylindrical emboss are equal to a quarter of a wave length and the minimum values for both cases are same. However, in the present analysis, the cylindrical pit with the depth of a quarter of a wave length dose not give the minimum of the sum signal output. It is also shown here that the sum signal characteristics for the cylindrical emboss mark are better than those for the cylindrical pit mark and, on the other hand, the differential signal characteristics for the pit mark are better than those for the emboss mark.

Coordinate Transformation Approach to the Problem of Three collinear Symmetrical Fibers

Jian Hua Zhu and Weigan Lin

University of Electronic Science and Technology of China,
Chengdu,610054,China

A Cassinian Oval is given by

$$(x^2 - y^2)^2 - 2c^2(x^2 - y^2) = a^4 - c^4 \tag{1}$$

in polar coordinates

$$\rho^2 = c^2 cos2\varphi + \sqrt{a^4 - c^4 sin^2 2\varphi} \tag{2}$$

and also can be written as $|z-c| \cdot |z+c| = a^2 = (e^{u/2})^2 = |e^{u+jv}|$, or

$$z = c(e^{u+jv} + 1)^{1/2} = a(e^w + 1)^{1/2} \tag{3}$$

from which we can obtain an Inverse Cassinian Oval

$$\bar{z} = c(e^w + 1)^{-1/2} \quad (c^2 - a^4)(x^2 + y^2)^2 - 2c^2(x^2 - y^2) + 1 = 0 \tag{4}$$

The useful peculiarity of (3) and (4) is that they consist of a pair of seperated ovals if $a < c$; they are lone ovals when $a > c$. When $u=0$, (3) gives a Lemntscate

$$z^2 = 2c^2 cos2\varphi \tag{5}$$

While (4) gives a hyperbola

$$x^2 - y^2 = 1/2 \tag{6}$$

The three parallel collinear fiber system consisting of an identical pair of fibers, of permitivity $\in_1$, seperatel by a dlistauce D, with a central fiber of permittivity $\in_2$ is now transformed into a three layered planar guiding system in the w-plane, where for $u < -u_1$, the permittivity is $\left|\frac{dz}{dw}\right|_1^2 \in_1$, for $-u_1 \leqslant u \leqslant u_2$, the permittivity is $\left|\frac{dz}{dw}\right|^2 \in_2$ and for $u > u_2 > 0$, the permittivity is $\left|\frac{dz}{dw}\right|_2^2 \in_2$. This planar layered guiding pyetem can he analyged with ease if we properly handle the factor $\frac{dz}{dw}$, $|\frac{dz}{dw}|^2 = \frac{a^2 e^{2u}}{4\rho_1^3}$, where p_1 is given in (2), from (1) we can find, $|\bar{z}| = |z| = a/\rho_1^{1/2}$, so we can write (15) as follows

$$|\frac{dz}{dw}|^2 = \frac{a^2 e^{2u}}{4} |\frac{z}{a}|^6, \text{and also,} |\frac{dz}{dw}|^2 = \frac{a^2}{4\sqrt{2}} \frac{e^{2u}}{(coshu + cosv)^{3/2}}$$

while in the W-plane, the logitudinal electric and magnetic field components E_z and H_z both satisfy the following wave equation

$$\frac{\alpha^2 E_z}{\alpha u^2} + \frac{a^2 E_z}{\alpha v^2} + k_i^2 |\frac{dz}{dw}|^2 = 0.$$

DIRECTIONAL WAVE FIELD DECOMPOSITION IN INTEGRATED OPTICS

by HANS BLOK and MATHÉ VAN STRALEN

Laboratory of Electromagnetic Research
Department of Electrical Engineering
Delft University of Technology
P.O. Box 5031, 2600 GA Delft, The Netherlands

Phone 31 15 2786291, Fax 31 15 2786194
E-mail h.blok@et.tudelft.nl

ABSTRACT

Directional wave field decomposition is a tool for analyzing and computing the propagation of waves in configurations with a certain directionality, such as waveguiding structures in photonic devices, e.g. tapers, Y-junctions and directional couplers (MMI's). In these devices the electromagnetic wave field mainly propagates along the longitudinal direction, while being gradually influenced by the variations in the material parameters. In this paper a new directional wave field decomposition, based upon the complete electromagnetic field equations is discussed. The approach is linked with ideas in seismics and underwater acoustics. The method consists of three main steps. First, the initial field at some reference plane is mathematically decomposed in waves travelling forward and backward in the preferred direction. The interaction between the forward and backward travelling waves due to inhomogeneities in the (preferred) direction of propagation is then described by a generalized Bremmer coupling series. If reflections can be neglected, only the first term corresponding to the direct wave needs to be determined and the scheme changes into a simple and fast, initial value problem, in which the longitudinal axis plays mathematically the role of a time axis. In general, a few terms of the generalized Bremmer coupling series must be taken into account. Finally, the forward and backward travelling waves are recomposed in the field at the desired positions. In the general case of lateral inhomogeneous medium, this decomposition procedure involves the symbol calculus of pseudo-differential operators and Fourier integral operators. The proposed approach results in a clear overview in which all other known BPM-type methods (like the method of lines, collocation method, mode expansion method, Lanczos method and wide-angle Padé BPM) can be placed.
In this paper, we discuss in detail the derivation of sparse matrix representations of the pseudo-differential operators. The matrix representation follows from a rational approximation of the square root quarter and the derivatives. The parametrization thus introduced lends itself to an overall optimization that minimizes the errors for a chosen discretization.
From an analysis of several numerical results the possibilities and the limits of the decomposition method will be discussed.

Degenerate points and guided modes in magnetooptical waveguides

Jaromír Pištora, Dalibor Ciprian, Roman Kantor, Romana Anýžová,
Jaromír Seidl, Kamil Postava, Petr Nencka

Department of Physics, Technical University Ostrava,
17.listopadu 1, 708 33 Ostrava - Poruba
Czech Republic

Based on 4x4 matrix formalism the conditions of waveguiding are investigated in absorbing and anisotropic film systems. The attention is paid on multilayered structures formed by ultra-thin magnetooptical films between dielectric layers. The polarisation of the guided modes is generally elliptical. Because of the absence of mode coupling for transversal configuration we can separate waveguide relations for two independent polarizations. In this case only reflection coefficient r_{pp} for p-polarised waves is dependent on off-diagonal elements of dielectric tensor.

Dispersion curves of guided modes in multilayers have been realized. The shapes of these dispersion curves are functions of the total thickness and geometry of the planar structure. The absorption of magnetooptical films has influence on dispersion curve shifts. This influence is a function of mode order and polarisation. For only dielectric planar waveguiding systems the refractive effective index of TE guided mode has higher value than one of TM polarised wave for the same mode order. In our magnetooptical and absorbing multilayered waveguides the crossover points, when TE and TM guided modes have the same effective indices of refraction, have been observed. These crossover points are referred to as degenerate points. The positions of the crossover points between the curves for hybrid modes in the multilayers have been analysed and a relationship to the degenerate points of TE and TM modes has been studied in detail. These effects are presented together with the field distribution across the magnetooptical multilayered structure. The discussed results allow a direct interpretation and applications in the analysis of the planar multilayered magnetooptical systems in the integrated optics and memory technology.

Multiple scale technique in photonics

Yijiang Chen
Optical Sciences Centre
Australian National University
Canberra, Australia

Abstract

Soliton propagation in an optical fiber or in a uniform medium is governed by the nonlinear Schrödinger equation. For an axial uniform Kerr medium, the governing equation is integrable by inverse scattering transform. However, when the propagation medium is axial nonuniform, such as dispersion tailored optical fibers, the nonlinear Schrödinger equation with variable coefficient is no longer integrable. When the axial variation is slow, we show that the perturbed nonlinear Schrödinger equation can be solved by multiple scale method. To the first order, the soliton solutions to the perturbed nonlinear Schrödinger equation are found to have the same form as that of the unperturbed system, but the amplitude, width and phase are function of the propagation distance. By keeping higher order terms, the form of the solution becomes complicated. Applications of the general solutions to various special cases of practical axial nonuniform media will also be discussed.

Progress in Electromagnetics Research Symposium, PIERS 1997 ISBN 962-442-097-1

Design Optimization of a Widened X-Branch Demultiplexer by Ion-Exchange in Glass at 1.31 and 1.523 μm

G.L. Yip and L.J.M. Babin

Guided-Wave Photonics Laboratory
Department of Electrical Engineering
McGill University
3480 University Street
Montreal, Quebec, Canada, H3A 2A7
Tel: (514) 398-7132, Fax: (514) 398-4470
E.Mail: yip@rosy.lan.mcgill.ca

Abstract

Wavelength division multiplex (WDM) has been used extensively to increase channel capacity in wide-band communication systems. Not surprisingly, WDM has become one of the key techniques currently being developed for signal processing in wide-band optical fiber communication in order to better utilize the enormous bandwidth capacity offered by a single-mode fiber. Among the many waveguide structures proposed and studied, this paper will present the design optimization of one wavelength multi/demultiplexer , which has the advantage of its simplicity both in configuration and operating principle and, hence, also in fabrication. The device consists of input and output waveguides in the form of two identical tapered directional couplers of length l_t connected adiabatically to a two-mode central waveguide of length L and width 2W. Each channel guide in the tapered region has a width W. This device works on the principle of interference between the two normal modes (TMI) (Neyer, 1983; Bernadi et al, 1989) supported by the structure, namely, the symmetric mode Ψ_s and the anti-symmetric mode Ψ_a. In each tapered region and the central region, the two propagation constraints β_s and β_a for Ψ_s and Ψ_a differ. Along the device length, the two modes accumulate a relative phase difference Φ. The power outputs are given by $P_l = P_{in} \cos^2(\Phi/2)$ and $P_x = P_{in} \sin^2(\Phi/2)$ where P_l denotes the device's power output from the output channel on the same side of the device's center line as the input channel for the input power P_{in} and P_x that from the other output channel . The device fabrication requires only one photomask in a single-step K^+-ion exchange in soda-lime glass. The design modelling involves the gradient-index profile modelling by the effective-index method (EIM), employing the numerical Runge-Kutta scheme. This is followed by the simulation of the beam propagation through the device, using a two-dimensional finite - difference vector beam propagation method (2-D FD-VBPM). This simulation enables the device performances to be design-optimized. A comparison between the theoretical and experimental results will be made to demonstrate the effectiveness of this design methodology.

SESSION 7P9

Tuesday, January 7, PM 1330-1610, Lecture Theatre 9, City University of Hong Kong

Analytical and Numerical Techniques in Photonics 2

Organizers: Kiyotoshi Yasumoto, Hung-chun Chang

Chairperson: Kiyotoshi Yasumoto, Kyushu University
Co-Chairperson: Yasumitsu Miyazaki, Toyohashi University of Technology

13:30 ***Transfer Function Statistics of Multi-Mode Systems*** 302
Harrison E Rowe
Stevens Institute of Technology

13:50 ***Low-Loss Transition Design in Optical Dielectric Waveguides*** 303
Tomohiro Mizuno, Mikio Tsuji, Hiroshi Shigesawa
Doshisha University

14:10 ***Analysis of Bent single-Mode Slab Waveguides with Finite Cladding Thinkness by Coupled-Mode Theory*** 304
Maria Mirianashvili, Kazuo Ono, Masashi Hotta
Ehime University

14:30 ***Accurate Modal Solutions of Optical Waveguides by Finite Elements*** 305
B M A Rahman
City University of London

14:50 ***Dynamic Coherent Characteristics of Waveguide Type Optical Amplifiers Using Garnet Crystal Films*** 306
Yasumitsu Miyazaki
Toyohashi University of Technology

15:10 **Break**

15:30 ***Efficient and Accurate Analysis of Photonic Devices with the Method of Lines*** 307
R Pregla, E Ahlers, S Helfert
FernUniversität

15:50 ***Scattering of Electromagnetic Waves by Multilayer Gratings with Periodic Surface-Relief*** 308
Tsuneki Yamasaki, Takashi Hinata, Toshio Hosono
Nihon University

TRANSFER FUNCTION STATISTICS OF MULTI-MODE SYSTEMS

Harrison E. Rowe

Department of Electrical Engineering and Computer Science
Stevens Institute of Technology
Hoboken, New Jersey 07030 USA

Mailing address:
9 Buttonwood Lane
Rumson, New Jersey 07760 USA

We study the transfer-function deviations due to random errors in multi-mode systems. Kronecker products play a central role in this work.

Multi-mode transmission occurs in two types of systems: 1. Oversize guides, such as millimeter waveguides or optical fibers. 2. Multi-layer optical coatings, designed as windows, mirrors, or filters.

Different modes in oversize guides are uncoupled if the guide is perfect; imperfections couple the modes together, the principal coupling occurring among forward-traveling modes. Such coupling is undesirable if independent transmission of the different modes is desired; mode coupling can improve the overall transmission under certain circumstances. The coupled line equations describe such systems.

Multi-layer coatings contain both forward and backward traveling waves; the thickness and electrical parameters of the individual coatings are designed to produce the desired transmission/reflection characteristics of the overall system. The Fresnel coefficients at the interfaces between different layers describe these systems.

In both cases the desired transmission performance is perturbed by random errors. Oversize guides are adversely affected by geometric and material imperfections, multi-layer coatings by departures of the thickness and electrical properties of the individual layers from their design values.

Kronecker products have greatly extended the scope of analysis of these systems, by the use of symbolic computation procedures, such as those of MAPLE. We illustrate the power of these methods with a variety of results for the transfer function statistics, including single- and multi-mode coherent and incoherent inputs, general imperfection spectra, exact solutions for white and multi-level Markov imperfections.

LOW-LOSS TRANSITION DESIGN IN OPTICAL DIELECTRIC WAVEGUIDES

Tomohiro Mizuno, Mikio Tsuji, and Hiroshi Shigesawa
Department of Electronics, Doshisha University,
Tanabe, Kyoto, 610-03 Japan

TEL: +81-774-65-6358 FAX: +81-774-65-6824 E-mail: mtsuji@mail.doshisha.ac.jp

A new design method is proposed for planar optical-dielectric-waveguide transitions. Any optical transition, usually used in open-waveguide configuration, is accompanied by undesirable continuous-spectral waves (or the radiation waves). The present authors presented, for the first time, a low-loss design method of Y-type transitions[1], in which the radiation waves are intentionally generated continuously along the transition and controlled in their magnitude and phase so that they could play an important role in reducing the transition loss due to radiation. The theoretical basis of that design method is on the invention of the spectral-composite modes[1], and its numerical basis is to approximate any transition by a number of infinitesimal step discontinuities which are connected in tandem through a uniform dielectric waveguide with variable segment length and guide width. Then these structural variables are solved by the modified Newton iteration method to fulfill the given constraint condition on the transition. The design approach mentioned above was indeed very accurate in general, but a drawback is much time consumption, and will become deadly in optical region.

To overcome this drawback, we propose here an alterative new method, by which a desired transition of open type is designed by putting it into a package box. It will be true that, if a transition of open type is successfully synthesized, both the guided modes and a continuum of the radiation waves must propagate being bound close to the transition structure, and the transmission characteristics cannot be affected significantly by the package walls assumed apart a distance from the structural axis. Then, time-consumed numerical integrations necessary in the previous method can be performed analytically because of the simple modal functions of the quantized radiation modes. In the present method, such a quantization is done into the twofold elements; one consists of the quantized modes when the walls are short circuited, while the other is obtained by the open-circuited walls. This idea is very effective to automatically reject spurious solutions in the optimization routine. The approach mentioned above is applicable to any frequency range. However, if we consider the optical devices with a small difference of the refractive indices between the core and the surrounding, the above approach is simplified further. For such a structure, the field distribution on a plane transverse to the transition axis does not significantly change as the wave travels. Then, we take only a few lower-order guided and quantized modes into account in the modified Newton iteration method. The techniques mentioned above useful in the optical region are very effective to relax the memory size and the cpu time.

Design examples for the Y branch in both the millimeter-wave and optical frequency ranges will be demonstrated at the talk. Both results are very compact compared to ones designed by ordinary methods, and the attained insertion loss is less than 0.1dB for both Y branch. For further investigation, it is necessary to develop a method available to three dimensional devices. A simple approximate method was already presented by the present authors[2], but a more accurate design method based on the FEM will be presented at the talk.

References

[1] H. Shigesawa, et al., "Theoretically zero-loss design of planar dielectric waveguide Y-branch," Digest of IEEE Intern'l Microwave Symp., Long Beach, CA, Z-5, June 1989.

[2] M. Tsuji, et al., "Challenge to 3-D discontinuous dielectric-waveguide circuit analysis," Digest of IEEE Intern'l Microwave Symp., New York, NY, X-5, May 1988.

Analysis of Bent Single-Mode Slab Waveguides with Finite Cladding Thickness by Coupled-Mode Theory

Maria Mirianashvili, Kazuo Ono and Masashi Hotta
Department of Electrical and Electronic Engineering
Faculty of Engineering, Ehime University
3 Bunkyo, Matsuyama 790-77, Japan
E-mail: ono@optgw.ee.ehime-u.ac.jp
Fax: +81-89-927-9792

Many numerical or approximate methods, that assume infinitely extended cladding, have been developed to study the propagation characteristics of bent optical waveguides and fibers. This article discusses the crucial practical problem of fundamental transmission properties of the bent single-mode waveguides with finite cladding thickness.

Two straight waveguides are connected by the bent slab waveguide, which runs along the arc of a circle. It is assumed that the cladding is finite and the buffer, outer region of cladding, is air. With the use of conformal transformation technique [1], a curved waveguide is replaced by a straight waveguide with an equivalent refractive index profile. For this nonuniform structure, the field propagation involves modal power exchange, which may be accurately described by coupled-mode formalism [2]. There are several possibilities to obtain the coupled equations, which arise from the different ways of describing the modes of the structure. We use the expansion in terms of ideal modes, which is particularly well suited to our case of waveguides with perfect geometry but inhomogeneous refractive index profile. As ideal modes for fibers are well known, the same expansion may be easily applied to these structures too.

The straight waveguide with the core refractive index equal to cladding refractive index is taken as an ideal case. After ignoring the radiation waves, the ideal modes are represented by finite number of bound normal modes only. This set of modes converts scalar wave equations to the system of coupled ordinary differential equations. The coupling coefficients for ideal modes have a simple general form. The equation system may be easily solved by Runge-Kutta method.

The numerical results show that the transmitted power in fundamental mode of the output waveguide varies with the parameters of the structure. The curvature of waveguide causes radiation from the core. As the cladding is finite, the radiated wave is reflected at cladding-buffer boundary and couples with the core fundamental mode. Thus, transmitted power is quasi-periodic function of the length of the bend [3]. The pure bend loss of the fundamental mode is derived from the slope of the transmitted power, which is dependent on propagation distance. The results are in good agreement with those obtained by Marcuse's analytical formula [4].

References:

[1] M. Heiblum and J.H. Harris, "Analysis of curved optical waveguide by conformal transformation", IEEE J.Quantum Electron., vol.QE-11, pp.75-83, 1975.
[2] D. Marcuse, "Theory of dielectric optical waveguides", 2nd ed., Academic Press, San Diego, CA, 1991.
[3] K. Ono, K. Oda and M. Hotta, "Bend loss in single mode optical planar waveguides with finite cladding thickness", Proc. PIERS'95, Seattle, Washington, USA, p.386, 1995.
[4] D. Marcuse, "Light transmission optics", 2nd ed., Robert E.Krieger, Malabar, FL, 1989.

ACCURATE MODAL SOLUTIONS OF OPTICAL WAVEGUIDES BY FINITE ELEMENTS

B M A Rahman
City University,
EEIE, Northampton Square, London EC1V 0HB, UK.

Since the advent of semiconductor laser and optical fibers, the emergence and progress of optical technology has been significant. To exploit the full potential of the new technology, the complexity of the optical devices and associated waveguides has also increased. The optical waveguides are the basic building blocks of more complex optical systems and accurate characterization of these waveguides is necessary for system optimization.

Although many semi-analytical and numerical methods have been introduced and used to analyze different types of optical waveguides, but however, the finite element method has been established as one of the most powerful and versatile techniques to analyze a wide range of practical waveguides. The use of irregular meshes which allows arbitrary variation of refractive indices is the main advantage of this method, and more recently adaptive re-meshing has been used to exploit this feature. The use of vector formulations, and particularly the use of vector **H**-field formulation provides *exact-solution-in-the-limit* for optical waveguides with two-dimensional confinement. This method has been further benefited by the development of the penalty technique to suppress spurious modes and the use of infinite elements to represent an open boundary optical structure. For the **H**-field formulation, efficient sparse solver has been developed, and by the use of perturbation technique this method has been further extended to characterize waveguides with loss/and gain media. Iteration procedure has been introduced to characterize optical field dependant nonlinear optical waveguides.

Modal solutions of a wide range of linear optical waveguides including multiple quantum well regions, surface plasmon layers, highly anisotropic, nonlinear and active optical waveguides and synchronous and nonsynchronous directional couplers with two-dimensional confinement will be presented.

Progress in Electromagnetics Research Symposium, PIERS 1997 ISBN 962-442-097-1

Dynamic Coherent Characteristics of waveguide Type Optical Amplifiers Using Garnet Crystal Films

Yasumitsu Miyazaki,
Department of Information and Computer Sciences,
Tempaku-cho, Hibarigaoka,
Toyohashi 440, JAPAN
Tel: 0532-47-0111, Fax: 0532-47-0152

Waveguide type optical amplifiers constructed by rare-earth ion doped garnet crystal film layers and channel waveguides on garnet crystals are very important for optical communication of fiber to home system and optical signal processing. These optical functional waveguide devices have non-linear characteristics for input optical signal and pumping signal generated by semiconductor lasers. Coherent and non-linear characteristics are important factors for optical waveguide amplifiers using input signal perturbed in transmission lines and small pumping sources. Optical amplification is one of non-linear characteristics concerned with optical mixing of two different partially coherent optical waves of disturbed input signal in random and dispersive transmission lines and pumping signal. Partial coherent characteristics of optical amplification in waveguide type optical devices are theoretically discussed considering the partially coherent interaction of optical signals with pumping waves.

High speed signal processing is an indispensable technique to costruct high speed and large parallel optical communication and information processing system. Dynamical analysis of partial coherent wave mixing in non-linear devices of optical amplifiers is considered with optical material constants of quantum structures such as energy level life time and relaxation time of rare-earth ions. Based on the study of dynamical coherent characteristics of waveguide type optical amplifiers, optimum systems of high speed and large capacity communication systems and information processing using integrated optics are shown to be realized.

Progress in Electromagnetics Research Symposium, PIERS 1997 ISBN 962-442-097-1

Efficicient and Accurate Analysis of Photonic Devices with the Method of Lines

R. Pregla, E. Ahlers, S. Helfert
FernUniversität, Allgemeine und Theoretische Elektrotechnik,
D-58084 Hagen, Germany
e-mail: R.Pregla@FernUni-Hagen.de

Photonic devices are complex structures composed by a high number of inhomogeneous layers. A special example is the vertical cavity surface emitting laser structure (VCSEL) sketched in Fig. 1.

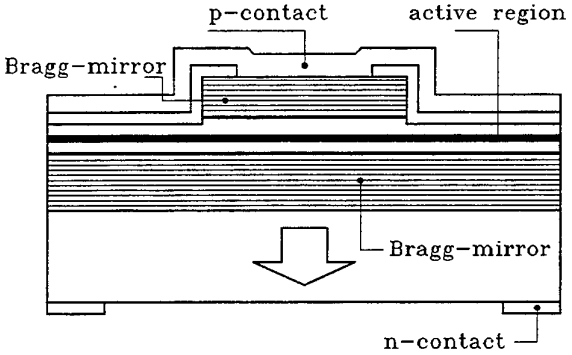


Fig. 1: Structure of a vertical cavity laser

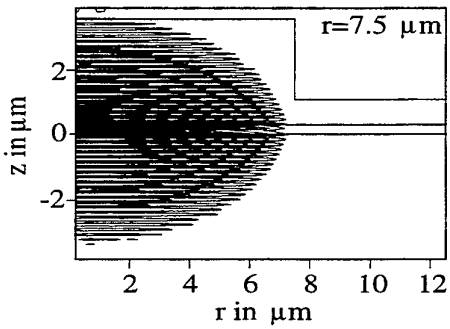


Fig. 2: Intensity distribution of the electric field

Each of the Bragg mirrors consists of a large number of cylindrical slices which are inhomogeneous in radial direction. This structure is an example for a general complicated photonic device. The analysis is based on the Method of Lines (MoL) which is a very stable algorithm. So, very accurate results are obtained. The MoL can be understood as a generalized transmission line theory. It consists of two main parts. First, the resonant frequency or the propagation constant has to be computed. For this purpose the general impedances are transformed from the outer layers (free space above and below) to the most important inner layers. In the VCSEL analysis the impedances are transformed to the upper and lower side of the active region. Fulfilling the conditions at this layer (or interface in other problems) an implicit eigenvalue problem for the field can be formulated. The solution of this equation leads to the resonant frequency or the propagation constant. It should be stated that the impedances at all interfaces are computed with a high degree of accuracy. The impedance transformation is possible even if the layers are of different radii (or of different widths).

The second main part is the calculation of the field in every point of the structure. Analyzing VCSELs, the knowledge of accurate values for the field in each layer is essential, especially the radiated field should be known "exactly". However, the computation of the field is a difficult task in a multilayered structure.

In the MoL the fields can be decomposed into forward and backward propagating parts. Using these parts together with the calculated impedances, the fields can be computed in each layer with high accuracy and without numerical problems.

As a numerical example the calculated intensity distribution of the electric field in a VCSEL is shown in Fig. 2.

The algorithm here described can also be used for the analysis of concatenated waveguide sections. Additionally, it should be mentioned that the MoL is useful not only to determine the optical field but also for the thermal analysis of the structure.

[1] E. Ahlers and R. Pregla, "Analysis of Multilayered and Multisectioned Circular Structures using the Vector-MoL-BPM in Cylindrical Coordinates", Proc: 7th European Conference on Integrated Optics, Delft, The Netherlands, April 3–6, 1995, 185–188

[2] R. Pregla, "The Method of Lines for Modeling of Integrated Optics Structures", in *Latsis Symposium on Computational Electromagnetics*, H. Baggenstos, Ed., ETH Zürich, 1995, pp. 216–229.

Scattering of Electromagnetic Waves by Multilayer Gratings with Periodic Surface-Relief

Tsuneki YAMASAKI , Takashi HINATA and Toshio HOSONO

Department of Electrical Engineering
College of Science and Technology
Nihon University , 1-8, Surugadai Kanda Chiyoda Ku
Tokyo, 101 Japan

Recentry, the refractive index can easily be controlled to make periodic structures by the development of manufactureing technology of optical devices. Accordingly, the numerical method which are applicable to inhomogeneous grating have been proposed.

In this paper, we have analyzed , using improved Fourier series expansion method and multilayer method , the scattering of a plane electromagnetic wave by multilayer gratings with periodic surface-relief whose interior distribution of permittivity is sinusoidally modulated in the direction of depth(=d) both TE and TM cases. In the analysis ,the Multilayer region is divided into an assembly of stratified thin layers with modulated index . In our method, the order of the matrix to be solved depends only on the modal truncation number, but not on the number of layers. Therefore, this method is applicable to a wide range of inhomogeneous dielectric gratings for both scattering and guiding problems.

Numerical results are given for the scattering proble on the transmi tted power for the following profiles:

(1) the surface profile $h(z)[0 \leq z <$p ,p :period of grating] of relief:

$$(A)h(z) = \frac{d}{2}\{\cos(\frac{2\pi}{p}z) - 1\}; \quad \text{sinusoidal profile}$$

$$(B)h(z) = \frac{d}{p}z - d; \quad \text{trianglar profile}$$

(2)the distribution of permittivity $\varepsilon(x, z)$ in the $-d < x \leq 0$; d: depth of grating

$$\varepsilon(x, z) \triangleq \begin{cases} \varepsilon_1 & ; \ h(z) \leq x < 0 \\ \varepsilon_A\{1 - \delta\cos(\frac{2\pi}{d}x)\} & ; \ -d \leq x < h(z) \end{cases}$$

$\varepsilon_A \triangleq$the average relative permittivity, $\delta \triangleq$the modulation index

In the numerical results, The influences of the incident angle ,and the frequency on the transmitted power are compared between the (A) type and the (B) type are discussed.

SESSION 7A8

Tuesday, January 7, AM 850-1230, Lecture Theatre 8, City University of Hong Kong

Photonics, Nonlinear Optics & Devices 1

Chairperson: P S Chung, City University of Hong Kong
Co-Chairperson: G L Yip, McGrill Univesity

8:50 ***A Study of Bending Waveguide for Semiconductor Photonics*** 310
Ching-Fuh Lin, Hsu-Feng Chou, Fuh-Hsiang Yang
National Taiwan University

9:10 ***Fractional Correlation Through Joint Transform Correlator*** 311
Yen Lo, Hsuan T Chang, Chung J Kuo
National Chung Cheng University

9:30 ***Inversion Techniques for Dispersive Optical Medium*** 312
An Ge, Paul A Richardson, Lakshman S Tamil
University of Texas at Dallas

9:50 ***A Novel Vector Theory for Second Harmonic Generation in Optical Waveguides*** 313
*N Hamelin, *Y T Chow, **P J Chandler
*City University of Hong Kong
**The University of Sussex

10:10 ***Optical Waveguide in Silicon Using Diffusion*** 314
E M W Wong, C F Lee, E Y B Pun, P S Chung
Optoelectronics Research Centre, City University of Hong Kong

10:30 **Break**

10:50 ***A Rigorous Analysis of the Lightwave and Microwave Interaction in a Mach-Zehnder Electrooptic Modulator*** 315
Philippe Zatta, Tchanguiz Razban
IRESTE

11:10 ***Coherent Cross-Talk Statistics of Feedback Buffer Memories*** 316
*D A C C Jayasinghe, **S J Madden, *W L R Perera, *P L Chu
*University of New South Wales
**Telstra Research Laboratories

11:30 ***Study on TSSL as Logic Components Employed in Optical Information Processing and Photonic Switching System*** 317
Zhijian Zhang, Yili Guo, Hanyi Zhang
Tsinghua University, Beijing

11:50 ***Integrated Optical Flip-flops*** 318
You-fa Wang
Merchant Marine College of Shanghai Maritime University

12:10 ***Analysis of Chaos in Intracavity-Doubled Laser by Using Dimension-Reducing Method*** 319
Dang Xiang, Zhenghong Jing, Ying Li
Jiading Campus of Shanghai University

A study of bending waveguide for semiconductor photonics

Ching-Fuh Lin(1), Hsu-Feng Chou(2), and Fuh-Hsiang Yang(1)
(1) Institute of Electro-optical Engineering
and Department of Electrical Engineering
(2) Department of Physics
National Taiwan University
Taipei, Taiwan, R.O.C.

Abstract

Photonics fabricated on semiconductor substrates has obtained growing interests in recent years. The bending waveguide is very important for applications in photonics, for example, in semiconductor interferemetric modulator, directional coupler switch, and monolithic integrated ring-cavity semiconductor laser. The bending waveguide is used to direct the lightwave to the target components on the same chip. The semiconductor waveguides are different from other waveguides by the characteristics of large refractive index in the materials and usually higher loss. Therefore, the study of light propagation in the semiconductor waveguide is important. In this presentation, we will report the simulation of light propagation in the semiconductor ridge waveguide and experimental properties of superluminescent diodes using such a bent ridge waveguide. Simulation works are based on Finite Difference Beam Propagation Method (FD-BPM). Simulation shows that, at the bending angle 7°, the light hardly propagates along the waveguide. Experimentally, superluminescent diodes are fabricated with a 220 μm straight waveguide and a 280 μm circularly bent ridge waveguide. The waveguide nearest to the output facet is bent at an angle of 7° from the normal of the cleaved facet. The light is observed to propagate along the waveguide and the output far-field pattern is therefore crescent-shaped. The discrepancy between the simulation and the experimental observation is due to the error of the FD-BPM at large bending angles. To improve the simulation, the circularly bent ridge-waveguide structure is conformally mapped into a straight waveguide. The FD-BPM is then applied in the transformed domain. Significant improvement on the simulation results at the bending angle 7° or larger is obtained. The simulation and the experiment both show that the field distribution in the semiconductor waveguide is highly asymmetric.

Fractional Correlation through Joint Transform Correlator

Yen Lo, Hsuan T. Chang & Chung J. Kuo

Signal and Media (SAM) Laboratory

Department of Electrical Engineering

National Chung Cheng University

Chiayi, Taiwan 62107

Abstract

Fractional correlation has been proposed recently. Fractional correlation is not always a shift-invariant operation. This operation leads to some new applications for fractional correlation as shift-variant image detection. In this paper, we modified the architecture of joint (Fourier) transform correlator (JTC) such that fractional correlation can be obtained. This system is thus named as joint (Fourier) transform fractional correlator (JTFC). The mathematical result of our JTFC is derived. In addition, simulation is used to verify our mathematical results.

†Please correspond with C.J. Kuo (kuo@ee.ccu.edu.tw) ‡Topic: #9

INVERSION TECHNIQUES FOR DISPERSIVE OPTICAL MEDIUM

An Ge, Paul A. Richardson and Lakshman S. Tamil
Broadband Communications Laboratory
Erik Jonsson of Engineering and Computer Science
University of Texas at Dallas, Richardson, TX 75083-0688

In a dispersive optical medium, the propagation constant varies with the wavelength of the light transmitted. Designing a wave guiding medium where different wavelengths can be transmitted with the same propagation constant are important in many applications such as optical amplifiers. The traditional way to design such a wave guiding system is by trial and error where an assumed refractive index profile of the medium is changed in an iterative fashion to achieve the desired transmission characteristics. This is an extremely difficult and time consuming procedure and the result is not always guaranteed.

We have developed inversion techniques that can be used to synthesize refractive index profiles of dispersive medium that can transmit different wavelengths with the same prescribed propagation constants. We achieve the objective by reformulating the wave equation as Schrodinger equation with an energy-dependent potential and the requirement that the waveguide should have the same propagation constant at different frequencies translates into a corresponding energy dependent potential supporting bound states of specified binding energies. Then a transformation reduces the inverse problem to a Schrodinger inverse problem for an energy-independent potential. The modified inverse problem can then be solved using analytical or numerical techniques. The translation of the potential into the refractive index profile of the medium involves solving a nonlinear differential equation.

We have solved both the cases of planar and cylindrical waveguides. Inversion procedures for both the cases along with numerical examples will be presented.

References

1. M. A. Hooshyar and L. S. Tamil, " Inverse scattering theory and the design of planar optical waveguides with the same propagation constants for different frequencies," Inverse Problems, vol. 9, pp. 69-80, 1993.

2. D. B. Ge, A. K. Jordan and L. S. Tamil, "Numerical inverse scattering theory for the design of planar optical waveguides," vol. 11, pp. 2809-2815, 1994.

A novel vector theory for second harmonic generation in optical waveguides

*N. Hamelin, *Y. T. Chow and **P.J. Chandler

*Electronics Engineering Department,
City University of Hong Kong
83 Tat Chee Avenue
Kowloon Hong Kong

** The University of Sussex
Maps Brighton BN1 9QH UK

Abstract:
Phase matching is a very important concept in non-linear optics. Active optical devices such as frequency converters would be useless if they were not fabricated in such way that their characteristics respect a phase matching condition. So far phase matching has been describe mainly with Maxwell equations In this article the authors give a new view of phase matching. We use Vector algebra to established the phase matching principles essential to non-linear optics. This paper also study the case of imperfect waveguides, such as lossy guides or waveguides with a non-uniform depth. Effects on the phase matching condition and the SHG signal output are study via a computer simulation. Such a view on phase matching is absent from the literature. It is more flexible than the Maxwell formulation and simulation of SHG phenomenon in the waveguide are readily produced.
This paper is divided into three main parts: In a first part we give a physical description of the principles of phase matching. In a second part we formulate the vector theory and finally a last part we study using vectorial algebra effects of losses and waveguides inhomogeinity.

Optical waveguide in silicon using diffusion

E. M.W. Wong, C.F. Lee, E.Y.B. Pun, and P.S. Chung
Department of Electronic Engineering
Optoelectronics Research Centre
City University of Hong Kong,
Tat Chee Avenue, Kowloon, Hong Kong

Abstract

Silicon is one of the most important materials in semiconductor electronics, and integrated electronic devices and VLSI processing technology is highly developed. Recently, there is an increasing interest in using silicon as a material for integrated optical devices, because of its optical transparency at wavelengths >1.2μm. Integrated optical modulators, switches, and integration of waveguides and photodetectors in silicon have been realized. Silicon based low cost integrated optical device will be a key element for applications such as optical interconnects in high speed computers, wavelength multiplexers/demultiplexers, and optical signal processing.

Different techniques for making optical waveguides in or on silicon have been demonstrated, these include lightly doped silicon on heavily doped silicon, diffusion using GeSi alloy, silicon-on-insulator (SOI), silicon-on-sapphire, and epitaxial grown GeSi layer. Among these techniques the simplest is diffusion, and expensive equipment like MBE (molecular beam epitaxy) and CVD (chemical vapour deposition) are not required.

In this paper, we report on our studies of optical waveguides in silicon substrates using SiGe indiffusion process. The diffusion source was alternate layers of Si and Ge thin films vacuum deposited onto Si substrate. The total thickness of thin film was 500nm. The temperature and the diffusion time used was 1200°C and 65h. The waveguide loss and the intensity profile of these channel waveguides were characterized at 1.3μm and 1.5μm. Below 4μm linewidth, the channel waveguide is single mode, and the propagation loss is ≈3 dB/cm.

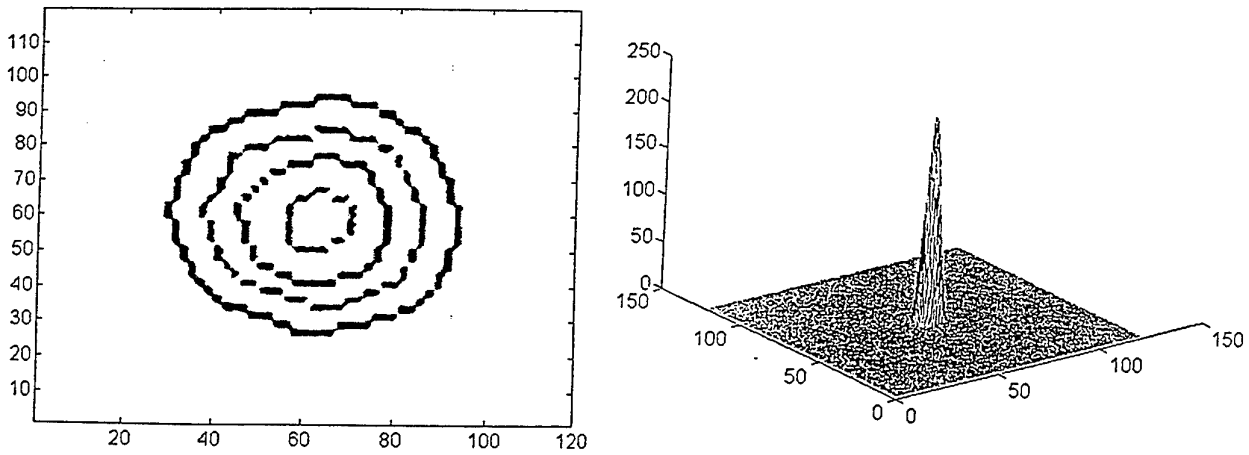


Fig.1 2D and 3D profiles of a 4μm Ge indiffused Si channel waveguide measured at 1.5μm wavelength

A RIGOROUS ANALYSIS OF THE LIGHTWAVE AND MICROWAVE INTERACTION IN A MACH-ZEHNDER ELECTROOPTIC MODULATOR

Philippe ZATTA and Tchanguiz RAZBAN
IRESTE, Laboratoire SEI EP CNRS 63
La Chantrerie, C.P 3003, 44087 Nantes Cedex 03, France
Phone: (33)-40 68 32 61, Fax: (33)-40 68 32 33, e.mail: pzatta@ireste.fr

Introduction

In the literature several wideband and low-driving voltage Ti:$LiNbO_3$ Mach-Zehnder electrooptic modulators operating around 20 GHz have been reported. Nevertheless, lightwave and microwave interaction has not been rigorously investigated. In this paper we point out lightwave and microwave signal electrooptic mixing and interaction in a Mach-Zehnder electrooptic modulator via the rigorously computation of the overlap fields integral.

I- Theorical formulation of the overlap fields integral

The overlap fields integral Γ of the optical wave and the microwave signal is evaluated by the disturbance wave theory as follows:

$$\Gamma = \frac{\iint_S \vec{E}_m \cdot \left|\vec{E}_o\right|^2 dS}{\iint_S \left|\vec{E}_o\right|^2 dS}$$

II- Analysis of the optical wave electric field in the Ti:diffused optical waveguide

The effective indices and multilayers combined methods are used to compute the electric field components and the propagation characteristics of the optical wave for both the TE and TM optical polarizations when no microwave signal is applied to the traveling wave electrodes.

IV- A rigorous analysis of the microwave electric field by the spectral domain method

We use the basic spectral domain method with several modifications to account for the particular nature of the modulator structure [1]. The microwave electric field pattern in the $LiNbO_3$ substrate and the propagation constant are accurately computed for any microwave frequency.

V- Analysis of lightwave and microwave signal interaction in an M.-Z. Electrooptic Modulator

Once the optical and microwave electric fields are separately analysed, lightwave and microwave signal interaction analysis is pointed out by the computation of the overlap fields integral.

Conclusion

Microwave and optical interaction is strongly related to the optical wavelength, the microwave frequency and the electrodes structure. The aim of our investigations is to accurately predict the performances of the microwave devices based on electrooptic modulators such as antennas [2].

References

[1] C. J. Railton and J. P. McGeehan, IEEE-MTT, Vol. 37, No.7, July 1989, pp. 1099-1104.

[2] T. RAZBAN and P. ZATTA, Congrès Européen OPTO'94, Paris 1994, pp.235-239

Coherent Cross-Talk Statistics of Feedback Buffer Memories

D.A.C.C. Jayasinghe, S.J. Madden†, W.L.R. Perera, P.L. Chu

Optical Communications Group, School of Electrical Engineering, UNSW, Sydney 2052, Australia.
†Telstra Research Laboratories 770 Blackburn road, Clayton, Vic 3168, Australia.

In this paper we report simulation results of cross talk in a feedback fibre buffer-loop memory. We show, how different architectures of space switches change the performance of the buffer under different traffic conditions.

This particular feedback memory is intended to be used in a wavelength routing all-optical ATM switch node (Fig.1)[1], where incoming packets are converted to wavelengths corresponding to each output port. The feedback buffer consists of a single substrate space switch made out of 2x2 couplers. A significant portion of crosstalk is accumulated on to the signal in this space switch. Here, we compare the binary tree architecture which offers fairly good crosstalk performance at the expense of a large switch count, with the cross-bar architecture space switch. Cross-bar is a simple architecture with a comparatively lower switch count[2].

In our analysis, random packets are generated with a bernoulli arrival process. Packets in the node, ie the space switch and the buffer are monitored throughout. When two packets of the same wavelength simultaneously passes through the same coupler or waveguide cross over, coherent crosstalk is added on to both the signals inphase, as randomly polarised crosstalk shows a tendency to interfere inphase[3].

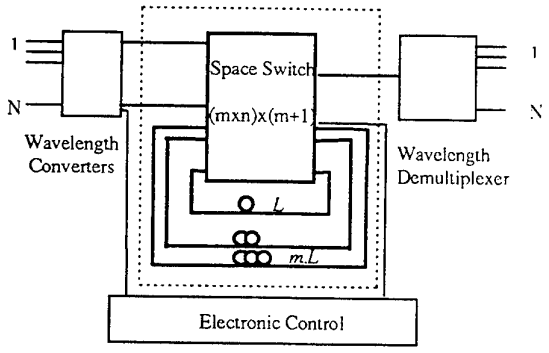


Fig1: Wavelength routing packet switch node with feedback fibre loop buffer

The cross talk accumulation on a certain packet at one point in time is a function of the arrival process, packets present in the switch and the buffer at that time and the load experienced.

In practical situations, all these factors are purely random, except for the load. Hence, the observed cross talk on a packet emerging out of the buffer is also random. We assume a realistic allowable cross talk to signal ratio level of -28dB for a cell to be accepted.

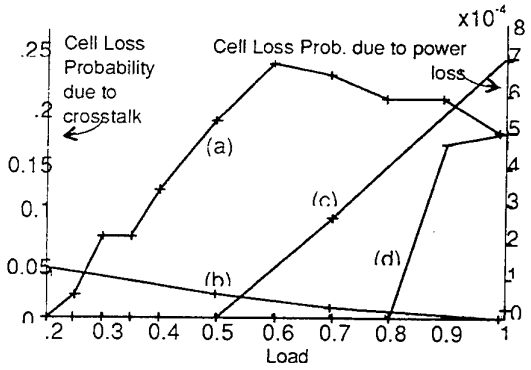


fig.2 Cell loss probability (i) due to crosstalk (a)cross-bar, (b)binary tree, (ii) due to power loss (c)binary tree, (d)cross-bar, : crosstalk .to signal ratio= -28dB, power loss= 5dB is allowed.

In the case of the cross-bar architecture, high traffic generates significant crosstalk levels.(Fig2(a)). However, in the binary tree, same wavelength packets are not simultaneously routed to the same outlet of the space switch. Hence, the major contribution to crosstalk would be from the wave guide cross overs (fig2(b)). On the other hand if the power loss in the buffer is considered, the cross-bar architecture seems to perform superior. (Fig 2 (c)&(d)).

Thus, under high traffic conditions, when the power loss is fairly low, the binary tree shows a significant performance improvement over the cross-bar architecture.

Reference

1. D.A.C.C. Jayasinghe et al. *to be published in proc. OECC'96*
2. S.J. Madden, *Appl.opt.* v 33 , 1994, pp8375-8386.
3. E.L. Goldstein et al *Photon. Tech. lett. v7 1995* pp 1345-1347.

Study on TSSL as logic components employed in optical information processing and photonic switching system

Zhijian Zhang Yili Guo Hanyi Zhang

Opto-electronic Div. E&E Dept. Tsinghua Univ. Beijing 100084, P.R.China

Photonic switching has received considerable attention because of its potential for high speed and large throughput optical network. Two-Section Semiconductor Laser (TSSL) is an important optical component for photonic switching system. It has two independent electrodes on active region and absorptive region respectively. By the injection of nonuniform field into different regions, nonuniform distribution of carriers, gain, refractive index and some nonlinear phenomena, such as gate switching, bistable and nonlinear amplifying, are formed. For this reason, TSSL can be used as notable elementary components in optical communication, photonic switching and optical information processing system.

The TSSL in our experiment was grown by two-step liquid-phase epitaxy. The length of the chip and absorptive region are 250μm, 20μm~60μm respectively. The depth and width of active region are 0.2μm and 2μm respectively. Some characteristics of TSSL about threshold current, optical spectrum, temperature and polarization influence are investigated. Also the TSSL was investigated to be used as logic components (and gate, or gate, or/non gate, and/non gate, other special logic gates) and nonlinear amplifier, switching array etc.

By composing TSSLs in series or parallel, high speed optical demultiplexer, optical pulse recoder and optical clock recover were demonstrated experimentally, which are very important components in optical communication and information processing.

An experimental photonic switching system employing TSSLs was setup. Ability of TSSL to switch optical pulse bits and optical data packets was demonstrated in this system. The interaction between electrical pulses and optical pulses was also investigated.

Integrated Optical Flip-flops

Wang You-fa
Merchant Marine College of Shanghai Maritime University
Pudong dadao 1550, Shanghai, P.R.China, 200135

Abstract

We present a series of integrated optical bistable triggers based on the saturating switching characteristics in the electro-optically controlled directional coupler switch in this paper. These optical bistable triggers include R-S optical flip-flop、D storage optical flip-flop、Clocked R-S optical flip-flop、Master-slave optical flip-flop、J-K optical flip-flop and optical pulse rising edge-triggered flip-flop. Each optical flip-flop has two types of input light–one is continuous laser which acts in the same way as the direct current voltage does in logic electric circuits, the other is optical pulse which acts as triggering signal or time clock pulse. In every optical flip-flop the input optical pulse and output optical pulse are the same in intensity, hence the optical output of the optical bistable triggers can be used as the triggering pulse of the next optical trigger. The principle of operation and basic properties of every optical flip-flop are described in this paper, and the results show that each optical flip-flop has the same function as the corresponding electronic flip-flop, which makes it easy to design integrated optical counters and shift registers.

Also discussed in this paper are the saturating switching characteristics of electro-optically controlled directional coupler switch, which has been discussed in detail in the other essays of mine. It is just the saturating switching characteristics that makes it easy to design integrated optical flip-flop using electro-optically controlled directional coupler waveguide switches and Mach-Zehnder interformeteric waveguide switches. The principle of operation of basic optical bistable device which, as the basic component of the integrated optical flip-flops, consists of two electro-optically controlled directional coupler waveguide switches as the introductions is mentioned at the beginning of the paper.

Analysis of Chaos In Intracavity-doubled Laser by Using Dimension-reducing Method

Dang Xiang Zhenghong Jing Ying Li

School of Communication and Information Engineering,
Jiading Campus of Shanghai University, Shanghai, China, 201800

Large amplitude fluctuations are observed when the doubling crystal *KTP* inserted into the laser cavity. The phenomenon is also called as greenlight chaos. The chaos in intracavity-doubled laser system arises from coupling of the various longitudinal modes by sum-frequency generation in the nonlinear crystal. We calculate the eigenvectors for the round-trip Jones matrix in the intracavity-doubled laser cavity, which combine to yield the electric fields at the doubled frequency. The multi-longitudinal-mode intensities are the magnitudes of field vector. At last the instablity of laser runing can be modled by a set of nonlinear rate equations about output intensities and gains. For a laser with *N*-longitudinal-mode oscillating, there are *2N* equations. The analysis and calculation become increasingly difficult for the laser with a large number of longitudinal modes. As we know, there is no report on simplifing these rate equation. A novel method presented here, based on the H.Haken's Slaving theory in synergetics, can reduce the dimension of rate equations from *2N* to *N*. According to Slaving theory , the variables in a complicate system can be devided into two types: the fast variables and slow variables. In the critical points, the development of system can only be determined by some slow variables. In the intracavity-doubled rate equations, we can eliminate longitudinal-mode intensities by using small-parameter method. So a set of *N* equations is obtained for *N*-longitudinal-mode. By the dimension-reducing, we have analysized some critical points at which the laser is running in various situations such as the stable, periodic and chaotic.

Key words: Chaos, Intracavity-doubled , Dimension-reducing.

SESSION 7P8

Tuesday, January 7, PM 1330-1650, Lecture Theatre 8, City University of Hong Kong

Nonlinear Optics & Applications

Organizer: E Herbert Li

Chairperson: E Herbert Li, University of Hong Kong
Co-Chairperson: B L Weiss, The University of Surrey

13:30 ***Ultrafast Laser-Induced Structural and Electronic Changes in Solids***+ 321
Eric Mazur, Eli N Glezer, Li Huang, J Paul Callan
Harvard University

14:10 ***Optical Information Processing by Using Anisotropic Diffraction in $BaTiO_3$*** 322
*Ming-Wen Chang, **Ching-Cherng Sun
*National Central University
**Chine Hsin College of Tech. & Commerce

14:30 ***Ultrashort Optical Pulses: Applications, Measurements and Generation*** 323
H K Tsang, L Y Chan, A H Liang, Y C Tong, Z Jiang, Zhijie Wang
The Chinese University of Hong Kong

14:50 ***Interdiffused Non-Square Quantum Wells for Applications in Optoelectronics*** 324
*K S Chan, **E Herbert Li
*City University of Hong Kong
**University of Hong Kong

15:10 Break

15:30 ***Porosity Determination Equation for Porous Silicon*** 325
De-liang Lian, K W Cheah
Hong Kong Baptist University

15:50 ***Effect of Control Pulsewidth on the Switching Efficiency of Nonlinear Optical Loop Mirror*** 326
W S Man, H Y Tam
The Hong Kong Polytechnic University

16:10 ***Analysis of Initial Frequency Chirp and Soliton Interaction on Nonlinear Pulse Propagation in a Dispersion-Shifted Fibre*** 327
P Shum, S F Yu, T I Yuk
University of Hong Kong

16:30 ***Effects of Cascading Second-Order Nonlinearities on Third-Harmonic Generation*** 328
Xue-Lin Yang, Sheng-Wu Xie
Shanghai Jiaotong University

+double time-slot (40 minutes)

Ultrafast Laser-Induced Structural and Electronic Changes in Solids

Eric Mazur, Eli N. Glezer, Li Huang, and J. Paul Callan
Division of Applied Sciences and Department of Physics, Harvard University
9 Oxford St., Cambridge, MA 02138

For over two decades the subject of laser-induced phase transitions in semiconductors has generated considerable interest. This interest is due to the technological importance of semiconductors and the research in this field was in part driven by the hope of developing better methods for the annealing of ion-implanted semiconductors. More recently, femtosecond laser pulses have made it possible to study highly non-equilibrium electron and lattice dynamics in semiconductors. In this talk we first present and overview of work on laser-induced structural and electronic changes in solids, and then describe recent work done in our group on GaAs.

In the experiments on GaAs we found that the optical excitation drives structural changes which strongly modify the bandstructure.[1-3] Using both linear and nonlinear optical techniques we have been able to directly observe the dielectric constant of GaAs during this phase transition, providing physical insight into the nature of the transition. Our data show that the laser pulse leads to a weakening of the covalent bonds in the sample. For high enough laser pulse energy, the covalent bonding changes dramatically and the resulting material becomes metallic above 2.5 eV.

Recently we developed a new broadband spectroscopic technique that allows us to simultaneously monitor, with 100-fs temporal resolution, the response of the dielectric function $\varepsilon(\omega)$ across the spectral range from 1.5 to 3.5 eV. The GaAs sample is driven by a 1.9-eV pump pulse and probed by a broadband probe pulse generated by strong self-phase modulation of a 70-fs 2.2-eV pulse in CaF_2. Reflectivities $R_1(\omega)$ and $R_2(\omega)$ are measured for p-polarized light at two incident angles, 60° and 76°, chosen to give high sensitivity to changes in the dielectric function. The reflectivity is determined by measuring both the reflected probe spectrum and a reference spectrum for each shot using an imaging spectrometer. The real and imaginary parts of the dielectric function are then determined from the experimentally determined reflectivies using the Fresnel equations. By varying the time delay between the pump and the probe, we observe the changes in the dielectric function in time as a result of the intense excitation. The broadband probe has a significant chirp, for which we compensate by temporally shifting the data based on a measured calibration of the dispersion.

The induced changes in the dielectric spectrum depend strongly on excitation strength. At 40% of the threshold for observable permanent change, the data display a drop in the real part and a broadening in the imaginary part of the dielectric function within a few hundred femtosecond after excitation. This initial change is probably due to the increase in carrier density. By 4 ps $\varepsilon(\omega)$ has changed considerably and agrees closely with the dielectric function of GaAs at 700 K,[4] indicating heating of the lattice by the electrons. At 65% of the threshold, the changes in $\varepsilon(\omega)$ are much more pronounced. The observed dielectric function in this regime is quite similar to that of amorphous GaAs[5] suggesting that the material becomes disordered. It is interesting to note that this occurs below the threshold for permanent change, indicating that the amorphization is reversible. Above threshold, these observed changes indicate changes in local bonding.

1. E.N. Glezer, Y. Siegal, L. Huang, and E. Mazur, Phys. Rev. B **51**, 6959 (1995).
2. E.N. Glezer, Y. Siegal, L. Huang, and E. Mazur, Phys. Rev. B **51**, 9589 (1995).
3. Y. Siegal, E.N. Glezer, L. Huang, and E. Mazur, Ann. Rev. of Mat. Sci. **25**, 223 (1995).
4. H. Yao, P.G. Snyder, and J.A. Woollam, preprint.
5. M. Erman et al., J. Appl. Phys. 56, 2664 (1984).

Optical information processing by using anisotropic diffraction in $BaTiO_3$

Ming-Wen Chang and Ching-Cherng Sun*

Institute of Optical Sciences, National Central University
Chung-Li 320, Taiwan, Republic of China

*Electronic Engineering Department
Chine Hsin College of Technology & Commerce
Chung-Li, Taiwan, Republic of China

Photorefractive crystals are the materials capable of recording dynamic phase volume holograms and they have been studied extensively for their potential applications of optical storage and real-time information processing such as optical correlation, optical phase conjugation and optical computing. $BaTiO_3$, due to its large electro-optic (EO) coefficient, is demonstrated to perform two-wave mixing, four-wave mixing, and self-pumped phase conjugation. In photorefractive phase volume holograms, there are two factors which determine the coupling effect of wave mixing, the first one is Bragg condition for volume holograms, and the other one is the EO tensor of the crystal.

Here this paper reports the review of the effects and the applications of optical information by using anisotropic diffraction in a normal-cut $BaTiO_3$. There are two special properties in the configuration that the optic axis is normal to the incident plane. One is that the refractive index change is as large as 2×10^{-4}; the other is that the diffraction process is permitted only when the polarizations of the probe beam and diffracted beam are mutually orthogonal, i.e., one is ordinary polarization and the other is extraordinary one. These characteristics cause anisotropic self-diffraction and make the crystal be used as a strong volume hologram. By using the characteristics, the applications of optical information processing, including matrix-matrix multiplication, contrast-reversible optical incoherent-to-coherent converter and the potential of optical storage, are presented.

Ultrashort Optical Pulses: Applications, Measurements and Generation

H.K.Tsang, L.Y.Chan, A.H.Liang, Y.C.Tong, Z.Jiang and Zhijie Wang
Department of Electronic Engineering,
The Chinese University of Hong Kong,
Shatin, New Territories, Hong Kong.
email:hktsang@ee.cuhk.edu.hk; Tel. +852-26098254; Fax: +852-26035558

Summary

Ultrashort optical pulses have many applications including soliton communications, nonlinear wavelength conversion, ultrafast all-optical switching and remote sensors. In this paper, recent work carried out at the Chinese University of Hong Kong on applications, methods of generation, and measurement of picosecond optical pulses at 1.3μm and 1.55μm wavelengths will be described.

The two-photon absorbtion (TPA) waveguide autocorrelator will be described and experimental results demonstrating its use for the pulse-width measurement of low power optical signals will be presented. The TPA autocorrelator has a sensitivity of 0.08 $(mW)^2$, which is over one order of magnitude better than a conventional second harmonic autocorrelator, and is particularly suited for measuring the pulse width of low duty-cycle ultrashort pulses generated by gain-switching or Q-switching a diode laser. The time resolution of the waveguide autocorrelator will be shown to be limited to about 10fs by waveguide modal birefringence.

Frequency chirp in ultrashort optical pulses will be considered theoretically, and a new pulse-width parameter called Laplacian pulsewidth will be introduced. The Laplacian pulse width is defined for a pulse $u(t)$ by

$$t_l \equiv \frac{1}{2}\left\{\frac{\int_{-\infty}^{+\infty}|u(t)|^2\,dt}{\int_{-\infty}^{\infty}\left[\frac{d|u(t)|}{dt}\right]^2 dt}\right\}^{0.5}$$

A new criterion for transform-limited pulses, based on the time-bandwidth product formed by the Laplacian pulse-width and RMS spectral width, will be described. The new criterion has the advantage of being independent of the pulse amplitude profile since the time-bandwidth product formed by the Laplacian pulse width and RMS spectral width is equal to 0.5 for all transform-limited pulses.

The generation of high power picosecond pulses from two-section tapered InGaAsP/InP laser diodes by Q-switching will be reviewed. Recent experimental results, including the generation of pulses with a peak power of 4W from a 1.3μm distributed feedback laser integrated with a tapered amplifier, will be presented and compared with numerical simulations. Other recent experimental results from two-section complex-coupled 1.5μm InGaAsP/InP distributed feedback lasers will also be presented.

Interdiffused Non-square Quantum Wells for applications in optoelectronics

K S Chan[#] and E Herbert Li[*]
Department of Physics and Materials Science
City University of Hong Kong;
* Department of Electrical and Electronics Engineering
University of Hong Kong.

Abstract

Interdiffused non-square single and multiple quantum well structures are currently attracting considerable interest for their applications in optoelectronics. This stems from both a fundamental point of view as well as for the realization of high performance devices and the fabrication of optoelectronic integrated circuits. The interdiffusion process is produced by using post-growth thermal annealing to induce the solid-state interdiffusion of atoms (such as Al and Ga) through the QW heterointerfaces (such as AlGaAs/GaAs) which alters the alloy composition profile(such as the spatial profile of the Al mole fraction along the QW growth axis) across the QW structure. In addition, the interdiffusion rate can be controlled by the techniques of impurity induced disordering and impurity-free vacancy interdiffusion. The optical properties of the quantum well, such as absorption, refractive index and gain, can be modified by the process of interdiffusion (due to band structure changes) so that it provides the ability to tune the operating wavelengths, reduce the power consumption and increase the switching time of photonic devices. It is also possible to confine photons between layers of as-grown and interdiffused QWs which have different refractive indices, which is due to the fact that both the band-gap and subband structure of the III-V semiconductor QW are a non-linear function of the alloy-composition. This latter ability to guide light both laterally and vertically in a planar structure is crucial to the monolithic integration technology of optoelectronic integrated circuits. In the present work, the optical properties such as absorption coefficient and optical gain of interdiffused quantum wells are analysed theoretically for applications in optoelectronic devices.

Porosity determination equation for porous silicon

De-liang Lian, and K.W. Cheah*

Department of Physics, Hong Kong Baptist University, Kowloon Tong, Hong Kong

(email address : kwcheah@hkbu..edu.hk)

In anodisation of silicon, the porosity of porous silicon formed is a function of etching current density, etching time and hydrofluoric acid. If the acid concentration is kept constant, it is possible to produce porous silicon with the desired porosity by varying the current density and etching time. Presently this process is based largely on experience and rule of thumb. This is inadequate if a more precise prediction is required, for example, a multilayer porous silicon with several different porosity layers is to be produced. Such multilayer porous silicon has the potential to produce narrow half width spectrum with higher luminescence intensity[1]. Here, we show that for porous silicon made from p-type silicon, there is an universal relationship among porosity, etching current density and etching rate. Using this relationship it is possible to determine (say) the change in porosity with respect to etching under a set etching current density. This relationship is checked against experimental data from several reports on these etching parameters, and they confirm the validity.

* - to whom all communication should be addressed to.

Effects of Control Pulsewidth on the Switching Efficiency of Nonlinear Optical Loop Mirror

W. S. Man, and H. Y. Tam

Department of Electrical Engineering
The Hong Kong Polytechnic University
Kowloon, Hong Kong

Abstract

The effects of control pulsewidth, with respects to the peak power of the control pulse, switching energy and switching efficiency, on all-optical control switching of soliton in nonlinear optical loop mirror (NOLM) are investigated numerically and the results are presented in this paper. In this work we considered an all-optical switching configuration in which the wavelengths of the control pulse and signal soliton straddles the dispersion zero to reduce pulse "walk-off". The central wavelengths of the signal and the control pulse are at 1560 nm and 1540 nm respectively.

The required peak power of the control pulse to achieve maximum switching efficiency decreases in proportional to the width of the control pulse. This is mainly due to the combined effect of the self phase modulation and group velocity dispersion. Our simulation shows that maximum switching efficiency of the NOLM occurred when the pulsewidth of the control pulse is three times of that of the signal and is independent of the loop length of the NOLM. However, the value of the maximum switching efficiency decreases with loop length. Our analysis also shown that to reduce the peak power of the control pulse by using a broader pulsewidth will always require more pulse energy. The switching efficiency of a NOLM with a loop length equivalent to four soliton period can be increased from about 90% to about 97% by using a control pulse with pulsewidth three times of that of the signal. In this case, the switching energy required to achieve maximum switching efficiency is about 25% more but the peak power required reduced to 56%. These results would be very useful in designing all-optical control switching of soliton in NOLM.

Progress in Electromagnetics Research Symposium, PIERS 1997 ISBN 962-442-097-1

Analysis of Initial Frequency Chirp and Soliton Interaction on Nonlinear Pulse Propagation in a Dispersion-Shifted Fiber

P. Shum, S. F. Yu and T. I. Yuk

Department of Electrical and Electronic Engineering, University of Hong Kong, Pokfulam Road, Hong Kong
Email : pshum@eee.hku.hk

Dispersive optical bistability in a Fabry-Perot, a distributed feedback (DFB), or a distributed Bragg reflector semiconductor laser has recently attracted much attention because of its potential for making highly functional optical devices. However these devices introduce initial frequency chirps to soliton pulses generated. Chirp is caused by a refractive index change in the semiconductor laser diode active layer, which can be due to changes in temperature or carrier density. This unwanted phenomenon is unavoidable whilst the laser is current modulated, and it causes chromatic dispersion or modal noise in practical optical fibre applications.

Optical solitons have been considered as potential information carriers in very high bandwidth optical fibre communication systems. In a digital soliton communication system, it is necessary to determine the optimum separation between adjacent solitons because the bit rate of digital signal transmission is inversely related to the time separation between neighbouring pulses. It is well known by now that soliton interaction can result in bandwidth reduction by a factor of 10 due to the variation of soliton separation as they travel down the fibre. Various methods are used to maintain the soliton separation : i) Phase alteration between neighbouring solitons. ii) Inclusion of the third-order dispersion term, the third order dispersion of an optical fibre can be used to reduce the mutual interaction between solitons when the fibre is operated nonlinearly. This provides a mean to improve the bandwidth of nonlinear fibre. iii) Unequal amplitude between neighbouring solitons, the larger the difference in amplitude, the more stable is the separation. Chirp can broaden the width of a soliton pulse with a larger portion of the input energy being transferred into unwanted dispersive tail. In a high bit-rate soliton communication system, the pulse broadening and the dispersive tail generated cause serious problems as the pulses are launched close to each other. It was found that positive initial chirp can enhance the interaction between pulses traveling in the two polarization axes of the fibre and thus can reduce the amplitude threshold for soliton trapping. However, at the same time, initially chirped pulses will broaden as they propagate along the fibre, which can diminish the maximum data transfer rate in a communication system. From the point of view of high bit-rate communication systems utilizing solitons, pulse broadening and the loss of energy from a chirped soliton to the highly dispersive non-soliton pulse can be a highly damaging effect.

Effects of cascading second-order nonlinearities on third-harmonic generation

Xue-lin Yang, Sheng-wu Xie

(Department of Applied Physics, Shanghai Jiaotong University, Shanghai 200030,CHINA)

Abstract

Since the second-order nonlinear optical interactions can be easily generated in acentric crystals, when we perform the direct third-harmonic generation (THG) process in these crystals, the cascading second-order interactions, i.e., two-step processes: SHG ($\omega_1+\omega_1=2\omega_1$) and frequency mixing ($2\omega_1+\omega_1=3\omega_1$), may happen simultaneously. That is to say, the observed third-harmonic signal may result from the cascading second-order interactions as well as the pure third-order one. Thus, the effective third-order coefficient should be the sum of the pure third-order susceptibility and effective third-order susceptibility of the cascading second-order interactions. We should take this effect into consideration when measuring the pure third-order susceptibility of crystals by THG method.

Generally speaking, there are phase mismatchings ΔK for the cascading second-order interactions in a phase matched THG process. In this paper, we have analyzed all the available cascading second-order interactions, and derived the formulae to calculate the phase mismatchings and the corresponding effective third-order coefficients, for both uniaxial or biaxial crystals. The results help us to distinguish the source of the observed third-harmonic signal, which is of great importance in the measurement of the pure third-order susceptibilities of crystals and in the design frequency conversion devices.

As an example, we have computed the phase mismatching ΔK and the effective third-order coefficient $\chi_{eff}^{(3)}$ for direct phase matched THG in lithium monohydrate (LFMH) biaxial crystals. The results show that, for the cascading second-order interactions in this case, ΔK is about $10^5 cm^{-1}$, and the corresponding $\chi_{eff}^{(3)}=10^{-18} esu$, which is about the same magnitude as the surrounding air. The effect in this case can be negligible. We conclude that the observed third-harmonic signal in our THG experiment is purely resulted from the third-order susceptibilities.

SESSION 7A7

Tuesday, January 7, AM 850-1250, Lecture Theatre 7, City University of Hong Kong

Bioelectromagnetic Image and Visualization

Organizer: Michio Miyakawa

Chairperson: Michio Miyakawa, Niigata University
Co-Chairperson: F Bardati, DISP Roma Tor Vergata University

8:50 ***Fundamental Study for Trans-body Imaging with Light*** 330
Koichi Shimizu,Katsuyuki Yamamoto
Hokkaido University

9:10 ***Reconstructed Images of Optical Tomography Using an Inversion Process*** 331
M R Jones,S G Proskurin,I W Kwee,Y Tanikawa,S Mizuno,Y Yamada
Ministry of International Trade and Industry

9:30 ***Real-time Reconstruction of NMR Images in NMR Fresnel Transform Technique*** 332
Satoshi Ito,Yoshifumi Yamada,Yoshitsugu Kamimura
Utsunomiya University

9:50 ***Virtual Images and Good Functioning of MR Equipments: Errors in Data Interpetration*** 333
*A A Russo, **R Delia
*Italian National Research Council
**Ministry of Health

10:10 ***Feasibility of Temperature Retrievals from Radiometric Data Measured In Vivo*** 334
*F Bardati, **P Tognolatti
*DISP Roma Tor Vergata Univ., **Universita dell'Aquila

10:30 **Break**

10:50 ***Computation of Microwave Radiometric Weighting Functions for Industrial and Medical Applications*** 335
K Ridaoui, B Bocquet, A Mamouni, Y Leroy
Institut d'Electronique et de Microelectronique du Nord

11:10 ***Microwave Radiometric Imaging by Deconvolution and Wiener Filtering*** 336
B Bocquet, S Mouty, R Ait-Abdelmalek, A Mamouni, Y Leroy
Institut d'Electronique et de Microelectronique du Nord

11:30 ***Analysis, Pre and Post-processing of a Hyperthermic Treatment for a Heterogeneous Phantom Model in Three Dimensions*** 337
*Y Kanai, **T Kashiwa, ***Y Saitoh, ***M Miyakawa
*Niigata Inst. of Tech., **Hokkaido Univ.,***Niigata Univ.

11:50 ***Computational - and Experimental - Visualization of Electromagnetic Power Absorbed by the Human Body****S Hoshina, *M Miyakawa, **Y Kanai 338
*Niigata University, **Niigata Institute of Technology

12:10 ***Measurement of Temperature and Blood Volume Change in Tissue During Hyperthermia Therapy by Impedance CT*** 339
Katsuyuki Sakamoto, Kitasato University

12:30 ***Light-Tissue Interaction and Evaluation of Color Information in Biomedicine*** 340
*M Akimoto, **T Asaeda, *Y Miyata, ***T Kikuta, ***H Namiki
*Nippon Medical School, **Color Consultant, ***Waseda Univ.

Fundamental Study for Trans-body Imaging with Light

Koichi Shimizu and Katsuyuki Yamamoto
Department of Bioengineering, Faculty of Engineering
Hokkaido University, N13 W8, Sapporo 060, Japan

With the recent progress of an optical technology, the feasibility of optical trans-body imaging has been pointed out. The strong scattering in body tissue has been identified as a difficult problem to realize the trans-body imaging. We have developed a technique to suppress the effect of the scattering using a differential principle.

In biomedical applications, we need to visualize the change in absorption that reflects the change in physiological functions such as ischemia and hypoxia. In the transillumination imaging, the spatial distribution of the absorption is strongly degraded by the scattering. Since the change in scattering property is much smaller than that of the absorption, we can suppress the effect of the scattering by taking the ratio (difference in log) of two images before and after some physiological change. In this way, we can visualize the physiological change inside a body in a transillumination image.

If we can suppress the scattering and get the light passed straight through the object, tomographic imaging becomes feasible using the same algorithm as an X-ray CT. We used the differential principle in the optical CT, as well. In this case, the effect of the scattering is suppressed by using a beam of collimated incident light and two detectors behind the scattering object.

The two detectors are placed on and off the optical axis of the beam of incident light. The on-axis detector receives three kinds of light. The first one is the light that experienced no scattering and propagated straight (ballistic photons). The second one is the light that was scattered along the optical axis of the incident light (snake photons). The third one is the light that was scattered and propagated in random direction in the tissue and reached the detector by chance. The first and the second kinds of light are useful in the CT imaging. However, with the mammalian tissues the first one is almost negligibly small, and even the second one is much smaller than the third one. The off-axis detector receives only the third component with the known angular distribution of diffuse scattering. Therefore, the randomly scattered component in transmitted light is greatly reduced by subtracting the output of the off-axis detector from the on-axis detector.

Using these scattering suppression techniques, we could obtain the following results. In the transillumination imaging, the local hypoxia in one of the mouse kidneys was visualized. The different types of local blood volume changes in the rat brain were visualized as well. In the CT imaging, the cross-sectional images of a living mouse were obtained. Due to the difficulties in an animal experiment, the spatial resolution was not satisfactory. However, the existence of a liver and kidneys was recognized in the CT images of a living mouse without using any contrast media.

Progress in Electromagnetics Research Symposium, PIERS 1997 ISBN 962-442-097-1

Reconstructed images of optical tomography using an inversion process

Matthew R. Jones, Sergei G. Proskurin, Ivo W. Kwee,
Yukari Tanikawa, Sho Mizuno, and Yukio Yamada
Mechanical Engineering Laboratory, Ministry of International Trade and Industry
1-2 Namiki, Tsukuba, Ibaraki 305, Japan

Abstract:

Optical tomography is a new modality of noninvasive diagnostic instrumentation. It has a capability of providing information on oxygenation status of living tissue through measuring the optical spectra of hemoglobin and/or myoglobin. However, the strong scattering of light by biological tissues makes very difficult optical tomography to be realized, and new algorithms for optical tomography must be developed. We have developed a new algorithm for optical tomography by using an inversion technique which is based on the photon diffusion equation. The propagation of light in strongly scattering and weakly absorbing media is modeled by the photon diffusion approximation, and the forward problem of light propagation is solved by using the Finite Element Method. The inversion process is a kind of quasi-Newton method with various regularization methods. Sample media for experiment were two cylindrical phantoms made of epoxy resin with titanium oxide particles mixed as scatterers. One of them was homogeneous in scattering and absorption while the other had inhomogeneity with an embedded small cylinder having increased absorption. The light source in near-infrared wavelength range was incident on the phantoms, and transmitted light was measured at many points around the cylinders. The measured data were processed by the new algorithm, and we have obtained a reconstructed image of the difference in the absorption coefficient between the homogeneous and inhomogeneous phantoms.

Real-time reconstruction of NMR images in NMR Fresnel transform technique

Satoshi ITO, Yoshifumi YAMADA and Yoshitsugu KAMIMURA

Department of Information Science, Utsunomiya Univ.

2753 Ishi-machi , Utsunomiya 321, JAPAN

Abstract

MRI high-speed imaging technique such as echo-planar imaging(EPI) has begun to be employed in commercial MRI system and data acquisition time may be shorten to less than 100msec. With this imaging system, if MR images were reconstructed in a moment, we would be allowed to get a real-time moving image. Optical computation has the advantage of very fast parallel processing and has the potential to overcome the time limitation related to image reconstruction. Holography is the most popular technique for optically reconstructing images.

Since the expression of NMR signal in the Fresnel transform technique is similar equation to that of the Fresnel diffraction equation in light, holographic reconstruction of NMR images is feasible, making a hologram from NMR spin-echo signal and reconstructing images using a coherent optical system.

In this paper, we describe a new method of opto-electronic reconstruction of NMR images using a liquid crystal-spatial light modulator(LC-SLM) as a hologram display, addressing a hologram electrically and using a coherent optical system. Experimental results show that considerably good images are obtained even by the commercially available LC-SLM. It indicates a possibility of real-time reconstruction of NMR images by combining the NMR high-speed imaging technique with this technique, because the hologram pattern on the LC-SLM is refreshed at a video-rate that is fully catch up with the data-acquisition time of high-speed imaging.

Virtual images and good functioning of MR equipments: Errors in data interpetration

A.A. Russo - Italian National Research Council - Safety and Prevention Department
Via di Pietralata, 190 - 00158 Rome (ITaly)
R. Delia - Ministry of Health - High Institute of Prevention and Work Safety
Ionizing and Non-Ionizing Radiation Laboratory -
ISPESL - Via di Fontana Candida, 1 - 00040 Monteporzio Catone (Rome) (Italy)

Introduction: In the 1985, a legislation on NMR (Nuclear Magnetic Resonance) equipment utilization in the medicine was promulgated in Italy. This low regards mainly the periodical quality control on the equipments. These controls allow to detect and so to remove the possible errors in the diagnostic results, which are produced by the virtual images, due to the artifacts often present, if the MR equipments are not good functioning.

Objective: The present study was aimed at assessing the effects of artifacts on the use of Magnetic Resonance Imaging (MRI).The objective of the present research is to develop and to apply a methodology, finalized to detect the virtual images, optimizing the times and the costs of the investigations.

Methods: During a period of five years of activity, 500 NMR equipments, with magnetic flux density from 0.2 T to 1.5 T, had been surveyed. On the basis of the obteined results, the authors have been set a standard protocol for the evaluation of the efficiency of the examined equipments. The measurement standard takes into account also the suggestions of the American Association of Physicists in Medicine . This methodology for the quality controls has been validated on a very great number of equipments and is suitable for almost all the diagnostic examinations, carried out by a NMR equipment.

Results and Discussion: Artifacts in MRI technology exist in prolific variety and many subtle artifacts are NORMAL to a properly functioning MRI system. Recognition and understanding of artifacts is important in order to distinguish those that are ABNORMAL and attributable to malfunctioning or mistuned equipment. In this paper the MRI artifacts are grouped in different categories on the basis of their appearance, recognizing that different sources may cause artifacts of similar appearance.

Feasibility of Temperature Retrievals from Radiometric Data Measured *In Vivo*

F. Bardati[1] and P. Tognolatti[2]

[1]DISP Roma Tor Vergata University
via della Ricerca Scientifica, 00133 Roma, Italy
[2]Dipartimento di Ingegneria Elettrica, Università dell'Aquila,
Poggio di Roio, 67040 L'Aquila, Italy

Multifrequency microwave radiometry has been considered for non-invasive thermal imaging of human body to a depth of a few centimetres from cutis. The feasibility of thermal retrievals has been investigated mostly with reference to synthesized noisy data. More recently, we have obtained retrievals of a subcutaneous hot spot from radiometric measurements performed in liquid phantoms simulating the electric properties of a muscle tissue. Despite these satisfactory indications, first inversions of *in vivo* data were inadequate. We refer to experiments on volunteers and to data that are obtained from a thigh during the thermal wash-out following a diathermy application. In this paper two main sources of errors of the technique are singled out when it is used during *in vivo* experiments.

The antenna used to collect the radiation from the body is a source of temperature-dependent thermal noise. This unwanted contribution must be subtracted from the data before their inversion. A theoretical model of the thermal behaviour of the contacting antenna has been developped and has been used for a comparison with the temperature variations measured at points of the antenna. Transient temperature patterns are obtained by immersion of the antenna open-end inside a water tank the temperature of which is accurately controlled.

A source of system errors is associated with the evaluation of the weighting (sensitivity) function that is the kernel of the radiometer integral equation. The weighting function is obtained from the deposited power pattern in the case where the radiometric antenna radiates onto the body itself. Numerical computations are performed by means of a FDTD code based on a 3D tissue map which, in turn, is interpolated from CT scans. Tissue complex permittivities and corresponding variations with temperature must be known. In this paper the accuracy of temperature retrievals is discussed in the presence of uncertainties of the electrical parameters.

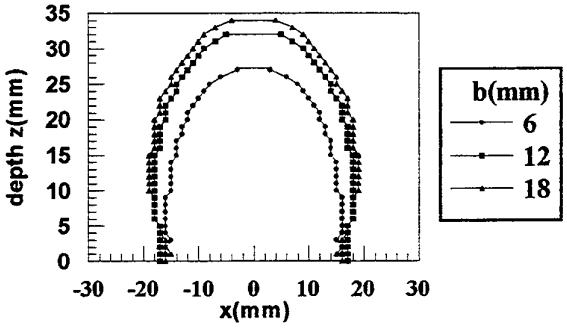
COMPUTATION OF MICROWAVE RADIOMETRIC WEIGHTING FUNCTIONS FOR INDUSTRIAL AND MEDICAL APPLICATIONS

K. Ridaoui, B. Bocquet, A. Mamouni, Y. Leroy

Institut d'Electronique et de Microélectronique du Nord
Département Hyperfréquences et Semiconducteurs U.M.R. CNRS 9929
Université des Sciences et Technologies de Lille 59655 Villeneuve d'Ascq Cedex FRANCE
Phone: +33-20 19 79 35 , Fax: +33-20 19 78 96 , e-mail: bertrand.bocquet@iemn.univ-lille1.fr

The measurement of the thermal noise in the microwave frequency range, leading to a non invasive thermometry, interests medical and industrial applications. The knowledge of the weighting functions is necessary to retrieve the temperature profile in the material ([1-3]). Recently, we have given a new definition of absolute weighting functions which represent the quantitative contribution to the radiometric signal of the different subvolumes of material.

A modal method of computation of the near field radiated by a wave guide in a lossy material is applied to homogeneous and multilayered structures [2-3]. The wave guide is rectangular and filled with a low loss dielectric. We consider the discontinuity between the two media, taking into account the mode matching technique of the transverse field components. We determine the electric field in three dimensions and deduce the radiometric weighting functions.



Example of limits of the coupling volumes for skin+breast in the section of the plane (xoz) for different sizes of the probe at 3 GHz

For example, we consider bilayered tissue (skin+breast) and different sizes of apertures (axb) of the probes (24mm x 6mm; 24mm x 12mm and 24mm x 18mm) and different frequencies (1.5; 3 and 4.5 GHz). We present examples of the weighting functions and the volume of material coupled to the probe. We demonstrate that the variation of size of the probe gives a variation of the weighting functions similar to a variation of the frequency.

The modal method cannot be applied to heterogeneous media, often met in industrial applications [4]. In this case, we use a finite element software. Examples of results are given for cylindrical thermal objects with a permittivity different to the surrounding material.

[1] A. Mamouni, Y. Leroy, B. Bocquet, J. C. Van de Velde, and Ph. Gelin, "Computation of near-field microwave radiometric signals: Definition and experimental verification" IEEE Trans. Microwave Theory Tech., vol. 39, pp. 124-132, Jan. 1991.

[2] B. Bocquet, P. Dehour, A. Mamouni, J. C. Van de Velde, and Y. Leroy, "Near field microwave radiometric weighting functions for multilayered materials", J. Electromagn. Waves Appl., vol. 7, no. 11, pp. 1497-1514, 1993.

[3] B. Bocquet, R. Aït-Abdelmalek, Y. Leroy, "Deconvolution and Wiener filtering of short-range radiometric images", Electronics Letters, Vol.29, n°18, pp1628-1632, 1993.

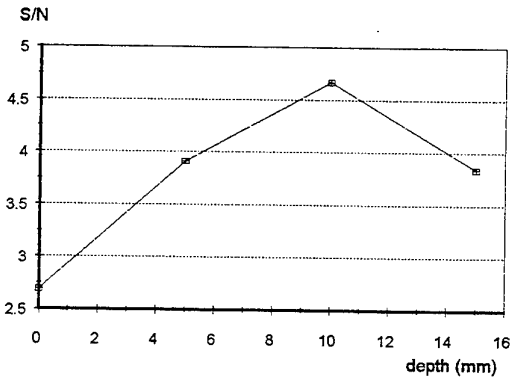
[4] B. Bocquet, J. C. Van de Velde, A. Mamouni, Y. Leroy, J. Ménard, O. Blondel, "Application de la radiométrie microonde au génie civil", 6ème JNM, juin 1989, Montpellier, France.

MICROWAVE RADIOMETRIC IMAGING BY DECONVOLUTION AND WIENER FILTERING

B. Bocquet, S. Mouty, R. Ait-Abdelmalek, A. Mamouni, Y. Leroy
Institut d'Electronique et de Microélectronique du Nord
Département Hyperfréquences et Semiconducteurs U.M.R. CNRS 9929
Université des Sciences et Technologies de Lille 59655 Villeneuve d'Ascq Cedex FRANCE
Phone: +33-20 19 79 35 , Fax: +33-20 19 78 96 , e.mail: bertrand.bocquet@iemn.univ-lille1.fr

Microwave Radiometric Imaging (MWI) is a non-invasive thermometric measurement in volume. A radiometer, centred around 3GHz, treats the thermal noise signal coming from hot volumes inside a body. The main application that we are looking for, is the detection and characterisation of breast tumours in terms of small size thermal volumes [1].

The development of a new inverse process permits to improve spatial resolution by taking into account the "instrument function" of the radiometric probe which are described by the weighting functions mentionned in the previous communication. These one depend on the frequency, size of the probe, structure and permittivity of the medium [2-3]. We have shown that the radiometric measurement is a convolution between these weighting functions and the physical temperature inside the body [4].



Experimental evolution of the signal to noise ratio in the image of a cylindrical thermal object of diameter 2.5cm with a temperature difference of 5°C with respect to surrounding matcrial, at a dcpth 10mm

We want to show that the deconvolution of the radiometric images by means of a well matched Wiener filtering improves the spatial resolution and permits quantitative informations. By inversion of the radiometric images with different slices of weighting functions, it is possible to retrieve size, temperature and depth of a cylindrical thermal object with a single frequency.

For example, the deconvolution of a thermal object of 2.5cm of diameter at $\Delta T=5°C$ gives an image more or less noisy. We analyse the signal to noise ratio in the image and we show that the best ratio is obtained for weighting functions corresponding to the real depth.

Generally, the use of a multifrequency radiometers permits to have these data [5-6]. The present method is an alternative to these rather complicated multifrequency radiometer.

[1] B. Bocquet, J.C. Van de Velde, A. Mamouni, Y. Leroy, G. Giaux, D. Delannoy, D. Delvallée, "Microwave radiometric imaging at 3GHz for the exploration of breast tumors", IEEE Trans. on MTT, Vol.38, n°6, 791-792, 1990

[2] A. Mamouni, Y. Leroy, B. Bocquet, J.C. Van de Velde, Ph. Gelin, "Computation of near-field microwave radiometric signals: definition and experimental verification," IEEE - MTT, Vol.39, n°1, 124-132, 1991

[3] B. Bocquet, P. Dehour, A. Mamouni, J.C. Van de Velde, Y. Leroy, "Near field microwave radiometric weighting functions for multilayered materials" J. of Elect. Waves and Appl., Vol.7, n°11, 1497-1514, 1993

[4] B. Bocquet, R. Aït-Abdelmalek, Y. Leroy, "Deconvolution and Wiener filtering of short-range radiometric images", Electronics Letters, Vol.29, n°18, pp1628-1632, 1993.

[5] F. Bardati, V.J. Brown, P. Tognolatti, "Temperature reconstruction in dielectric cylinder by multifrequency microwave radiometry", J. of Elect. Waves and Appl., Vol.7, n°11, 1549-1571, 1993

[6] S. Mizushina, T. Shimizu, K. Suzuki, M. Kinomura, H. Ohba, T. Sugiura, "Retrieval of temperature depth profiles in biological objects from multifrequency radiometric data", JEWA, Vol.7, n°11, 1515-1548, 1993

Analysis, pre- and post-processing of a hyperthermic treatment for a heterogeneous phantom model in three dimensions

Yasushi Kanai*, Tatsuya Kashiwa**, Yoshiaki Saitoh*** and Michio Miyakawa***
*Department of Information and Electronics Engineering, Niigata Institute of Technology,
1719 Fujihashi, Kashiwazaki 945-11 JAPAN
**Divison of Information and Communication Electronics, Hokkaido Univ.
N13-W8, Kita-Ku, Sapporo 060, JAPAN
***Department of Information engineering, Faculty of Engineering, Niigata Univ.,
8050 Ikarashi-2, Niigata 950-21, JAPAN

Hyperthermia is a method for cancer treatment in which induced heat is used to kill tumor cells. A hyperthermia system is required to raise the temperature of a selected volume of tissue to 42-45 °C, while other areas that surround the selected volume remain unharmed. For safety reasons and a more efficient use of the hyperthermic system, before clinical test, analysis of the heating characteristics under different conditions are carried out. Analysis based on numerical computations will be applied to estimate the heating performance under various conditions. In fact, numerical analysis will be indispensable even at the stage of clinical application in order to predict the temperature distribution inside the human body.

Previous computations usually have been carried out for two dimensional heterogeneous models. For these models, only the electromagnetic field is calculated and then the Specific Absorption Rate (SAR) is evaluated. When the SAR is evaluated, blood flow, which greatly affects the temperature is ignored.

This paper investigates the analysis, pre- and post-processing of a hyperthermic treatment for a heterogeneous phantom model in three dimensions [1]. We have used 3-D Finite-Difference Time-Domain method to analyze the heating phenomena by a reentrant resonant cavity applicator [2]. A 3-D heterogeneous phantom model is divided into variable finite-difference cells by our automatic mesh generator, then the electromagnetic field is calculated and heating energy is evaluated. Heat-transfer equations are solved for a heterogeneous phantom model with and without the blood flow.

By comparing electromagnetic energy and temperature distributions, we found that considering the blood flow is indispensable when predicting precise temperature distributions during a hyperthermic treatment. Temperature rises for various organs are also shown to be very important to assure the raising temperature of a selected volume to 42-45 °C, while the surrounding tissue remains at a safe temperature.

References

[1] Y. Kanai, et al., *IEEE Trans. Magn.*, Vol. 33, May, 1996 (in press).
[2] Y. Saitoh, et al.,*6th Int'l Congress on Hyperthermic Oncology*, Vol.1, 337, Apr. 1992.

Computational- and experimental-Visualization of electromagnetic power absorbed by the human body

S. Hoshina*, M. Miyakawa*, Y. Kanai**
*Niigata University, Faculty of Eng., Dept. of Info.
8050, Ikarashi 2, Niigata, 950-21 JAPAN, Tel: (025)262-6755, Fax: (+81) 25 261 2512
E-mail: hoshina@tibig.info.eng.niigata-u.ac.jp
**Niigata Institute of Tech., Information and Electronics Engineering.
E-mail: kanai@iee.niit.ac.jp

Recently, there has been a increasing interest in the effects of electromagnetic fields on biological systems. Particularly, the absorbed electromagnetic power by a human head has been a matter of great concern by many researchers.

This paper investigates the visualization of the absorbed electromagnetic power inside a human head. To visualize the absorbed power, we have used a newly developed gel phantom whose optical character changes from transparent to white and then opaque. The region which exceeds a certain temperature (clouding point) becomes white and then opaque. Because the clouded region is determined by the density, specific heat and clouding point and the initial temperature of the phantom and the power applied to the phantom, the power absorption can be estimated reversely by the infinitesimal region at border of the clouded region. The cylindrical phantom which has 30 cm-diameter and 30cm-high has been used to model a human head. The phantom material has almost the same electric property as biological tissues and the clouding point is designed to be 25C°. A helical antenna has been contacted to the phantom, then the power of 20 Watts at the frequency of 144 MHz has been applied for 30 minutes. Figure 1 shows the clouded region in which temperature exceeded 25C° due to power absorption from the helical antenna. From the figure, the absorbed power seems to decrease gradually as the distance from the antenna becomes larger.

To validate the absorbed power distribution estimated by the clouded region in the phantom, the absorbed power distribution has been computed by the Finite-Difference Time-Domain(FD-TD) method. Because the cylindrical phantom and an electric line source with the infinitesimal length are assumed, the computations have been carried out in two dimensions. Absorbed power distribution obtained by the calculation for the human head model noted above is shown in Fig. 2. As can be seen from the figure, the absorbed power decreases abruptly as the distance from the surface of the model increases, which is slightly different from the result obtained by the experiment. Since the power was supplied to the phantom for 30 min in the experiment, the thermal conduction in the phantom can no longer be neglected, then the difference between calculated and experimental results occurred. The clouded region observed in the phantom, however, agrees well with the region of large absorbed power obtained by the calculation. This means that the newly developed gel phantom can has a great potential to visualize the electromagnetic energy pattern absorbed by a human body.

Acknowledgments
We would like to thank Dr. T.Kashiwa of Hokkaido Univ. for providing the basic source program list of FD-TD method.

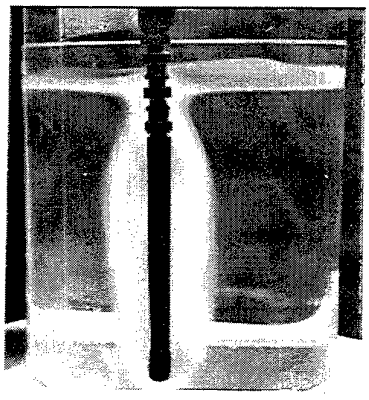


Fig.1 The cloud region absorbed power in the cylindrical phantom

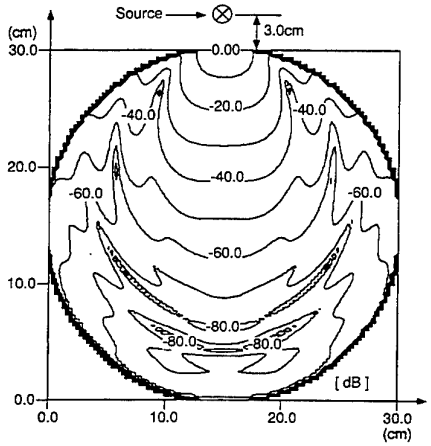


Fig.2 The calcucurated distribution of absorbed power acrosse the cylindrical phantom

Measurement of temperature and blood volume change in tissue during hyperthermia therapy by Impedance CT

Katsuyuki Sakamoto
Department of Clinical Engineering, School of Allied Health Sciences,
Kitasato University

Abstract

As everybody knows, the impedance of living tissue changes with the change of temperature of itself. The temperature coefficient is about -2%/°C. Therefore, if we measure the impedance change of a tissue which is heated up during hyperthermia therapy by impedance CT(IMPCT), we could estimate the temperature change of it. But IMPCT method for measuring the tissue temperature change has two fatal problems.

One is that since the current supplied through a point electrode widely spreads in the tissue and again converges to the opposite point electrode, it is very difficult to obtain a reconstructed impedance image of a cross section of the body from data obtained through electrodes arranged around the cross section. The data include not only information about the cross section but also 3 dimensional information.

Second problem is that when the temperature of a tissue increases, not only resistivity of the tissue decreases, but also blood flow and volume increase in order to keep the normal tissue temperature. Because resistivity of blood is much lower than that of other tissues, even though, the temperature of tissue does not change, if blood volume included in a tissue increases, the resistivity of the tissue decreases. Therefore, we should eliminate the effect of blood volume change to measure the temperature change of the tissue heated up by IMPCT.

Here, we propose the new IMPCT algorithm for obtaining the reconstructed impedance change image in a cross section and the new method for measuring the temperature and blood volume change in a tissue at the same time by IMPCT.

We use the modified sensitivity IMPCT algorithm(MSM). The new algorithm we propose here is a kind of modified MSM under the following process.

We assume that we can find or know the cross section in which hot spots caused by some heating system are. Therefore, we can arrange electrodes around the cross section. The resistivity of these hot spots changes due to blood volume and temperature changes. Because the only 3 dimensional sensitivity at these hot spots changes, we could estimate the sensitivity change by comparing 3 dimensional calculated sensitivity with 2 dimensional calculated sensitivity if the resistivity change is small enough. By using the sensitivity obtain here, we can estimate the impedance change value and location in the cross section by MSM algorithm.

In lower frequency region than about 300kHz, the electrical characteristics of blood can be assumed to be pure extra-cellular fluid resistance. Therefore, when a living tissue is heated up, extracellular fluid resistance Re decreases due to blood volume and tissue temperature change. And intracellular fluid resistance Ri decreases only by rising tissue temperature. Therefore, if we know the changes of Re and Ri by IMPCT, we could estimate blood volume and tissue temperature changes in the body.

Light-Tissue Interaction and Evaluation of Color Information in Biomedicine

Makio Akimoto[1], Teruo Asaeda[2], Yuhei Miyata[1], Toshiteru Kikuta[3] and Hideo Namiki[3]

[1] Department of Pharmacology, Nippon Medical School,
1-1-5, Sendagi, Bunkyo-ku, Tokyo 113, Japan

[2] Color Consultant, 4-21-18, Okusawa, Setagaya-ku, Tokyo 158, Japan

[3] Department of Biology, School of Education, Waseda University,
1-6-1, Nishi-Waseda, Shinjuku-ku, Tokyo 169-50, Japan

The increasing use of electromagnetic waves has stimulated a great amount of research for medicine and biology[1]. In recent years, there has been an increasing interest in interactions between electromagnetic radiation and biomedical tissues dependent on the wavelength of radiation[2]. Especially, biological materials are a very important application of color imaging in clinical analysis. Researchers in optical biomedical imaging are pursuing a dream that someday soon they will develop non-invasive modalities enabling doctors to peer inside the human body by optics. On the other hand, the optical microscope, despite its limited lateral resolution and long history of use, retains several attributes not readily replaced by other, newer imaging or diffracting devices that provide greater resolution.

We developed a new colorimetry combined with image analysis of charge-coupled-device(CCD) camera. To quantify color information as we percept color vision is becoming possible by using computer assisted-CCD camera system. The instrument consists of an optical unit equipped with a high resolution CCD camera, an image processing unit and a microcomputer. The image signal from the camera was processed by an image processor controlled by a microcomputer. The analysis of images is bringing quantification and objective assessment to diagnostics in histology and cytopathology. With the video imaging, we can: readily examine a wide field of view; follow dynamic changes in the specimen nondestructively and in real time; generate contrast in several modes reflecting optical and finestuctural characteristics of the specimen; distribution of antigenic and other reactive molecules with high specificity; and directly image optical sections. Algorithms are also adapted and developed both to enhance and restore the captured images. From the viewpoint of color specification, it is desired that the image be represented by color features which constitute a space possessing uniform characteristics, such as the CIE-L*a*b* color coordinate system. The system is best fit to the perceptual color space and very useful to realize visual imaging. The whole system is expected to produce a practical and cost-effective means of the routine assessment of biological tissues quality.

It is recognized from the above experimental that the colorimetry is very useful for measuring the color of tissue. The total system has both research and diagnostic potentials. We believe that capability will be invaluable for the study of biological tissues, especially during their development, not only because of the images generated, but also because the processes observed can be described quantitatively.

[1]C.Polk and E.Postow, Handbook of Biological Effects of Electromagnetic Fields, CRC Press, Boca Raton (Florida), 1988.

[2]M.Akimoto et al., Progress in Electromagnetics Research Symposium (PIERS-1995), Seattle, Washington, USA, 24-28, July, 1995.

SESSION 7P7

Tuesday, January 7, PM 1330-1510, Lecture Theatre 7, City University of Hong Kong

Medical Applications & Biological Effects 1

Chairperson: Koichi Ito, Chiba University
Co-Chairperson: R Van de Walle, Ghent University Hospital & University of Ghent

13:30 ***Fast Motion Detection in Projection Reconstruction MR Imaging*** 342
*R Van de Walle, **I Lemahieu
*Ghent University Hospital
**University of Ghent

13:50 ***Heating Characteristics of Multiple Coaxial-Slot Antenna for Interstitial Microwave Hyperthermia*** 343
Lira Hamada, Takafumi Kitada, Rong Wang, Koichi Ito
Chiba University

14:10 ***Improvement of Optical CT Image by PSF Deconvolution*** 344
Yoichi Onodera, Yuji Kato, Koichi Shimizu, Katsuyuki Yamamoto
Hokkaido University

14:30 ***Performance of Microwave Disinfector for Deactivating Bacteria*** 345
Qun Wu, Daoli Sun
Harbin Institute of Technology

14:50 ***Biological Effects of Cancer Cells Radiated by Ka-Band MMW*** 346
*H Bai, **D G Zhang
*People's Hospital of Shenzhen
**Shenzhen University

15:10 **Break**

Fast Motion Detection in Projection Reconstruction MR Imaging

R. Van de Walle[1,2] and I. Lemahieu[1]
[1]ELIS Department, University of Ghent, Sint-Pietersnieuwstraat 41, B-9000 Ghent, Belgium
[2]MR Department, Ghent University Hospital, De Pintelaan 185, B-9000 Ghent, Belgium

[Introduction] In this paper, projection reconstruction (PR) imaging is considered. We present a quantitative technique that allows to check when motion occurred during a PR experiment. No a priori information about the motion is required since only the measured MR (Magnetic Resonance) signals are used in the calculations.

[Theory] In PR imaging, a set of 1D projections $P_\theta(r)$ of the complex transverse magnetization is considered, where $\theta = 0, \frac{1}{N}\pi, \frac{2}{N}\pi, \ldots, \frac{N-1}{N}\pi$ are the projection angles, N is the number of projections and r is a place variable along each projection axis.

We found earlier that in case of translational motion with a frequency that is smaller than a critical frequency of typically 100 Hz, the projections' amplitudes $P^*_\theta(r) = |P_\theta(r)|$ are almost not distorted. Then, images without relevant artifacts can be reconstructed from the set $\{P^*_\theta(r)\}$.

The difference π/N between two successive projection angles is small in all practical situations. Therefore, the difference between two successive projections will be relative small as well when no relevant motion occurs. Consider the root mean square deviation

$$RMSD(\theta) = \sqrt{\frac{\sum_r \left(P^*_\theta(r) - P^*_{\theta-\pi/N}(r)\right)^2}{N}},$$

When $RMSD(\theta)$ becomes large for a certain value of θ, it can therefore be concluded that rotational motion or translational motion with high motion-frequency components occurred during the measurement of $S_\theta(k)$.

[Materials and methods] Images of a volunteer's brain were investigated. The corresponding MR signals were measured by using a PR sequence on a 1.5 T Siemens SP63 whole-body scanner. Each signal $S_\theta(k)$ corresponds with the Fourier transform of $P_\theta(r)$, with respect to r. All images had a resolution N of 256.

In a first experiment, the volunteer's head was moving during two time intervals, corresponding with the measurement of the 17th through 41st signal and the 114th through 137th signal respectively. The head movement was continuous and contained both translational and rotational components. The maximum displacement in the direction perpendicular to the image plane was 0.5 cm, while the maximum in-plane displacement was 5 cm.

In the second experiment, the volunteer's head was moving in a similar way but only during the measurement of the 47th trough 56th signal.

For each experiment, the intervals during which motion occurred were determined by calculating $RMSD(\theta)$ on a relative scale between 0 and 100 for all projection angles θ. When $RMSD(\theta)$ was higher than 10, it was decided that motion occurred during the measurement of $S_\theta(k)$.

[Results and discussion] Using the mentioned threshold for $RMSD(\theta)$, the motion intervals could be estimated. For the first experiment, these motion intervals corresponded with the measurement of signals 17 through 40 and during the measurement of signals 113 through 137. The motion interval for the second experiment corresponded with the signals 47 through 57.

Obviously, our motion-detection method proves to be able to detect motion intervals in PR signals with high accuracy: the maximum difference between the estimated intervals and the actual motion intervals is 1 signal number or 1 repetition time, both in case of long and repetitive motion and in case of relative short motion.

Heating Characteristics of Multiple Coaxial-Slot Antenna for Interstitial Microwave Hyperthermia

Lira HAMADA, Takafumi KITADA† , Rong WANG and Koichi ITO†

Graduate School of Science & Technology, Chiba University
† Department of Electrical and Electronics Engineering,
Faculty of Engineering, Chiba University
1-33 Yayoi-cho, Inage-ku, Chiba-shi, 263 Japan

The multiple coaxial-slot antenna is an applicator for interstitial microwave hyperthermia to heat localized deep-seated tumors and large volume tumors. The antenna is made from a thin coaxial semi-rigid cable of about 1 mm in outer diameter. Several ring slots are cut on the outer conductor and the tip of the cable is short-circuited. A thin plastic catheter covers the antenna for medical safety.

This antenna controls its heating patterns by varying the intervals and the numbers of its ring slots. In this report the characteristics of the antenna will be investigated theoretically and experimentally. In the numerical analysis, the antenna is modeled as a vertical antenna penetrating the interface between the air and the human body considered as homogeneous muscular tissue. The catheter around the antenna is replaced with the equivalent polarization current. The electric field source at the ring slot is replaced by a narrow strip of magnetic current generated by feeding voltage at the slot. The analysis can be performed by using the transmission line theory for internal region of the antenna, and by using the moment method for external region. For example, when one antenna whose Lts (length from the tip to the slot near the boundary surface) = 20 mm with four slots is inserted into the body in 70 mm long at 430 MHz, heating region where the SAR is more than 50% is about 20 mm along the antenna. Under the same condition, heating region of more than 30 mm long is generated by the antenna whose Lts = 30 mm with six slots.

REFERENCES. (1) J.W. Hand and J.R. James (Eds.) :" *Physical techniques in clinical hyperthermia*", Research Studies Press, UK, 1986.

(2) M. S. Wu, et al.:"Basic study of multiple coaxial-slot antenna for interstitial microwave hyperthermia", Technical Report of the Institute of Electronics, Information and Communication Engineers (IEICE), A·P 95-24, 1995 (in Japanese).

(3) J.H. Richmond and E.H. Newman:"Dielectric coated wire antennas", Radio Science. Vol.11, No.1, pp.13-20, 1976.

Improvement of Optical CT Image by PSF Deconvolution

Yoichi Onodera, Yuji Kato, Koichi Shimizu and Katsuyuki Yamamoto

Graduate School of Engineering, Hokkaido University,
North 13 West 8, Kita-ku, Sapporo-shi, Hokkaido, 060 Japan

With the recent progress of an optical technology, the optical cross-sectional imaging or an optical CT has been pointed out. The strong scattering at biological tissue is one of the most difficult problems to realize an optical CT. To suppress the scattering effect in a reconstructed image, a fundamental study has been conducted on the deconvolution technique using a point spread function (PSF). The image blurring due to the scattering can be considered as the convolution of the PSF of a scattering medium. If we know the PSF, we can suppress the effect of scattering by a deconvolution technique.

In the translate-rotate scan of CT imaging , we consider a collimated set of a light source and a detector in a scattering medium. The depth d is defined as the distance from the detector in the direction to the light source. The PSF varies depending on d. Thus, it was not easy to apply the deconvolution technique directly to the projection data in tomography which were the sum of the absorption in different depths.

We have developed a technique to apply the deconvolution technique in the reconstruction of a CT image with the translate-rotate scan. In this technique, the d-dependent PSF is obtained first in a measurement or a computer simulation of light scattering. Then, it is applied to the CT image degraded by the scattering effect.

To examine the effectiveness of this technique, the computer simulation was conducted. As the d-dependent PSF, the Gaussian functions with different FWHM's were used. Fig.1 shows the numerical phantom given. Fig.2 is the image reconstructed with the projections blurred by the PSF. Fig.3 shows the results of this technique. The image was improved considerably.

Through this study, the fundamental feasibility of the scattering suppression in an optical CT was verified.

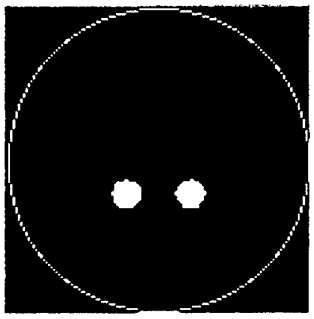


Fig. 1 Numerical phantom

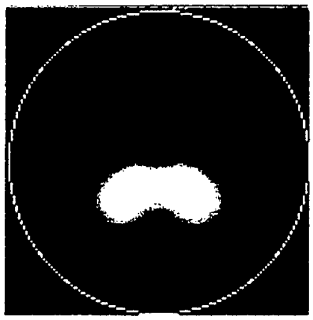


Fig. 2 Reconstructed image (conventional FBP)

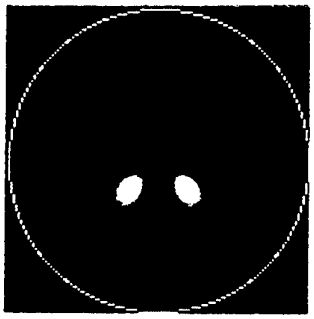


Fig. 3 Reconstructed image (proposed method)

PERFORMANCE OF MICROWAVE DISINFECTOR FOR DEACTIVATING BACTERIA

Wu Qun Sun Daoli
Department of Radio Engineering
Harbin Institute of Technology
Harbin City,Heilongjiang Province,P.R.China

Disinfection is one of the important measures to prevent infectious diseases from spreading. With the continuous rise in living conditions and cultural level,more and more disinfection applications are needed by the human race. In order to meet the needs for every field in daily life, disinfec- tion techniques have been developing ,too. Microwave energy has a stronger ability to penetrate dielectric materials and makes thermal effects or non-thermal effects on microbes.As a newly-developed technique, microwave disinfection has been attracting a lot of researchers to extensively explore the interaction machnism of microwave on bacteria. Especially for conventional disinfection,it is nearly impossible to sterilize items such as paper,bonds,paper money,documents,files,books and report lists of chemical examinations for infectious diseases in hospitals and so on. Whereas microwave energy is more effective and more favourable for disinfecting those items.According to the superiority of disinfection, a specially- designed microwave disinfector using high-power microwave energy was made. A series of disinfection experiments have been made to determine the effect of microwave energy on indicator bacteria such as Bacillus subtilis var.nigaor, Bacillus stearothermophilus, Bacillus pumilus E601, Staphylococcusaureas, Bacillus cereus.In order to observe the performance of the disinfector for deactivating bacteria and the effects of microwaves on those indicator bacteria under different conditions,and find out the optimum time and power needed for killing the indicator bacteria,we choose some items as representive ones with materials such as papers,wood,and china for simulation Finally,an important conclusion has been obtained.i. e. , the Bacillus subtilis can be chosen as an optimun indicator bacterium for microwave disinfection. This conclusion provides an important evidence with microwave disinfection rescearch.The expanded manuscript will discribe the apparatus, structure, composition,and experimental results and final conclusions.

Progress in Electromagnetics Research Symposium, PIERS 1997 ISBN 962-442-097-1

Biological Effects of Cancer Cells Radiated by Ka-Band MMW

H. Bai, B.Sc.(Medi)
Dept. of Cancer
People's Hospital of Shenzhen
518020 Shenzhen, P.R. China

D.G. Zhang, B.Sc.(EE), Ph.D.
Advanced Technology Res. Center
Shenzhen University,
518060 Shenzhen, P.R.China

Telephone:(86-755) 5533018-2497

Facsimile: (86-755) 6660182

Abstract

The biological effect of electromagnetic wave is the biomedical changes brought about when a biological system conducted by an electromagnetic field of a certain intensity at a given frequencies. The electromagnetic biomedical effect lay the foundations of biomedical applications of electromagnetic wave and sanitary standard of electromagnetic radiation. In this study, several experiments have been done to determine whether the electromagnetic wave can lead to biological changes or not. If the answer is 'yes', what type of biological changes it will lead to?

Several types of cancer cells under the radiation of a certain millimeter wave are analyzed experimentally. Cell SMMC-7721 of liver cancer, cell HEP-2 of throat cancer and cell MGC 80-3 of stomach cancer was radiated by a electromagnetic wave at Ka-band, respectively. The electromagnetic intensity is 1~3 mw/cm^2 and the frequency is 36 GHz. The duration are 30 minutes per day, totally 3 days. The injurious modification of cell form is observed by electronic-scanning microscope. The taking shape ability of monoclonal antibody have been decreased rapidly to $\rho<0.01$. The content of DNA also have been reduced quickly to $\rho<0.01$ by DNA quantitative analysis of image-scanning analyzer.

Cell MGC 80-3 of stomach cancer combined with HPD was radiated by a electromagnetic wave with a intensity of 3 mw/cm^2 at the frequency of 39 GHz. In this time, it endure 20 minutes per day, totally 3 days. It is noticed that the Ka-band millimeter wave along with HPD can execute cancer cells reasonably.

There still have much to learn about the biomedical effect for the meaning of medical application as well as the determination of sanitary standard.

Author Index

A

Aberle,J T 128
Abhari,R 574
Aboul-Seoud,Ahmed K 76
Achkar,Joseph 160
Adams,D M 115
Advokatov,V R 698
Agarwal,G S 288
Ahland,A 609
Ahlers,E 307
Ahn,Joon Tae 514
Ait-Abdelmalek,R 336
Aitchison,C S 587
Akerson,J J 279
Akhavan,H G 575
Akimoto,M 340
Akyel,Cevdet 162
Alfas,Swen 122, 125
Aliev,YuM 456
Allal,D 454
Alsewede,R H 90
Altintas,Ayhan 232
Amari,Smain 96
An,Tongyi 186, 187, 589, 594
Anandan,V K 670, 671
Anderson,S J 75, 77, 253
Andersson,L-E 480
Ando,Makoto 378, 389
Andrenko,Andrey 378, 389
Aneburg,E L 246
Ang,C K 158
Ansari,N A 533
Antar,Y M M 364
Anyzova,Romana 298
Ao,Farliang 635, 636
Arora,B M 726
Arsenyan,T 697
Asaeda,T 340
Asakura,Toshimitsu 498
Augustin,V 666
Avenhaus,B 640
Awai,I 239
Awata,Aki 85
Azevedo,Joaquim A R 377

B

Babin,L J M 300
Babu,G Sathish 579
Baginski,M E 415, 691
Bai,H 346
Bakar,Ahmad Hairi Abu 549, 550
Balamuralidhar,P 670
Banerjee,Partha P 528
Bao,Jiashan 626, 627, 628
Bapiraju,B 675
Barbara,A K 693, 694, 695
Barbier,Christian 280
Barbosa,A M 684
Barchloui,N Komjani 577
Bardati,F 334
Barman,M K 693
Basha,Aleem H 675
Bashkuev,Yu B 698
Basu,A 54
Bates,A P 410
Batoroev,A S 28
Bauer,Peter 272
Baum,E 23
Belot,D 146
Benson,T M 112
Berkovits,Richard 473
Bertolotti,M 107
Besada,José Luis 148
Besieris,Ioannis M 525
Beyer,Adalbert 94, 437, 441
Biebl,Erwin M 393, 630
Binh,Le Nguyen 713
Bjerede,Bjorn 583
Blanchard,Andrew J 489
Blok,Hans 297
Blot,J P 368
Blouvac,J 146
Bocquet,B 335, 336, 454
Boerner,W M 246, 251, 253, 555
Boley,Daniel 504
Bollmeier,T 640
Boone,Francois 210
Borghi,R 502
Borisov,V V 418, 419
Bosisio,Renato G 156, 157, 161
Botten,L C 680, 682, 683
Brandfass,M 257
Brench,Colin 620
Brock,J C 53
Buah,P A 507
Budkewitsch,P 482
Bujakas,V I 380
Burke,P T 717
Button,T W 643
Byun,Dongjin 705

C

César,Amílcar Careli 207
Callan,J Paul 321
Cao,J 66
Cao,M S 266
Caorsi,S 84
Carbonne,D 146
Carolan,Shawn 44

Caron,Martin 162
Casem,Merv 551
Casimiro,António Manuel E S 377
Catreux,Severine 96
Ceremuga,Janina 641
Chai,Shunlian 200
Chan,B 739
Chan,C H 41, 48, 392
Chan,K K 405
Chan,K S 324
Chan,K W 547
Chan,L Y 323
Chan,Michael C Y 116
Chan,T K 47, 283
Chan,W H 632
Chan,Wing Shing 655, 656
Chan,Yuk 455
Chandler,P J 313, 704
Chang,A 271
Chang,Alfred T C 266, 268, 269
Chang,Fung-Yuel 613, 622
Chang,Hsuan T 311, 523
Chang,Hung-chun 292, 509
Chang,Hung-Wen 417
Chang,J Y 709
Chang,Kai 59, 131
Chang,L A 690
Chang,M W 322, 709
Chang,P C Y 728
Chang,The-Nan 32, 36
ChangTsurng-Jeng 12
Chapin,Elaine 252
Chatterjee,Monish R 529
Chavez,Jose 381
Cheah,K W 325
Chen,B 140
Chen,Chih-fan 396
Chen,Chun Hsiung 33
Chen,Dongqun 730
Chen,Fushen 637
Chen,Hai-ying 741
Chen,Hong-Twu 9, 12
Chen,Horng-Dean 9, 10
Chen,Jiayu 216
Chen,K M 413, 548
Chen,K S 399
Chen,Kangsheng 225
Chen,Kuo-Cheng 238
Chen,Nan-Cheng 8
Chen,R M M 178, 180
Chen,S 91
Chen,Shih-Tun 529
Chen,Wenhong 143, 569
Chen,Wen-Shyang 11
Chen,X Y 121
Chen,Yijiang 299
Chen,Yinchao 610, 612
Chen,Yiyuan 426, 644
Chen,Yong H 618
Chen,Yung-Hong 36
Chen,Z N 371
Chen,Zhiyu 558
Chen,Zhuming 218, 220, 425
Cheng,Feng 607
Cheng,M 158
Cheng,Q H 645, 649
Cheng,Yuan-Tung 9, 12
Cheung,Cho-Wai 243
Cheung,Philip 106, 504
Cheung,W N 710, 712
Chew,Weng C 44, 45, 46, 82, 618
Chiang,K S 515, 532, 535, 537, 540
Chin,Mee K 510
Chinjen,C 709
Chiu,Cheng-Nan 33
Chiu,Chien-Wen 38
Chiu,L 271
Chiu,Long S 268, 269
Choi,Jee Yon 516
Choquette,Kent D 111
Chou,C K 547
Chou,Hsu-Feng 310
Chou,Yong 188
Chow,K Y 373
Chow,Wah Yan 656
Chow,Y L 176, 229, 390, 445, 647
Chow,Y T 313, 535, 704
Choy,W C H 718
Christopher,S 601, 602
Chu,B C B 515, 537
Chu,Kwang-Uk 513
Chu,P L 316
Chu,Qing-Xin 613, 622
Chu,S C 526
Chu,Tah-Hsiung 79
Chuang,Cheng H 523
Chuang,Shang-Jen 10
Chuang,Wei-Ching 34
Chuang,Zuon-Min 711
Chung,P S 314
Chung,Shyh-Jong 59, 131
Ciprian,Dalibor 298
Ciric,I R 169, 406
Cloude,S R 247
Costa,D 586
Cui,S M 182
Cullen,A L 448, 544
Cwik,Tom 41

D

d'Assuncao,A G 142
D'Iorio, M A 482
Dai,Kailiang 599
Dai,Y 644
Daribazaron,E Ch 86, 87, 88
Darizhapov,D D 86, 87, 88

Darlington,C N 640
Das,Alok K 725
Das,N K 133
Das,P 519
David,J P R 450
Davidson,Kenneth L 491
Davis,L E 366, 643
Day,Chuen-Chen 270
Dea,J Y 555
DeCusatis,C 519
Deen,M Jamal 117
Deguchi,Hiroyuki 151
Delaveaud,Ch 565
Delia,R 333
Delisle,G Y 264
Dembelov,M G 698
Deming,R W 481
Deri,R J 103
Derrick,G H 682
Desplanches,B 369
DeSwiet,Thomas 376
Detlefsen,Juergen 97
Devaney,A J 290, 481
Devi,M 693, 694, 695
DiJaili,S P 103
Dilworth,I J 545, 564
Ding,K H 279
Ding,Yiyuan 218, 220, 425
Ding,Zhi 415, 416
Dirassen,B 739
Dong,X P 515, 537
Dong,Xingqi 589
Dou,W B 213, 219
Dowden,R L 484
Dozier,J 492
Dreher,A 571
Drossos,G 366, 643
Duan,G-H 113
Duan,Yuxiang 216
Dugarzhapova,D B 28
Dumoulin,J G 149
Durand,D 544
Dutta,Gopa 675
Duttagupta,S 694

E

Ebeling,K J 720
Eccleston,K W 449
Edimo,M 563
Edwards,Paul J 712, 714
Ehrich,Matthias 703, 738
Eibert,Thomas F 92
El-Badawy,El-S A 240
Elbers,J-P 101
El-Hennawy,H M 240
El-Motaafy,H A 240
Elsherbeni,Atef Z 617, 621
Emanuel,M A 103
Emori,Yoshihiro 171

F

Fagen,Mike 237
Faggetter,D 390
Fan,Yong 424
Fan,Z 364
Fang,D G 140, 182, 226, 392
Fang,Jian 593, 598
Fedotov,N 697
Felbach,Dirk 97
Felbacq,D 681
Feng,Xiangchu 401
Feng,Zuwei 614, 623
Fiallos,M 394
Finkele, Rolf 81
Flood,B 480
Frölind,P-O 480
Franceschetti,Giorgio 74
Freilikher,V 465
Frezza,F 502
Friedsam,Gerhard 630
Fu,Chengpeng 631
Fujimoto,M 700, 701
Fujimoto,Takafumi 129
Fujimura,Sadao 274, 275

G

Gaikovich,K P 478
Gal,M 717
Galati,Gaspare 71
Galocha,Bélen 148
Gan,Xiaobing 401
Gao,Yifan 199
Ge,An 312
Ge,D B 197
Geints,Yu E 198
Genack,A Z 497, 501
Gentle,David 152
Gerlach,J 526
Geudtner,D 482
Ghannouchi,Fadhel M 162
Ghatak,A K 541
Ghodgaonkar,Deepak K 550
Glezer,Eli N 321
Glingener,C 101
Golden,Kenneth M 490
Gong,Jianping 225
Gong,Ke 64
Gonschorek,Karl-Heinz 21
Gonzalez,F 658, 659
Gopinath,Anand 106
Gorbachev,A A 696
Gori,F 289, 502
Goyal,I C 541
Gragnani,G L 84
Granherr,M. 720
Grattan,K T V 507

Green,S D 72
Grey,R 450
Griffiths,H D 69, 544
Grilo,Alberto J V 377
Gu,C K 121
Gu,Hong 402
Gu,Q 581, 583
Gu,Zeji 546
Gu,Zu Han 284, 285
Gubanov,V P 244
Guo,Hua-Dong 493
Guo,J S 379, 453
Guo,Lixin 196, 403
Guo,Wei 190
Guo,Wenyan 408, 409
Guo,Yili 317
Guo,Ziqin 611
Gustavsson,A 480
Gvamichava,A S 380

H

Habash,Riadh W Y 549, 550
Hadley,Ronald G 100, 111
Hagiwara,Seiji 358
Halevi,Peter 686
Hall,Richard C 135
Hamada,Lira 343
Hamelin,N 313, 704
Han,Seon Gyu 512, 513
Hanada,Tatsuyuki 471
Hanaizumi,Hiroshi 275
Haneishi,M 134
Hansen,P M 381,555
Hansen,Volkert 92
Hara,Y 279
Hara,Yoshihisa 276
Harada,Takashi 22
Hareesh,M 673, 674
Hasabe,Nozomu 360
Hashimoto,Masahiro 407
He,Jianguo 386
He,Ling 635, 636
He,Liquan 214
He,M 645
Heldring,Alexander 174
Helfert,S 105, 307
Hellsten,H 480
Hensley,Scott 252
Herberthson,M 480
Herring,J 167
Hill,G 450
Hinata,Takashi 308
Hirasawa,K 63
Hirayama,Tomoaki 469
Hirose,K 132
Hitatuka,Toshiro 236
Hodges,Richard E 43
Hoefer,W J R 167
Holm, William A 263
Holm,Andreas 95
Hong,J 640
Hong,Wei 426
Hong,Y 271
Hongo,Kohei 195
Hopcraft,K I 410, 688, 728
Hoshina,S 338
Hosono,Toshio 308
Hotta,Masahi 304
Hou,Xinyu 411, 568
Hsu,C C 279
Hsu,Powen 39
Hsu,Wei-Chen 13
Hsun,Chang-Zheng 114
Huang,C Y 709
Huang,C-F 31
Huang,F 640
Huang,Hung-Chia 536
Huang,J 138, 271
Huang,Jhin-Fang 189, 605
Huang,Jifu 208
Huang,Li 321
Huang,Shumji 29
Huang,W P 115
Huang,Y 545, 548
Huang,Y X 227
Huang,Yan-Ming 417
Hui,H T 228
Huntsman,Lee L 551
Hwang,Y 192,572

I

Ibrahim,B A W 567
Ibrahim,S H 240
Iguchi,Toshio 267
Iio,Kenichi 236
Ikuno,H 294
Ilinski,A S 603
Ilyushenko,V N 734, 735, 736
Inn,Arba'iah 550
Isele,B 93, 439, 440
Ishiguro,Masato 151
Ishii,J 239
Ishii,N 367
Ishikawa,Yohei 211, 236
Ishimaru,A 47,283
Ishizaka,Hiroyuki 209
Ito,Koichi 137, 343
Ito,Satoshi 332
Ito,Shigeo 462
Itoh,K 367
Itoh,T 51, 54, 67
Iwamoto,Masafumi 276

J

Jäger,D 90

Jagadish,C....717
Jain,A R....670
Jakal,A Z....567
Jakeman,E....410
Jamnejad,Vahraz....41
Jarem,John M....528
Jarriel Jr,G W....415, 691
Jayasinghe,D A C C....316
Jecko,B....560, 565
Jeon,Min-Yong....514
Jeong,Jaesik....705
Jiang,Lijun....573
Jiang,M M....645
Jiang,Z....323
Jiang,Zhi Ping....217
Jin,B B....645
Jin,Canmin....590, 600
Jin,D X....182
Jin,Jian-Ming....44
Jing,D....629, 632, 645
Jing,Zhenghong....319
Johnson,J Michael....617
Jones,M R....331
Jonsson,T....480
Jordan,Mary S....491
Josse,M....285
Jou,Chewn-Pu....16
Jung,W S....517

K

Kühn,E K....166
Kadir,Nabil M Abdul....549, 550
Kagami,Yoshiharu....225
Kamimura,Yoshitsugu....58, 332
Kanai,Y....337, 338
Kaneko,Yasuhisa....702
Kanemoto,Yutaka....275
Kanevsky,M B....486, 494
Kang,K....184, 185
Kang,L....645
Kantor,Roman....298
Kaplan,Ben-Zion....553
Kapustin,U U....603
Karaev,V Y....486, 494
Karikomi,Masahiro....355
Karnychev,V I....249
Karouta,F....717
Kartmann,Uwe....25
Karunasiri,Gamani....719
Kashiwa,T....337
Kasuya,Yoshihiro....60
Kataria,N D....648
Katchalova,G B....254
Kato,Yuji....344, 469
Kaveh,Moshe....496
Kawabata,Kyosuke....276
Kawai,Tadashi....60
Kawamata,S....122, 123
Kawanishi,T....463
Kawasaki,Shigeo....56
Kawata,Y....277
Ke,Shyh-Yeong....16
Kendall,P C....112
Khomyak,E M....86, 87, 88
Kikuchi,H....122, 123
Kikuta,T....340
Kim,Gyeungho....705
Kim,Ho Young....514
Kim,Hye-Young....512, 513
Kim,Ki Hong....516
Kim,Kyong Hon....514
Kim,Y....717
King,Yen C....523
Kingsley,S P....72, 450
Kishore,P....667, 672, 673, 674
Kitada,Takafumi....343
Kiyasu,Senya....274
Klimov,A I....244
Koch,Barry....106
Kogan,Eugene....496
Kohler,C R....279
Kojima,Toshitaka....295
Kokotoff,D M....128
Kokubo,Yoshihiro....60
Kong,Fanli....391
Kong,J A....276, 279
Kong,K S....438
Konishi,Yoshihiko....561
Kooi,P S....35, 37, 42, 61, 62, 66
Korolenko,P....697
Korovin,S D....244
Kotsuka,Youji....20
Kozlov,A I....248, 260, 262
Kozu,Toshiaki....267
Kremer,Dennis....98
Krishna Murthy,B V....666
Krishnan,Sivanand....449
Krogager,E....251, 263
Ku,W H....586
Kubina,S J....384
Kuga,Yasuo....47, 283
Kuhlmann,Joachim,....703, 738
Kum,Dong-Hwa....705
Kumar,Ashok....733
Kumar,M Jaya....648
Kumon,Yasunori....359
Kuo,C J....311, 523
Kuo,P-H....31
Kuo,Tsung-Hua....270
Kuroda,Takao....110
Kuroki,Futoshi....205
Kusaka,T....277
Kwee,I W....331

L

Lacey,D....643

Lah,D S 517
Lahart,Martin J 505
Lai,A K Y 400
Lai,Henry 543
Lan,Gao 459
Lan,Kang 592
Lancaster,M J 640
Langenberg,K J 257
Larsson,B 480
Las-Heras,Fernando 148
Lau,Yuen-Pat 613, 622
Le,Charlie T C 283
Lee,C F 314
Lee,Ching-Her 13, 93
Lee,Ching-Ting 711
Lee,D 149
Lee,El-Hang 514
Lee,Hak Kyu 514
Lee,Hung-Mou 194
Lee,Hyuek Jae 512, 516
Lee,Hyung Jong 512, 513
Lee,Jeng-Hong 707
Lee,K F 127
Lee,K O 540
Lee,Kun-Yi 34
Lee,Myung-Hyun 512, 513
Lee,Wei-Yu 34
Leger,James 106
Lemahieu,I 342
Lemaire,Philippe 280
Leong,M S 35, 37, 42, 61, 62
Leonhard,S 104
Leroy,Y 335, 336, 454
Leskova,T A 458
Lesnak,Michael 556
Leung,K W 371, 373
Leung,S W 19
Leveque,Ph 565
Levery,David B 241
Li,Alex Tak Ho 531
Li,Chuanlu 435, 730
Li,E H 116, 324, 718
Li,Fang 689
Li,H H 428, 649
Li,Ji 156
Li,Jun-Fei 493
Li,K 584
Li,Keren 554
Li,L W 35, 37, 42, 62
Li,Lin 223
Li,Man Shi 655
Li,Ming 408
Li,Shizhi 143, 569
Li,Simin 634
Li,X 115
Li,Xiangsheng 730
Li,Ying 319
Li,Yong 214
Lian,De-liang 325
Liang,A H 323
Liao,Guo-Ju 509
Lim,Dong Sung 514
Lin,C M 392
Lin,Ching-Fuh 310
Lin,Deyun 606, 611
Lin,F J 66
Lin,Jiun-Hwa 82
Lin,L Y 51
Lin,Leon 583
Lin,Shangpin 408, 409
Lin,Shijie 190
Lin,Wei 711
Lin,Weigan 215, 221, 296, 427, 430, 432, 592, 593, 598, 599
Lin,Yikun 421
Lindenmeier,Stefan 165
Ling,F 140
Ling,Gensheen 730
Litovchenko,Konstantin 280
Litva,John 616
Liu,C H 668
Liu,Gin-Rong 270
Liu,H S 19
Liu,Hongwei 215
Liu,Kecheng 386
Liu,Shenggang 447, 595
Liu,Shizhong 606
Liu,Tiejun 188
Liu,W M 596
Liu,Y W 173, 175, 176, 178, 179, 180
Liu,Yong Gui 435
Lo,Kai Ming 531
Lo,Terry Kin-chung 572
Lo,Yen 311
Logvin,A I 248, 260, 262
Lokanadham,B 669
Lomonosov,V 697
Lopez,J M 146
Lor,K P 535
Loutin,E A 255
Lu,Cai-Cheng 45, 46
Lu,H B 645
Lu,Hsin-Chia 79
Lu,Jui-Han 15
Lu,Jun Q 284
Lu,Qi Sheng 217
Lu,Shih-Wen 39
Lu,Xiang-Rong 355
Lu,Ying 190
Luk,K M 127, 173, 175, 176, 365, 371
Luneau,P 264
Luo,Xizhang 421
Luo,Y L 175
Luo,Yi 114
Lyon,G M 731

M

Müller, Thomas....630
Müller,Alf....94
Ma,Hon Wah....26, 651, 654
MacGregor,D M....31
Madden,S J....316
Madr,Vilém....556
Madsen,Soren....252
Maeda,Atsushi....20
Maeda,Hiroshi....293
Mahdjoubi,K....563
Mahmood,N....507
Mahmoud,Samir F....483
Mait,Joseph N....527
Makimoto,Mitsuo....235
Makino,T....115
Mambo,Philip....208
Mamouni,A....335, 336
Man,W S....326
Manap,Lilywati....550
Mangold,T....93
Mao,Jun-Fa....414
Mao,Junjie....386
Mao,Zhunjie....200
Maradudin,Alexei A....282, 285, 458
Margineda,Jose....159
Marques,A....394
Mars,Dan E....702
Marti,Fausto....71
Marvin,A C....24
Masciulli,P....107
Masuda,Masanori....151
Matsumoto,Yuji....370
Matsuo,Michiaki....235
Matsuoka,Tsuyoshi....476
Matsuzawa,Shin-ichiro....137
Matystak,Lubomír....556
Maurin,David....444
Mayer,K....257
Maystre,D....681
Mazur,Eric....321
McDouglall,J A....547
McEwan,N J....567
McGurn,Arthur R....282
McNair,Peter....152
McPhedran,R C....680, 682, 683
Mei,K K....173, 175, 176, 179
Meier,Hans....95
Melichov,S V....233
Meng,Zhi-Qi....471
Merza,A....161
Mezentsev,V K....90
Miao,Jing-Feng....203
Michalzik,R....720
Migliaccio,Maurizio....74
Mikuteit,S....584
Minett,James W....19
Mirianashvili,Maria....304
Mirotznik,Mark S....527
Mirshekar-Syahkal,D....564, 575
Mishra,S R....149
Mitsunaga,Naohiro....293
Mittra,Raj....612
Miwa,Takashi....80
Miyahara,Norio....151
Miyakawa,M....337, 338
Miyata,Y....340
Miyazaki,Yasumitsu....306
Mizumoto,Tetsuya....171
Mizuno,S....331
Mizuno,Tomohiro....303
Mochida,Hideo....372
Mohanty,A....133
Moiseeva,L G....662
Mooney,Jon E....416
Moreno,F....658, 659
Morgan,G B....651
Morimoto,Eiji....561
Morioka,T....63
Mouty,S....336
Mrozynski,G....23
Mudaliar,S....661
Munkoev,V E....28
Munoz,Juan....159
Muramoto,M....367
Murat,Zunaira....550
Murch,R D....356
Musher,S L....90

N

Nagai,Y....122, 123, 124
Nagpal,P C....733
Naito,Yoshiyuki....171
Naka,Y....294
Nakagawa,Shigeru....702
Nakamura,S....700, 701
Nakano,H....132, 375
Nakayama,Junichi....459
Naldi,Maurizio....71
Namiki,H....340
Nanbu,Yukihisa....475
Narsale,A M....726
Nauwelaeres,B....161
Nencka,Petr....298
Neto,M I....544
Netzler,Dirk....703, 738
Neves,Jose....732
Ney,R....665
Ng,M W R....440
Ng,S S K....178, 180
Ng,Sze Kui....729
Nguyen,T H....279
Ni,Ming....217
Nicorovici,N A....680, 682, 683
Nie,Zaiping....49

Niitsuma,Hiroaki 80
Nilsson,S 480
Nishida,Hiroshi 211
Nishimoto,M 294
Niu,G F 180
Niu,Maode 631
Niwa,Atsuko 110
Noguchi,Y 239
Norgren,Martin 685
Norman,A 413, 548
Nothofer,A 24
Nyquist,D P 413

O

Ofli,Erdem 232
Ogura,H 460, 461, 463, 465
Ohta,Isao 60
Ohtoshi,Tsukuru 110
Ohtsuka,Masataka 561
Ojiro,Y 63
Okamura,Yasuyuki 468
Olbrich,G R 242
Oliveira,J R S 142
Oliver,Chris 70
Olyslager,Frank 692
Omar,A S 166
Ono,Kazuo 304
Onodera,Yoichi 344
Ooi,B L 61
Oristaglio,Michael L 618
Ortiz,E M 658, 659
Osada,Yoshihito 225
Oumansour,K 258

P

Paiva,C R 506, 684
Pak,Kyung 464, 466
Palumbo,Stefano 73
Pan,C J 668
Paoletti,D 289
Parfitt,Andrew J 130
ParkGu ,Bum 225
Pastorino,M 84
Pathak,Nirbhaya 578
Patro,Y G K 726
Patterson,F G 103
Pavlasek,T J F 145
Pei,Jinming 186, 187
Peik,S 229
Pekonen,Olli 65
Pellerin,Tony 384
Peng,Chang 504
Perera,W L R 316
Peyton,A J 731
Pistora,Jaromír 298, 556
Pitsch,A 257
Polifko,David 237
Poon,T C 525, 526
Poon,Y W 398
Porch,A 640
Postava,Kamil 298
Pottier,E 247
Powell,J 640
Prabhakran Nayar,S R 666
Prakash,V V S 602
Prather,Dennis W 527
Pregla,R 98, 105, 307
Proskurin,S G 331
Pun,E Y B 314

Q

Qassim,K A S 567
Qian,Bao Liang 435
Qian,Yongxi 67
Qin,Jiayin 421
Qin,Yaokun 230
Qiu,Kun 422
Qiu,Y L 37, 62
Quek,C L 35, 42

R

RÖttger,J 668, 676
Raβhofer,Ralph H 393, 630
Rahal,A 161
Rahman,B M A 305, 507
Rahman,H 170
Rahmat-Samii,Yahya 43, 147, 617
Rajarajan,M, ... 507
Raju,R R 675
Ramahi,Omar M 620, 621
Ramesh,B V 579
Ramon,Ceon 551
Ramos,P M 506
Ramos-Mendieta,F 686
Ranieri,P 107
Rao,D N 667, 672, 673, 674
Rao,P B 670, 671
Rao,S V B 667, 672, 673,674
Rao,T N 674
Rao,Y S Raja 579
Rappaport,Carey M 546
Rashwan,Hanaa M 76
Razban,Tchanguiz 315, 566
Reddy,G Ramachandra 671
Reddy,John 153
Reddy,K K 672
Redmond,D 271
Reed,G T 724
Reed,M 112
Reindl,L 443
Reiner,G 720
Ren,Kening 362
Ren,Wei 470, 474, 476, 477
Ren,Xianfeng 377
Rensburg,D 149
Revankar,U K 579

Revathy,K....666
Riccio,Daniele....74
Richardson,D J....538
Richardson,Paul A....312
Ridaoui,K....335
Riggs,Lloyd S....416
Rinkevich,A B....557
Risler,Ulrike....95
Rius,Juan M....177
Rocha,Armando....732
Rodger,Craig J....484
Rodriguez,Ernesto....252
Rogatkin,D A....662
Rojo,Marta....159
Rolland,C....115
Rosen,Paul....252
Rossum,M Van....161
Roth,Bernd....441
Rothwell,E J....413
Row,Jeen-Sheen....17
Rowe,Harrison E....302
Rowell,C R....356
Roy,K K....485
Royer,K W....440
Ruan,Y Z....596
Ruile,Werner....95
Russer,Peter....165, 439, 440
Russo,A A....333
Ruthowski,Jacek....437
Rybakova,A G....380
Ryzhenkova,I V....90

S

Sado,S....277
Safaai-Jazi,A....520
Sagawa,Morikazu....235
Saillard,J....258, 259
Saito,Atsushi....211
Saitoh,Y....337
Saiz,J M....658, 659
Sakaguchi,Koichi....360
Sakamoto,Katsuyuki....339
Samir,W....533
Sammut,R A....533
Samokhin,A B....603
Sampath,V....264
Santarsiero,M....289, 502
Sanyal,Ashis....638
Sarkar,B K....646
Sarytchev,V A....254
Sasaki,Hideki....22
Sasaki,K....367
Sasano,Yasuhiro....278
Sato,A....63
Sato,Moyoyuki....80
Sato,Ryoichi....660
Satoh,Chiaki....276
Schaeffer,E C....691
Schanz,Lars....272
Schettini,G....502
Schiinemann,K....447
Schlüter,H....456
Schneider,John B....619
Schneider,Ralph....95
Schreck,Andreas....81
Schreurs,D....161
Schulz,D....609
Sedunov,N A....486
Seger,O....480
Seguin,G....145, 149, 364
Seidl,Jaromlr....298
Seifert,F....443
Sen,Pabitra N....376
Sewell,P....112
Shaalan,Ahmed E....76
Shafai,L....139, 150
Shao,K....645
Shao,Yun....493
Sharaiha,A....368, 369, 563
Sharma,M U....733
Sharma,Sanjay....695
Sharygin,G S....261
Shen,Dacai....188
Shen,X C....649
Sheng,Ping....678
Sheng,Xinqing....224
Shenq,Meng-Huei....417
Shi,Jiancheng....492
Shi,Pengyu....64
Shi,S Y....197
Shi,W M....184, 185, 629, 632
Shi,Zhendong....215
Shibasaki,S....63
Shigesawa,Hiroshi....303, 442
Shih,Y C....55, 438
Shimizu,Koichi....85, 330, 344, 469
Shinomiya,G....700, 701
Shirai,Hiroshi....660
Shirai,T....498
Shirasaki,M....539
Shivarova,A....456
Shlager,Kurt L....619
Shum,P....327
Shum,S M....365
Sibilia,C....107
Sihvola,Ari....692
Singh,A K....485, 602
Singh,Narendra P....543
Siu,Y M....19
Skriabine,Anatoli....663
Smith,Charles E....621
Smith,P....643
Smith,Paul D....241
So,P P M....167
Sobhy,M I....440
Solaimani,M....574, 577

Somekh,M G 728
Song,Haipin 186,589
Song,J M 46
Song,Liqun 447
Song,Xue Bin 431
Song,Y M 226, 392
Sou,I K 723
Soukoulis,M 679
Sourdois,C 146
Souza,Rui Fragassi 207
Spagnolo,G Schirripa 289
Srivastava,G P 648
Srivastava,S M 485
Stöhr,Christian 703, 738
Stenström,G 480
Stoytchev,M 497, 501
Stritzker,B 640
Stukach,O V 734, 735, 736
Su,C D 708
Su,C-W 31
Su,Hsin-Cheng 14
Su,S Y 668
Su,Ying-Wem 189, 605
Sudbo,Aasmund 102
Suissa,Uri 553
Sulivan,P J 586
Sultan,N 149, 364, 384
Sun,C C 709
Sun,Ching-Cherng 322
Sun,Daoli 141, 345
Sun,Z L 213, 219
Suppanitchakij,V 520
Suratkar,P P 726
Swatek,D R 406

T

TaftiH,A 118
Taga,Tokio 355
Taguchi,Mitsuo 129
Taguchi,T 700, 701
Takada,Jun-ichi 370, 372
Takahashi,Norio 562
Takeuchi,Tetsuya 702
Tam,H Y 326
Tam,W Y 398
Tamil,Lakshman S 312
Tamura,Yasuhiko 459
Tan,H H 717
Tanaka,Kazumasa 129
Tanaka,Masato 562
Tang,H 647
Tang,X H 742
Tang,Xiaohong 424
Tanikwa,Y 331
Tanizaki,Toru 211
Tarn,Chen Wen 521
Tassoudji,M Ali 581
Tatarinov,S V 249, 250
Tatarinov,V N 249, 261
Tateiba,Mitsuo 470, 471, 474, 475, 476, 477
Tayeb,G 681
Tcherny,V V 662
Temae,Takahiro 163
Terret,C 368, 369, 563
Tertuliano,H 394
Teshirogi,Tasuku 562
Thieme,Markus O 393
Thomas,K 691
Thompson,C 716
Titov,V I 486
Tognolatti,P 334
Tong,Chi-Lun 451
Tong,K F 127
Tong,Ming-Sze 610
Tong,Y C 323
Topa,Antonio L 684
Torabian,A 445
Torres,F 560, 565
Tran,H T 533
Tremblay,F 405
Truehafft,Bob 252
Trueman,C W 384
Tsai,Kun-Hua 34
Tsang,H K 323
Tsang,K F 184, 185, 629, 632, 653, 654
Tsang,L 48, 464, 466
Tsou,R H 709
Tsuji,Mikio 303, 442
Tsukiji,Takehiko 359
Tsunekawa,Koichi 358
Tu,C 526
Tu,Yuan-Kuang 711
Turitsyn,S K 90
Turnbull,L 24
Tzeng,Y C 399
Tzuang,C-K C 238

U

Ulander,L M H 480
Urasaki,Shuji 561
Ustinov,V V 557
Uysal,S 449

V

Vachon,P W 482
Vahldieck, R 91
Valle,P J 658, 659
Valon,Marcel 160
Van Stralen,Mathe 297
Van Zyl,Jakob 252
Varughese,Suma 601
Vasenkov,A A 696
Vaughan,Rodney G 354, 357, 361
Vaya,P R 118, 721
Vicalvi,S 289
Vinagre,L 69

Voges,E 101, 609
Vokurka,V U 154
Vorobiev,V G 248, 260, 262

W

Wada,K 239
Wagner,Holger 21
Wait,James R 484
Wakabayashi,Kenji 295
Walle,R Van 342
Wallinga,G 413
Walliser,Beate 95
Walter,Marc 94
Wan,Goubin 411, 568
Wan,Qing 231
Wan,Wei 411, 568
Wang,C F 226
Wang,Chi-Yu 711
Wang,H B 649
Wang,Hanyang 564
Wang,Huazhi 387
Wang,Huilian 488
Wang,J R 690
Wang,J-J 31
Wang,Kai 712
Wang,L A 708
Wang,L F 279
Wang,Manshu 186
Wang,Paul J 546
Wang,Rong 343
Wang,Shuzhong 608
Wang,W Z 428
Wang,Way-Seen 707
Wang,Weiyan 83
Wang,Wenbing 383
Wang,Wenxiang 595
Wang,Y 258, 259
Wang,Y Y 644, 645
Wang,Yong 730
Wang,You-fa 318
Wang,Z L 460, 461, 465
Wang,Zhen-song 472
Wang,Zhijie 323
Wang,Zhong 29
Wanielik,Gred 81
Wash,Carlyle H 491
Watanabe,Koki 508
Waterhouse,R B 128
Weigel,R 93,95,443
Weigl,B 720
Weiss,B L 716, 718
Wellhofer,F 640
Wen,Geyi 591
Wen,Guo-Peng 114
Wen,J D 227
Werner,Chales 252
Wilheit,T 271
Wilson,Julian 73
Wing,Omar 414
Wolf,Emil 287
Won,Yong Hyub 512, 513, 516
Wong,Chak Nam 26, 652, 653
Wong,E M W 314
Wong,G K L 723
Wong,K S 723
Wong,Kin-Lu 8, 14, 15
Wong,W P 532
Wongcharoen,T 507
Woodall,P 640
Wu,Chen 616
Wu,Cheng-Wen 292, 509
Wu,Doris I 135
Wu,Ke 156, 168, 204, 208, 210, 444
Wu,M C 51
Wu,P H 645, 649
Wu,Qun 141, 345, 409
Wu,R X 645
Wu,Ruey-Beei 38
Wu,Wen 402, 607
Wu,Xiangying 625
Wu,Z 366, 643
Wu,Zhengde 424, 428
Wu,Zhensen 196, 383, 403

X

Xavier,B 586, 587
Xia,Jun 397
Xiang,Dang 319
Xiang,Jiazhen 582
Xie,Chongjin 387
Xie,Sheng Wu 328
Xin,Y-L 120
Xu,Changqing 193
Xu,Chen 401
Xu,Deming 625, 631
Xu,Feng 614, 623
Xu,Jiadong 590, 600
Xu,Jie 65
Xu,Jun 423
Xu,Kexi 626, 628
Xu,Liang 383
Xu,S F 645
Xu,Shanjia 224
Xu,W W 649
Xu,Yansheng 157
Xu,Zhi Cai 433, 434
Xue,Liangjin 423
Xue,S Q 428, 649

Y

Yabuki,Hiroyuki 235
Yaccarino,Robert G 147
Yam,Yu-On 243, 451
Yamada,Kazuhiro 468
Yamada,Norihide 702
Yamada,Y 700, 701

Yamada,Yoshifumi....58, 332
Yamada,Yukio....331
Yamamoto,Katsuyuki....85, 330, 344
Yamamoto,Sadahiko....468
Yamasaki,Tsuneki....308
Yamashita,Eikichi....67
Yamashita,Sadao....236
Yan,Y....447
Yang,Eric....276
Yang,Fan....576
Yang,Fuh-Hsiang....310
Yang,Jianyu....220, 425
Yang,Jinn-Chyuan....11
Yang,Quanrang....402, 607
Yang,Szu-Wen....292
Yang,Xiaobo....220, 425
Yang,Xue Lin....328
Yang,Y E....279
Yang,Yexin....230
Yang,Z....723
Yao,De-miao....200, 385
Yasumoto,Kiyotoshi....293, 508
Yata,A....294
Yau,Patrick....616
Yeh,C-H....31
Yeh,Y H....517
Yellaiah,G....669
Yeo,S P....158
Yeo,T S....35, 37, 42, 62
Yin,Shizhuo....522
Yin,Xing Hui....433, 434
Yip,G L....300, 524
Yokota,Tatsuya....278
Yokoyama,Kiyoyuki....109
Yoneyama,Tsukasa....163, 202, 206
Yu,chen-Kuo....194
Yu,Francis T S....522
Yu,Guofen....595
Yu,P K L....52
Yu,S F....327, 722
Yu,Tiejun....642
Yu,Z Z....731
Yuan,F Y....581, 585
Yuan,Hongjun....576
Yuan,Naichang....386
Yuan,Xiaokang....582
Yuen,Chung Ming....651, 652, 653, 654
Yuk,T I....327
Yun,Xiaohua....223
Yung,Edward K N....173, 175, 176, 179, 228, 371, 455, 742
Yurkevich,I....465

Z

Zaboronkova,T M....696
Zatta,Philippe....315, 566
Zemlyanov,A A....198
Zengerle,R....104
Zhang,D G....346, 742
Zhang,Dekun....634, 635, 636
Zhang,Guifu....464, 466
Zhang,Hanyi....317
Zhang,Hong....422
Zhang,Hua Fang....431
Zhang,J....548
Zhang,J Z....644, 645
Zhang,Jihong....29
Zhang,Linchang....362
Zhang,Peng....488
Zhang,Shourong....83
Zhang,Tao....422
Zhang,W X....183,184, 185
Zhang,Xianmin....225
Zhang,Xuexia....573, 576, 642
Zhang,Y....279
Zhang,Y P....192
Zhang,Yerong....49
Zhang,Yongchuan....216
Zhang,Yonghong....423
Zhang,Yongling....391, 608
Zhang,Z Q....499
Zhang,Zhaofeng....214
Zhang,Zhijian....317
Zhang,Zuyin....190
Zhao,F R....120
Zhao,Jiasheng....29
Zhao,Minggui....193
Zhao,Yushen....592, 593, 598, 599
Zhao,Zhi-zhong....385
Zheludev,N I....534
Zheng,H....379, 453
Zheng,Xingshi....421
Zhong,Ming....183
Zhou,Dong....422
Zhou,H J....596
Zhou,Jianyi....607
Zhou,Qin....400
Zhou,Shiping....625, 626, 628
Zhou,Y L....645
Zhu,Bocheng....143, 569
Zhu,Dajun....447
Zhu,Jianhua....221, 296, 427, 430, 432
Zhu,Sheng-chuan....27, 452, 740, 741
Zhu,Shouzheng....187, 594
Zhu,Xiang....594
Zhu,Xiaowei....426
Zou,Chuanyun....635, 636
Zuffada,Cinzia....41
Zuikova,E M....486